KCDC User Manual

KCDC - the **K**ASCADE **C**osmic Ray **D**ata **C**entre

Open Access Solution for the

KArlsruhe **S**hower **C**ore and **A**rray **De**tector (**KASCADE)**

KIT - University of the State of Baden-Wuerttemberg
and National Research Centre of the Helmholtz Association

Authors:	Jürgen Wochele, Donghwa Kang, Doris Wochele, Andreas Haungs, Sven Schoo
Address:	Karlsruhe Institute of Technology (KIT) Institute for Astroparticle Physics (IAP) Hermann-von-Helmholtz-Platz 1 76344 Eggenstein-Leopoldshafen
Internet:	kcdc.iap.kit.edu www.kit.edu
DOI:	https://doi.org/10.17616/R3TS4P
Version:	V.3.2
Last update:	2024-11-22

TABLE OF CONTENTS

III

1

1

VI

1

1

1   INTRODUCTION

The KCDC Manual provides detailed explanation of data taken by the KASCADE/KASCADE-Grande Collaboration and made publicly accessible with the KCDC Project Internet Application. The KCDC-team is quite aware of the fact that not all details concerning data acquisition and data analysis can be described in this manual.

1.1   KCDC - THE KASCADE COSMIC RAY DATA CENTRE

KCDC is the **'KASCADE Cosmic Ray Data Centre'**, where via a web-based interface data of the astroparticle physics experiment KASCADE are made available via various so called 'DataShops' for the interested public.

The KASCADE experiment, financed by public money, was a large-area detector for the measurement of high-energy cosmic rays. These charged particles (fully ionised atomic nuclei) are accelerated in active cosmic objects, propagated through the intergalactic and interstellar medium of the Universe, and reach our Earth for energies above 10^{14} eV with a rate of less than one per minute and square meter. Hitting our Atmosphere, they subsequently interact with nuclei and generate a cascade of millions of secondary particles, which partly reach the Earth surface and can be detected. This phenomenon is called an extensive air shower: EAS. With an array of particle detectors this secondary cosmic radiation of individual EAS can be detected and the parameters of the impinging primary particle reconstructed. In a second step, the energy spectrum, elemental composition and the arrival distribution of the primary cosmic rays are investigated and by this, the astrophysical question to the origin of cosmic rays is studied. KASCADE was extended to KASCADE-Grande in 2003 to reach higher energies of primary cosmic rays where the rate decreases to less than one per day and square meter. KASCADE-Grande stopped finally the active data acquisition of all its components end of 2012 and is already decommissioned. The international collaboration of the experiment, however, continues the detailed analysis of nearly 20 years of data.

Moreover, with KCDC we provide to the public the edited data, i.e. the reconstructed parameters of the primary cosmic rays measured via the detection of EAS with the KASCADE-Grande experiment, via a customized web page. The aim of this particular project is the installation and establishment of a public data centre for high-energy astroparticle physics. In the research field of astroparticle physics, such a data release is a novelty, whereas the data publication in astronomy has been established for a long time. But, due to basic differences in the measurements of cosmic-ray induced air showers compared with astronomical data, KCDC provides the first conceptional design, how the data can be treated and processed so that they are reasonably usable outside the community of experts in the research field. The first goal of KCDC is to make to the community the data from the KASCADE experiment available to external users.

In November 2013 we published in a first step 15 parameters of reconstructed and calibrated data, which we thought are necessary to do simple astroparticle physics analysis, e.g. the time, arrival direction and energy of events, etc.

With every new release we want to add more data sets or more quantities to enable the users to perform more complex and more sophisticated analysis with the KASCADE data. As the preparation of the data for public usage is rather time consuming and the KCDC team is rather small, we ask you to be a little patient if not all parameter you would like to do analysis with, can be made available at once. With the latest release PENTARUS we added a second experiment based as well on the KASCADE-Grande data, but analysed in a completely different way, which cannot be compared to formerly published KASCADE data sets.

The following chapters describe in detail the experimental setup of KASCADE and KASCADE-Grande, the parameters as well as the procedure of the reconstruction of extensive air showers in KASCADE.

Information on the matching KASCADE Simulations can be found in the '**KCDC Simulations Manual**' and in the simulation manuals of the other experiments published in KCDC fro example the **'KCDC-Combined Simulations Manual'**.

1.2 KCDC MOTIVATION

The aim of Astroparticle Physics is to investigate the nature of the Cosmic Radiation manifesting in many ways. In various air shower experiments all over the world the cascades of particles are detected, generated in interaction processes between the particles of the Cosmic Radiation and the atmosphere of the earth. As the Air Showers consist of a huge number of particles which are spread over a vast area, big detectors are required to measure a number of parameters of these showers. The combined analysis of observations of various components of the cosmic radiation like charged particles, gamma rays and neutrinos is widely known as "Multi Messenger Astroparticle Physics". From this presently as "hot topic" classified field we hope to gain new and exciting information to extend our knowledge of the origin and transport of what we understand as Cosmic Radiation.

Necessary to achieve such a challenging aim is a free access to the data of various experiments measuring cosmic radiation by different methods and techniques. This is likewise interesting for the community of scientists as well as for all public interested in this topic.

A first step in this direction is to provide the data as well as the tools to analyse the data measured with the KASCADE / KASCADE-Grande Experiment for public use. This project is called the 'KASCADE Cosmic Ray Data Centre', "KCDC".

Our motivation is based on three ideas:

The idea of open data as it is laid down in the "Berlin Declaration on Open Access to Knowledge in the Sciences and Humanities" from 22.10.2003. There we read :

"Our mission of disseminating knowledge is only half complete if the information is not made widely and readily available to society. New possibilities of knowledge dissemination not only through the classical form but also and increasingly through the open access paradigm via the Internet have to be supported. We define open access as a comprehensive source of human knowledge and cultural heritage that has been approved by the scientific community."

and

1 Introduction

"In order to realize the vision of a global and accessible representation of knowledge, the future Web has to be sustainable, interactive, and transparent. Content and software tools must be openly accessible and compatible."

The Helmholtz Alliance and the KIT plead for further use and for re-examination of the measured data based on this declaration.

Furthermore, KASCADE was financed by taxpayer's money, which implies that the collected data are public property. We want to prepare our data in a way that the general public will be able to access and use the data.

The data have to be preserved for future generations in a way that they should not only be able to re-perform all analysis steps and conclusions which led us to our widely approved results manifested in a lot of international publications, but also to be able to use the data far beyond the lifetime of the experiment which has in fact been shut down already end of 2012.

This approach is new in Astroparticle Physics as well as in the neighbouring fields like Nuclear Physics and High Energy Physics, but well known from Astronomy. Therefore, it is our aim to provide a consistent 'bundle' of hard- and software applicable for cosmic ray data. KCDC will handle questions like calibration of the raw data, applied quality cuts, data formats but also internet access via a web portal and the associated questions like legal rights and so on from the very beginning.

Because of the huge amount of available data it is not feasible to offer all data in a 'tarball' for download. Moreover, we offer a way to apply reasonable selection cuts to reduce the variety of data and parameters adapted to the requirements of the analysis the user intends to perform.

We try to achieve this by means of a flexible web portal providing a modern software solution for publishing the KASCADE / KASCADE-Grande data for a general audience based on open source software. KCDC as a WEB portal offers software as a service without installation by the user with the advantage of a worldwide access via web browsers to data and processing facilities. We also supply meta information on the detectors and the available data.

Moreover, we provide example analysis to encourage teachers and pupils to use our data for their first step into the exciting field of cosmic radiation and astroparticle physics.

In a second step we will release our software as Open Source for free use by other experiments to publish their data in a similar way.

1.3 KCDC DATA OVERVIEW

The list provided is intended to give a brief overview of the data from the KASCADE-Grande experiment that has been published to date with the latest release PENTARUS.

DataShop	Detector	Component	Nr of Events
KASCADE	**KASCADE-Grande**	array	433,209,340
		grande	35,310,393
		calorimeter	100,655,080
		lopes	3058
		general	433,209,340
COMBINED	**KASCADE-Grande**	combined	15,635,550
		lopes	1430
		general	15,635,550

1.4   THE KCDC TEAM

Fig. 1.3.1   *The KCDC-Team*

2 THE KASCADE-DETECTORS

2.1 THE KASCADE-GRANDE EXPERIMENT

KASCADE-Grande is an extensive air shower experiment array to study the cosmic ray primary composition and the hadronic interactions in the energy range $E_0=10^{14}$–10^{18}eV. The experiment is situated on site of the KIT, Campus North (the former Forschungszentrum Karlsruhe) (49.1°N, 8.4°E) at 110m a.s.l, corresponding to an average atmospheric depth of 1022g/cm^2. One of the main results obtained by KASCADE is a picture of increasingly heavier composition above the 'knee' caused by a break in the spectrum of the light components. Conventional acceleration models predict a change of the composition towards heavier components.

The KASCADE Grande experiment consists of four major detector components (see fig.: 2.1.1). An array of 252 detector stations housing separate electron and muon detectors, a central detector for measuring the hadron component with additional muon detection area, a tunnel with streamer tubes to record individual muon tracks and a second array with 37 detector stations for electron detection which extends the effective KASCADE array area from 200x200 m² by a factor of 10 built in 2003 by reassembling 37 stations of the former EAS-TOP experiment running successfully between 1987 and 2000 at Campo Imperatore, Grand Sasso Laboratories, Italy.

 An additional small trigger Array half way between the centres of the KASCADE and KASCADE-Grande detector arrays (Piccolo) provides trigger information for showers far away from the KASCADE array. Furthermore, an array of radio antennas is co-located with the KASCADE array (LOPES) which uses the KASCADE trigger and the well-calibrated information of air shower properties to study radio emissions of cosmic rays.
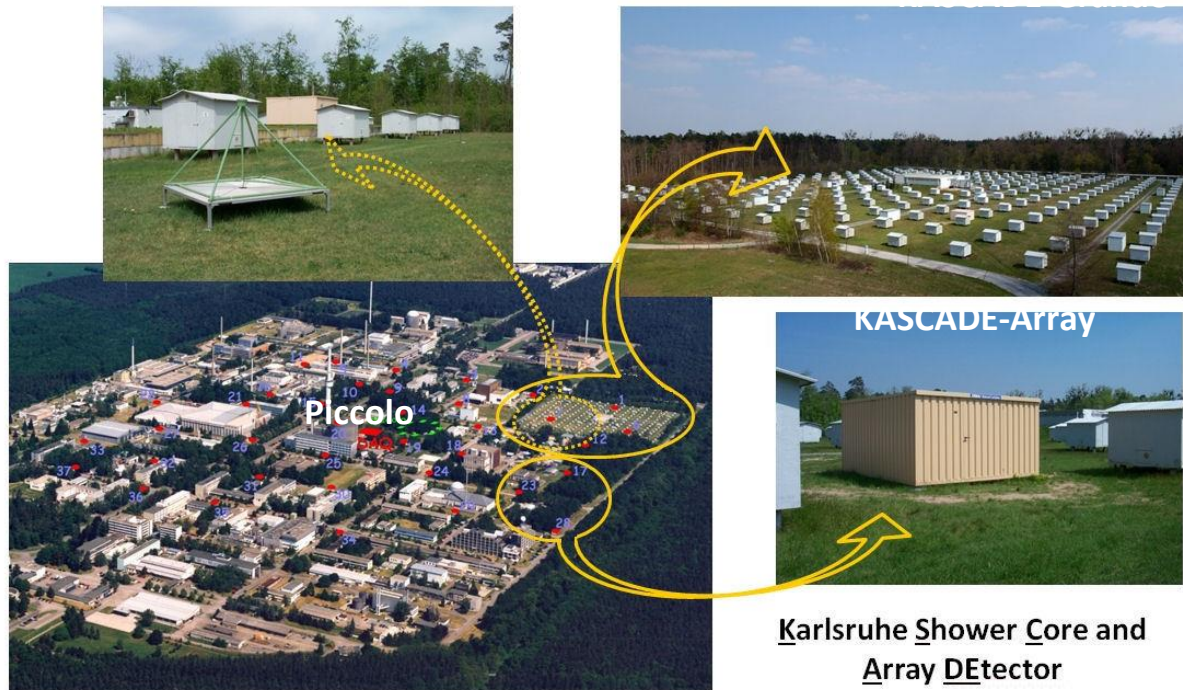
Fig. 2.1.1   *Location of the KASCADE detector arrays*

2.2   THE KASCADE DETECTOR ARRAY

The field array consists of 252 detector stations arranged on a rectangular grid with a distance of 13 m covering an area of 200x200 m² organized in 16 clusters 4x4 stations each with an electronics container in the centre (see fig 2.2.1). The stations are equipped with unshielded and shielded detectors for the measurement of the electromagnetic and muonic shower components simultaneously and independently. The charged component of the air shower's secondary particles above 3 MeV threshold is detected in the liquid scintillation counters above the shielding while the muonic component is measured underneath lead and iron absorber sheets (10cm Pb and 4cm Fe) in 3.2 m² of plastic scintillators.
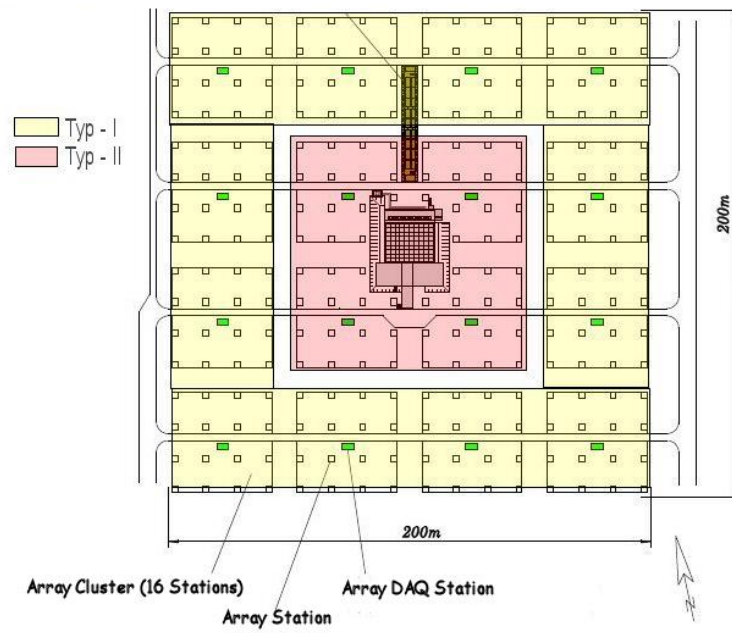
Fig. 2.2.1   *Array setup, schematic view of the KASCADE detector array*

Two different detector setups are realised in the KASCADE array. The inner 4 clusters (marked red in fig. 2.2.1), consist of only 15 stations, (the 16th position is blocked by the Central Calorimeter) and are equipped with 4 liquid scintillator cones with an effective area of 3.14m² to measure the shower core. As the probability of punch through of hadrons and electrons is increasing closer to the shower core, only the outer 12 cluster have μ-detectors (marked yellow in fig 2.2.1). Underneath only two liquid scintillation e/γ-detectors, a shielding of 10 cm Pb and 4cm Fe is located. Below the shielding only the muonic shower component is present and detected above 230 MeV (see fig 2.2.2). Each of the e/γ liquid scintillation detectors is equipped with one photomultiplier, to monitor the electromagnetic component of an air shower for timing and particle density measurements.

Each of the 16 clusters is able to take data independently. Data are accumulated in the electronic station of each cluster and transmitted to the data acquisition system (DAQ). The time resolution of the detector is 0.77 ns. This excellent timing leads to an angular resolution of about 0.1° for the arrival directions of the showers which enables us to search for large-scale anisotropies as well as for cosmic ray point sources.

Main task of the array is the determination of the shower core position, the number of electrons and muons in a shower, its lateral particle distribution and its incident direction.

Type-I Station

Detector Station

HV- and Signal Connectors

Photomultiplier Tube

Light Guide

Pressure Balance Vessel (Ar filling)

e/gamma-Detectors Liquid Scintillator

Lead Absorber (10 cm)

Iron Absorber (4 cm)

Muon-Detectors Plastic Scintillators

Concrete

2400mm

Type-II Station

Detector Station

HV- and Signal Connectors

Photomultiplier Tube

Light Guide

Pressure Balance Vessel (Ar filling)

e/gamma-Detectors Liquid Scintillator

Concrete

2400mm

Fig. 2.2.2   *Array station setup, schematic view of Type-I and Type-II detector stations*

As an example of KASCADE Array events, the screenshots from the Array Event Display are shown in fig 2.2.3. On the left sides you see the energy deposits in the 252 Array stations, top the e/γ-detectors, bottom the μ-detectors. The warmer the colour the higher the energy. On the right sides the corresponding arrival times. The warmer the colour the bigger the time stamp measured. As the colours used are normalised to the difference between the first and the last time stamp, it cannot be used as a measure for the zenith angle of the incident particle.
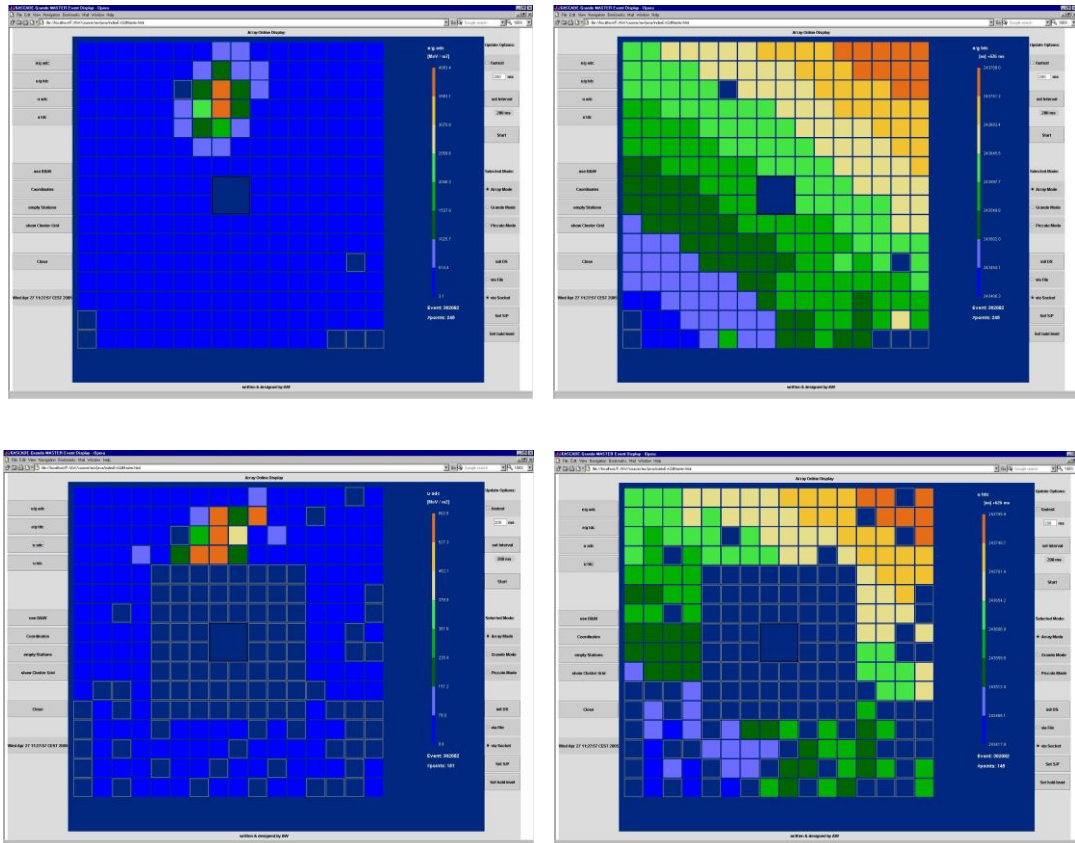
fig. 2.2.3   *Array event No. 302082 from 27.4.2005; energy deposit (left), arrival times (right)*

2.3   THE GRANDE DETECTOR ARRAY

During 2003 the Grande array was added to the KASCADE experiment. It extended its effective area, and thereby its upper energy limit, by a factor of ten.

The Grande array is composed of 37 detector stations installed over an irregular triangular grid with an average spacing of 137 m. It covers an area of approximately 0.5 km² (fig. 2.3.1).
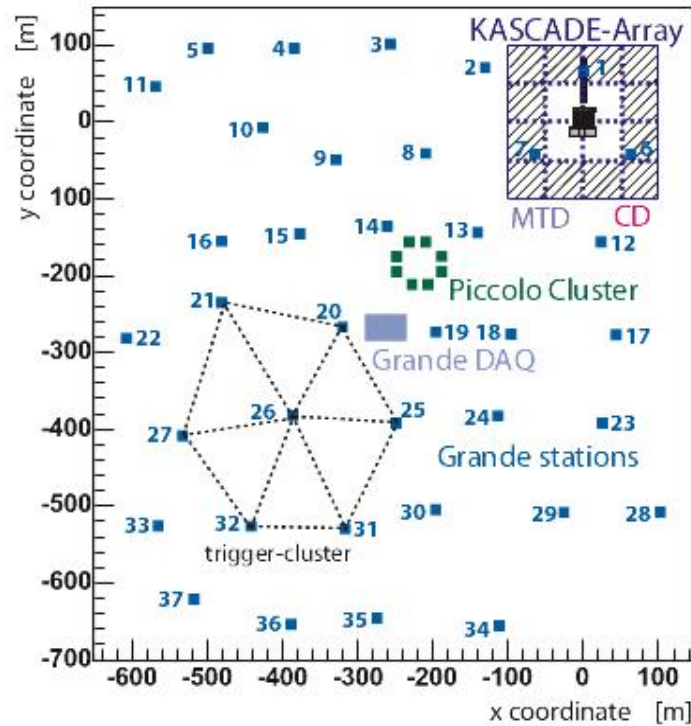
Fig. 2.3.1   *KASCADE-Grande detector setup*

Each detector station includes a total of 10m² of plastic scintillator subdivided into 16 individual modules each viewed from the bottom by a photomultiplier. Each stainless steel box has a wall thickness of 1mm, housing a 80×80×4 cm^3 NE102A plastic scintillator slab and a photomultiplier (PMT). The inside of the boxes is painted with a diffusive coating. The scintillators are viewed from the bottom at a distance of 30 cm by a XP3462B photomultiplier for timing and particle density measurements (High Gain PMTs). The four central modules are equipped with an additional PMT of the same type which is operated with a lower high voltage value optimised for high linearity even at large particle densities (Low Gain PMTs). A sketch of the 16 modules of a station is depicted in the fig. 2.3.2.
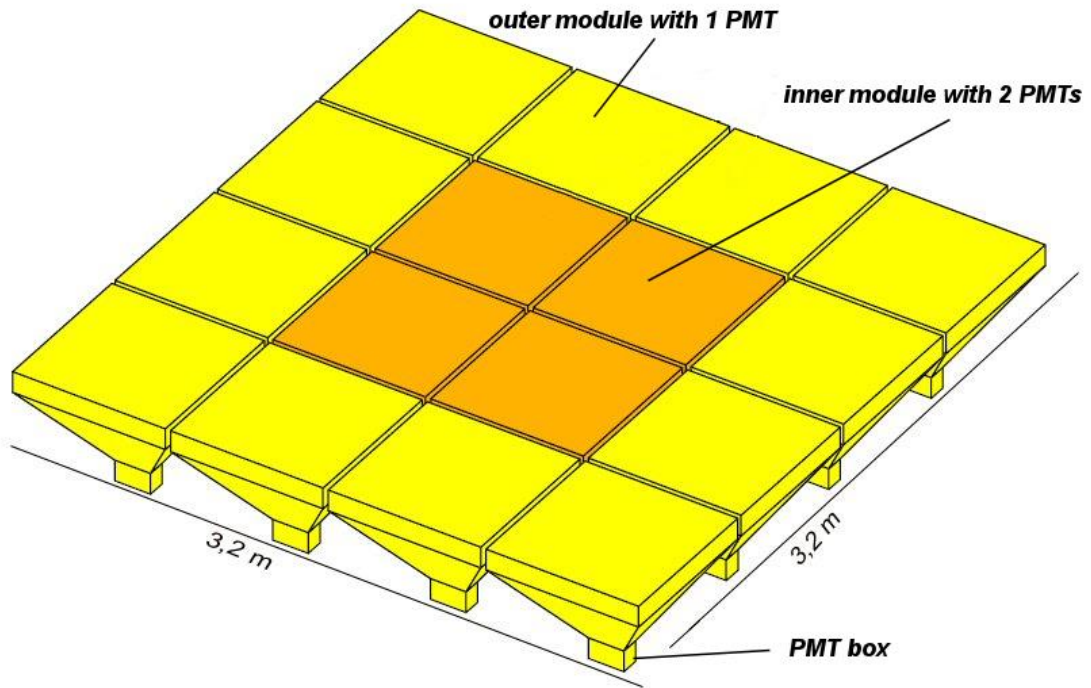
Fig. 2.3.2   *KASCADE-Grande detector station setup*

The GRANDE Array operates independently from the KASCADE Array and measures the same parameters of the electromagnetic component as the KASCADE Array.

The 37 Grande stations are organized in 18 overlapping trigger clusters (see fig 2.3.3). Each cluster includes seven detector stations: six in a hexagonal shape and a central one. The data acquisition is triggered by either a 4/7 coincidence from a cluster (4 stations in a compact configuration, trigger rate: ˜5 Hz) or by a central trigger coming from KASCADE (trigger rate: ˜3.5 Hz). In addition, any full 7/7 coincidence (rate: ˜0.5 Hz) from one of the 18 clusters is transmitted also to KASCADE as a KASCADE-Grande trigger to start KASCADE-Grande event acquisition.
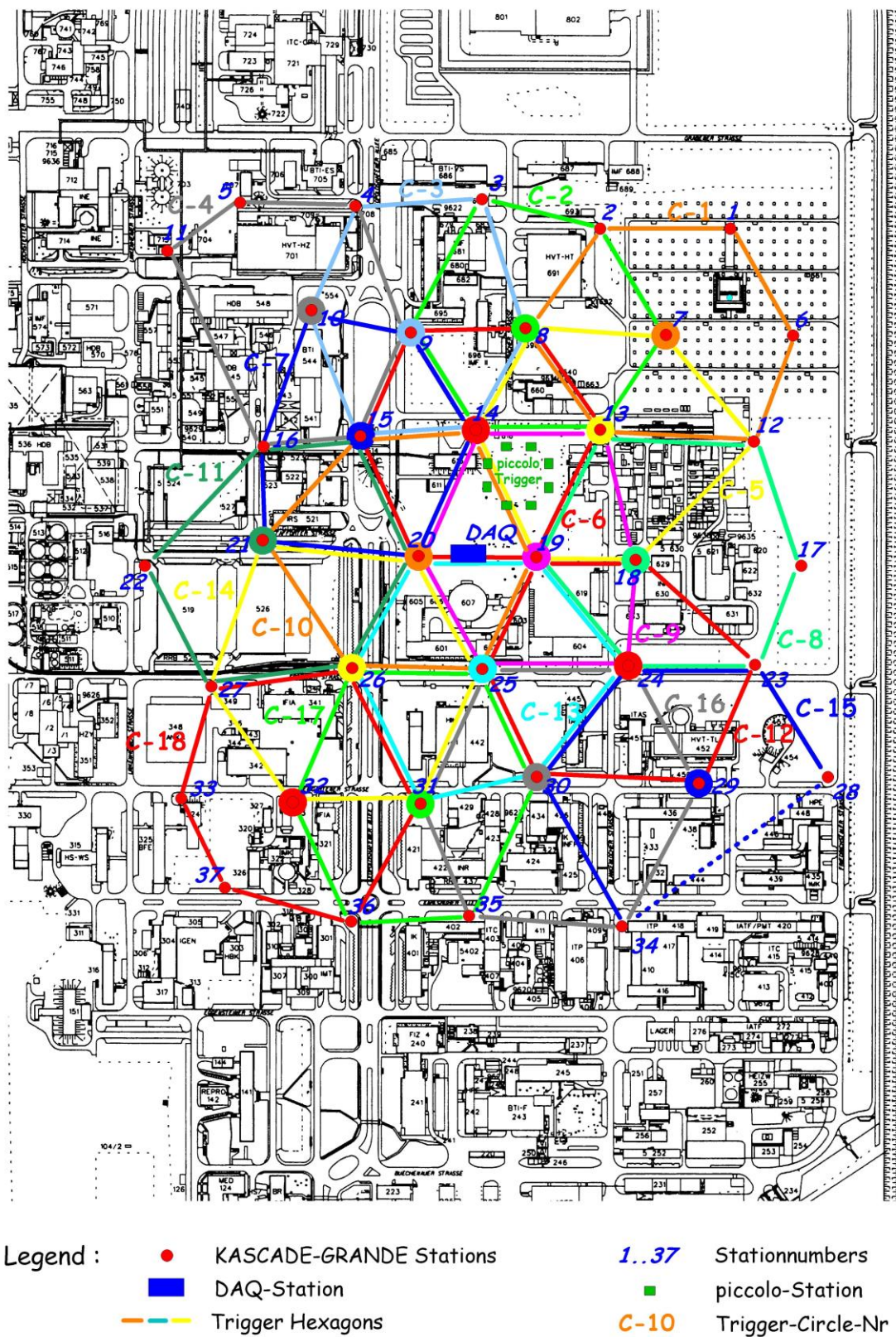
Fig. 2.3.3   *KASCADE-Grande trigger setup*

As an example of Grande Events the screenshots from the Grande Event Display are shown in fig. 2.3.4. On the left sides you see the energy deposits in the 37 Grande stations. The warmer the colour the higher the energy. On the right sides the corresponding arrival times. The warmer the colour the bigger the time stamp measured. As the colours used are normalised to the difference between the first and the last time stamp, it cannot be used as a measure for the zenith angles.
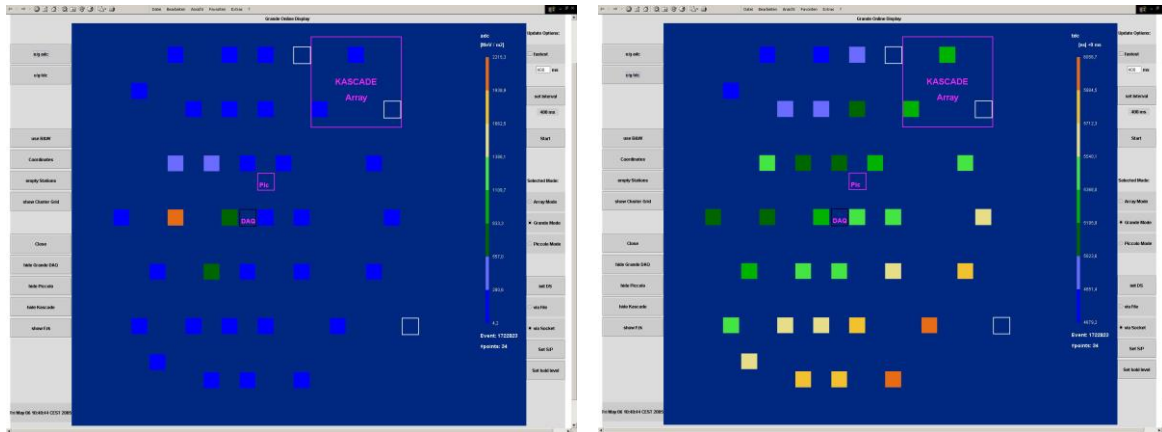
fig. 2.3.4   *Grande event No. 1722823 from 6.5.2005; energy deposit (left), arrival times (right)*

2.4   THE CENTRAL DETECTOR

The central detector houses several distinct experimental setups. A hadron sampling calorimeter as its major component, a layer of scintillation detectors (the so called Trigger Layer) for trigger purposes and for studies of time structure of showers, a high energy muon tracking facility consisting of multiwire proportional chambers (MWPC) and a limited streamer tube (LST) layer (fig. 2.4.1).

The central calorimeter is shifted by +5.19m against the centre of the KASCADE array to the north. North in this sense is not geographical north but 'KASCADE north' twisted by 15° to the east. This information is vital for cuts applied on quantities related to the central calorimeter.

Ionisation Chambers

Top Cluster

Trigger Layer

Lead Shielding

Iron

16 m

20 m

Muon Chambers

Concrete

Streamer Tubes
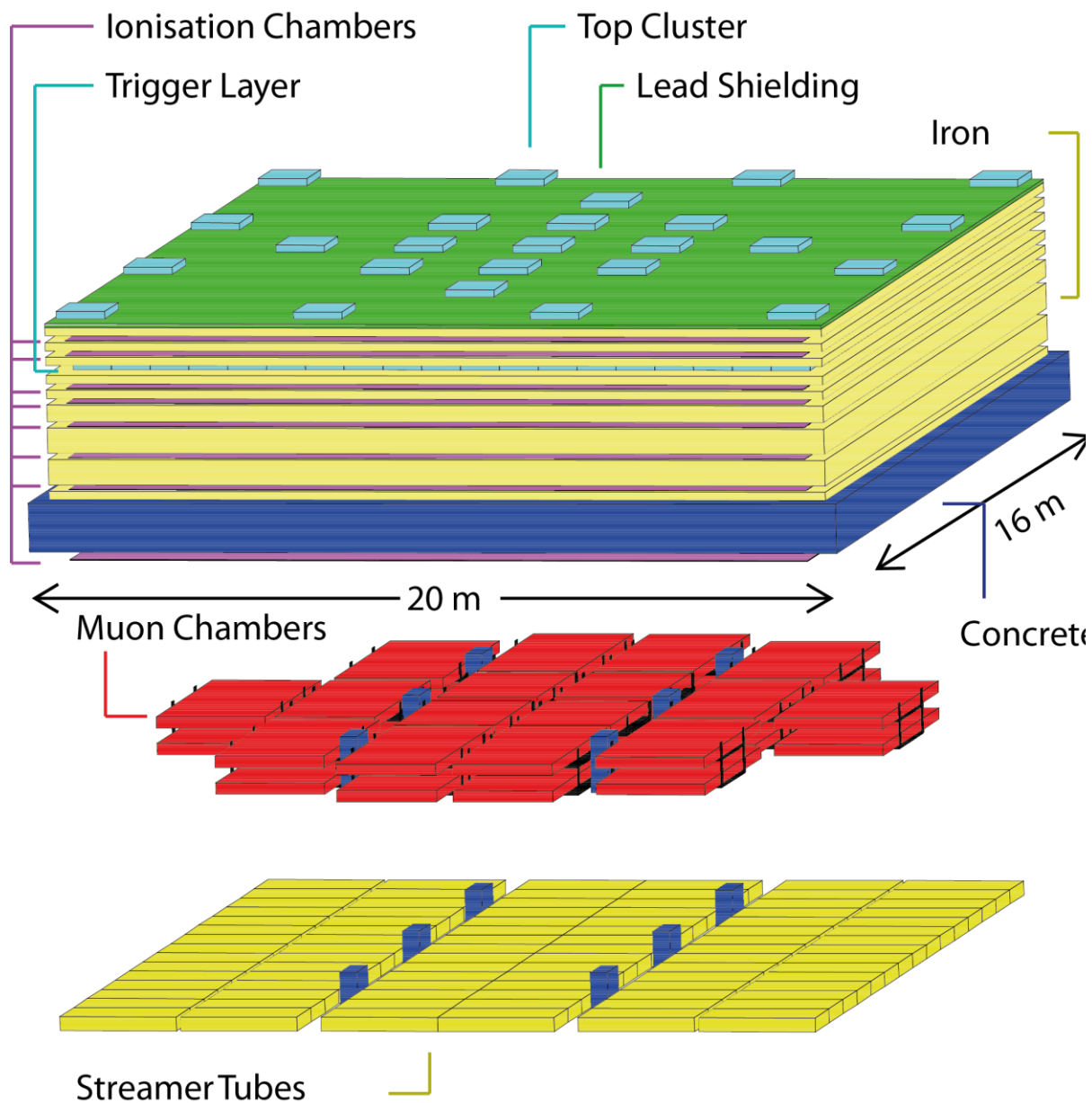
fig. 2.4.1   *Layout of the KASCADE central calorimeter*

2.4.1   THE HADRON CALORIMETER

An important part of the information about the mass and energy of the shower inducing primary particle is transported within the hadronic air shower component to the observation level. The hadrons and their interactions are vital for the understanding of the shower development within the atmosphere. Therefore, the hadron calorimeter is one of the major components of KASCADE, located in the centre of the KASCADE array.

The hadron calorimeter is an Iron-Sampling Calorimeter 16×20m² in size designed to measure the hadronic component of an air shower which hits the KASCADE array centrally. The parameters derived from the calorimeter measurements are the number of reconstructed hadrons, their energy deposits, their core position and their direction. The size of the hadron calorimeter corresponds to the size of the shower core of high-energy air showers. Hadrons up to an energy of about 25 TeV can be absorbed in the calorimeter completely.

The absorber consists out of several layers of iron with a thickness of 12 cm in the upper part increasing to 24 cm and 36 cm in the lower part, respectively. A 5 cm lead filter on top of the calorimeter serves to suppress the electromagnetic component. The 77 cm concrete ceiling of the detector basement acts as last absorber layer. The absorber corresponds to 1460 g/cm^2 or 11.4 hadronic interaction lengths (see fig. 2.4.2).
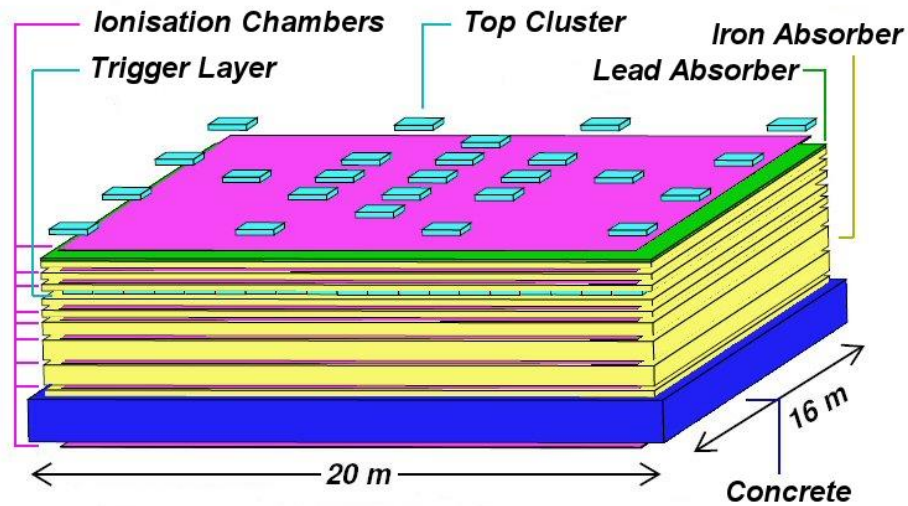
fig. 2.4.2   *Setup of the KASCADE hadron calorimeter*

More than 10,000 liquid ionisation chambers serve as active components, installed in eight layers between and below the iron absorbers, a ninth layer is located above the lead absorber. The ionisation chambers are based on a new detector technology developed at the Institute for Nuclear Physics of the KIT. The KASCADE hadron calorimeter is the first experiment using warm ionising liquids for a large detector. The chambers achieve a large dynamic range of about 6×10^4, only limited due to the amplification electronic. Therefore, signals from a minimum ionising particle as well as from hadrons in the shower core can be measured up to primary energies of 10^{16} eV without saturation. Due to the fine lateral segmentation and the

read-out of the calorimeter in more than 40,000 electronic channels, hadrons with an energy E_{had}>20 GeV can be measured in the calorimeter. They can be separated from each other when the distance of their shower axis is above 40 cm. The spatial resolution of the calorimeter is about 11 cm and the angular resolution is in the order of 5°. The energy resolution is 30% for hadrons with 100 GeV decreasing to 15 % for E_{had}=25 TeV.

As an example of a hadron induced event reconstructed in the calorimeter the screenshots from the Hadron Event Display are shown in fig. 2.4.3. On the left side you see the energy deposits in the several layers caused by a shower core which hits the detector centrally. The middle picture shows 3 individual hadron tracks while on the right hand side an unaccompanied hadron has been reconstructed. The warmer the colour the higher the energy. The black lines are the hadrons tracks as reconstructed by the data analysis software.
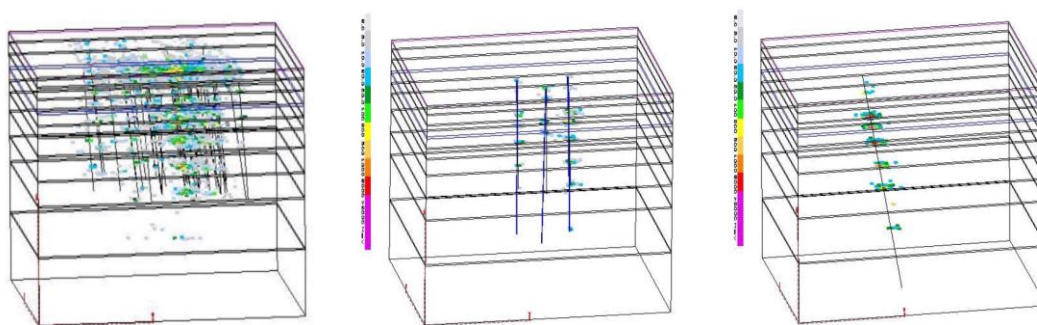
fig. 2.4.3   *Hadron tracks reconstructed: left: one shower core; middle: 3 single tracks; right: one 25TeV unaccompanied hadron*

The room-temperature liquids Tetramethylsilan (TMS, Si $(CH_3)_4$) and Tetramethylpentan (TMP, C_9H_{20}) are used as ionisation media. These liquids are good insulators, on the other hand they are exhibiting a large conductivity for free electrons due to the spherical structure of the molecules. The liquids have a large gap between the conductivity and the valence band similar to metals but with a distance of about 8 eV.

One advantage of such chambers compared with gas chambers is the larger density of the medium and therefore a higher energy deposition per active volume. The induced signals can be measured directly with low noise amplifiers. Due to this, the uncertainties caused by gas

amplification can be eliminated and the detectors can be calibrated absolutely. In addition, good lateral and energy resolutions is achieved due to a compact setup.
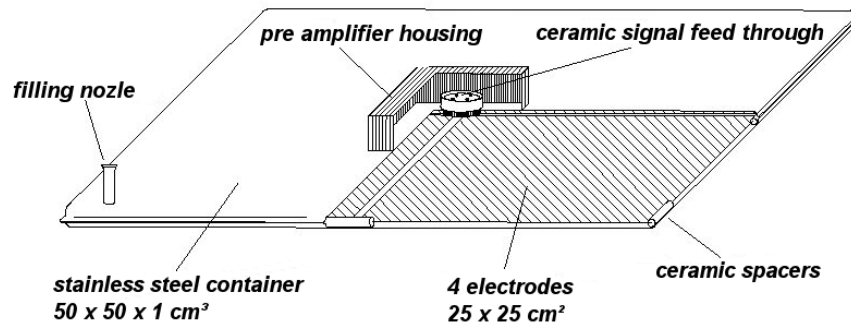
fig. 2.4.4   *Setup of a liquid ionisation chamber*

A ionization chamber consists of a 50x50x1 cm^3 stainless steel box containing four electrodes (25x25 cm^2) positioned in the mid-plane of the box by ceramic spacers (see fig. 2.4.4). A ceramic feed-through allows to apply high voltage to the electrodes and to read out their signals independently, ensuring a fine spatial segmentation of the calorimeter. One chamber is filled with approximately 1.75 l ionisation liquid.

2.4.2   THE TRIGGER LAYER

The third layer of the sampling calorimeter is equipped with a highly segmented trigger and fast timing facility, which enables accurate measurements of the arrival time distributions of muons. For muon identification, the trigger detectors operate in coincidence with the multi-wire proportional chambers MWPC in the basement of the hadron calorimeter. It is built up of 456 scintillation detector elements covering 64 % of the total central detector area (see fig. 2.4.5).

one detector box
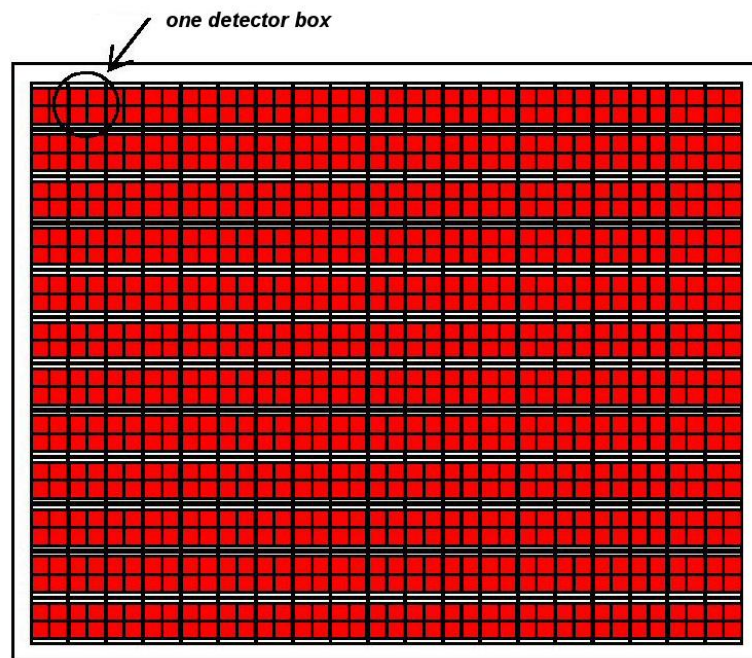
fig. 2.4.5   *Setup of the Trigger Layer*

Each single detector element consists of two quadratic scintillator sheets of 3 cm thickness read out via a wavelength shifter bar and a 1.5 " photomultiplier. Two of the detectors are housed, optically separated, in a detector box. The time resolution of the trigger detectors is 1.8 ns. This detector triggers the read out of the hadron ionisation chambers as well as the muon chambers.

detector box
98 x 125 cm²

plastic scintillator

wavelength shifter

photomultiplier 1,5"
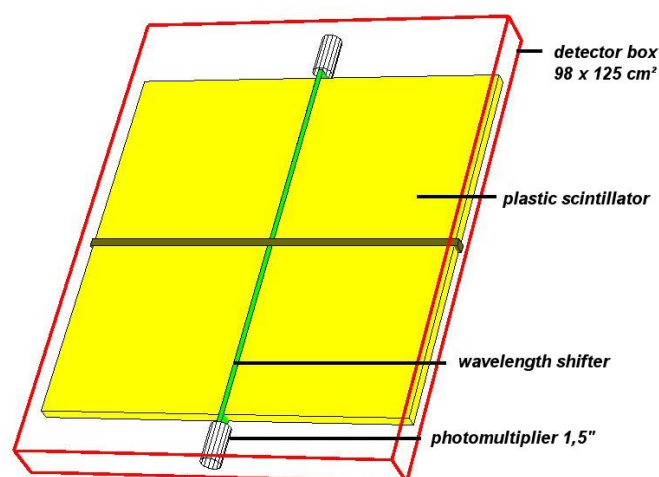
fig. 2.4.6   *Setup of one trigger box*

As an example of an event reconstructed in the Trigger Layer the screenshots from the Trigger data analysis is shown in fig. 2.4.7. On the left side you see the energy deposits in the trigger layers. The warmer the colour the higher the energy. On the right sides the corresponding arrival times.
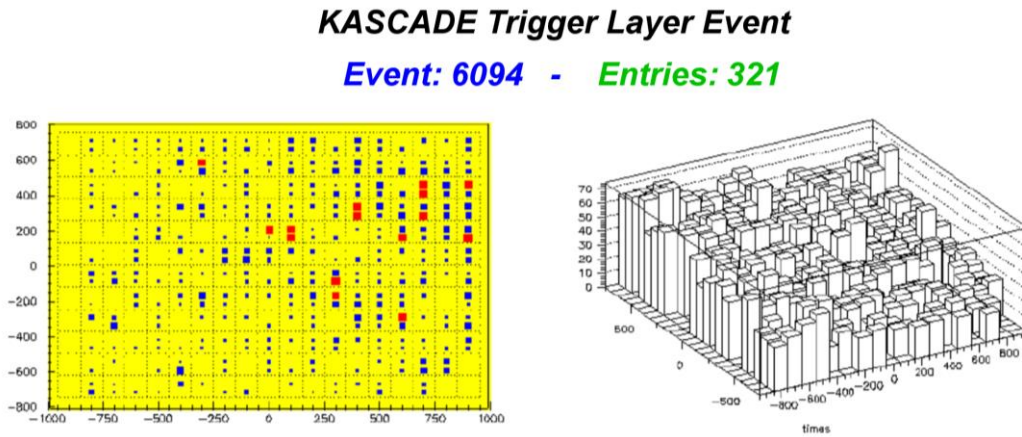
fig. 2.4.7   *Trigger Layer Event: energy deposit (left), arrival time distribution in [ns] (right)*

                           left: energy deposits 2<E<320 MeV (blue); >320MeV (red)

2.4.3   THE MUON CHAMBERS (MWPC)

Two layers of MWPC chambers (16 modules in each layer) are housed below a shielding of 11 nuclear interaction lengths in the basement of the hadron calorimeter. They provide measurements of positions and angles for high energetic muons above an energy threshold of about 2.4 GeV. For unique identification, the multi-wire proportional chambers operate in coincidence with the detectors of the trigger layer.

sensitive area
2 x 122 m²
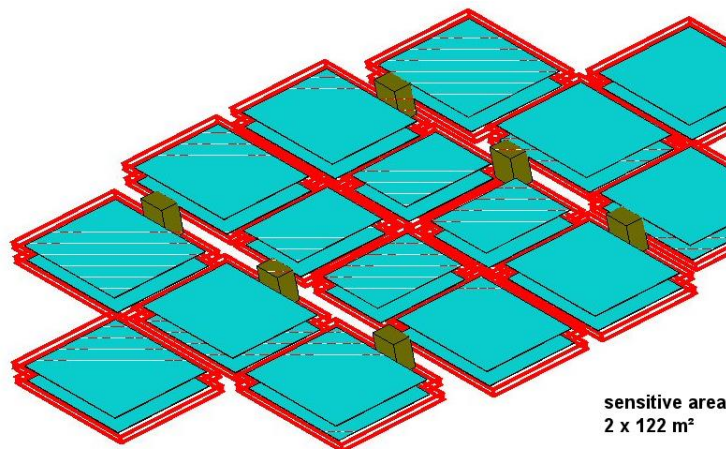
fig. 2.4.8   *Setup of the MWPCs, 32 modules in two layers*

Every chamber contains of three layers of wires and stripes in an 18 mm gas volume. The crossed layers allow estimating the crossing points of penetrating particles in high accuracy (see fig. 2.4.9).
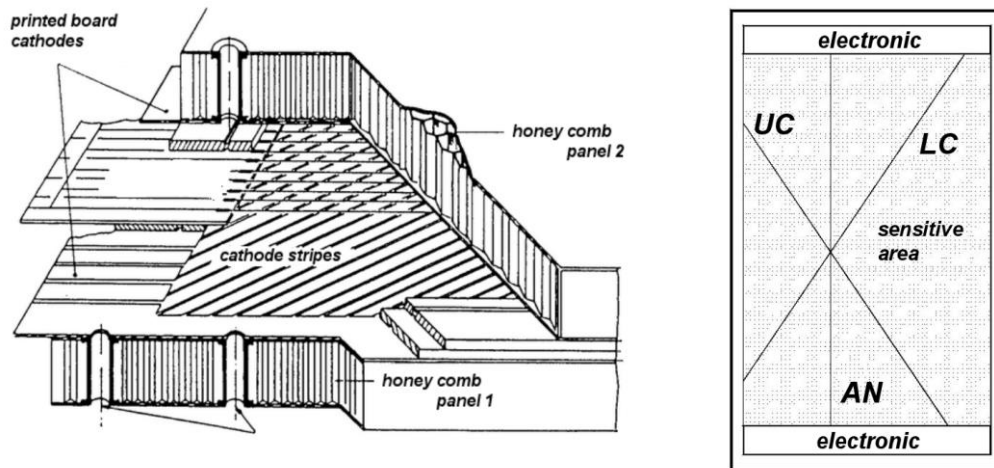
Fig. 2.4.9.   *3 crossed layers in one MWPC module*

2.4.4   THE LIMITED STREAMER TUBES

Underneath the MWPCs was a layer of limited streamer tubes with pad readout installed. This layer was designed to reduce ambiguities at higher densities where the MWPCs saturate (densities > 2 particles per m²), especially near the shower axis. Their arrangement in six rows with 15 modules each is sketched in fig. 2.4.1. As an example of muon detection in the inner part of an extensive air shower, the reconstructed hits are shown in fig. 2.4.10.
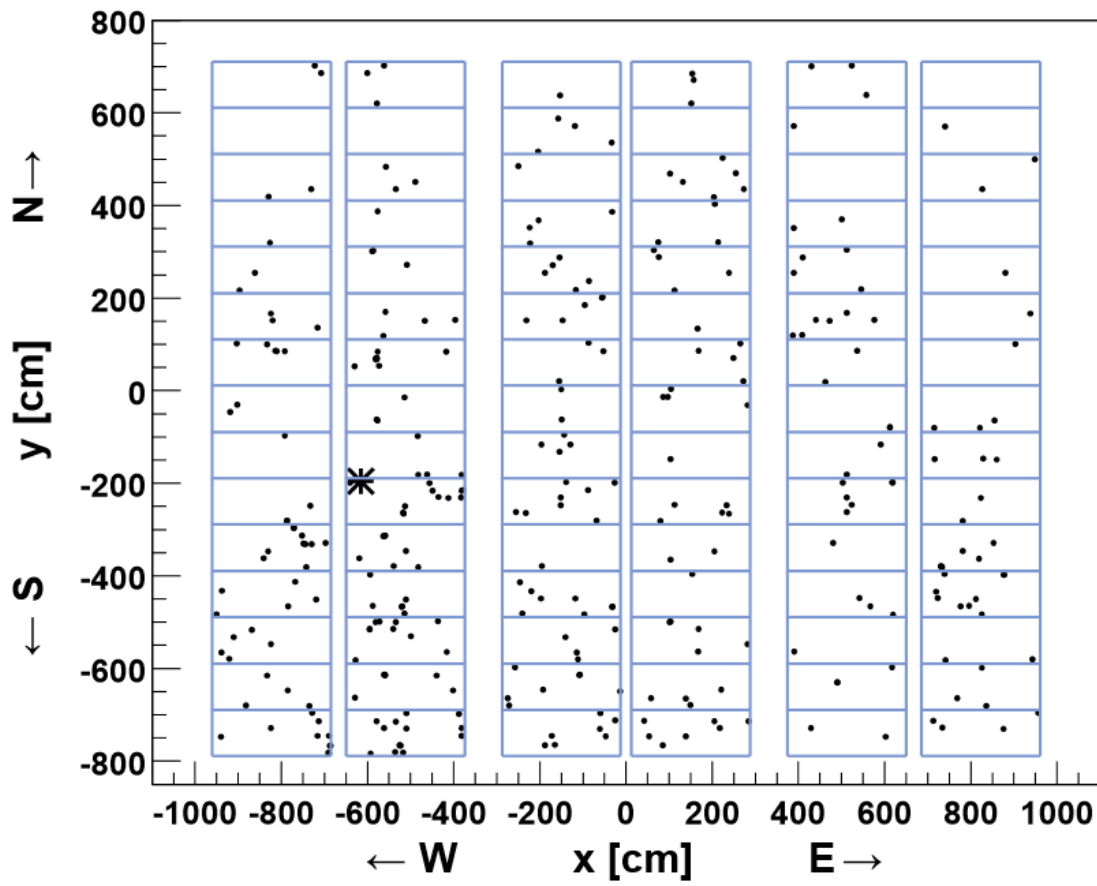
Fig. 2.4.10   *Example of hit distribution in the LSTs. The (∗) marks the shower core as reconstructed by the Array*

2.4.5   THE TOP TRIGGER CLUSTER

The Top Trigger Cluster, located on top the Central Detector, was designed to collect information on the electromagnetic component of an air shower at the location of the Central Detector to complete the measurements from the KASCADE Array. Furthermore, it is used as an independent trigger source on the electromagnetic shower component for the Central detector components. The modules are identical to those used in the Trigger Layer. The Top Trigger Cluster consists of 25 detector modules (50 independent detectors) arranged as shown in fig 2.4.11. The tighter layout in the centre of the Top Trigger Cluster was chosen to lower the threshold to detect smaller showers and to increase the angular resolution. The total active area of the Top Cluster is 22.6m² covering 7.4% of the area of the Central Detector.
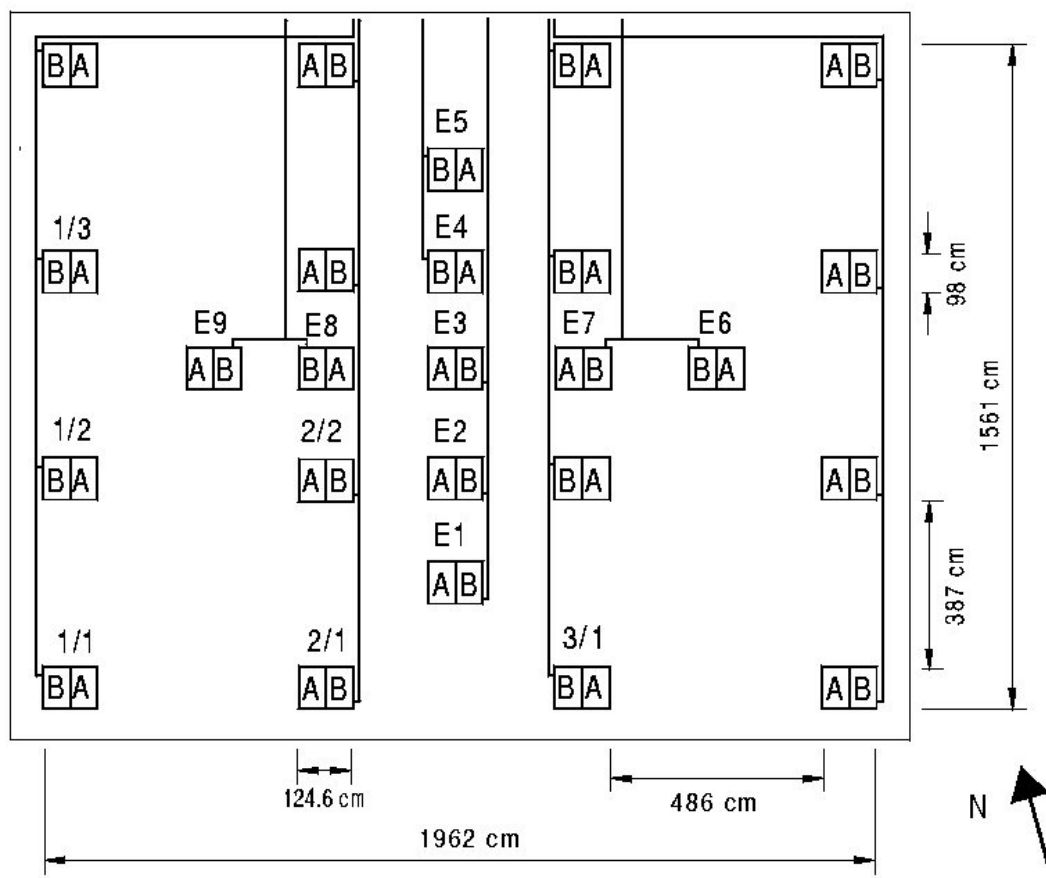
Fig. 2.4.11   *Setup of the Top Trigger Cluster*

2.5   THE MUON TRACKING DETECTOR

The underground tunnel of size 5.5x48 m² houses 3 horizontal layers of limited streamer tubes, each layer covering an area of 128 m². Under a shielding of about 18 radiation lengths concrete, iron and soil, they provide tracking of singles muons with high angular resolution. Additional modules covering the sides of the detector setup increase the solid angle for the detection of inclined tracks (see fig. 2.5.1 & 2.5.2).
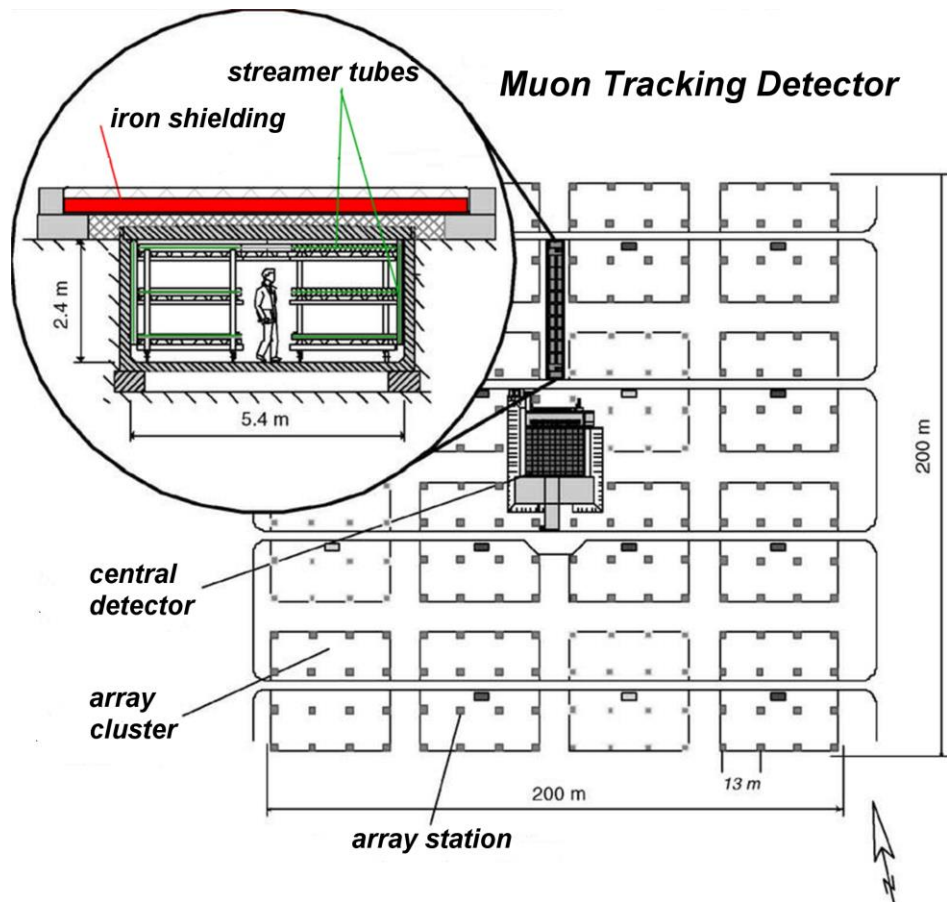
Fig. 2.5.1   *location and setup of MTD*

Due to the high accuracy in the order of 0.5°, the MTD aims, beside others, to measure the production heights of muons by triangulation.
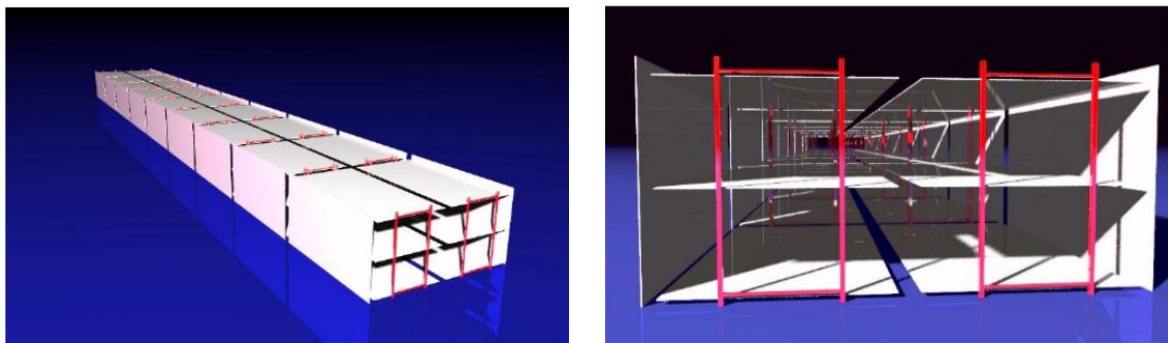
Fig. 2.5.2   *setup of the MTD's streamer tubes*

2.6 THE PICCOLO TRIGGER DETECTOR

The main aim of the Piccolo Array is to provide an external trigger for the KASCADE experiment and the extension KASCADE-Grande. Since the large area of the Grande Array leads to events with large distances to the KASCADE detector, the particle densities become too low to build a local trigger signal using the KASCADE detectors. On the other hand, the delay of the arrival time of the showers, which hit the Grande Array far away from KASCADE, is too big to send the Grande trigger via cable to KASCADE especially for inclined showers. To solve this problem a small scintillator array called PICCOLO has been placed near the centre of the Grande array, used to create a trigger signal, which is sent directly to KASCADE and KASCADE-Grande (see fig. 2.6.1). Piccolo reaches 100% efficiency over nearly the whole area of Grande for all primary particles above 10^{16} eV. Thus, it guarantees full operational efficiency of all the detector components of KASCADE over the Grande area.
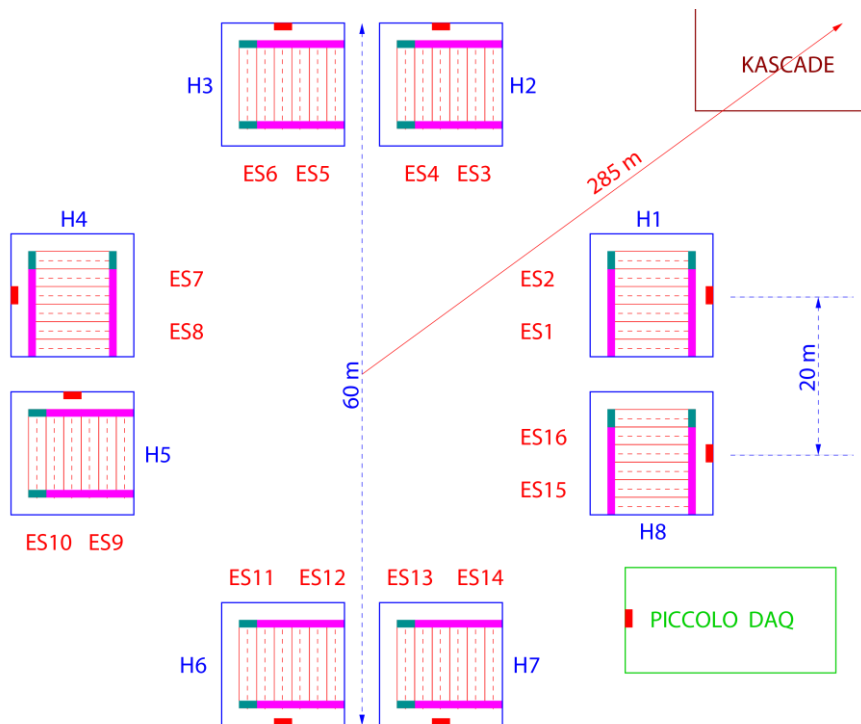
Fig. 2.6.1   *setup of the Piccolo Trigger Array*

2.7 THE LOPES RADIO ANTENNAS

The radio antennas of the LOPES experiment (**LO**far **P**rototyp**E S**tation), distributed over the KASCADE detector array (fig. 2.7.1), are designed to measure the radio emission of cosmic ray air showers in the frequency range from 40 to 80 MHz. In an offline analysis LOPES is using reconstructed parameters provided by the KASCADE-Grande data processing from the particle detectors such as location of the shower core, shower direction, energy deposited in the particle detectors, reconstructed total number of electrons and muons at ground level. Although LOPES data were never part of the KASCADE main data stream, the detectors got a time stamp from the KASCADE clock and a status word was written in the KASCADE event header to indicate that LOPES has received a KASCADE trigger and was recording data for this event.
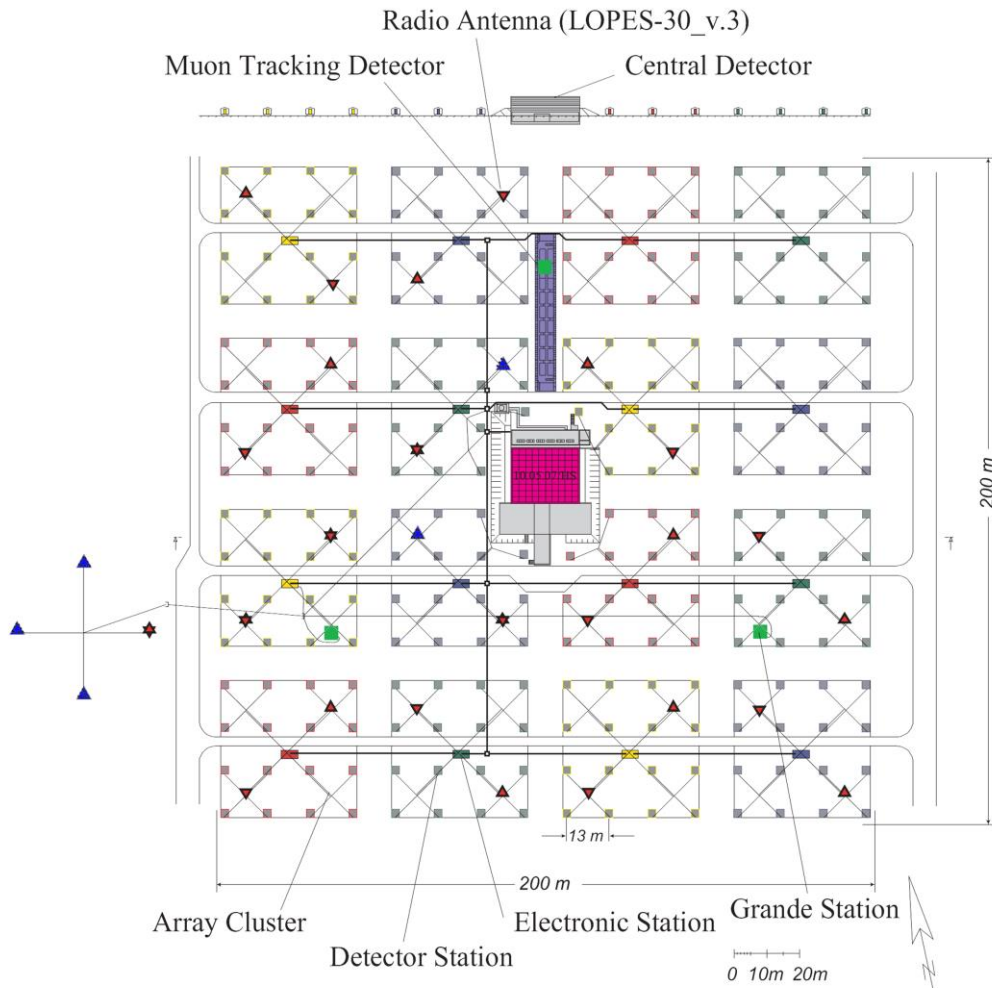
Fig. 2.7.1   *Setup of the LOPES-30 radio detector array. Details see text.*

The Trigger signal sent to LOPES was either from the KASCADE Array a so called '10/16 Array cluster coincidence' activated when 10 out of the 16 Array clusters have recorded signals above the threshold, or a valid GRANDE trigger invoked by one complete GRANDE trigger hexagon. This leads to an energy threshold of 10^{16}eV for LOPES events and to a data rate of about two events/minute. When LOPES receives a trigger signal data from a time interval of 410 µs before and after the trigger signal are recorded.

The capability to digitally form a cross-correlation beam (CC-Beam see Glossary) with the electric field strength traces of all antennas makes LOPES a radio interferometer. A beam is formed by shifting the electric field strength traces of each antenna accordingly to the arrival time of the radio pulse (geometrical delay), in order that the radio pulse of each trace overlaps (fig. 2.7.2a). After shifting the traces, they can either be added in square to form the power beam, or a cross-correlation between them is calculated to form the cross-correlation beam (CC-beam) (fig. 2.7.2b). The cross-correlation amplitude is a measure for the strength of the air shower induced radio pulse. Usually the CC beam is used for the analysis of the LOPES data. It turned out as a useful tool to reconstruct the air shower arrival direction, the primary energy, and mass.
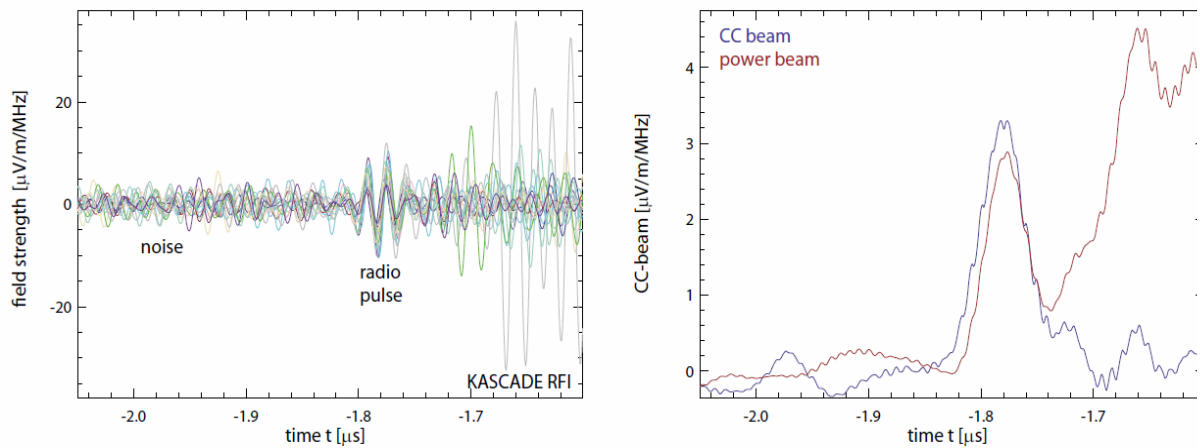
Fig. 2.7.2   *example of a typical LOPES event: electric field strength in individual antennas (different colours) (left) which are calibrated and corrected; cross-correlation and power beam (right).*

In the centre of the LOPES detector area an e-field mill is installed, recording the atmospheric electric field every second. In 'normal' weather conditions these values lie between -100 V/m and -200 V/m. Changes are then slow with a typical time scale of minutes (fig. 2.7.3a). Moving

clouds are noticeable by larger field strengths, but even then the changes are continuous. However, when a thunderstorm occurs, the conditions change quite dramatically. Ground field strength may exceed ± 20 kV/m (fig. 2.7.3b). In addition, lightenings are visible as discontinuities in the recorded data. The size and direction of the jumps depends on the location and type of discharge. From the field strength and the occurrence of jumps, thunderstorms can be detected reliably and automatically. They have to be excluded in normal radio data analyses.
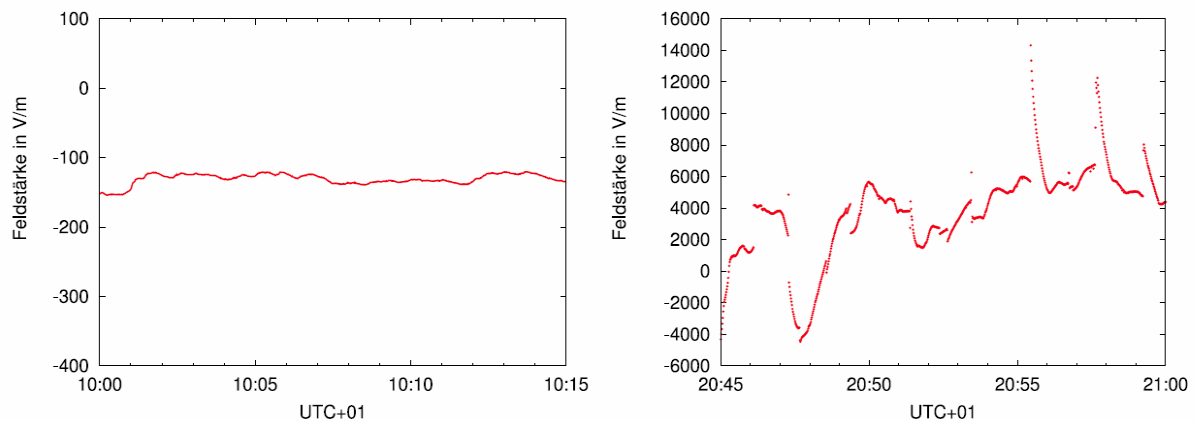
Fig. 2.7.3   *example of an e-filed mill measurement;*

left: during fair weather; right: during a thunderstorm

In KCDC we publish radio data from the LOPES-30 experiment in the time range 2.12.2005 to 26.10.2009. During this time the setup of the radio antennas was changed a few times. In the beginning, all 30 antennas were aligned in East-Western direction indicated by the blue and red triangles in fig. 2.7.1. In 2006 half of the antennas have been rotated to North-South alignment ('LOPES-30 Dual') to allow the measurement of the complete electric field vector. Red triangles pointing upwards indicate East-West alignment, pointing downwards means North-South alignment. Five antennas were equipped with both N-S and E-W. Stations indicated by the blue triangles have been dismantled when switching to the 'LOPES-30 Dual' setup. Details of the changes are outlined in appendix C.3.

2.8   LOCATION OF KASCADE AND THE KSACADE COORDINATE SYSTEM

KASCADE is located at 49.099436°N, 8.437485°E (centre of KASCADE) on site of the KIT, Campus North (the former Forschungszentrum Karlsruhe) at 110m a.s.l, corresponding to an average atmospheric depth of 1022g/cm^2.

The regular orientation of the KASCADE Array has an offset of about +15° towards East against the real northern direction (fig 2.8.1.), caused by the fact that the conditions of the location allows only this orientation. This offset is corrected for in the data analysis.

The zenith angle is measured against the vertical direction, which means that θ=0° is pointing upwards and 90° denotes a horizontal shower. The azimuth is defined as an angle measured clockwise starting in real northern direction (90° is east).
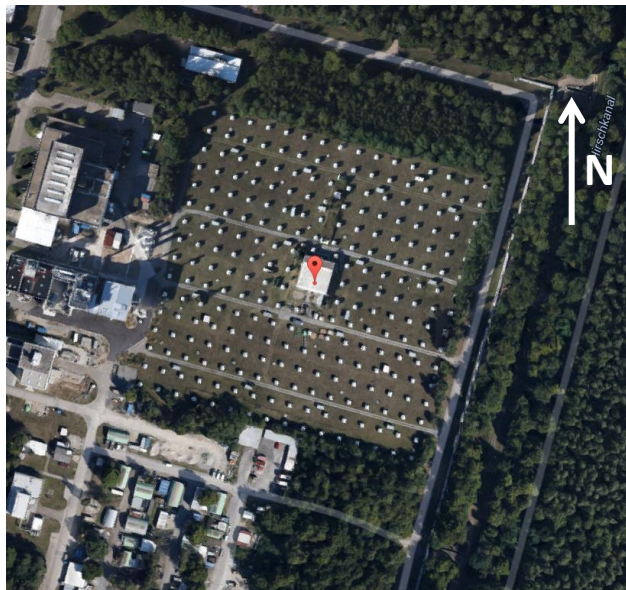
Fig. 2.8.1   *Location of KASCADE array*

2.9   ACTIVE TIME OF THE DETECTOR COMPONENTS

The 10 different detector components of the KASCADE Grande Experiment were most of the nearly 20 years of operation not working at the same time. Fig. 2.9.1 shows their 'active time'. The solid lines denote the 'active time', dashed lines denote their installation stages. The table below gives a more detailed overview of the active times of the various components.

Some Components of the Central Detector like Hadron Calorimeter, Trigger Layer and Top Trigger Cluster were switched off in 2005 after having collected enough data to perform high quality analysis. At the end of 2009 the Muon Tracking Detector switched to stand-alone mode which means that the data recorded were no longer included in the KASCADE-Grande main data stream. Thus, the events recorded have to be merged offline with the KASCADE-Grande events.
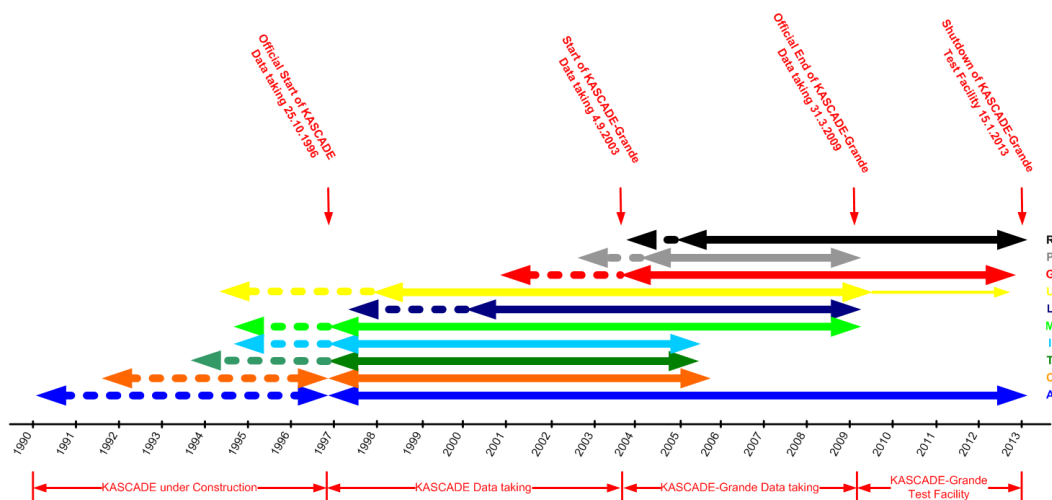
Fig. 2.9.1   *Schedule of the ‚active times' of the various detector components of KASCADE-Grande*

A: KASCADE Detector Array (blue)   *C: Hadron Calorimeter (orange)*

T: Trigger Layer (green)   *I: Top Trigger Cluster (light blue)*

M: Muon Chambers (light green)   *L: Limited Streamer Tubes (dark blue)*

U: Muon Tracking Detector (yellow)   *G: KASCADE-Grande Array (red)*

P: Piccolo Trigger Detector (grey)   *R: LOPES Radio Antennas (black)*

Detector Component	First Run	First Event Time	Last Run	Last Event Time
ARRAY (A)	282	25.10.1996; 15:19 UTC	7417	15.1.2013; 9:40 UTC
MWPC (M)	282	25.10.1996; 15:19 UTC	6691	31.3.2009; 13:07 UTC
Trigger (T)	282	25.10.1996; 15:19 UTC	5448	5.8.2005; 1.38 UTC
Top Cluster (I)	282	25.10.1996; 15:19 UTC	5418	4.7.2005; 7:15 UTC
Calorimeter (C)	282	25.10.1996; 15:19 UTC	5496	12.10.2005; 11:20 UTC
MTD (U)	637	26.11.1997; 15:27 UTC	6731	3.6.2009; 12:25 UTC
LST (L)	2364	1.3.2000; 15.26 UTC	6691	31.3.2009; 13:07 UTC
Grande (G)	4685	20.12.2003; 3:40 UTC	7407	5.11.2012; 10:14 UTC
Piccolo (P)	4753	26.2.2004; 13:54 UTC	6691	31.3.2009; 13:07 UTC
LOPES (R)	5530	28.11.20054; 9:47 UTC	7417	15.1.2013; 9:40 UTC

3 DATA ACQUISITION AND EVENT BUILDING

Each of the various components of the KASCADE-Grande detector system is an independent experiment with its own data acquisition and control system. Part of each system is besides the control and monitoring of the hardware, the preparation of the data recorded and the transmission to the Central Event Builder (EVB). The main task of the Central Event Builder is to merge time information and the recorded data of all running detector components and to transfer it to a mass storage system.

3.1 KASCADE GRANDE TRIGGERS

3.1.1 TRIGGER SOURCES

Five detector components were designed to serve as trigger sources. The **KASCADE Array [A]** as a fast trigger for all components, the **Trigger Layer [T]** as trigger source mainly for the detector components inside the Central Detector, the **Top Trigger Cluster [I]** triggering on very small showers which hit the central detector, the **Piccolo Array [P]** for showers far away from the KASCADE Array and the **Grande Array [G]**. Fig. 3.1.1 is a schematic view of the various trigger sources and the trigger signal directions.
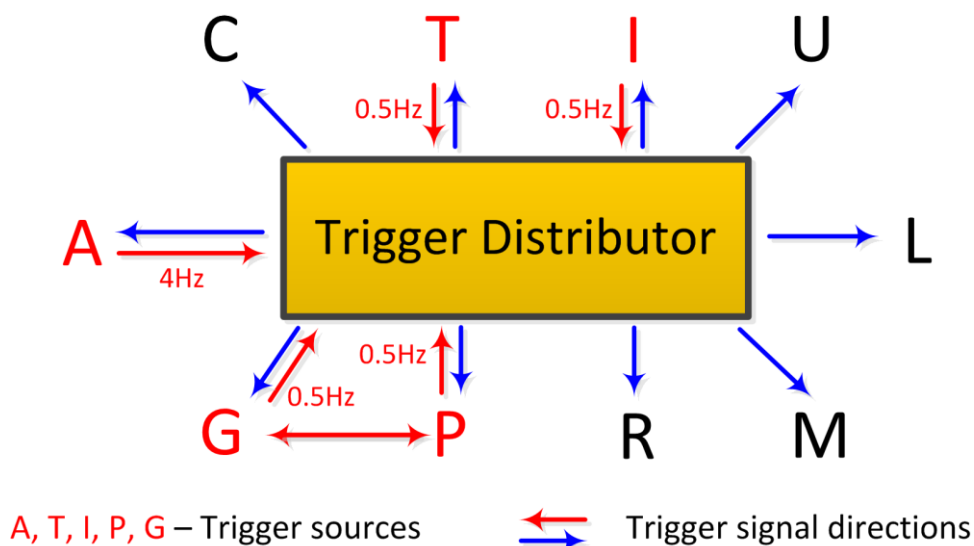
Fig. 3.1.1 *Scheme of the sources and distribution of the trigger signals in KASCADE*

3.1.2 TRIGGER CONDITIONS AND TRIGGER THRESHOLDS

The conditions to generate a trigger are defined in the local processes of the detector components without any control by the Event Builder. Most of the components have defined '*internal triggers'* which differ from the conditions building the signal sent to the Trigger Distributor. These '*internal triggers'* are used for monitoring and test purposes and were normally not sent to the Trigger Distributor. Their data are not included in the KASCADE main data stream merged by the Event Builder. Only the signals transmitted to the Trigger Distributor are accepted for the data acquisition.

Heart of the trigger generation and trigger distribution in KASCADE is the so call 'Distributor Box' where trigger signals from various sources are processed and fed through the outputs to all detector components simultaneously.

For the **KASCADE Array** the trigger condition was generated from the '*Cluster Triggers'* which were set differently for the inner 4 and the outer 12 clusters (details see chapter 2.2). In the inner four clusters, where each of the 15 stations is equipped with 4 e/γ-detectors, the condition is set to 20/60 detectors, while in the outer 12 clusters, where each of the 16 stations is equipped with only 2 e/γ-detectors, the condition is set to 10/32 detectors corresponding to an energy deposits per station of about 8 MeV. If, within a time window of 400ns, this condition is fulfilled in one the 16 clusters, a trigger signal is sent to the central Trigger Distributor. The trigger rate is about 4 Hz.

The resulting thresholds of the measurements is a few times 10^{14} eV, depending on the zenith angle and the primary mass. The upper limit of the experiment is defined by the size of the detector array to roughly 10^{17} eV. In most events the array trigger is accompanied by a muon multiplicity trigger from the Trigger Layer or the Top Trigger Cluster of the Central Detector.

For the **Trigger Layer** the trigger conditions are either a multiplicity trigger of at least 8 fired scintillators out of the 456 modules ('*Muon Trigger'*) or one firing detector with a large energy deposit ('*Single Hadron Trigger'*). The threshold for the '*Muon Trigger'* corresponds to 30% MIP (Minimum Ionising Particle, see Glossary). The threshold for the '*Single Hadron Trigger'* , used to study the flux spectrum of unaccompanied high-energy hadrons was set to 50*MIP resulting in a rate of about 0.5 Hz.

The 37 stations of the **Grande Array** are organized in 18 overlapping trigger clusters (see fig. 2.3.3). Each cluster includes seven detector stations, six in a hexagonal shape and a central one. A trigger signal is generated and transmitted to the Trigger Distributor if all stations from one of the 18 clusters have recorded data above the threshold of 3 MeV (7/7 coincidence). The Grande trigger rate is about 0.5 Hz.

For the **Top Trigger Cluster** the multiplicity trigger condition was set to 10 modules out of 50 designed to read out the whole experiment in case of low energy central shower events.

For the **PICCOLO Trigger Array** the trigger condition is 2 out of 8 stations. The low level processing applied ensures a fast distribution of the trigger signal to all the detector components. Piccolo reaches 100% efficiency over nearly the whole area of Grande for all primary particles above 10^{16} eV.

3.2   EVENT BUILDING

To correlate the data from different parts of KASCADE, event building is based on two common clock signals, a 1Hz signal derived from a GPS/DCF77 clock system and a 5 MHz signal generated locally. These two signals are distributed to all detector components where the 1Hz Clock serves as a common reset for the 5MHz clocks in all components. The clock synchronisation of the detector components is done online by the central event builder (EVB). From the first 10 events of each run the time offset of each detector component is calculated and stored. This offset is then added by the EVB to the time stamp received with the data packages.

If a detector is triggered, either by its own or by an external trigger, it transfers the data from the local readout processors to the central workstation together with an associated local time label. For this purpose, a private network is installed where each component opens a socket to send data to the Central Event Builder. There the data blocks are stored in chained lists sorted by detectors and the offset corrected time. Data from different components within a time window of 8μs are considered as part of the same event. When the Grande array was introduced in 2003 this event time had to be increased to 12μs taking into account the 6μs integration time of Grande. After the merging, the data are written to a mass storage device

in the CERN ZEBRA bank structure. This data structure can be read by the KRETA data analysis program.

If one running detector component does not send any data packages for more than 120 sec the respective component is marked as 'dead' and the event builder is starting a new run without it.

During its operation time from 25.10.1996 until 15.1.2013 the KASCADE/KASCADE-Grande experiment has recorded 1.76 billion events on 54,910 files, a total data volume of about 20 TB (including LOPES). Not all detector components were running the whole time except the KASCADE array. The Grande array started operation in the end of 2003 and took data up to final experiment shutdown.

Apart from a very rough online inspection, all data are analysed offline using the data reconstruction program KRETA (**K**ASCADE **R**econstruction of **E**x**T**ensive **A**ir showers).

Radio LOPES data have not been included in the KASCADE data stream because of the huge amount of data stored. The data sets have been merged offline.

4   KASCADE DATA IN KCDC

The measured air showers in KASCADE are analysed using the reconstruction program KRETA (*Kascade Reconstruction for ExTensive Airshowers*), which reads the raw data, performs the calibration and reconstructs the basic shower observables, storing all the results in the form of histograms and vectors of parameters (ntuples).

The reconstruction procedure starts after the calibration phase and develops internally over three levels using an iterative process to come to the final results.

From about 200 observables obtained in the analysis we choose 15 in a first release to be published in KCDC which could be selected and applied cuts via the KCDC Data Shop as **Quantities**. The number of measured and reconstructed Quantities published in with release NABOO is 29 including the newly added detector component GRANDE. Adding the radio **LOPES** detector component with the release OCEANUS has almost doubled the number of quantities.

Based on data generation and data handling we distinguish between:

Measuring Data

    Corresponding to data which are directly measured or reconstructed by the KASCADE analysis software like core positions and angles.

Calibration Data

    Used to calibrate the data sets on an event-by-event basis like air temperature and air pressure.

Event Information

    Used to characterise an event uniquely like run number and event time.

Quantity	Description	Unit	ID
Measuring Data			
Energy	first order reconstructed Energy	eV	E

Quantity	Description	Unit	ID
Core Position X	location of the reconstructed shower core x-position	m	Xc
Core Position Y	location of the reconstructed shower core y-position	m	Yc
Zenith Angle	reconstructed zenith angle with respect to the vertical	° (degree)	Ze
Azimuth Angle	reconstructed azimuth angle with respect to the north	° (degree)	Az
Electron Number	reconstructed number of electrons (fit)	(number of)	Ne
Muon Number	reconstructed number of Muons (fit)	(number of)	Nmu
Age	Shower shape parameter		Age
e/γ - energy deposits	Energy deposit in MeV / station	(MeV)	EDeposit
μ - energy deposits	Energy Deposit in MeV / station	(MeV)	MDeposit
Arrival Times	Arrival Times / station	ns	Arrival
Calibration Data			
Air Temperature	temperature on site at event time	°C	T
Air Pressure	air pressure on site at event time	hPa	P
Event Information			
Run Number	internal KASCADE counting number	(number of)	R
Event Number	internal KASCADE counting number	(number of)	Ev
Event Date	event date	UTC	Datetime
Global Time	event date time in seconds since 1.1.1970	s	GT
Micro Time	event time in 200 ns steps	(number of)	M

Quantity	Description	Unit	ID
UUID	Universally Unique IDentifier		*UUID*

The plots schown in this chapter are only examples, mostly based on a subsample of the data sets published. So, applying user cuts either in the KCDC Data Shop or in your own analysis can change these spectra drastically.

4.1   ENERGY (E)

One of the main goals of the air shower measurement is to determine the energy spectrum of the cosmic rays. Due to uncertainties in the hadronic interactions and the huge fluctuations in the shower size, this determination of energy and mass is rather challenging. In KASCADE, we measure the electromagnetic and muonic components of air showers separately. By using both observables, we perform a transformation matrix in order to convert the number of electrons and muons to the energy of primary particles taking into account the angle of incidence. The parameters of the formula of the energy estimator are derived from extensive air shower simulations.

4.1.1   MEASURED DATA

Each detector station of the KASCADE array is equipped with e/γ-detectors, which is a liquid scintillator with a height of 5 cm, for the measurements of the electromagnetic components (charged particles). The e/γ-detector reaches its full efficiency at $lgN_e > 4.25$, with a strong decrease for small showers.

The outer detector stations of the array are additionally equipped with muon detectors underneath an absorber of 10 cm lead and 4 cm iron. The efficiency of the muon detector is related to the e/γ-detectors, because the trigger as well as the shower parameters like the shower centre are determined by the e/γ-detectors.

From the measurements we derive the number of charged particles for each of the 252 detector stations separately. The number of muons is taken for each of the 192 outer detector stations. If the shower core is inside the KASACDE array (and not too close to the

border), one can fit a function to the charged particles and muons separately. Due to saturation and punch through μ-detector stations within a radius of 40m around the reconstructed shower core are not taken into account. The area underneath this so-called LDF (Lateral Density Function) is a measure for the number of charged particles and Muons. Subtracting the two curves and integrating leaves the number of Electrons (N_e). These two parameters are the basic input to the Energy Estimator.

4.1.2 SIMULATED DATA

For the air shower simulations the CORSIKA program (**CO**smic **R**ay **SI**mulation for **KA**SCADE) has been used by applying the hadronic interaction model of QGSjet-II-02 (Quark-Gluon-String Model, version II-2) for laboratory energies above 200GeV. The low energy model Fluka 2002_4 has been used for energies below 200 GeV. All particles have been tracked down to the observation level at 110 m.a.s.l. The output of CORSIKA was fed into the detector simulation program CRES (**C**osmic **R**ay **E**vent **S**imulation) where the response of all detector components is taken into account by using the the CERN GEANT3 package. The predicted observables at ground level, such as the number of electrons and muons are then compared to the measurements. Showers of five different mass groups indicated by five different primaries (*p*, *He*, *O*, *Si* and *Fe*) have been simulated. The simulations cover the energy range of $1·10^{14}$ to $3·10^{18}$ eV with zenith angles in the interval 0° - 42°. The spectral index in the simulations was -2 to safe time and then corrected for the real spectral index of the cosmic rays to -2.7. For details please refer to the "KCDC Simulations Manual".

For the Parametrisation, the air showers are divided into two zenith angel ranges, from 0° to 18° and from 18° to 25°. Both angular bins have the same acceptance. The selected data between $E = 10^6 GeV$ and $E = 3.2 \cdot 10^9 GeV$ are divided in 15 logarithmical equidistant energy intervals, where the mean values e/γ- and μ -distributions are determined.

4.1.3 FORMULA FOR ENERGY ESTIMATOR

Primary energy function as reconstructed by KASCADE by means of air shower simulations done with the simulation models *QGSjet-II-02 (above E$_{lab}$=200GeV)* and *Fluka 2002_4 (below E$_{lab}$ =200 GeV)*.

atmospheric depth at KASCADE level (110 m.a.s.l.)

D=(-186.5562)+(1222.6562)*exp(-110.*100./994186.38)
xatte = 158.0
xattm = 823.0

transform to average sizes for vertical showers 0-18 deg

dwb1 = (D/cos(theta_rad)) - (D*1.025)
$\lg(N_e) = \lg(N_e) + (dwb1/xatte/\log(10.))$
$\lg(N_\mu) = \lg(N_\mu) + (dwb1/xattm/\log(10.))$

$\lg(E/eV) = 1.93499 + 0.25788*\lg(N_e) + 0.66704*\lg(N_\mu) + 0.07507*\lg(N_e)^2 + 0.09277*\lg(N_\mu)^2 - 0.16131*\lg(N_e)*\lg(N_\mu)$

The spectrum of the reconstructed energy of the primary particle is shown in Fig. 4.1.1.
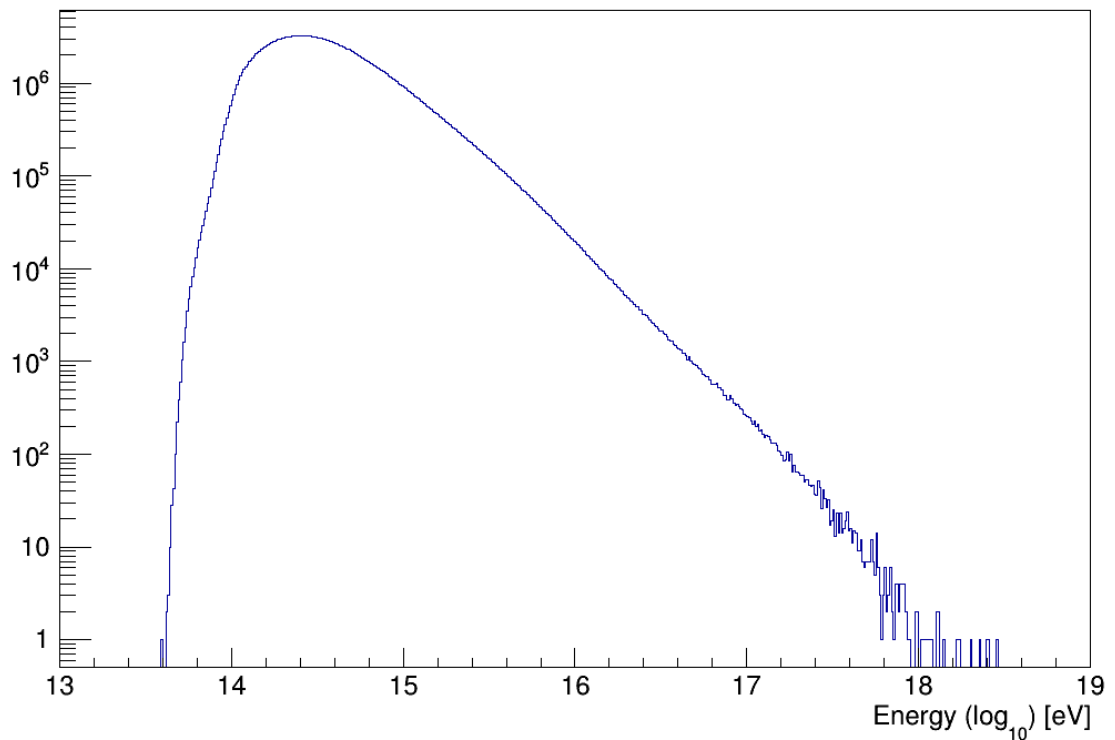
Fig. 4.1.1   *The reconstructed energy spectrum in log-log scale*

The table below illustrates the strong dependency of the number of remaining events from the cuts applied on the Quantity ‚*Energy*' for the events published in MERIDIAN.

Energy Cut	Nr of Events remaining
E > 1.0*10^{13}	147,979,836
E > 5.0*10^{13}	143,125,811
E > 1.0*10^{14}	140,752,178
E > 5.0*10^{14}	39,618,180
E > 1.0*10^{15}	14,231,390
E > 5.0*10^{15}	906,980
E > 1.0*10^{16}	239,611
E > 5.0*10^{16}	11,487
E > 1.0*10^{17}	3,017
E > 5.0*10^{17}	82

4.2   NUMBER OF ELECTRONS AND NUMBER OF MUONS (NE, NMU)

In KASCADE, the energy deposits of electrons and muons at ground level are measured, as well as their arrival time. From these measurements, the arrival direction of the shower, its impact point on ground (shower core) and the total number of electrons and muons in the shower, i.e. the electron and muon shower sizes are reconstructed. Reconstruction is performed in three so-called levels.

4.2.1   LEVEL 1

A station classification is performed to identify the properly operating stations and the very first estimation of the shower core and arrival direction is carried out.

In the first step, the shower core is determined by using a neural network and the shower direction by using a gradient method with the arrival times of the first particles in the detector stations. With an empirical formula, the numbers of electrons and muons are

first approximated. The parameters obtained from the first step give starting values for the next reconstruction level.

4.2.2 LEVEL 2

The total number of charged particles in the shower is obtained through the fit of lateral distribution to the energy deposits and the shower axis is conclusively determined, as well as the muon size for the KASCADE array. In the next level, the measured energy deposits are corrected with the Lateral Energy Correction Functions (LECF) and converted to particle densities. In the e/γ and μ detectors, electrons and muons as well as other particles are registered.

To take into account the contribution of these particles, the LECF is required, which is obtained by Monte Carlo simulations. It describes the energy deposits of different particles in the detector as a function of the distance to the shower core. In KASCADE, there are four different LECFs: two of them are for the energy deposits of the muons in the e/γ and μ detectors, and two others for the energy deposits of electrons, e/γ and hadrons in both detectors.

The reconstruction of the shower direction is improved as well in this level. The shower direction, which gives the best transformation of the measured arrival times into the shower plain, is obtained by a χ^2 minimisation and a parametrisation.

With the improved information on the shower direction and the particle densities, the lateral distribution is determined by using a modified NKG function. The modified NKG function is given by

$$\varrho_{e,\mu}(r) = C(s) \cdot N_{e,\mu} \left(\frac{r}{r_m^{e,\mu}}\right)^{s-\alpha} \left(1 + \frac{r}{r_m^{e,\mu}}\right)^{s-\beta}$$

with

$$C(s) = \frac{\Gamma(\beta - s)}{2\pi r_m^2 \Gamma(s - \alpha + 2)(\alpha + \beta - 2s)}$$

The shower core, the electron number N_e and the age parameter s of the electron lateral distribution are simultaneously determined, whereas the muon number N_μ is a free parameter. The Moliere radii r_m as well as α and β and for both electrons and muons are estimated by Monte Carlo simulation, which are r_m = 89 m and 420 m for electrons and muons, respectively.

4.2.3   LEVEL 3

In the last level, the electron shower size is estimated. The energy deposits are calculated again by using the LECF and the improved shower direction and shower core from Level 2. With this improved information, the performance of the shower reconstruction is repeated. After that, the NKG function is applied to the lateral distributions of electrons and muons.

The electron number is determined by taking into account the number of muons from Level 2 and by correcting for the contribution of muons in the e/γ detectors, while the number of muons is the same as in Level 2.

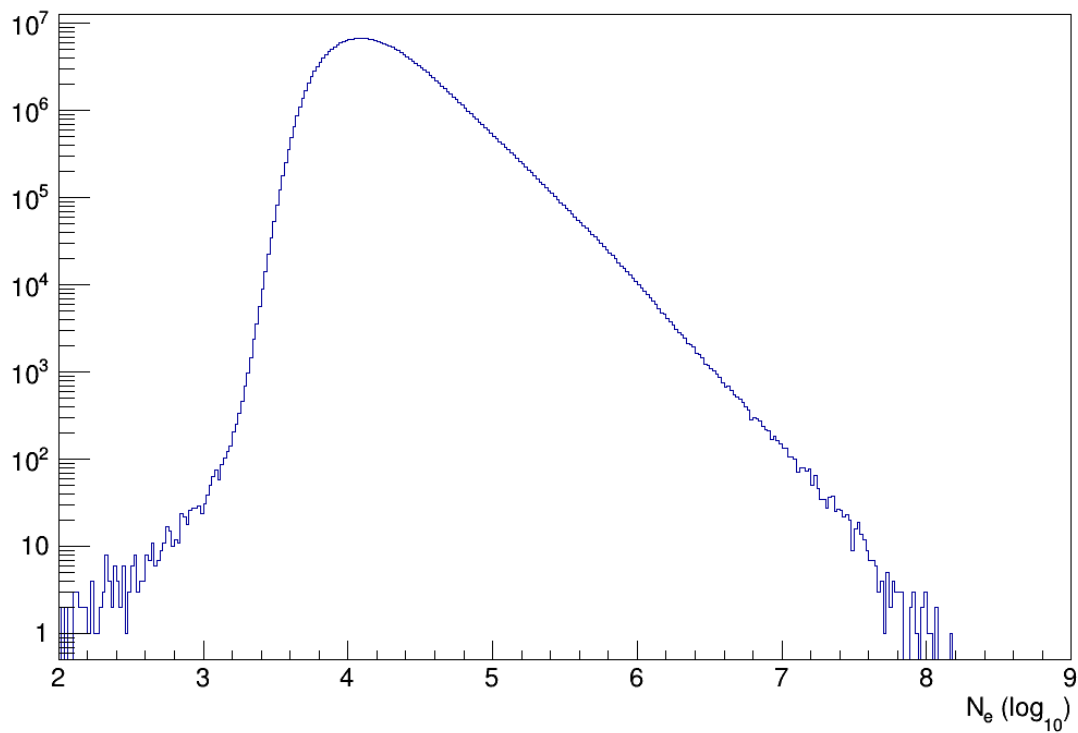Fig. 4.2.1   *The spectrum of the number of electrons*

Figures 4.2.1 and 4.2.2 show the N_e and N_μ distributions in a log-log scale. The structure clearly visible in the N_μ spectrum at low energies is an artefact for low muon numbers close to the threshold.
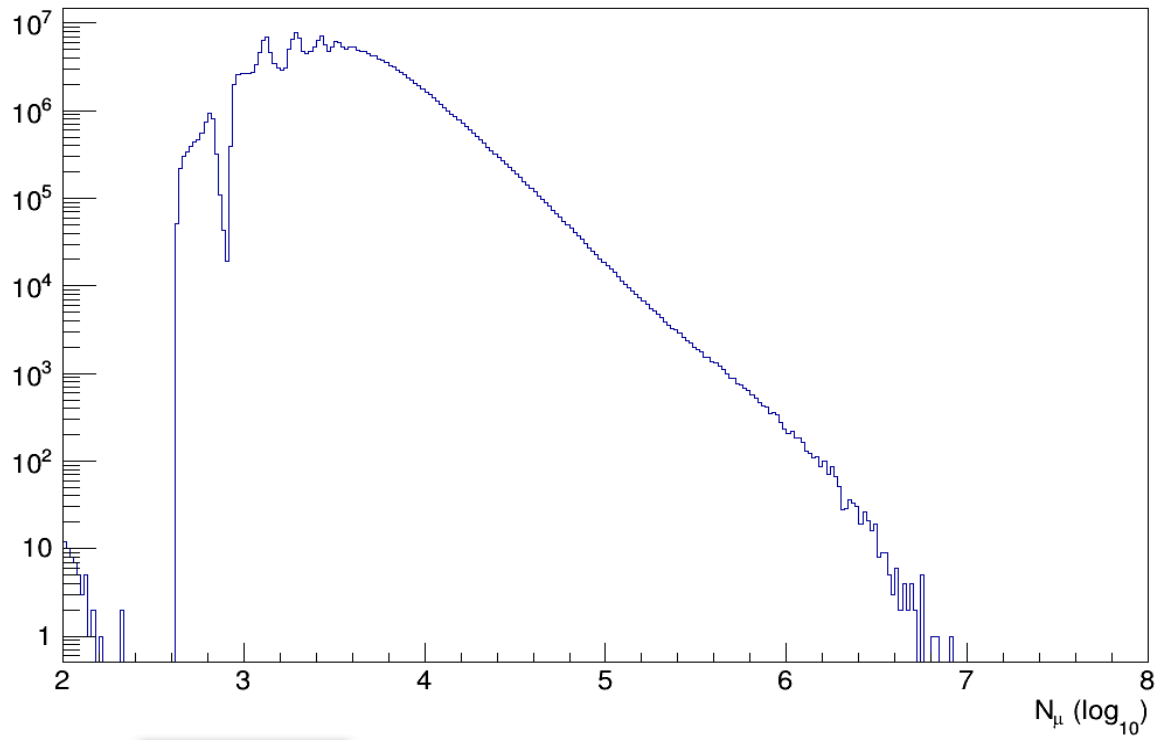

Fig. 4.2.2　　　*The spectrum of the number of muons*

Fig. 4.2.3 shows the $lgN_\mu - lgN_e$ distribution measured by KASCADE.
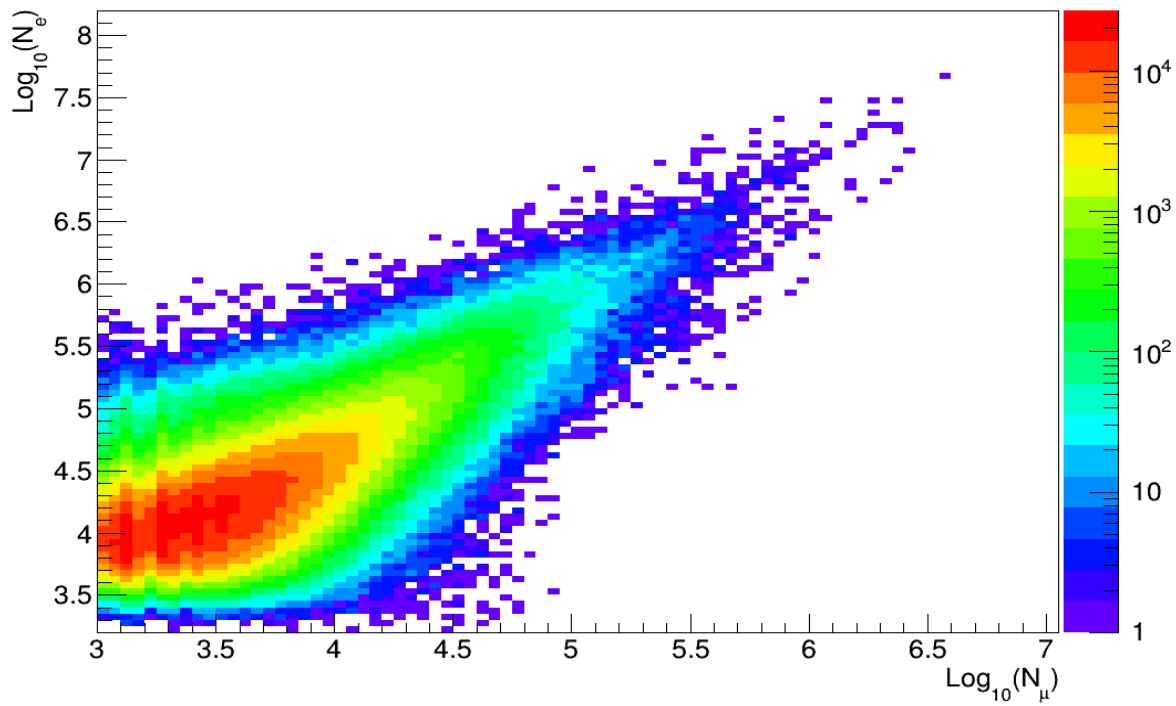
Fig. 4.2.3   *$lgN_\mu - lgN_e$ distribution measured by KASCADE*

4.3   AGE (AGE)

Contrary to variables like number of electrons N_e or number of muons N_μ, the value of the age parameter has no absolute meaning, as it depends on the choice of the lateral distribution function, which is fitted, to the shower data. It may also be called **lateral shape parameter** because it describes the steepness of the lateral electron density distribution. KASCADE uses a modified NKG-function to fit the lateral shower shape. Within this function, the age parameter values are limited theoretically to a range from 0.1 to 1.48. Common shower values however range from 0.6 to 1.3. Lower values describe steeper lateral distributions.

The shape (steepness) of the lateral density distribution of a given shower depends on the energy of the primary particle, as well as on its nature. The higher the shower energy, the steeper the lateral distribution. A heavy primary particle with the same energy as a light one gives rise to a flatter lateral distribution, as the shower starts earlier in the atmosphere. When reaching ground, the shower is "older", which gives the age parameter its name. The age parameter therefore may help (in combination with number of electrons) to distinguish between primary particles of different mass.

Fig. 4.3.1 shows the distribution of the Age parameter within its valid range.
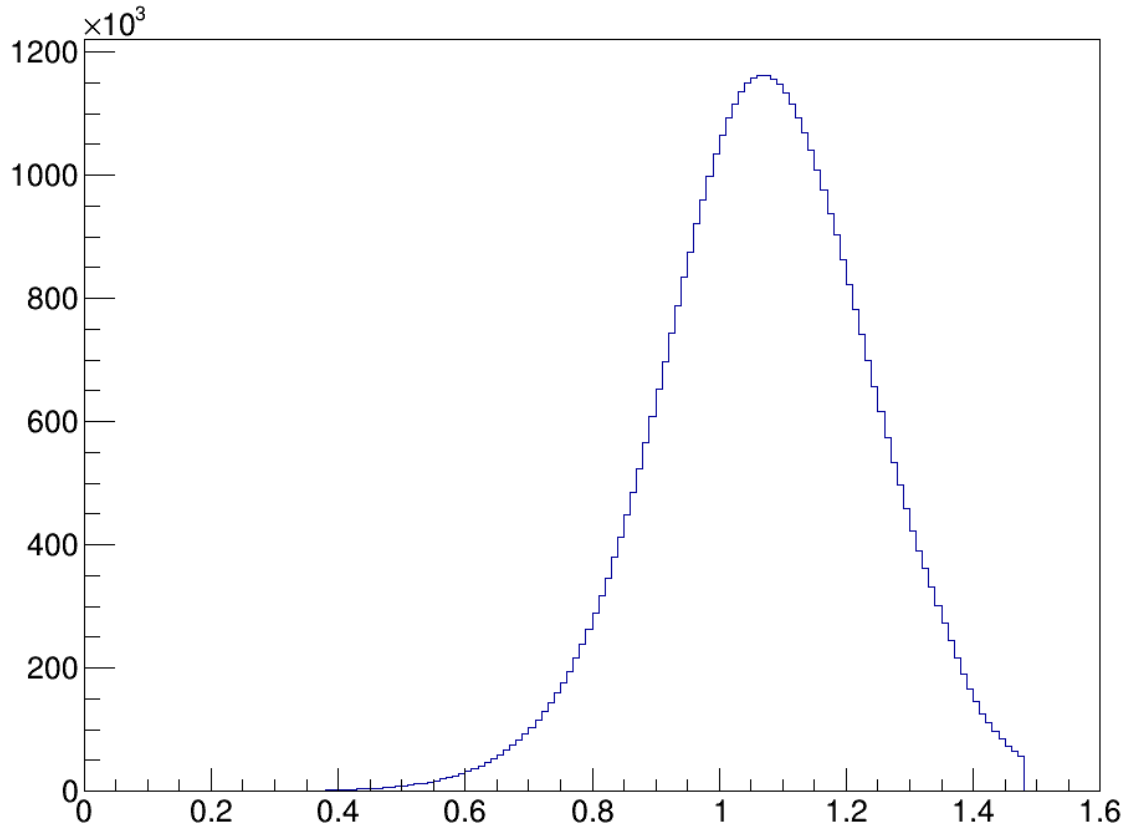
Fig. 4.3.1   *The AGE distribution from the modified NKG function for reconstructed showers.*

4.4   SHOWER CORE POSITION (XC, YC)

The Core Position is the reconstructed location of the shower centre at KASCADE level derived from the energy deposits of each detector station of one event. The unit of the core position is [m].

For the reconstruction of the core position in the KASCADE array basically the particle densities in every detector station are taken. By means of an *neural network algorithm* which combines high efficiency for the identification of the shower core with good rejection capability for showers that fall outside the fiducial area, the core can be determined to a precission of about 1m. In addition, this method offers a simple approach to identify events with subcores.
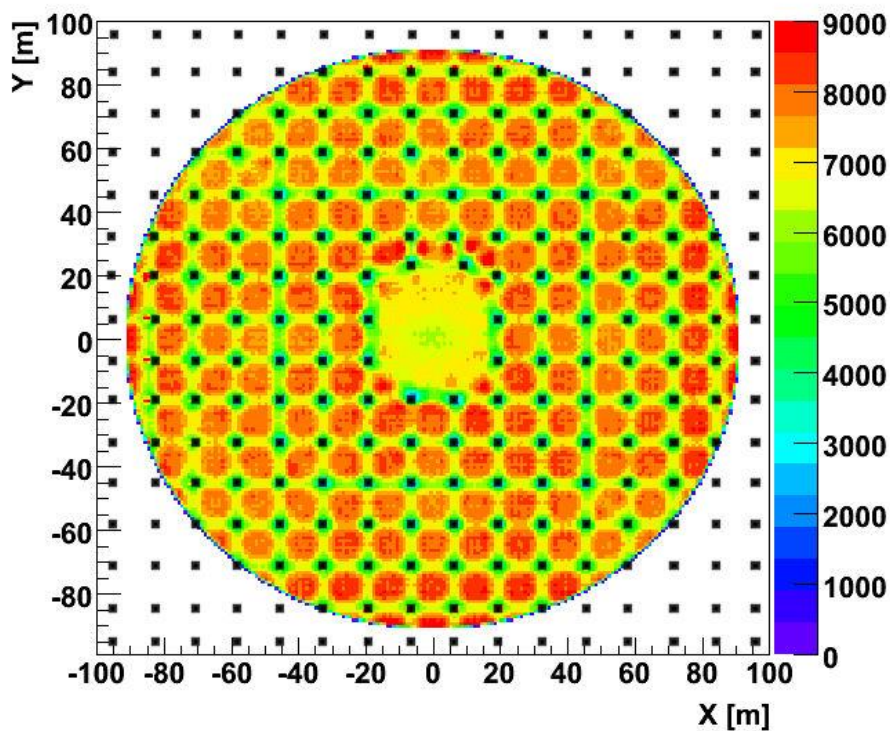
Fig. 4.4.1   *Shower core distribution with KASCADE array detector stations*

The distribution of the shower core is plotted in the fig. 4.4.1. Extensive air showers with a core position outside the detector area have a great probability for beeing incorrectly reconstructed. Therefore, only showers with a maximum core distance less than 91 m radius from the centre of the detector area are taken into account which reduces the fuducial area by about 35%.

The regular structure in the above picture is caused by an artefact in the reconstruction algorithm, which causes the centre of the shower core to be drawn between the stations with the highest measured energy deposits, which is usually between four neighbouring stations. For low energies the reconstruction algorithm draws the centre of the shower core towards the stations with the highest measured energy deposit. In the centre of the array the Central Calorimeter is located, thus four stations are missing. The two detector stations north of the Central Calorimeter are a little dislocated because of the main building.

4.5   SHOWER DIRECTION (ZE, AZ)

In KASCADE coordinates, the zenith angle is measured against the vertical direction, which means that θ=0° is pointing upwards and 90° denotes a horizontal shower. The azimuth is defined as an angle measured clockwise starting in northern direction (90° is east). The regular orientation of the KASCADE Array has an offset of about +15° against the real northern direction, caused by the fact that the conditions of the location (KIT, Campus North) allows only this orientation. This offset is corrected for in the data analysis. The unit of the azimuth and zenith angles is [°].

The KASCADE detectors measure the arrival times and the energy deposits of air shower particles, so that the shower directions are determined by evaluating the arrival times of the first particle in each detector station and the total particle number per station.

To calculate this shower centre the differences in the arrival times of the shower particles of the array stations are used. After an individual time calibration of all stations where delay times and cable properties and electronics including the PMTs are taken into account, the differences of the times compared to the signal of the first station arriving at the central data acquisition are taken. To increase the accuracy, the energy deposits are taken into account when the direction of the shower disk is calculated.

In the first level of the reconstruction, the shower direction is estimated by a gradient method. This method is very fast and works without a minimisation procedure. It can deliver good starting values for the following reconstruction levels.

More detailed:

With a square root of the energy deposit $\sqrt{E}$, the weighted gradients $\frac{d_t}{d_x}$ and $\frac{d_t}{d_y}$ were filled in a histogram over each other. The gradient with the most entries from the channel was used to determine the shower direction. The angular resolution with these methods is 0.3 ° up to 1 ° depending on the shower energy. This is to account for the probability of an early particle at low densities.

In the second and third reconstruction levels, the shower direction is determined by the fitting of the function to the lateral distribution of the time signals. The form of the function has a significant effect on the size of the statistic and systematic errors of the estimated values. In the standard reconstruction of KASCADE, the fitting of the arrival time is performed with a conical surface, i.e. the shower disk is not flat but a spherical segment.

The angular resolution drops significantly above about $\theta > 40$ °, caused by the fact that the reconstruction algorithm has been fine-tuned to zenith angles below 40°. Even though the published data sets include events with zenith angles up to 60°, the KASCADE collaboration has set limits in their analysis to 40°. This restriction reduces the number of analysed showers by about 5%.

In figure 4.5.1 the distributions of the azimuth angle is shown.
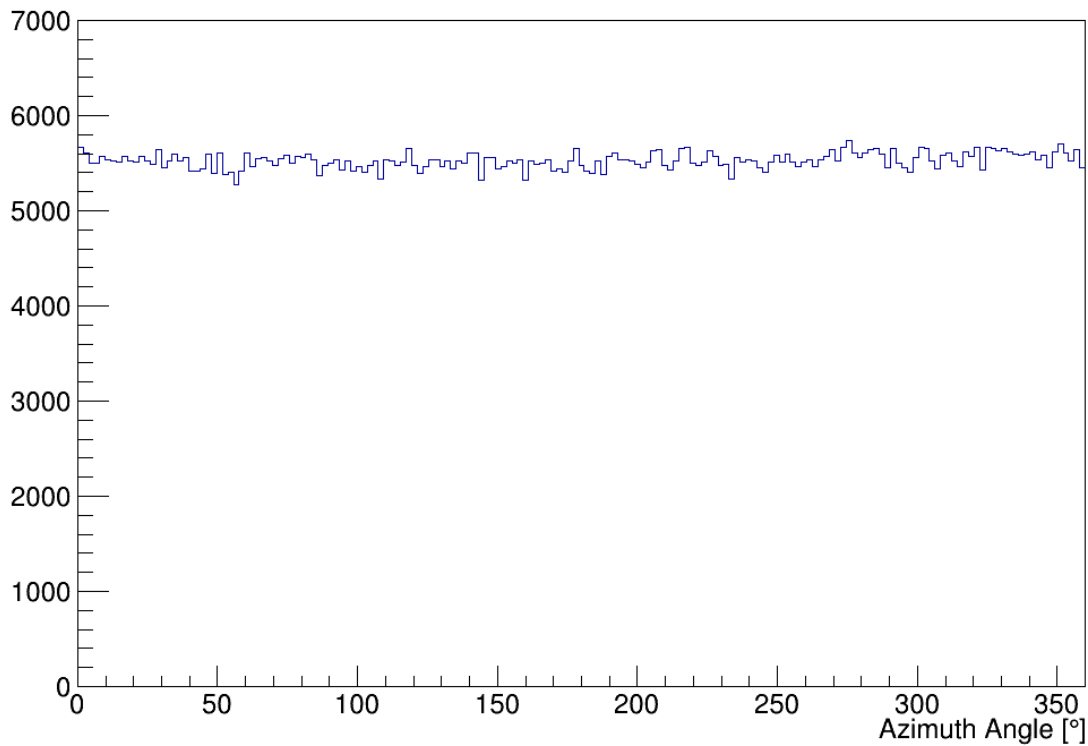

Fig. 4.5.1   *The distribution of the reconstructed azimuth angle*

The distribution of the zenith angle shown if fig 4.5.2 indicates that the loss of events above 60° is negligible.
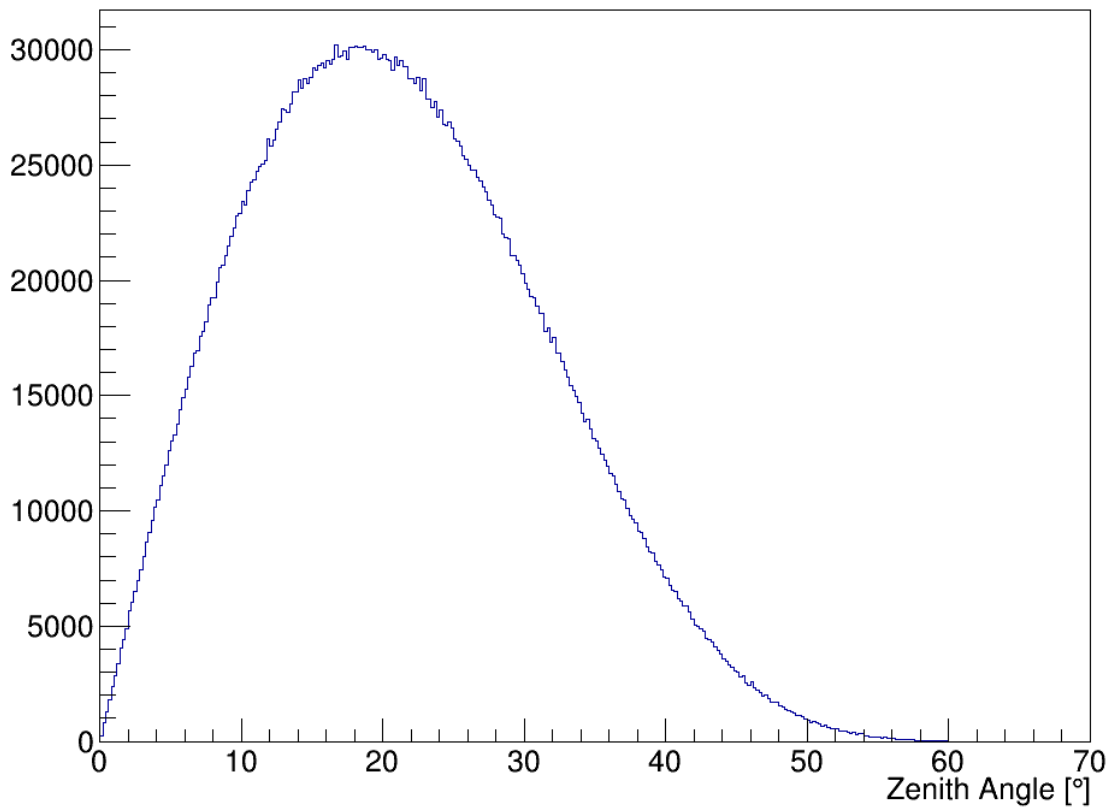
Fig. 4.5.2   *The distribution of the reconstructed zenith angle*

4.6   ENERGY DEPOSITS PER STATION (EDEPOSIT, MDEPOSIT)

The publication of the energy deposits offers a new quality of KCDC to perform analysis with the KASCADE data. Available are the energy deposits of each single detector station independently measured in the e/γ- and in the μ-detectors.

In a former KCDC release MERIDIAN we published the particle densities/station, normalised to track length and effective detector area, which is different for the two types of KASCADE array detector stations.

We decided to switch to energy deposits because we think that it makes more sense to publish a measured value than a corrected one. This offers the users the unique possibility to build their own Lateral Energy Correction Function (LECF) to recalculate the densities/station by just knowing the angle of incidence (Ze) and the effective detector area (see 4.6.1.4) besides the deposited energy.

A detector station has to fulfil several conditions to be treated as 'active detector station' in the sense that their energy deposits (EDeposit) and their muon energy deposit (MDeposit) values are provided.

- the station was flagged as 'active'
- no overflow was detected in the station
- the station was not deselected for various reasons

Active detector stations which had no signal above the threshold are as well taken into account. No energy value of these 'silent' stations is given, just the station ID (EDepositS) is stored.

Note: on the quantities 'Energy Deposit' no cuts can be applied

Note: in chapter 8.4 are examples on how to handle the quantity 'Energy Deposit'

4.6.1   E/γ – ENERGY DEPOSITS

Handling the **'e/γ Energy Deposits'** quantity mostly requires some additional information either on the absolute coordinates of the detector station or on the distance to the reconstructed shower core. Therefore, the quantity **EDepositS** is always supplied with the energy values. Furthermore, the number of detector stations with valid energy deposit information (**EDepositN**) is provided as well.

Thus, if the quantity '**e/γ Energy Deposit'** is selected in the KCDC DataShop you will always be supplied with the following data sets:

EDepositN	number of active e/γ-detector stations with energy deposit ≥ 0
EDeposit	energy deposit per station in MeV
EDepositS	detector station ID [1...252]

4.6.1.1.   Number of active e/γ-detector stations (EDepositN)

The range of active e/γ-detector stations stored in **EDepositN** is between 1 and 252. The distribution for **EDepositN** is shown in Fig. 4.6.1. The lower limit is given by the selection condition that at most 2 array clusters (32 stations) may be missing in the respective event. As there may be more single stations flagged as '*inactive'* the number can be below 220. The peak structure is caused by the cluster geometry of the KASCADE array (see chapter 2.2) i.e. the probability that a whole cluster is missing.

Note: only active stations are used for further analysis and shown in the plot.

Note: This value is always shipped if the 'e/γ Energy Deposit' Quantity is selected but only in root and hdf5 files not in ASCII.
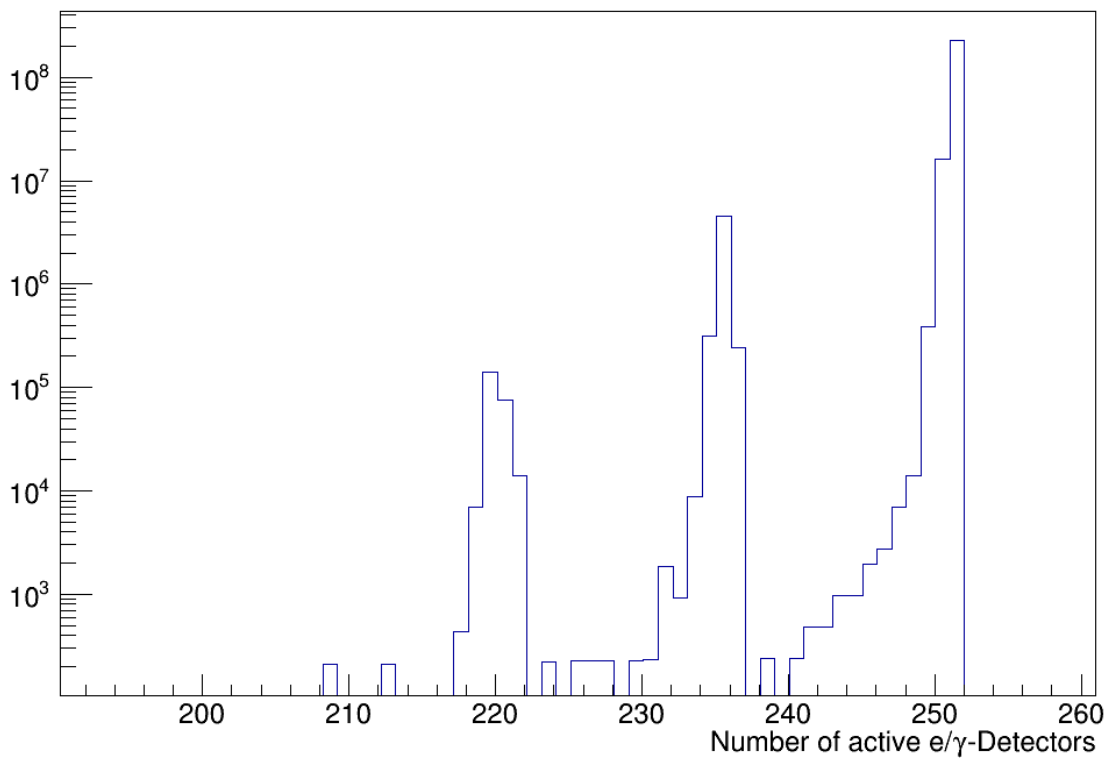

fig. 4.6.1   *Distribution of the number of active e/γ –detector stations*

4.6.1.2.   Number of e/γ-detector stations with hits

The distribution of the number of **e/γ**-detectors with *EDeposit>0* in this event is given in fig 4.6.2.
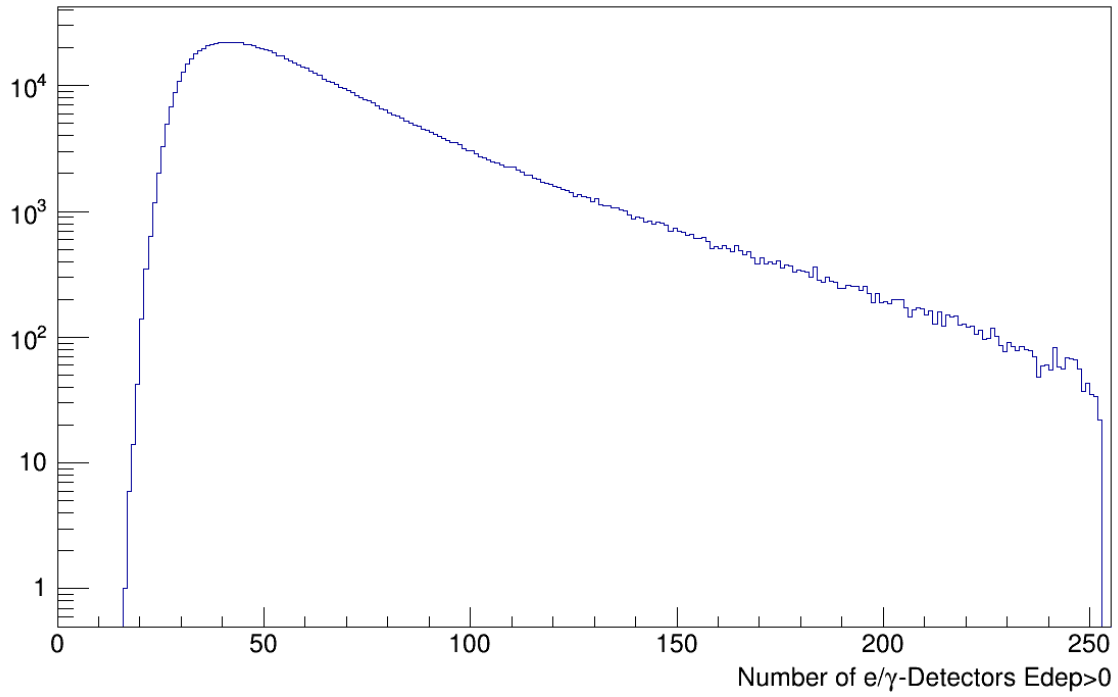
fig. 4.6.2   *Distribution of the number of e/γ –detector stations with hits*

4.6.1.3.   e/γ Energy Deposit for each detector station (EDeposit)

The Energy deposits are derived from the stored ADC values for each detector station by means of a calibration procedure where the influences of electronics and cabling are included. EDeposit values are given in MeV. In fig 4.6.3 the energy deposits for a subsample of KASCADE data are plotted.
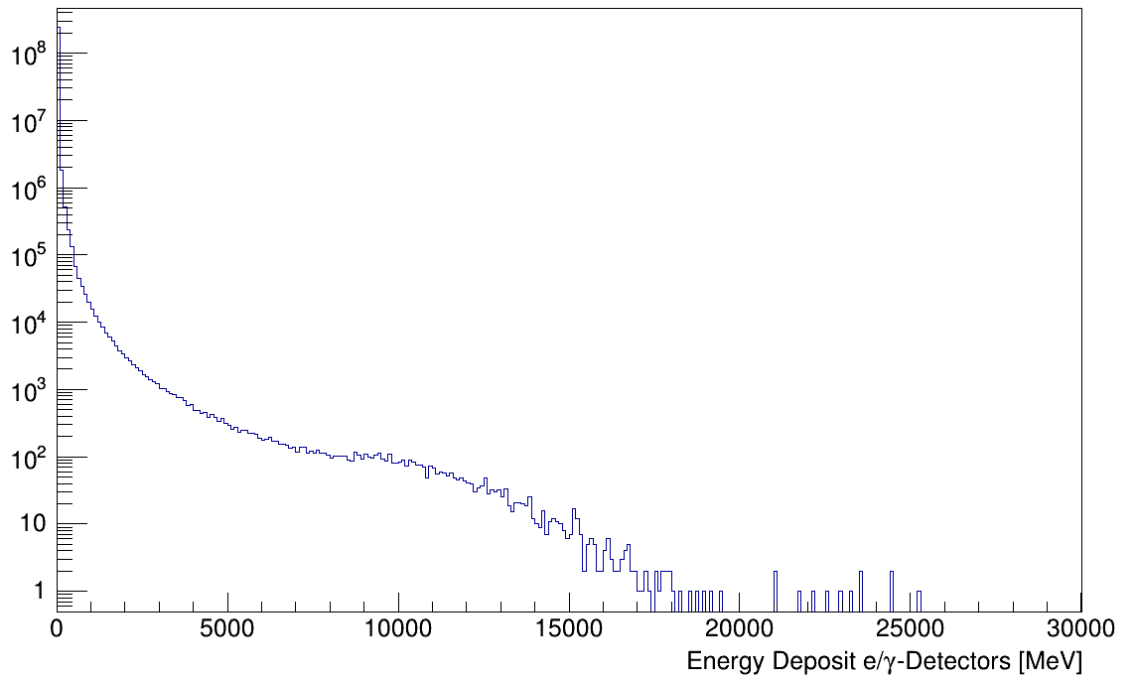
fig. 4.6.3   *Distribution of the calibrated e/γ –Energy Deposits of all active stations*

4.6.1.4.   Station ID (EDepositS)

The station ID holds the information of the location of the respective detector station. The transformation from the station ID to the true detector position in KASCADE coordinates of the respective Array detector station is described in chapter 8.4 and Appendix A.

Fig 4.6.4 shows the distribution of station IDs of the active e/γ-detector stations. The steps in the otherwise very flat spectrum indicate that one station or a whole cluster (16 stations) were missing for some time.

Note: This value is always shipped if the 'e/γ Energy Deposit' Quantity is selected but only in root and hdf5 files not in ASCII.
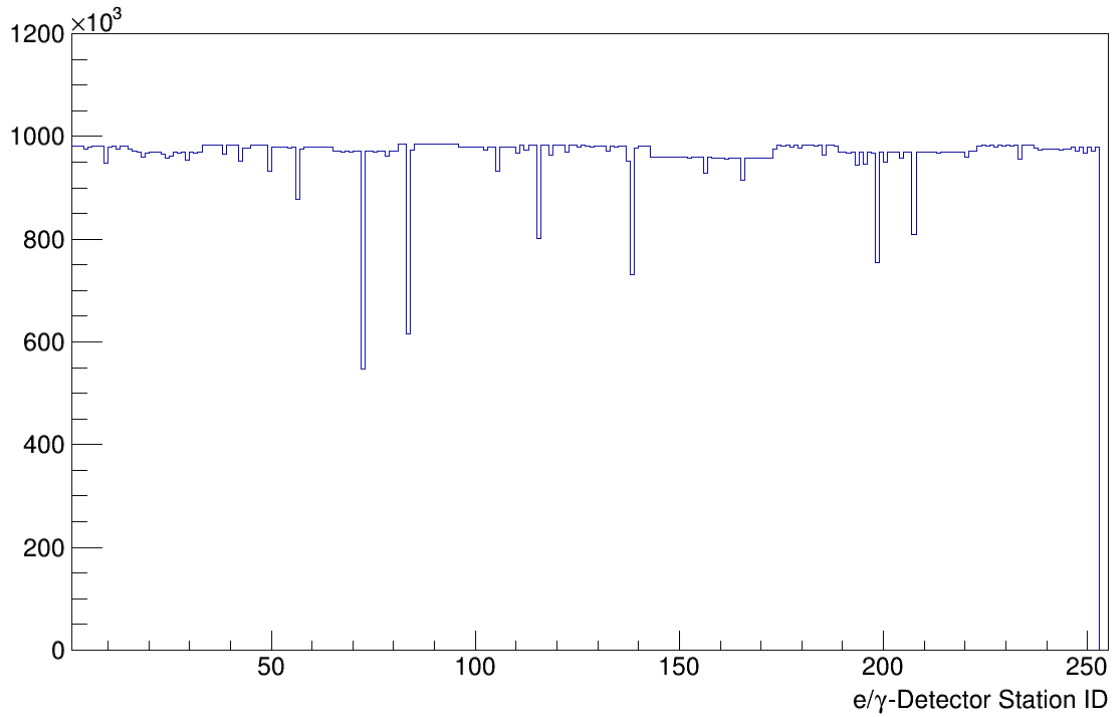
Fig. 4.6.4   *Distribution of station IDs for active e/γ-detector stations*

For further studies the effective e/γ –detector area for a given station can be derived from the station ID. As described in chapter 2.2 two different detector setups are realised in the KASCADE array. The inner 4 clusters consist of only 15 stations, (the 16th position is blocked by the Central Calorimeter) and are equipped with 4 liquid scintillator cones with an effective area of 3.14m² to measure the shower core. The outer 12 cluster have two liquid scintillation e/γ-detectors with an effective area of 1.57m² (see fig. 4.6.5). The table below shows the correlation between station ID and effective detector area.

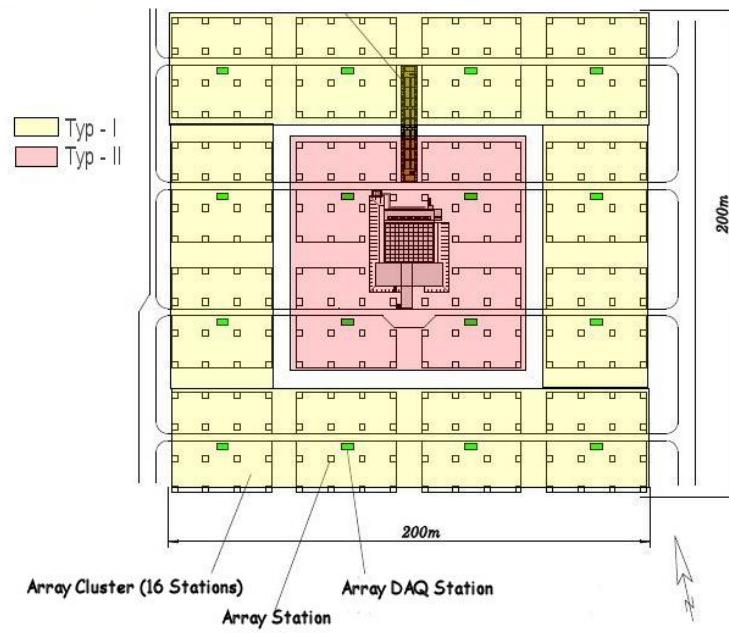| Station ID	Area [m²]	Area Code
1 - 80	1.57	0
81 – 110	3.14	1
111 – 142	1.57	0
143 – 172	3.14	1
173 – 252	1.57	0

Fig. 4.6.5   *Array setup, schematic view of the KASCADE detector array*

yellow: two e/γ-detectors ,1.57m² ; red: four e/γ-detectors, 3.14m² per station;

4.6.1.5.   Distance to shower core

The distance from the e/γ –detector station to the reconstructed shower core can be cal-culated from the station ID **EDepositS** and the shower core coordinates Xc and Yc. The structure in the distribution in fig 4.6.6 clearly visible around the maximum of the distance to the shower core distribution is caused by the reconstruction algorithm which 'draws' the reconstructed shower core between the stations with the highest energy deposits measured. The spacing of 13m of the detector stations is mapped here (see also fig. 4.4.1). The structures diminish with increasing cut on energy.
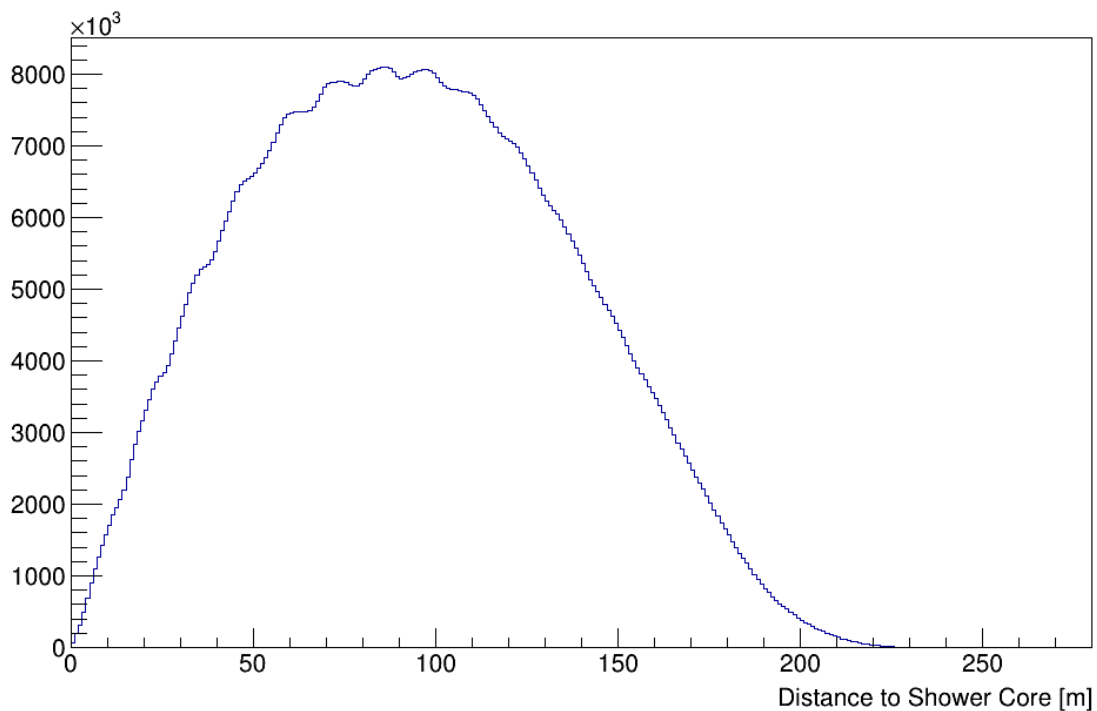
fig. 4.6.6   *Distribution of the distances to the shower core of the e/γ –detector stations*

4.6.2   MUON – ENERGY DEPOSITS

Handling the '**Muon Energy Deposits'** quantity mostly requires some additional infor-
mation either on the absolute coordinates of the detector station or on the distance to
the reconstructed shower core. Therefore, the quantity **MDepositS** is always supplied
with the Energy Deposit values. Furthermore, the number of detector stations with valid
energy information (**MDepositN**) is provided as well.

Thus, if the quantity **'Muon Energy Deposit' ('MDeposit')** is selected in the KCDC
DataShop you will always be supplied the following data sets:

MDepositN   number of active μ-detector stations with energy deposit ≥ 0

MDeposit   muon energy deposit per station in MeV

MDepositS   detector station ID

4.6.2.1   Number of active µ-detector stations (MDepositN)

The range of **MDepositN** is between ca. 1 and 192. The distribution for **MDepositN** is given in Fig. 4.6.7. The lower limit is given by the selection condition that at most 2 array clusters (32 stations) may be missing in the respective event. As there may be more single stations flagged as '*inactive*' the number can be below 160. Furthermore, µ-detectors within a radius of 40m around the reconstructed shower core are not used because of the saturation and the punch through which cannot be estimated accurately and thus not cor-rected for.
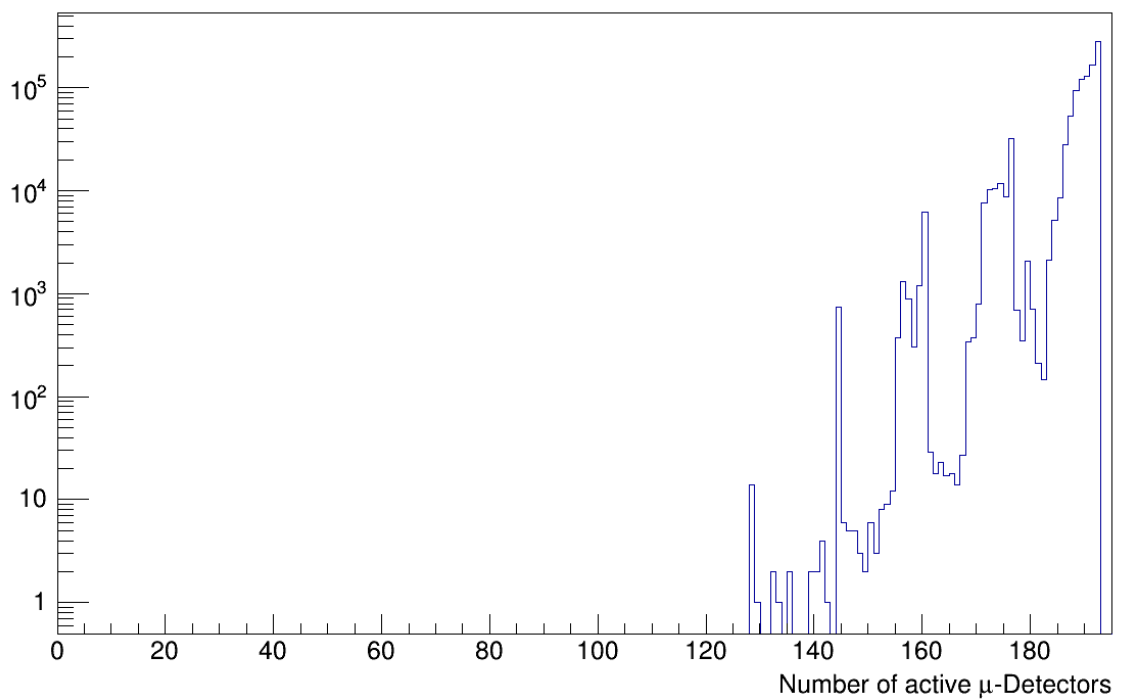

fig. 4.6.7   Distribution of the number of active µ–detector stations

Note: This value is always shipped if the 'Muon Energy Deposit' Quantity is selected but only in root and hdf5 files not in ASCII.

4.6.2.2 Number of μ-detector stations with hits

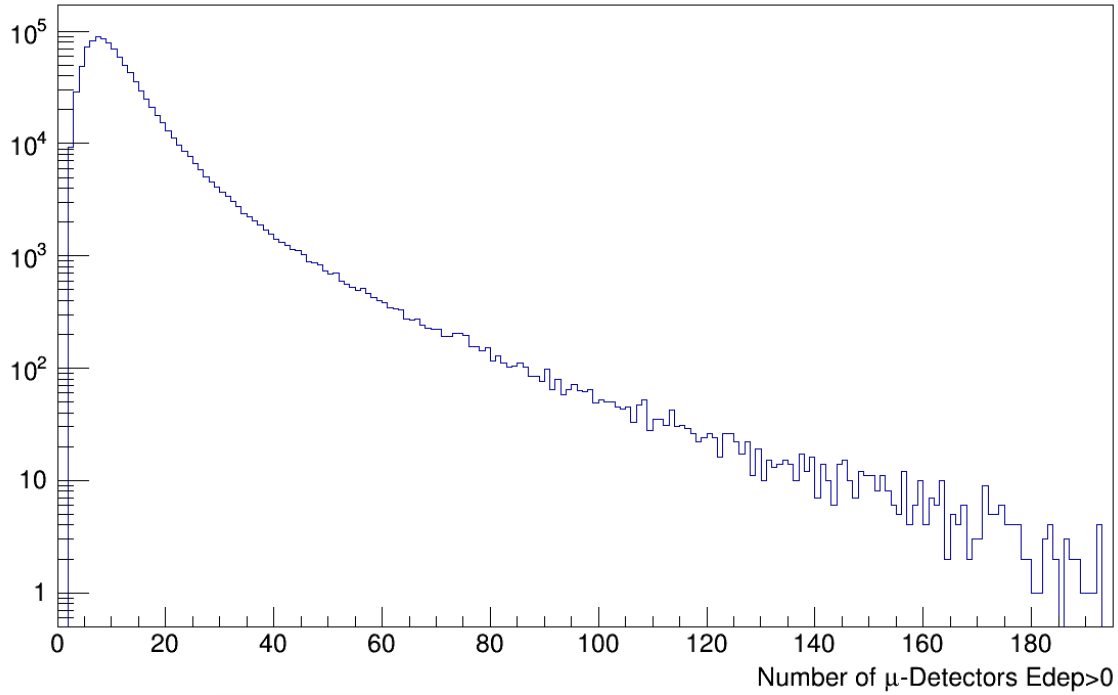The distribution of the number of μ-detectors with energy deposit *MDeposit>0* in this event is given in fig 4.6.8.

fig. 4.6.8   *Distribution of the number of μ–detector stations with hits*

4.6.2.3 μ-Energy Deposit value for each detector station (MDeposit)

The Energy deposits are derived from the stored ADC values for each μ detector station by means of a calibration procedure where the influences of electronics and cabling are included. **MDeposit** values are given in MeV. In fig 4.6.9, the energy deposits for a sub-sample of KASCADE data are plotted.

Note: Muon energy deposits within a 40m radius around the reconstructed shower core are not in the data samples because of the saturation and the punch through effects, which cannot be estimated and thus not corrected for.
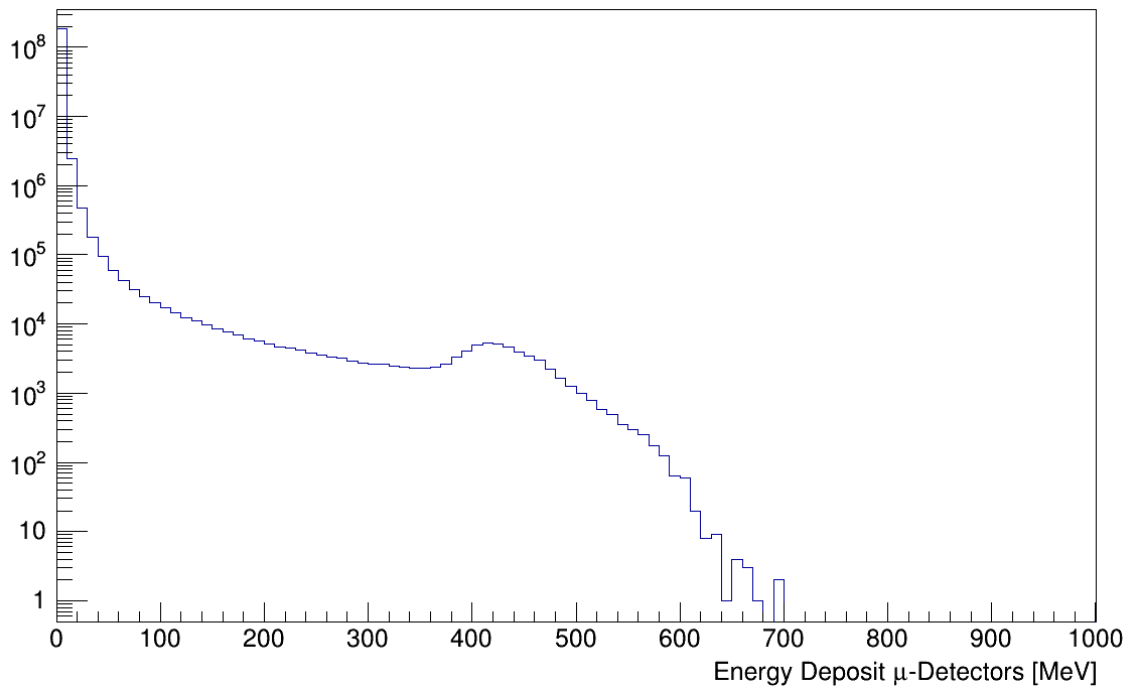
fig. 4.6.9   *Distribution of the corrected μ energy deposits of all active stations*

4.6.2.4   Station ID (MDepositS)

The *station ID (same as for e/γ-detectors in 4.6.1.4)* holds the information of the location of the respective detector station. The transformation from the *station ID* to the KASCADE coordinates of the respective Array detector station is described in chapter 8.4 and Appendix A.

Fig 4.6.10 shows the distribution of station IDs of the active μ-detector stations. The two regions not populated represent the 4 inner array clusters, which are not equipped with μ-detectors (see chapter 2.2). The other steps in the otherwise very flat spectrum indicate that one station or a whole cluster (16 stations) were missing for some time.

The effective μ–detector area for all 192 stations is 3.24 m² (yellow area in fig 4.6.5).

Note: This value is always shipped if the 'μ Energy Deposit' Quantity is selected but only in root and hdf5 files not in ASCII.
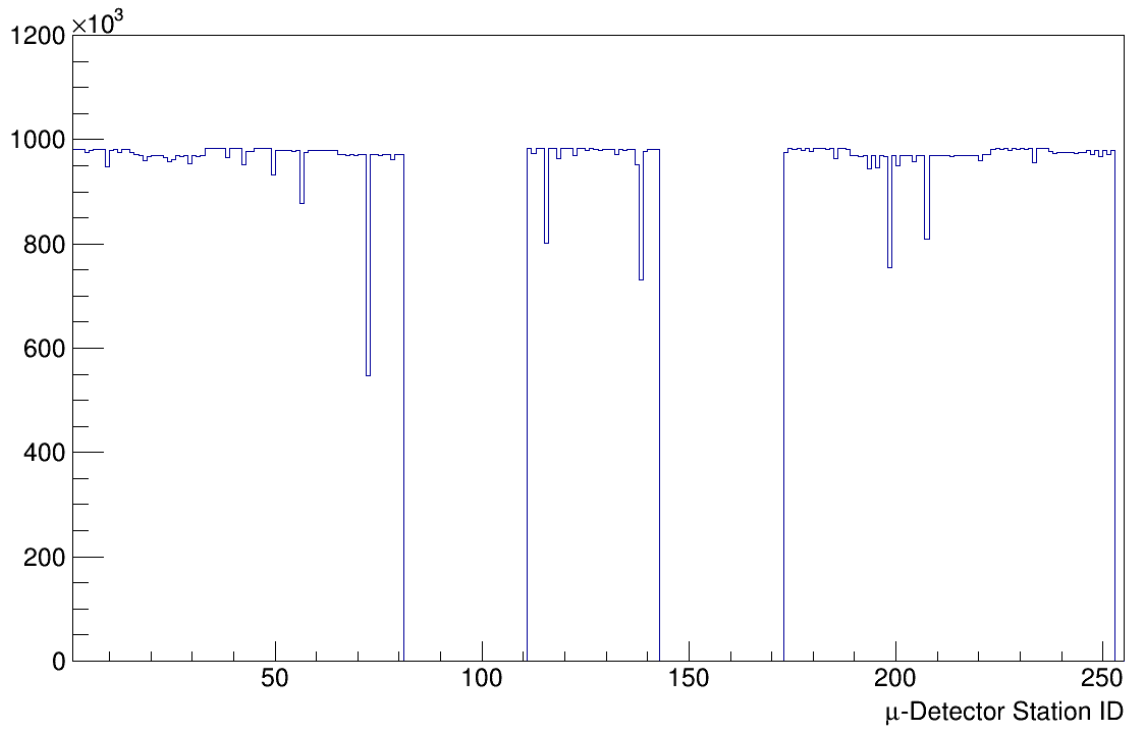
Fig. 4.6.10   *Distribution of station IDs for μ-detector stations*

4.6.2.5   Distance to shower core

The distance from the μ –detector station to the reconstructed shower core can be calculated from the station ID **MDepositS** and the shower core coordinates Xc and Yc. Due to saturation and punch through μ-detectors within a radius of 40m around the reconstructed shower core are not taken into account. The structure in the distribution in fig 4.6.11 clearly visible around the maximum of the distance to the shower core distribution is caused by the reconstruction algorithm which 'draws' the reconstructed shower core between the stations with the highest energy deposits measured. The spacing of 13m of the detector stations is mapped here (see also fig. 4.4.1).

The structures diminish with increasing cut on energy. The structure clearly visible around the maximum of the distance to the shower core distribution in fig 4.6.10 is caused by the reconstruction algorithm which 'draws' the shower core towards the closest detector station with the highest energy deposit measured. The spacing of 13m of the detector stations is mapped here (see also fig. 4.4.1). The structure diminishes with increasing energy.
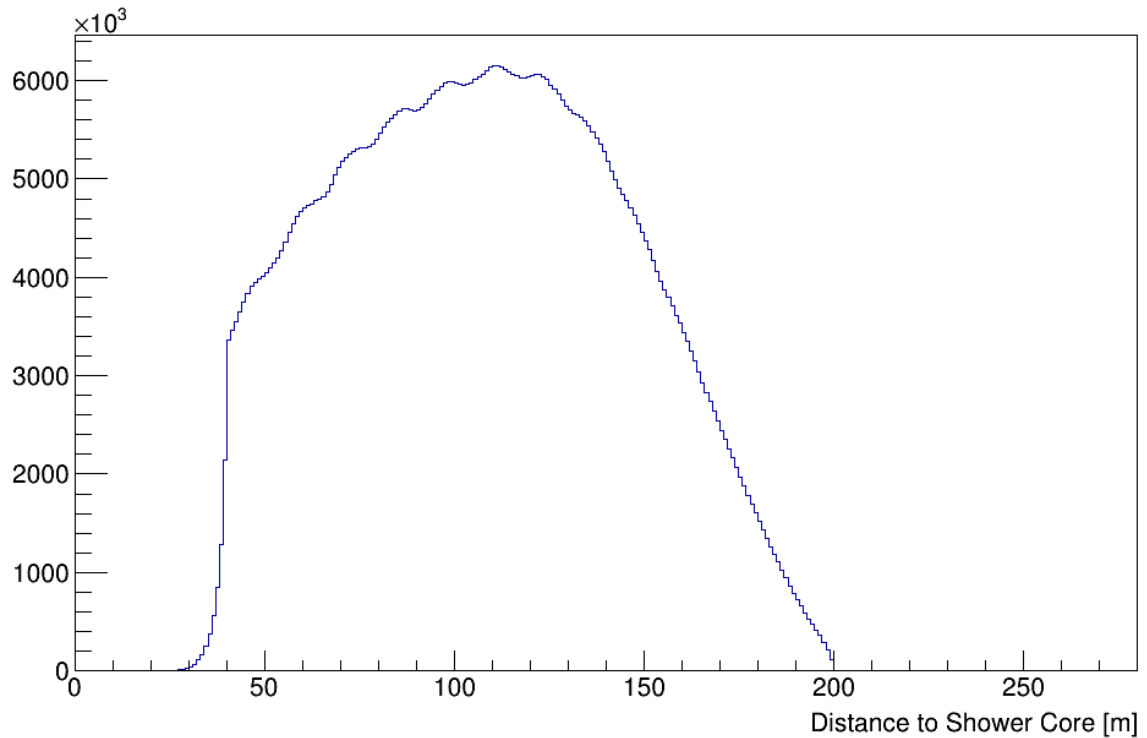
Fig. 4.6.11   *Distribution of the distances to the shower core of the μ –detector stations*

4.7   ARRIVAL TIMES

The '**Arrival Times'** of each KASCADE array station represents the first time stamp of each detector station that has been hit by a charged particle. When the electronic has recorded a signal above a certain threshold a signal is sent to the central data acquisition system. The first signals of each station represent the shower front and are used to determine the shower direction.

The quantity '**Arrival Time'** offers the possibility to reconstruct the shower disc and the arrival direction of the extensive air shower.

The values of the arrival times are taken from the e/γ –detector's data.

A detector station has to fulfil several conditions to be accepted as 'active detector station' for arrival time analysis.

- the station was flagged as 'active'

73

- no overflow was detected in the station

- the station was not deselected for various reasons

A detector station which did not provide any time information was treated as 'silent station'.

Note: on the quantity 'Arrival Times' no cuts can be applied

Note: in chapter 8.4 are examples on how to handle the quantity 'Arrival Times'

Handling the '**Arrival Times'** quantity mostly requires some additional information either on the absolute coordinates of the detector station or on the distance to the reconstructed shower core. Therefore the quantity **ArrivalS** is always supplied with the times values. Furthermore, the number of detector stations with valid arrival time information (**ArrivalN**) is provided as well.

Thus, if the quantity '**Arrival Times'** is selected in the KCDC DataShop you will always be supplied with the following data sets:

ArrivalN	nr of active e/γ-detectors for this event (0 … 252)
Arrival	Arrival time in [ns] bins
ArrivalS	detector station ID [1…252]

4.7.1 NUMBER OF DETECTOR STATIONS WITH VALID ARRIVAL TIMES (ARRIVALN)

The range of **ArrivalN** is between about 15 and 252. The distribution is shown in fig. 4.7.1. The lower limit is given by the trigger condition described in chapter 3.1.2.
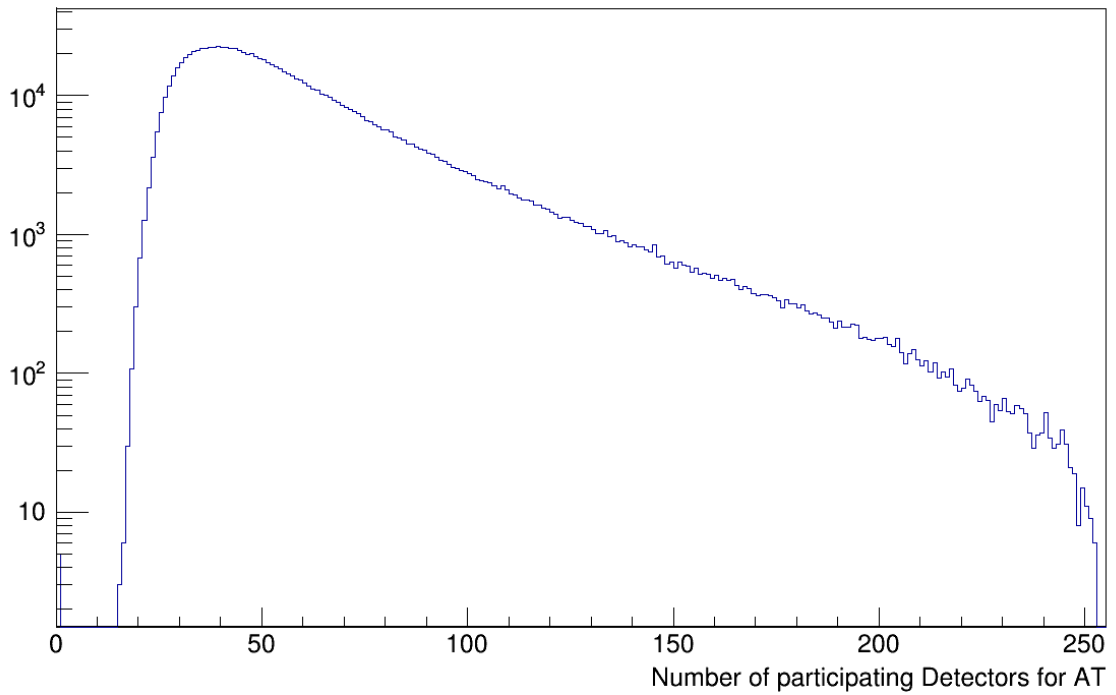
fig. 4.7.1. *Distribution of the number of detector stations with 'Arrival' information*

4.7.2 ARRIVAL TIMES PER STATION (ARRIVAL)

The arrival times are given with a resolution of 1ns/bin. Fig 4.7.2 shows the 'arrival'– distribution. The values of the arrival times can be negative due to the fact that the reference to calculate the individual time stamps is not the first signal above a certain threshold but the time of coincidence that matches the trigger condition set in the hardware. The structure clearly visible is caused by small showers corresponding to low energies. Going to higher Energies the negative Arrival Time values and the structures will disappear as indicated in the red curve of fig. 4.7.2 where a cut as been applied on $N_e > 50,000$.
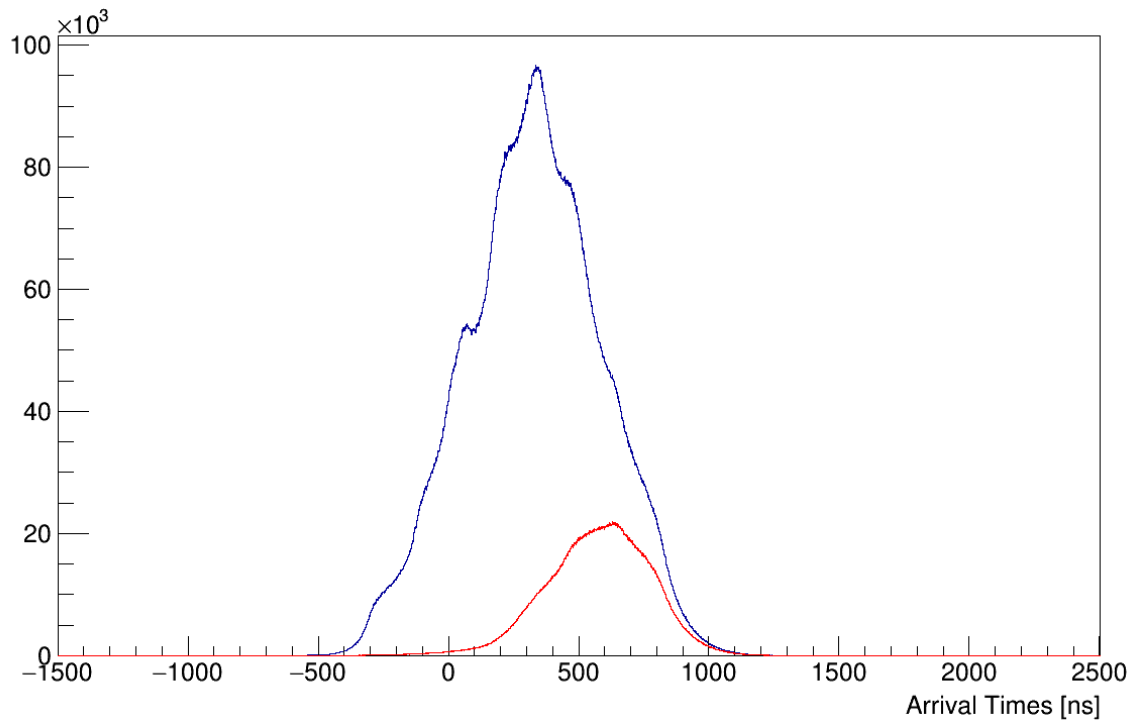
fig. 4.7.2   *Arrival time distribution; no N_e cuts(blue); N_e>50,000 (red)*

4.7.3   STATION ID (ARRIVALS)

The station ID (same as in 4.6.1.4) holds the information of the location of the respective detector station. The transformation from the *station ID* to the KASCADE coordinates of the respective Array detector station is described in chapter 8.4 and Appendix-A.

Fig 4.7.3 shows the distribution of station IDs of the active e/γ-detector stations. The two regions with the higher population mark the four inner clusters which have a detection area twice the size of the outer 12 clusters (see fig. 4.6.5).

Note: This value is always shipped if the 'Arrival' Quantity is selected but only in root and hdf5 files not in ASCII.
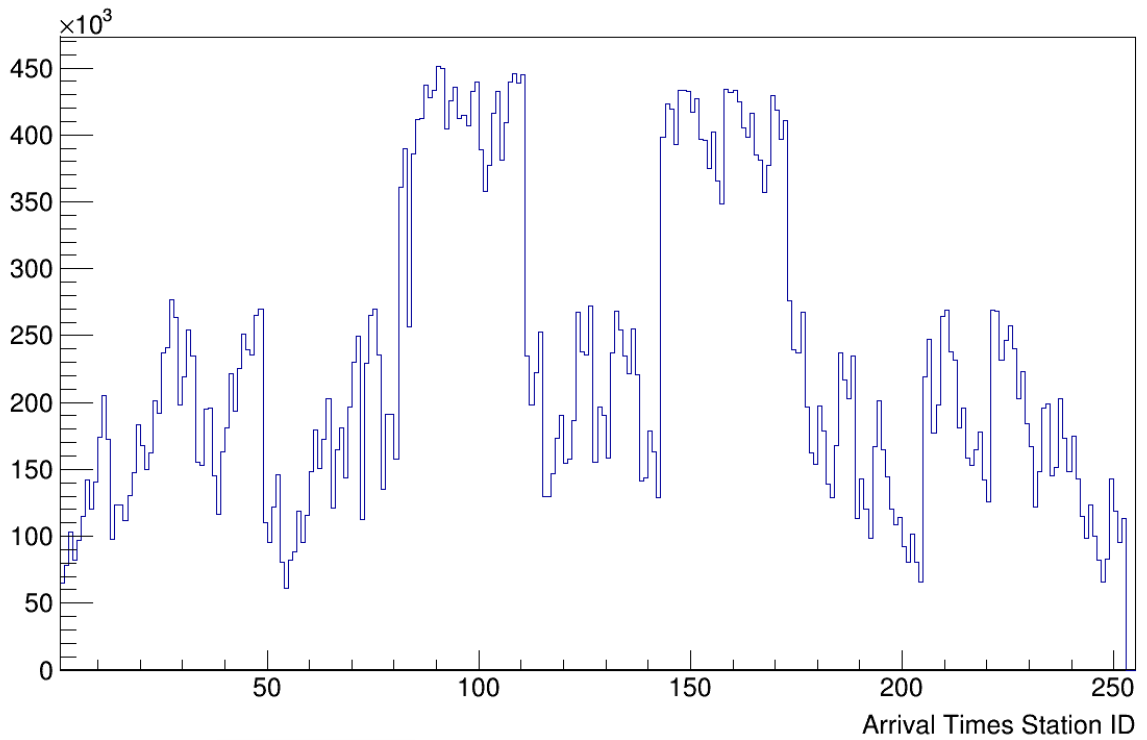
fig. 4.7.3   *Distribution of station IDs for e/γ-detector stations with valid Arrival Times*

4.7.4   DISTANCE TO SHOWER CORE

The distance from the e/γ –detector station with a valid arrival time to the reconstructed shower core can be calculated from the station ID **ArrivalS** and the shower core coordinates Xc and Yc. The structure in the distribution in fig 4.7.4 clearly visible around the maximum of the distance to the shower core distribution is caused by the reconstruction algorithm which 'draws' the reconstructed shower core between the stations with the highest energy deposits measured. The spacing of 13m of the detector stations is mapped here (see also fig. 4.4.1). The structures diminish with increasing cut on energy.
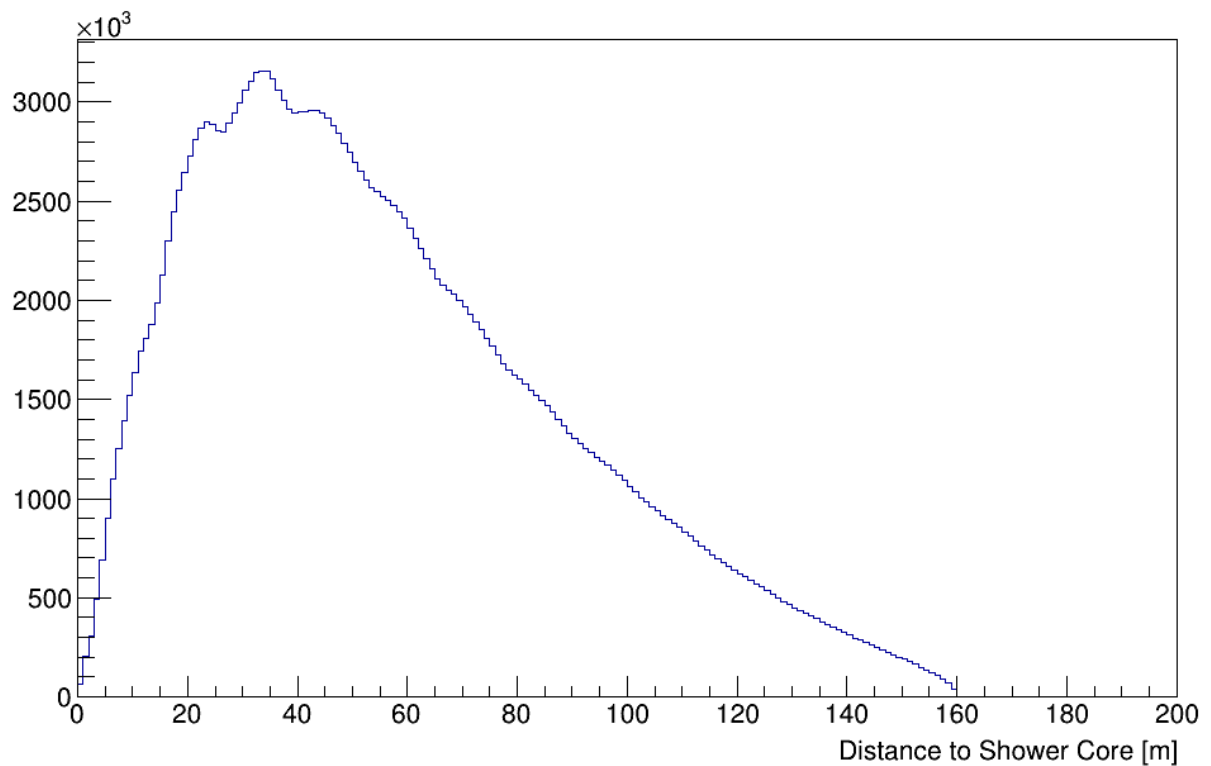
fig. 4.7.4   *Distribution of the distances of e/γ-detector stations to the shower core with valid Arrival Times*

4.7.5   EXAMPLE

An example for the arrival time distribution of one event is given in fig 4.7.5. The warmer the colour the bigger the time difference which usually corresponds to larger zenith angles. The arrival time distribution and the large difference in the arrival time of about 600ns indicate that the shower is coming from south-west direction at a zenith angle of about 30°.
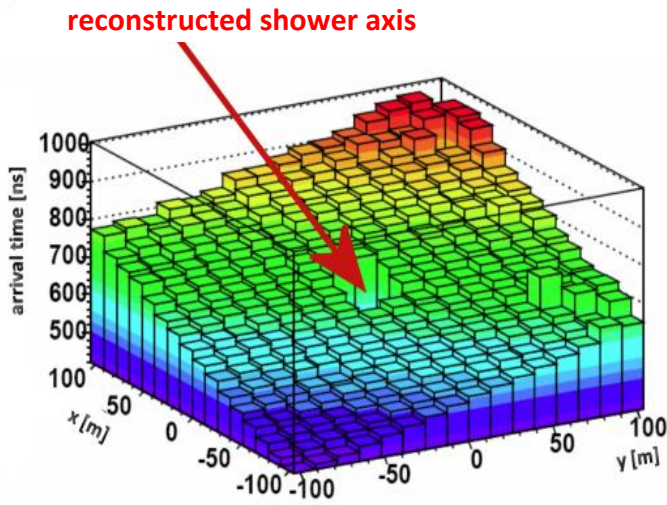
reconstructed shower axis

Fig. 4.7.5   *Example of an arrival time distribution with the reconstructed shower direction*

4.8   EVENT TIME (DATETIME, GT, MT)

In KASCADE an event is stored when the trigger condition is fulfilled (details see chapter 3.). As all events recorded are triggered either by the KASCADE Array or by the GRANDE Array, these conditions are based on the layout of the two detector arrays. For the KASCADE Array the 252 detector stations are subdivided in 16 clusters (4x4 stations each, the 4 inner clusters have on 15 stations each). The trigger condition is fulfilled when at least one cluster has recorded a signal above a certain threshold. For the GRANDE Array the trigger condition is fulfilled when at least all seven stations of one trigger hexagon (see 2.3.3) have recorded a signal above the threshold. The time of the first trigger either from KASCADE or from GRANDE is stored as the event time.

The event time is always given in UTC which is affected with an offset of -2h for summer time (CEST) and -1h for winter time (CET). As a redundant time information we use at KASCADE the *Unix Time,* a system timestamp counting the number of seconds elapsed since 1. January 1970 (midnight UT), which is internally referenced as *Global Time*. To get a high precision time stamp the Micro Time information is used.

Based on the cycle of a 5 MHz clock which is reset and synchronised every second, we obtain an accuracy of +/- 200 ns for the event time.

For a better accuracy of the absolute time, we utilize the Global Positioning System (GPS), which is a high-precision satellite navigation system. The absolute accuracy is better than 1 μs.

With an integration time of 200 ns, the electronics of each station is ready for the next measurement after about 1.2 μs. Taking into account the trigger rate of about 4 Hz, the total dead time due to the data acquisition is 5 μs.

Due to the difference of the cable lengths between the array clusters, i.e. transmission path, the differences in the transmission time are determined by a time calibration and corrected for.

4.9   AIR TEMPERATURE AND PRESSURE (T, P)

The earth's atmosphere has a small influence on the development of the extensive air showers and thus cannot be neglected, in particular for anisotropy studies of cosmic rays. Thus data can be corrected for effects of temperature and pressure on an event-by -event basis in analyses.

The meteorological data are received from the Institute of Meteorology and Climate Research at KIT. The measurements are taken from sensors placed 2m above ground level for the temperature readings and 1.5m above ground for the air pressure measurements on site of KIT, Campus North, about 1 km from the KASCADE experiment. All climate observables were recorded every 10 minutes.

The figure 4.9.1 presents the distribution of the temperature between 1998 and 2013. The spectrum shows the seasonal variation and the distribution is stable.
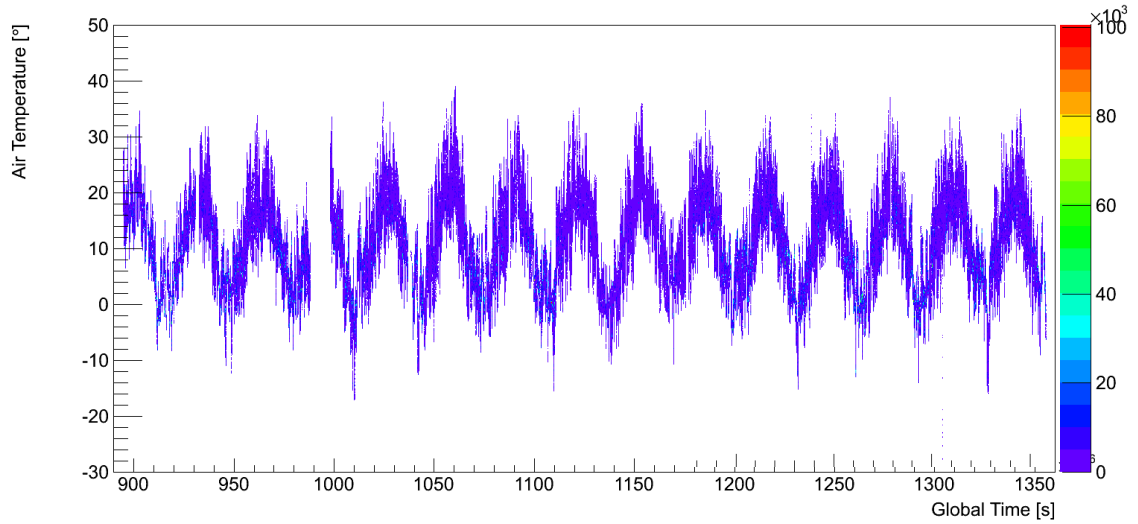
Fig. 4.9.1   *The spectrum of the temperature as a function of the Global Time measured at*
ground level for the time period 8.5.1998 – 15.1.2013 in [10⁶ s]

In general, the number of charged particles decreases exponentially after their shower maximum and it varies with the zenith angle, as well as with the atmospheric pressure. Therefore, the attenuation can be described with the attenuation length λ_N by:

$$\langle N_e(X) \rangle \propto exp\left(-X_0/\lambda_{N_e} \cos \Theta\right)$$

where $N_e(X)$ is the number of electrons of the extensive air shower at the slant depth $X[g/cm^{-2}]$. The X_0 is a definite initial atmospheric depth after the maximum of the longitudinal shower development and it is 1020 g/cm^{-2} at KASCADE

A variation of the slant depth by the pressure $p(t)$ with an average atmospheric pressure p_0 is given by

$$X\big(p(t)\big) = \frac{X_0}{\cos \Theta} + \frac{p(t) - p_0}{g \cdot \cos \theta}$$

The fluctuation of the rate because of the pressure variation can be up to 20%. By means of tuning a polynomial function, the atmospheric influences on the rate can be well corrected.

The variation of the pressure for the measuring period 1998-2013 is given in fig 4.9.2.
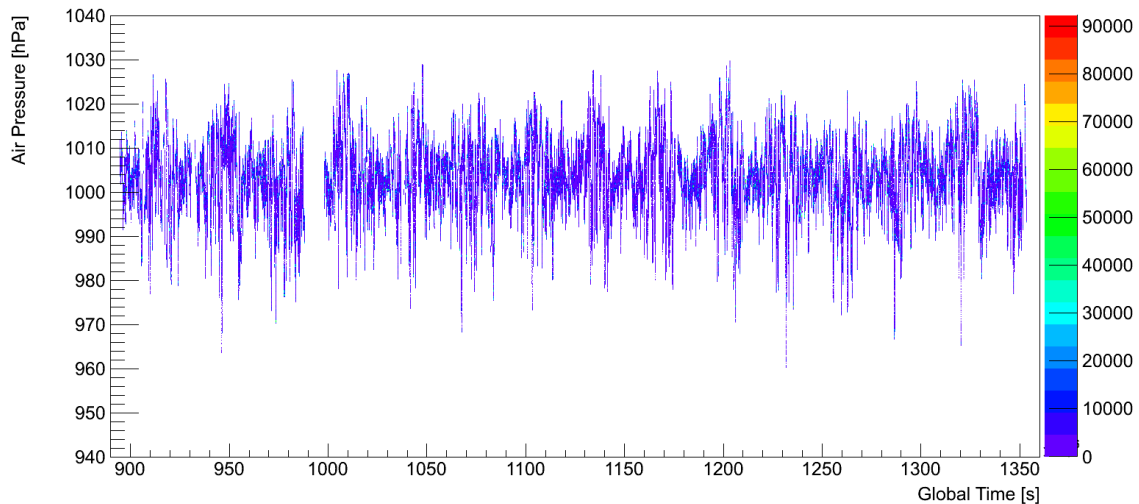
Fig. 4.9.2

The spectrum of the air pressure as a function of the Global Time measured at ground level for the time period 8.5.1998 – 15.1.2013 in [10⁶ s]

4.10   RUN NUMBER & EVENT NUMBER

Run Number and **Event Number** are two parameters which characterise an event uniquely. They will always be supplied with the data sets. A run is in KASCADE defined as a set of events recorded under the same hardware conditions. An automatic procedure in the data recording system caused the data taking to stop and to start with a new run if the hardware conditions of one of the various detector components has changed, p.e. loss of one detector component.

The Event Number starts at '1' with each run and is increased with every valid hardware trigger which invokes data recording. KASCADE recorded within its lifetime more than 1.7 billion events of which only 433 million passed our quality cuts.

4.11   UUID

The **UUID (Universally Unique Identifier)** has been introduced to identify a single event by one unique string. This identifier is required to match the KCDC data with the data of

the TAIGA/TUNKA experiments published within the GRADLC Initiative (**G**erman-**R**ussian **A**stroparticle **D**ata **L**ife **C**ycle **I**nitiative).

A unique UUID represents an object independent from versions and the reference is immutable. Records that were once published in KCDC are frozen by versions, which means that even if the data are extended or changed the reproducibility is maintained.

5 CALORIMETER DATA IN KCDC

The main component of the KASCADE Central Detector is an Iron-Sampling-Calorimeter 16×20 m² in size. The hadrons and their interactions are important for the understanding of the shower development within the atmosphere. The parameters reconstructed from the calorimeter measurements are the Number of hadrons and their energy sum.

Quantity	Description	Unit	ID
Measuring Data			
Hadron Number	reconstructed number of Hadrons (fit)	*(number of)*	*Nhad*
Hadron Energy Sum	Sum Energy of all hadrons reconstructed	*(eV)*	*Ehad*

5.1 HADRON NUMBER

Due to the fine lateral segmentation and the read-out of the calorimeter in more than 40,000 electronic channels, hadrons with an energy $E_{had}>20$ GeV can be measured in the calorimeter. They can be separated from each other when the distance of their shower axis is above 40 cm. The spatial resolution of the calorimeter is about 11 cm and the energy resolution is 30% for hadrons with 100 GeV decreasing to 15 % for $E_{had}=25$ TeV. The analysis algorithm allows reconstructing up to 500 separated tracks in a shower core.

Fig. 5.1.1 shows the distribution of the reconstructed numbers of hadrons per event for all events reconstructed.

'No hadrons were reconstructed' does either mean that the hadron energy was below 20GeV, the shower core was well outside the active detector area or the reconstruction algorithm failed because too few active layers have been hit.
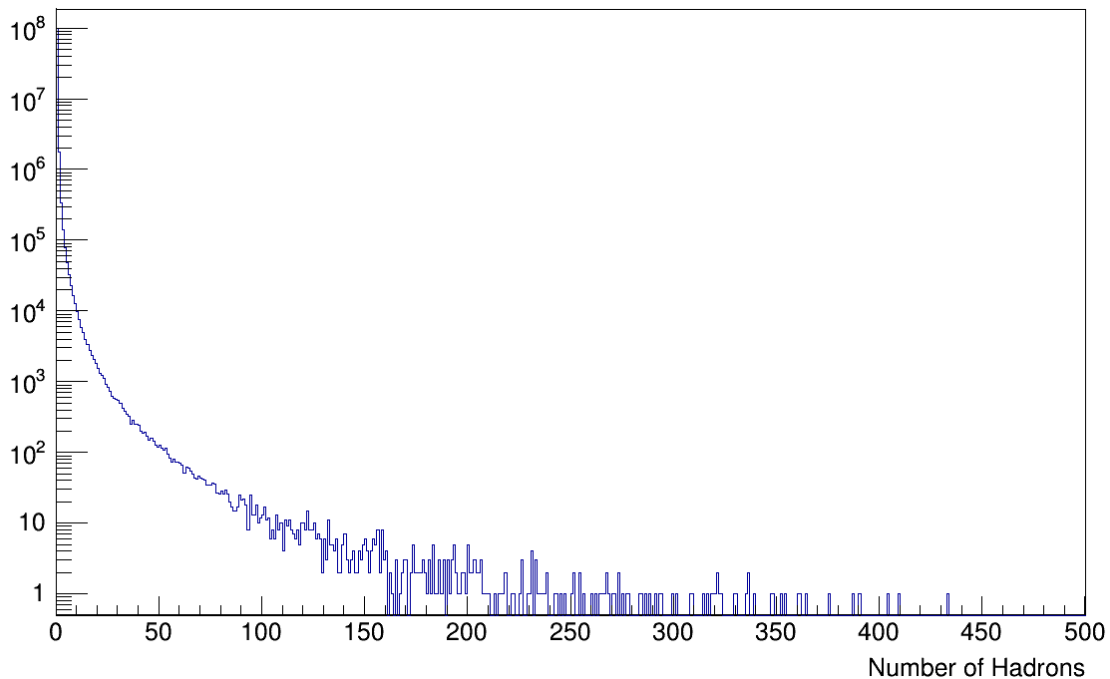
85

Fig. 5.1.1   *The distribution of number of hadrons*

The range of values is described in the table below:

N_{had} Value	Description
no value	The Hadron Calorimeter was not running i.e. no information available
0	The Hadron Calorimeter was running but no hadrons were reconstructed
1 - 500	# hadrons reconstructed in the Hadron Calorimeter

5.2   HADRON ENERGY

The value given here for the hadron energy is actually the sum of all hadron energies reconstructed in the hadron calorimeter in $log_{10}[eV]$. Due to the fine segmentation of the calorimeter and the detection of the shower development in 9 active layers interspaced by iron absorbers, up to 500 hadrons can be separated and reconstructed individually. The range of the energy sum is between 20 GeV (lower threshold for one hadron) and about 10^7 GeV.

In fig. 5.2.1 the distribution of the energy sum of all reconstructed hadrons per event for all events reconstructed is given.
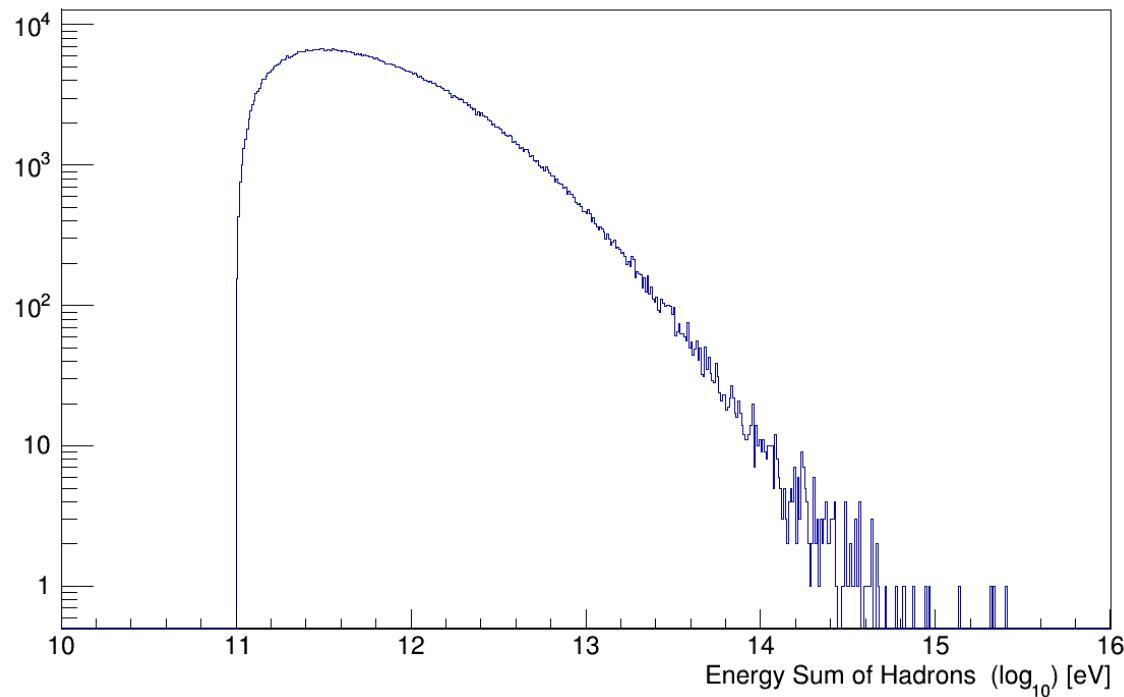

Fig. 4.8.2   *The distribution of the energy sum of all of hadrons reconstructed*

The range of valid values is described in the table below:

E_{had} Value	Description
no value	The Hadron Calorimeter was not running i.e. no information available
0	The Hadron Calorimeter was running but no hadrons were reconstructed
10 - 16	Energy sum in log10[eV] for all reconstructed hadrons

Note:

Events where the Hadron Calorimeter was not running are set to '-1' in the row map file.

6   GRANDE DATA IN KCDC

The measured air showers in the KASCADE-Grande array (GRANDE) are analysed using the reconstruction program KRETA (*Kascade Reconstruction for ExTensive Airshowers*).

From the observables obtained in the analysis we choose 9 to be published in KCDC which can be selected and mostly applied cuts on via the KCDC Data Shop as **Quantities**.

If not stated otherwise, the GRANDE quantities are reconstructed in the same way as the KASCADE array quantities. Merely the parameters for the fits are different. Described here are only the GRANDE measuring data. Calibration data and event information are explained in detail in chapter 4.

GRANDE Quantity	Description	Unit	ID
Measuring Data			
Core Position Xc	location of the reconstructed GRANDE shower core X-position	m	Xc
Core Position Yc	location of the reconstructed GRANDE shower core Y-position	m	Yc
Zenith Angle	zenith angle reconstructed by GRANDE with respect to the vertical	° (degree)	Ze
Azimuth Angle	azimuth angle reconstructed by GRANDE	° (degree)	Az
Number of Charged Particles	number of charged particles reconstructed by GRANDE	(number of)	Nch
Muon Number	number of Muons (fit) reconstructed by GRANDE	(number of)	Nmu
Age	GRANDE Shower shape parameter		Age
Energy Deposits	energy deposit per GRANDE detector station	(MeV)	GDeposit
Arrival Times	Arrival Times per GRANDE detector station	(ns)	GArrival

During its lifetime we recorded 88,459,522 GRANDE triggered events of which 27,399,720 survived all quality cuts and are made available for public usage.

The plots shown in this chapter are only examples, mostly based on a subsample of the data set published. So, applying user cuts either in the KCDC Data Shop or in your own analysis can change these spectra drastically.

For GRANDE we do not give an estimation of the energy of the primary particle because this value strongly depends on the simulation model and the cuts applied. As a rough estimator one can use

$$\lg(E_{Grande}/eV) = (1.402 + 0.9266 * \lg(N_{ch})) + 9.0$$

for Grande energies given in log10/eV.

6.1 NUMBER OF CHARGED PARTICLES AND NUMBER OF MUONS IN GRANDE (N_{CH}, N_{MU})

In GRANDE, we can only measure the energy deposit of charged particles and photons together. There is no way to distinguish between electromagnetic particles and muons. Thus, the measured data are the energy deposits of charged particles at ground level and their arrival times. From these measurements, the arrival direction of the shower, its impact point on ground (shower core) and the total number of charged particles in the shower, i.e. the shower size are reconstructed. The given muon number is derived from the muon detectors of the KASCADE stations. The reconstruction is performed similar to KASCADE but with different parameters. The number of Muons (N_μ) are taken from the KASCADE detector stations participating in the respective event with a simplified method. As there are normally only few KASCDE detector stations with muon information when GRANDE has been triggered, the number of detected muons is compared to a shower with a normalised shower size. When the GRANDE core position is known, the average value of the ratio of '*measured muon number*'/'*expected muon number*' over all detectors are formed and stored as N_μ.

Figures 6.1.1 and 6.1.2 show the N_{ch} and N_{μ} distributions in a log-log scale.
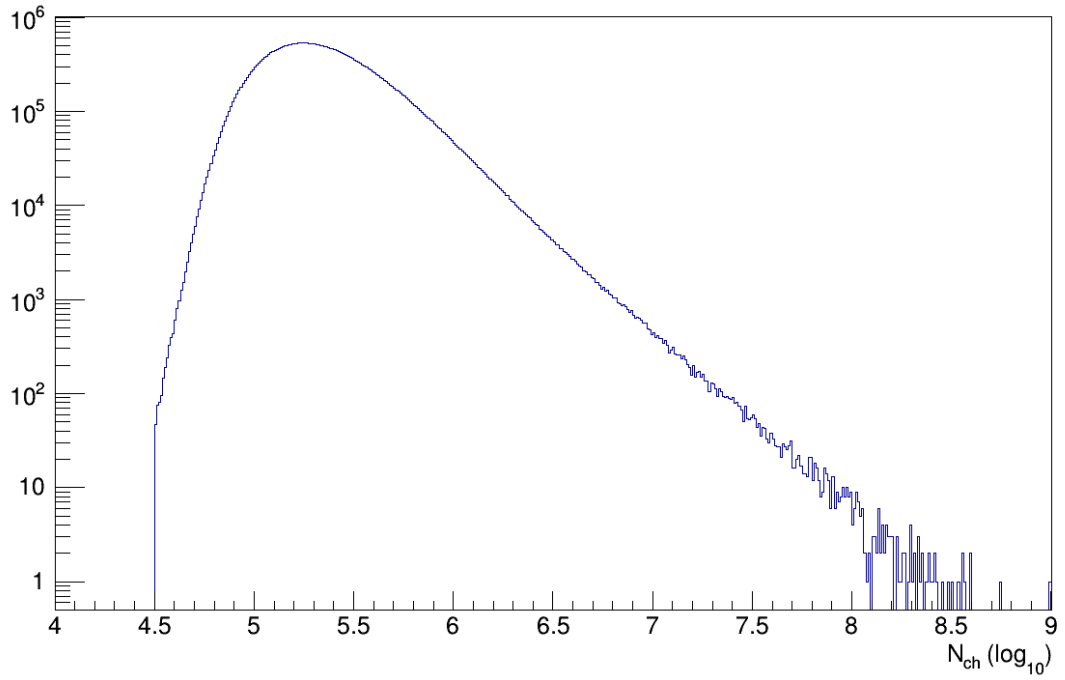

Fig. 6.1.1   *The spectrum of the number of charged particles in GRANDE*
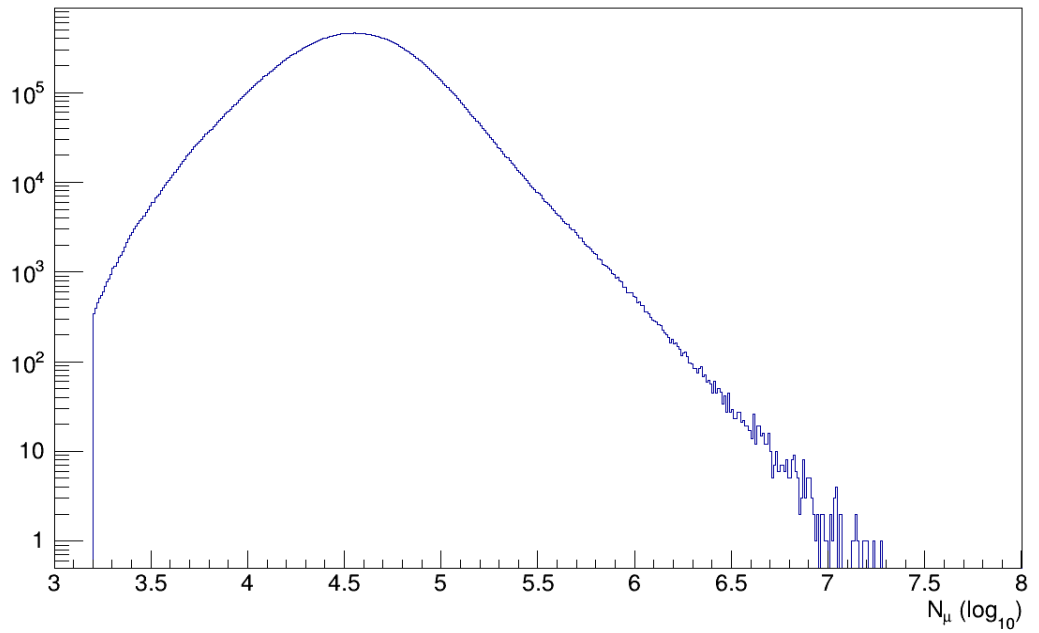

Fig. 6.1.2   *The spectrum of the calculated number of muons in GRANDE*

6.2 GRANDE AGE (AGE)

Contrary to variables like number of charged particles N_{ch} or number of muons N_{μ}, the value of the age parameter has no absolute meaning, as it depends on the choice of the lateral distribution function which is fitted to the shower data. It may also be called **lateral shape parameter** because it describes the steepness of the lateral electron density distribution. Like KASCADE, GRANDE uses a modified NKG-function to fit the lateral shower shape but with different parameters. Within this function, the age parameter values are limited theoretically to a range from -0.385 to 1.485. Common shower values however should not be negative. Lower values describe steeper lateral distributions.

The shape (steepness) of the lateral density distribution of a given shower depends on the energy of the primary particle, as well as on its nature. The higher the shower energy, the steeper the lateral distribution. A heavy primary particle with the same energy as a light one gives rise to a flatter lateral distribution, as the shower starts earlier in the atmosphere. When reaching ground, the shower is "older", which gives the age parameter its name. The Age parameter therefore may help (in combination with number of charged particles) to distinguish between primary particles of different mass.

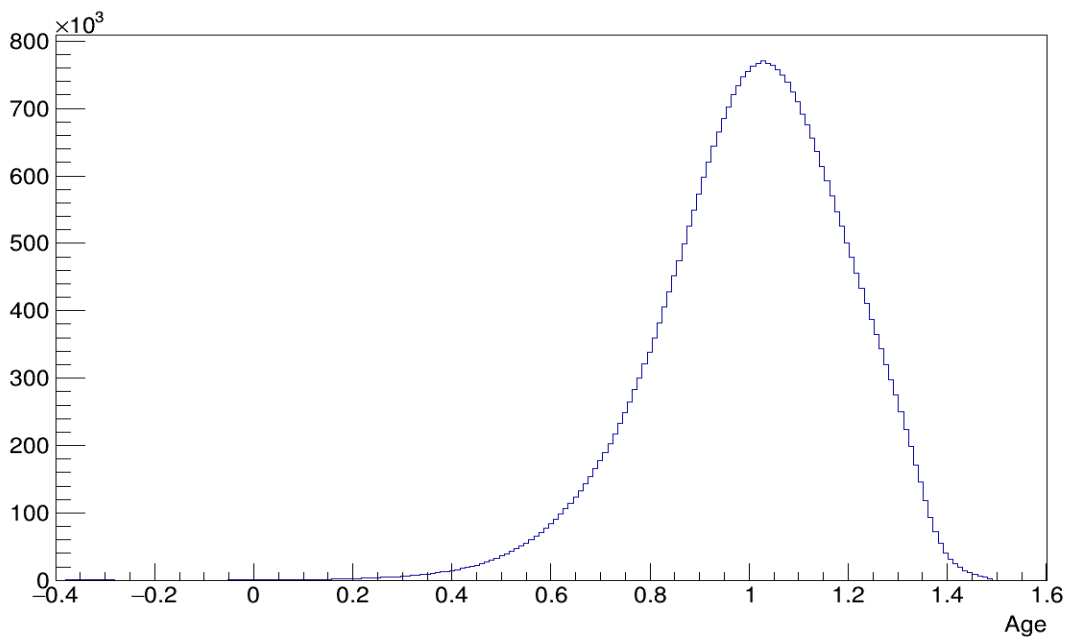Fig. 6.2.1 shows the AGE distribution.

Fig. 6.2.1 *The GRANDE Age distribution for reconstructed showers.*

6.3 GRANDE Shower Core Position (Xc, Yc)

The GRANDE shower core position is the reconstructed location of the shower centre at GRANDE level (same as KASCADE level) derived from the energy deposits of each of the 37 detector stations of one event. The unit of the core position is [m].

For the reconstruction of the GRANDE core position like at the KASCADE array basically the particle densities in every detector station are taken. The core can be determined to a precission of about 10m.
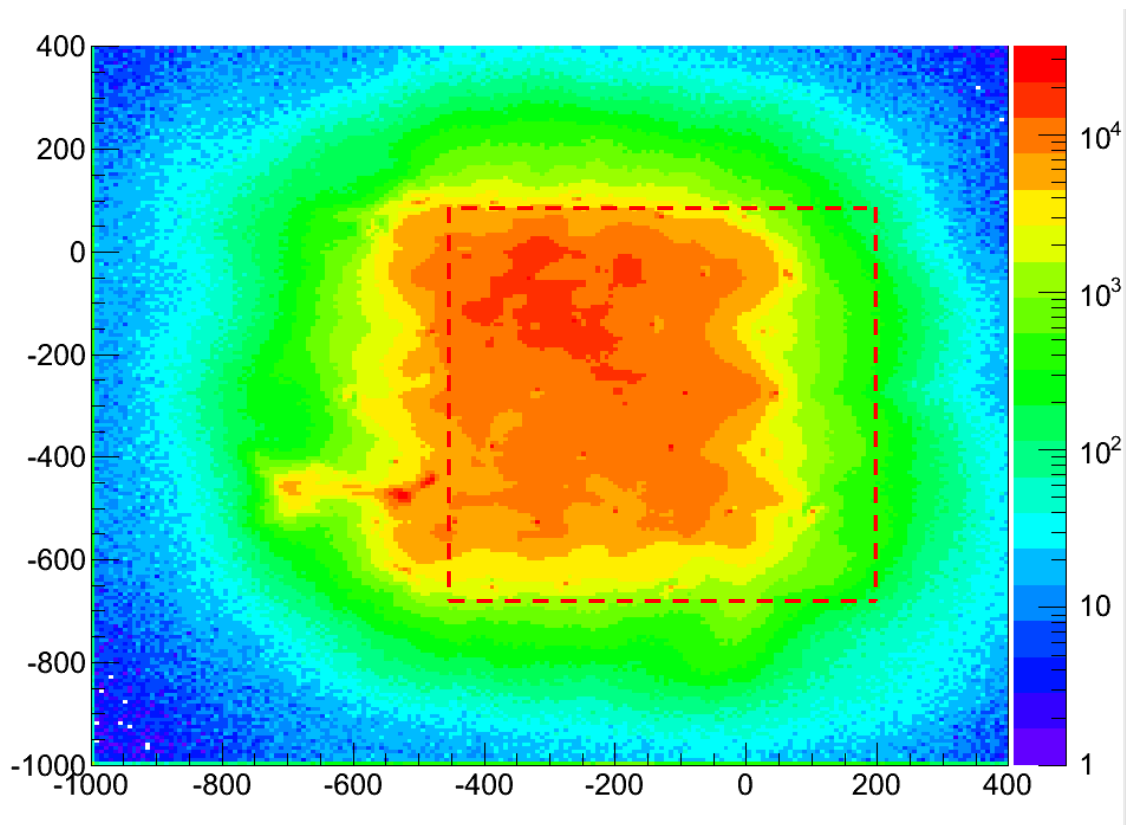

Fig. 6.3.1   *Shower core distribution with GRANDE array detector stations*

The distribution of the shower core is plotted in the fig. 6.3.1. Extensive air showers with a core position outside the detector area have a great probability for beeing incorrectly reconstructed. Therefore, only showers with a core inside the dotted line are taken into account.

6.4 GRANDE SHOWER DIRECTION (ZE, AZ)

Like in KASCADE the GRANDE zenith angle is measured against the vertical direction, which means that $\theta=0°$ is pointing upwards and 90° denotes a horizontal shower. The azimuth is accordingly defined as an angle measured clockwise starting in northern direction (90° is east). The orientation of the GRANDE Array has an offset of about +15° against the real northern direction. This offset is corrected for in the data analysis. The unit of the azimuth and zenith angle is [°].

In figure 6.4.1 the distributions of the GRANDE azimuth angle is shown. The distribution of the zenith angle is shown in fig 6.4.2.
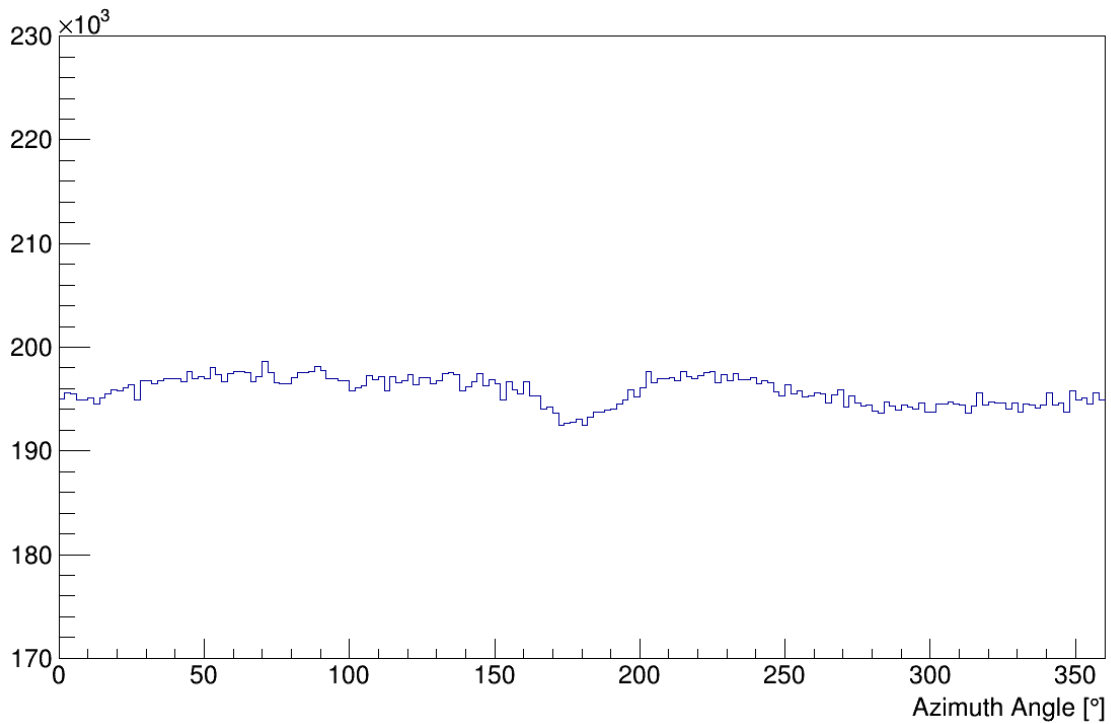
Fig. 6.4.1   *The distribution of the reconstructed GRANDE azimuth angle*
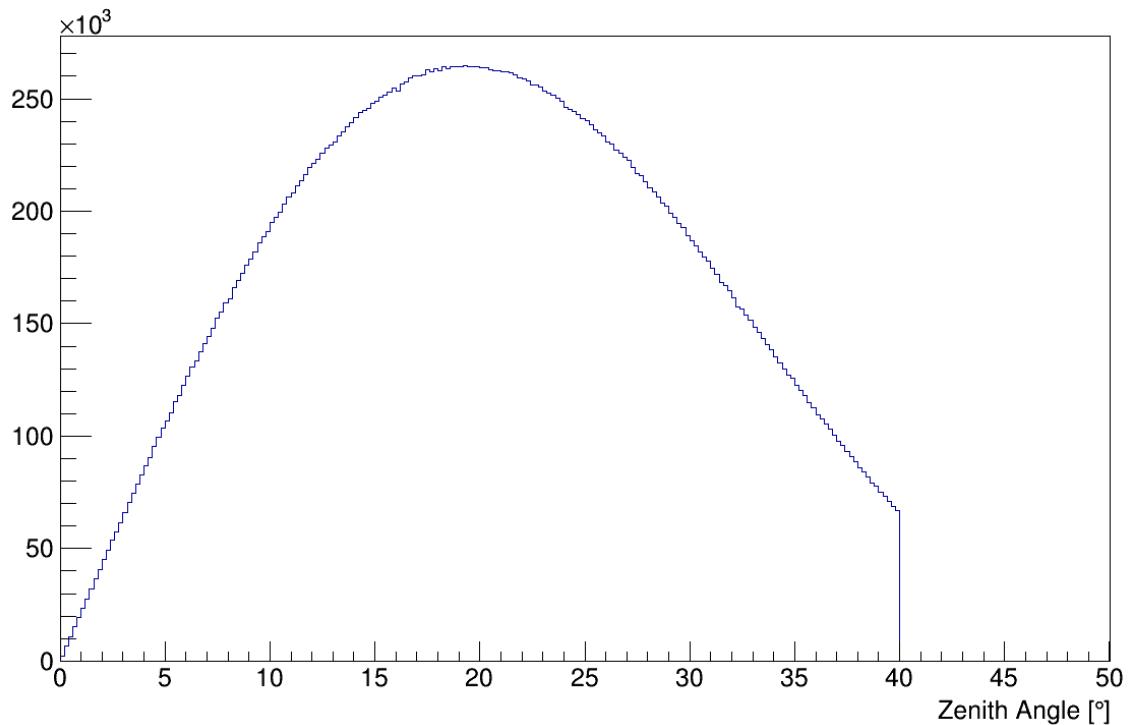
Fig. 6.4.2   *The distribution of the reconstructed GRANDE zenith angle*

6.5   GRANDE ENERGY DEPOSITS PER STATION (GDEPOSIT)

Available are the GRANDE energy deposits of each of the 37 detector stations.

A detector station has to fulfil several conditions to be treated as 'active detector station' in the sense that their energy deposits and arrival times are provided.

- the station was flagged as 'active'
- no overflow was detected in the station
- the station was not deselected for various reasons

Active detector stations which had no signal above the threshold are as well taken into account. The energy value of these 'silent' stations is set to '0'.

Note: on the quantities 'GRANDE Energy Deposit' no cuts can be applied

Note: in chapter 8.4 are examples on how to handle the quantity 'GRANDE Energy Deposit'

Handling the **'GRANDE Energy Deposits'** quantity mostly requires some additional information either on the absolute coordinates of the detector station or on the distance to the reconstructed shower core. Therefore, the quantity **GDepositS** is always supplied with the energy values. Furthermore, the number of detector stations with valid energy deposit information (**GDepositN**) is provided as well.

Thus, if the quantity '**GDeposit**' is selected in the KCDC DataShop you will always be supplied with the following data sets:

GDepositN	number of active GRANDE detector stations with energy deposit ≥ 0
GDeposit	energy deposit per station in MeV
GDepositS	detector station ID [1…37]

6.5.1   NUMBER OF ACTIVE GRANDE DETECTOR STATIONS (GDEPOSITN)

The range of **GDepositN** is between roughly 25 and 37. The distribution for **GDepositN** is given in Fig. 6.5.1.

Note: only active stations are used for further analysis and shown in the plot.

Note: This value is always shipped if the 'GRANDE Energy Deposit' Quantity is selected but only in root and hdf5 files not in ASCII.
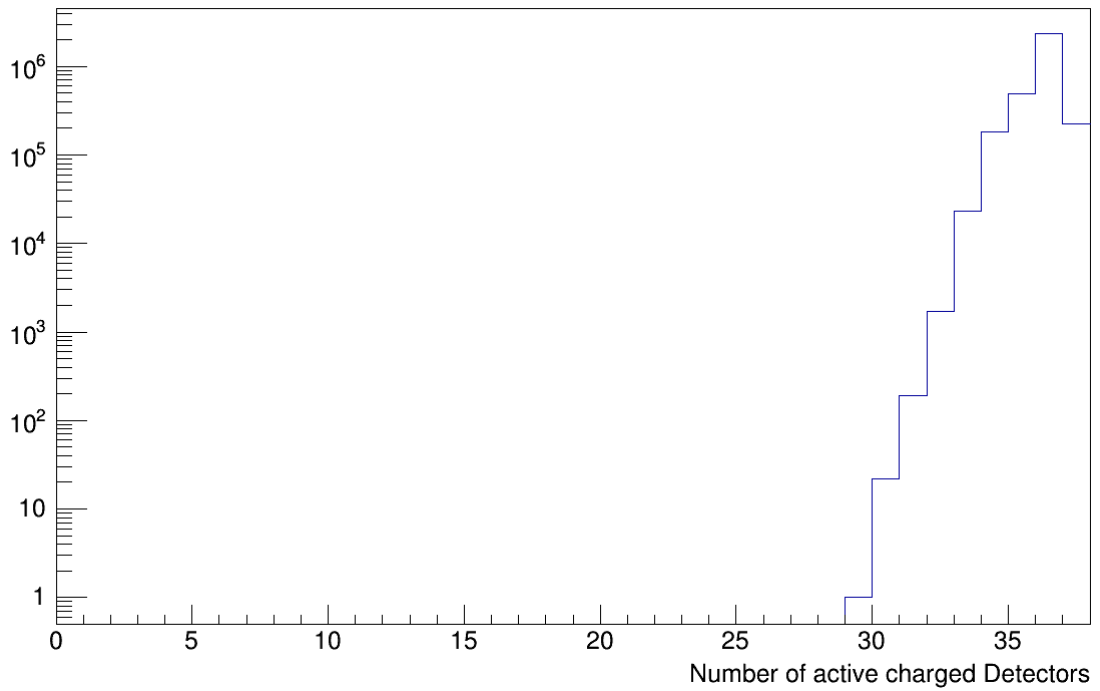
fig. 6.5.1   *Distribution of the number of active GRANDE detector stations*

6.5.2   GRANDE ENERGY DEPOSIT FOR EACH DETECTOR STATION (GDEPOSIT)

The Energy deposits are derived from the ADC values for each GRANDE station by means of a calibration procedure where the influences of electronics and cabling are taken into account. **GDeposit** values are given in MeV. In fig 6.5.2 the energy deposits for a subsample of GRANDE data is plotted.
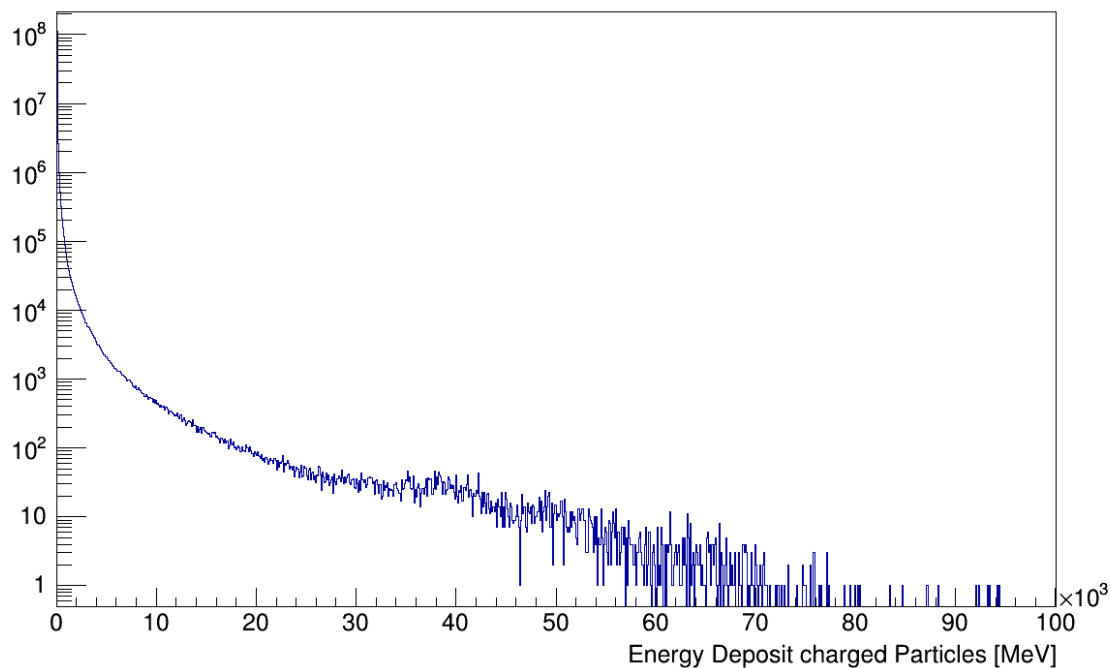
fig. 6.5.2   *Distribution of the GRANDE Energy Deposits of all active stations*

6.5.3   Station ID (GDeposits)

The station ID holds the information of the location of the respective detector station. The transformation from the station ID to the true detector position in KASCADE coordinates of the respective GRANDE detector station is in detail described in chapter 8.5 and Appendix B.

Fig 6.5.3 shows the distribution of station IDs of the active GRANDE detector stations. The step in the otherwise very flat spectrum indicates that a single station was missing for some time.

Note: This value is always shipped if the 'GRANDE Energy Deposit' Quantity is selected but only in root and hdf5 files not in ASCII.
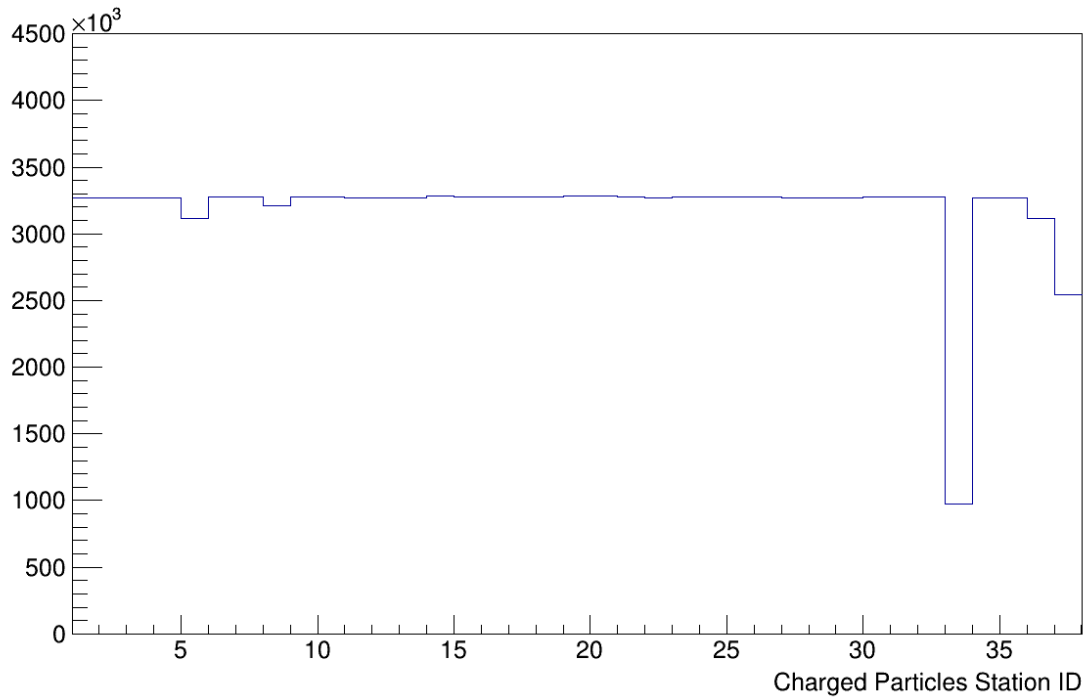
Fig. 6.5.3   *Distribution of station IDs for e/γ-detector stations*

6.6 ARRIVAL TIMES

The '**GRANDE Arrival Times'** of each GRANDE array station represents the first time stamp of each detector station that has been hit by a charged particle. When the electronic has recorded a signal above a certain threshold a signal is sent to the central data acquisition system, the GRANDE DAQ. The first signals of each station represent the shower front and are used to determine the shower direction.

The quantity '**GRANDE Arrival Time'** offers the possibility to reconstruct the shower disc and the arrival direction of the extensive air shower which hit GRANDE.

A detector station has to fulfil several conditions to be accepted as 'active detector station' for GRANDE arrival time analysis.

- the station was flagged as 'active'
- no overflow was detected in the station
- the station was not deselected for various reasons

A detector station which did not provide any time information was treated as 'silent station'.

Note: on the quantity 'GArrival' no cuts can be applied

Note: in chapter 8.4 are examples on how to handle the quantity 'GRANDE Arrival Times'

Handling the '**GArrival'** quantity mostly requires some additional information either on the absolute coordinates of the detector station or on the distance to the reconstructed shower core. Therefore the quantity **GArrivalS** is always supplied with the times values. Furthermore, the number of detector stations with valid arrival time information (**GArrivalN**) is provided as well.

Thus, if the quantity '**GRANDE Arrival Times'** is selected in the KCDC DataShop you will always be supplied with the following data sets:

GArrivalN	number of active GRANDE detector stations for this event [0 … 37]
GArrival	Arrival time in [ns] bins
GArrivalS	detector station ID [1…37]

6.6.1 Number of GRANDE detector stations with valid arrival times (GArrivalN)

The range of **GArrivalN** is between about 25 and 37. The distribution is shown in fig. 6.6.1. The lower limit is given by the trigger condition described in chapter 3.1.2.
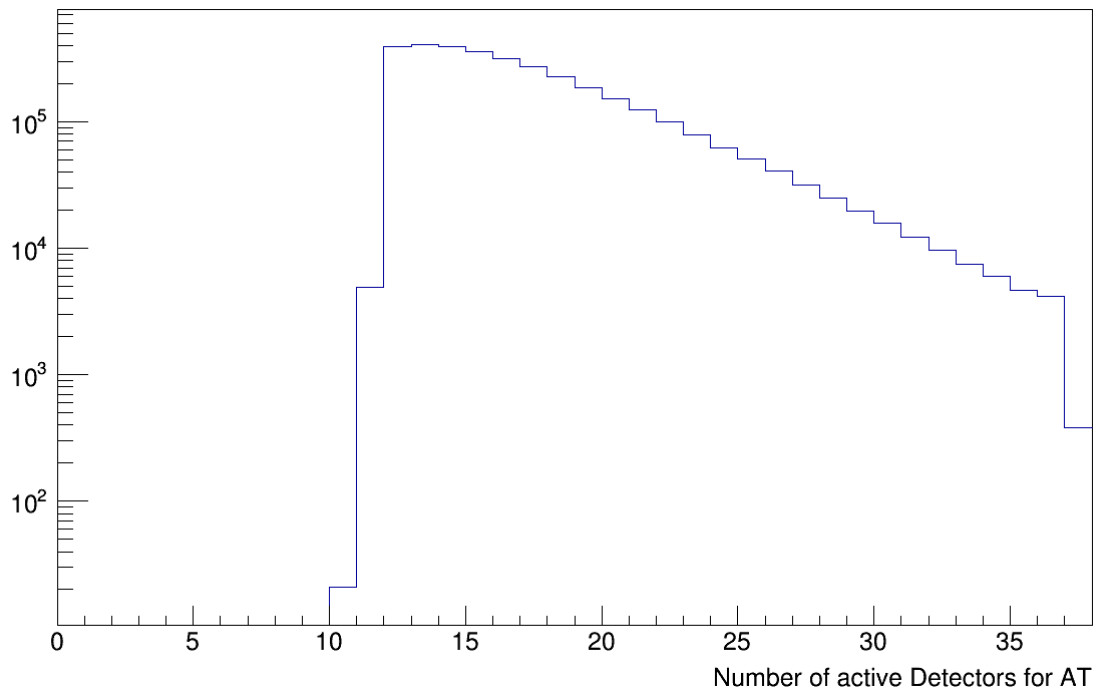
fig. 6.6.1.   *Distribution of the number of active detector stations for 'Arrival Times'*

6.6.2   Arrival Times per Station (GArrival)

The '**GRANDE Arrival Times**' are given with a resolution of 1ns/bin. Fig 6.6.2 shows the 'arrival time'– distribution.
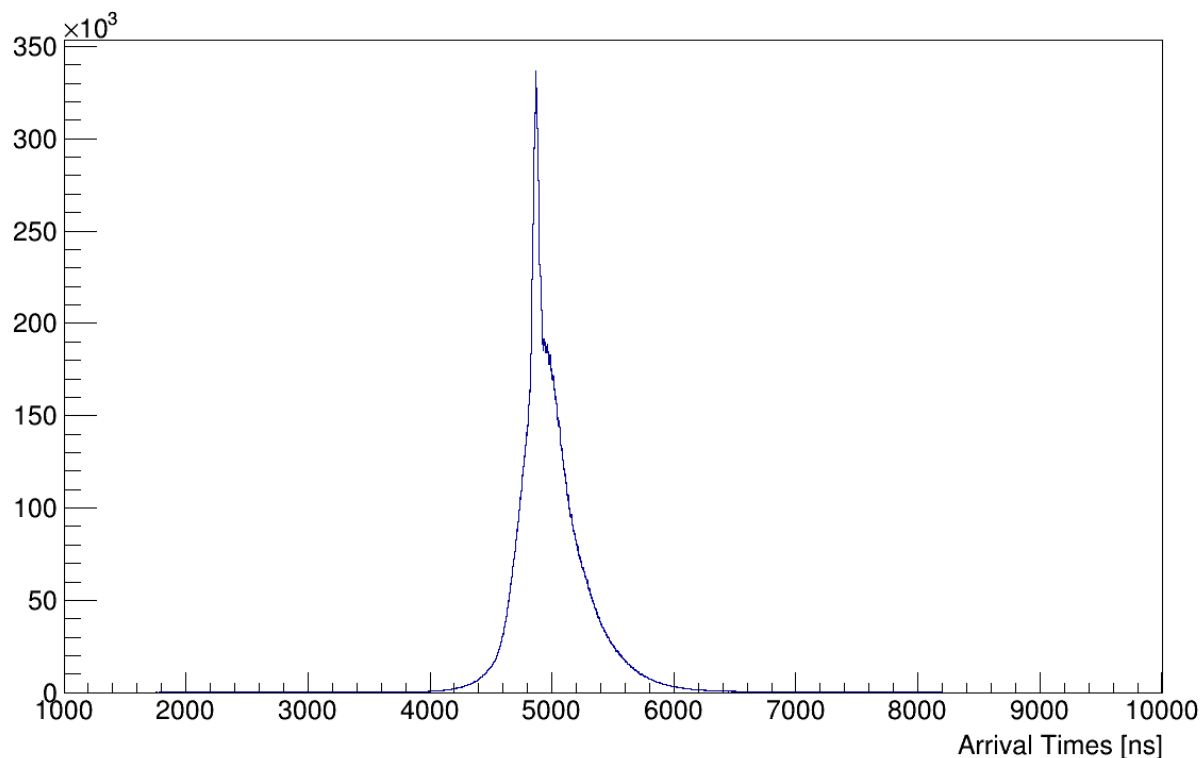
fig. 6.6.2   *GRANDE Arrival time distribution*

6.6.3   STATION ID (GARRIVALS)

The station ID holds the information of the location of the respective detector station. The transformation from the station ID to the GRANDE coordinates of the respective Grande detector station is in detail described in chapter 8.5 and Appendix B. Fig 6.6.3 shows the distribution of station IDs of the active detector stations. The structure is mostly caused by the area cut for the effective area in the core position of the GRANDE showers where some stations are outside these limits.

Note: This value is always shipped if the 'GRANDE Arrival Times' Quantity is selected but only in root and hdf5 files not in ASCII.
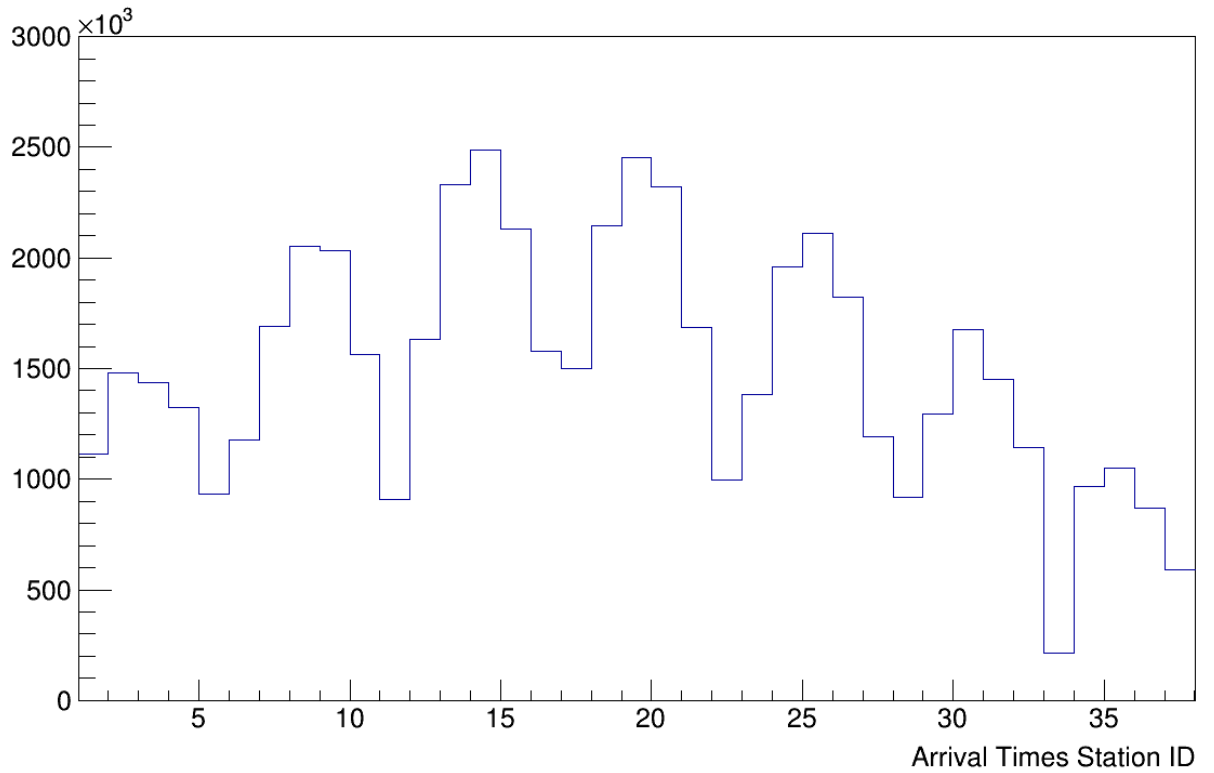
Fig. 6.6.3   *Distribution of station IDs for GRANDE detector stations with valid arrival times*

6.6.4   EXAMPLE

An example for the arrival time distribution of one event is given in fig 6.6.4. The warmer the colour the bigger the time difference which usually corresponds to larger zenith angles. The arrival time distribution and the large difference in the arrival time of about 1400ns indicate that the shower is coming from north-east direction at a zenith angle of about 25°.
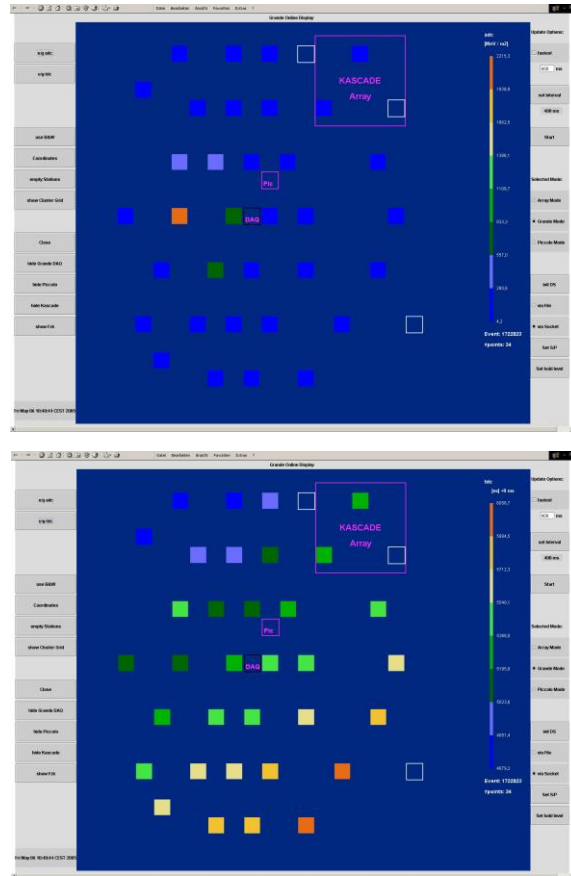
fig. 6.6.4   *Grande event No. 1722823 from 6.5.2005; energy deposit (left), arrival times (right)*

7 LOPES Data in KCDC

As described in chapter 2.7 the measured air showers from the radio antenna array LOPES (**LO**far **P**rototyp**E** **S**tation), are not part of the KASCADE main data stream. Nevertheless, they got a time stamp from the KASCADE trigger system to merge the measured data offline.

From the observables obtained in the analysis we choose 26 to be published in KCDC which can be selected and mostly applied cuts on via the KCDC Data Shop as **Quantities**.

LOPES Quantity	Description	Unit	ID
Measuring Data			
EfieldMaxAbs	maximum atmospheric electric field as measured by e-field mill	V/m	EfieldMaxAbs
Azimuth E-W	azimuth of LOPES CC beamforming reconstruction (East-West)	$°(degree)$	AzL_EW
Azimuth N-S	azimuth of LOPES CC beamforming reconstruction (North-South)	$°(degree)$	AzL_NS
Elevation E-W	elevation of LOPES CC beamforming reconstruction (East-West)		ElL_EW
Elevation N-S	elevation of LOPES CC beamforming reconstruction (North-South)		ElL_NS
CCheight E-W	amplitude of smoothed cross-correlation beam (East-West)	$\mu V/m/MHz$	CCheight_EW
CCheight N-S	amplitude of smoothed cross-correlation beam (North-South)	$\mu V/m/MHz$	CCheight_NS
Xheight E-W	amplitude of X-beam (East-West)	$\mu V/m/MHz$	Xheight_EW
Xheight N-S	amplitude of X-beam (North-South)	$\mu V/m/MHz$	Xheight_NS
rmsCCbeam E-W	RMS of CC beam in noise window (East-West)	$\mu V/m/MHz$	rmsCCbeam_EW

rmsCCbeam N-S	RMS of CC beam in noise window (North-South)	μV/m/MHz	rmsCCbeam_NS
Number of Antennas E-W	number of antennas contributing to CC beam (East-West)	(number of)	NCCbeamAntennas _EW
Number of Antennas N-S	number of antennas contributing to CC beam (North-South)	(number of)	NCCbeamAntennas _NS
ConeAngle E-W	cone angle rho of hyperbolic wave-front reconstructed with CCbeam forming (East-West)	°(degree)	coneAngle_EW
ConeAngle N-S	cone angle rho of hyperbolic wave-front reconstructed with CCbeam forming (North-South)	°(degree)	coneAngle_NS
Eta E-W	slope parameter of exponential LDF (East-West)	1/m	eta_EW
Eta N-S	slope parameter of exponential LDF (North-South)	1/m	eta_NS
Eps E-W	amplitude parameter of exponential LDF (East-West)	μV/m/MHz	eps_EW
Eps N-S	amplitude parameter of exponential LDF (North-South)	μV/m/MHz	eps_NS
Geomag Angle	angle between geomagnetic field and KASCADE shower axis	°(degree)	geomag_angle
Geomag AngleG	angle between geomagnetic field and GRANDE shower axis	°(degree)	geomag_angleg
Reconstruction	Reconstruction used as Input for LOPES: A = KASCADE ('array') 65; G = Grande 71		reconstruction
LOPES Component Identifier	used to identify an event with Lopes data 1 = with LOPES data 0 = no LOPES data		Lopes_Comp_ID
Height	amplitude of pulse (after correction for noise)	μV/m/MHz	height[30]

Distance	distance of antenna position to shower axis	m	dist[30]
EnvelopeTime	time of maximum envelope	ns	envelopeTime[30]
Polarization	alignment of antennas (EW or NS)		polarization[30]

The plots shown in this chapter are only examples. So, applying user cuts either in the KCDC Data Shop or in your own analysis can change these spectra drastically.

7.1   EFILEDMAXABS

The e-field has been measured on KASCADE site in the centre of the LOPES array by means of an e-field mill 3m above the ground taking data every second.

During fair weather, the electric field at ground level has a value between -100 V/m and -200 V/m. Occurring small changes are slow, with a typical time scale in the range of minutes. However, when a thunderstorm occurs, the conditions change quite drastically. Ground field strength may exceed ± 20 kV/m. In addition, lightenings are visible as discontinuities in the recorded data. Thus for 'normal' analyses a cut is applied removing events recorded during conditions with an e-field higher than 3000 V/m.
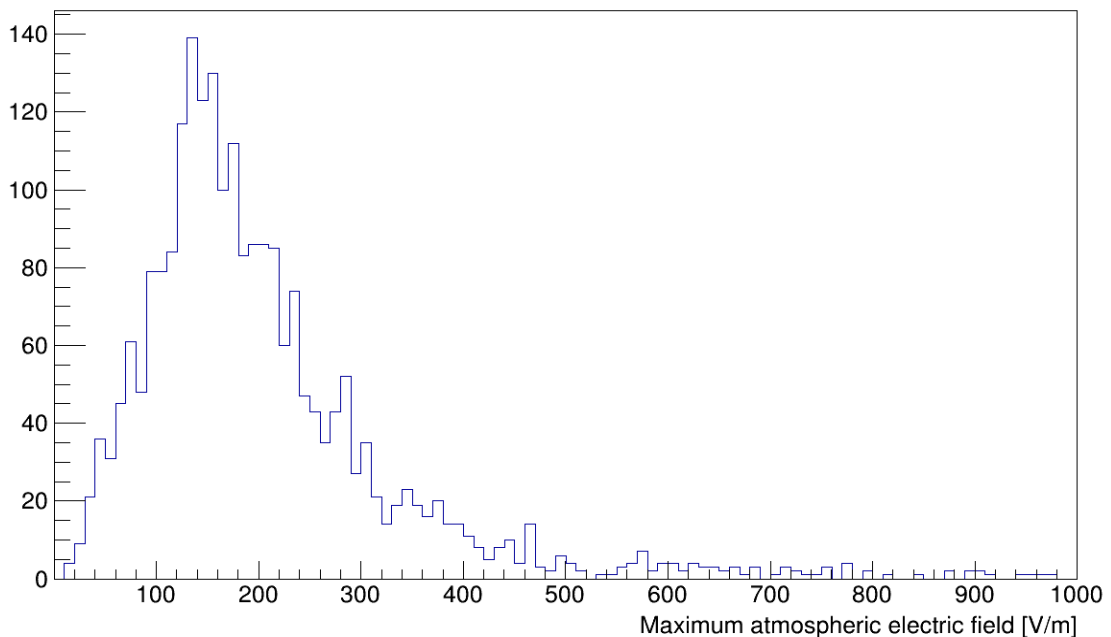
fig. 7.1.1   *E-filed distribution as measured by the e-field mill (absolute value)*

7.2 AzL_EW & AzL_NS AND ElL_EW & ElL_NS

AzL_EW/AzL_NS and ElL_EW/ElL_NS describe the direction reconstructed using the cross-correlation beamforming for the east-west and north-south aligned antennas respectively. The LOPES coordinates are defined analogously to KASCADE. So the Azimuth AzL is defined as Az, the Elevation ElL equals 90°-Ze, so ElL=90° points upwards. During the maximization of the CC-beam, the assumed arrival direction of the shower is changed according to a defined grid on the sky. This grid is centred on the arrival direction reconstructed by KASCADE(-Grande), which is used as a starting value. For each arrival direction the expected time difference of the LOPES time trace is calculated and corrected for. Then the CC-beam is maximized using a simplex fit varying the direction, see also 7.3. Thus, the reconstructed direction is those yielding the maximum value for the smoothed CC-beam.
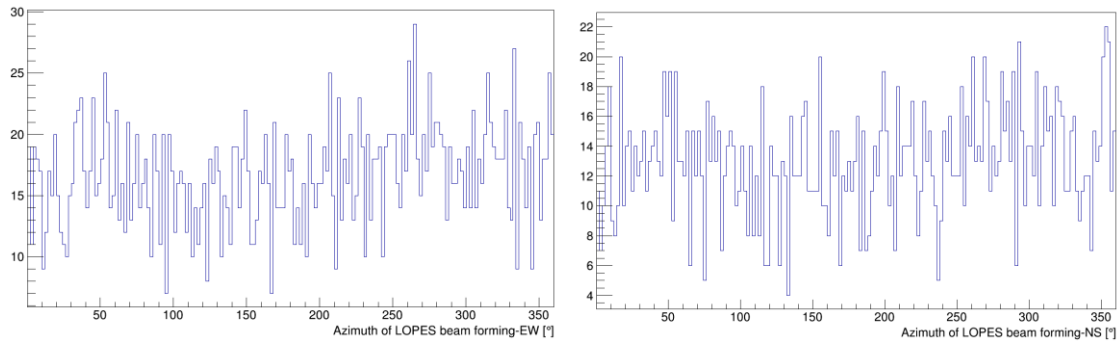
fig. 7.2.1   *Azimuth of LOPES CCbeam forming reconstruction*

left: East-West orientation; right: North-South orientation
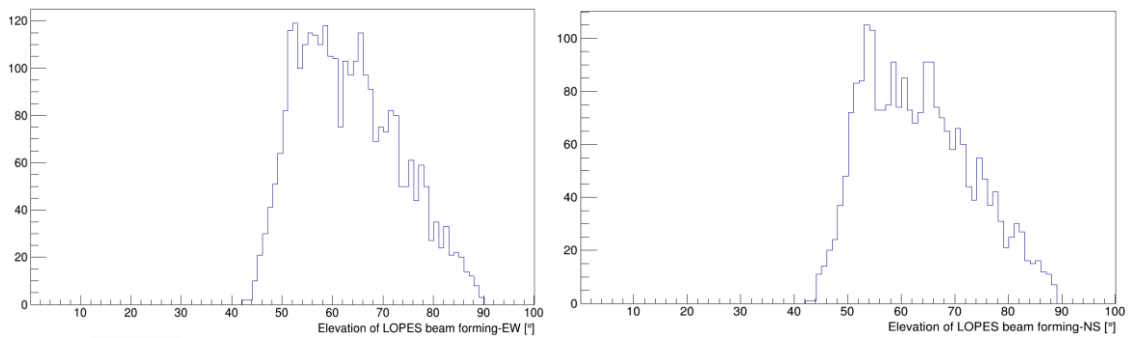
fig. 7.2.2   *Elevation of LOPES CCbeam forming reconstruction*

left: East-West orientation; right: North-South orientation

7.3 CCHEIGHT_EW & CCHEIGHT_NS AND RMSCCBEAM_EW & RMSCCBEAM_NS

The CCheight is the maximum value of the smoothed cross-correlation beam which is determined as follows:

According to the arrival direction and the distance of the air shower a geometrical delay of the signal in each antenna is calculated. The shower core is given by KASCADE-(Grande). This delay depends on the shape of the radio wave front. Investigations on measured and simulated radio signals show that a hyperbolic shape is the best approximation for the radio wave front. For larger distances this hyperboloid approaches an asymptotic cone. Such a hyperbolic shape is parametrized using the following formula:

$$c\tau(d, z_s) = \sqrt{(dsin\rho)^2 + (cb)^2} + z_s cos\rho + cb$$

With the lateral distance of the antenna to the shower axis d, the distance of the antenna to the shower plane z_s and the two parameters ρ for the opening angle of the asymptotic cone and b describing the time offset between the hyperboloid and the asymptotic cone at the shower axis. According to the expected arrival time of the signal, calculated with the formula above, the time traces are shifted in such a way that after the shift the radio signal is seen at the same time in all antennas.

Then the directional sensitivity of the antenna is considered by the application of the antenna gain. In a final step the cross correlation beam, CC-beam, is calculated using the following equation:

$$cc(t) = \pm \sqrt{\left| \frac{1}{N_{pairs}} \sum_{i=1}^{N_{Ant}-1} \sum_{i>j}^{N_{Ant}} s_i(t) \cdot s_j(t) \right|}$$

With N_{Ant} being the number of Antennas, N_{pairs} the number of unique pairs, the time t and the time-shifted traces of the particular antennas $s_{i/j}(t)$.

To suppress fine structure coming from the bandpass filtering, the CC beam is smoothed by applying a block-averaging over the lengths of three raw samples (37.5 ns; which contain more than three samples when upsampling is used in the reconstruction). Then the

arrival direction and the cone angle ρ are changed according to a defined grid on the sky and the CC-beam is maximized using a simplex fit. The arrival direction reconstructed by KASCADE-Grande is used as a starting value.

Finally, a Gaussian function is fitted to the CC-beam which provides the information on time and height of the CC-beam. The time is used to identify the time of the signal in the individual antennas, see 7.11.

Additionally, the RMS value of the CC-beam is calculated which is a measure for the background. The ratio of the CCheight and the RMS of the CC-beam, thus, is a signal-to-noise ratio.A cut is applied rejecting events with a low ratio, where the threshold is 14 or lower, depending on the number of antennas contributing to the CC-beam:

$$CCheight/rmsCCbeam > 14 * \sqrt{(N_{Ant}/30)}$$
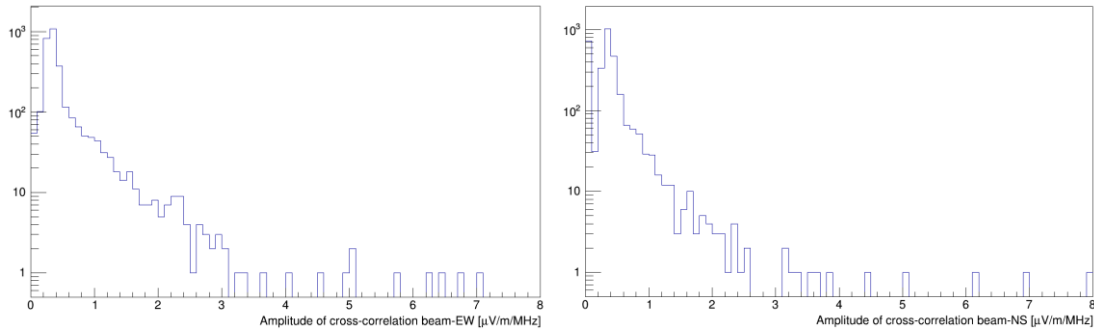
fig. 7.3.1   *Amplitude of smoothed cross correlation beam*
                    left: East-West orientation; right: North-South orientation

7.4   XHEIGHT_EW & XHEIGHT_NS

The X-beam or excess beam x(t) is calculated from the block averaged (BA) CC-beam and power beam like:

$$x(t) = cc(t) \cdot \left| \frac{\langle cc(t) \rangle_{BA}}{\langle p(t) \rangle_{BA}} \right|$$

Then a Gaussian function is fitted providing the height of the X-beam. The Xheight is used as quality cut for the radio data: The fraction of power in the CC-beam compared to the

total power is an important quantity for the quality of LOPES events and can be determined from the ratio of the Xheight divided by the CCheight, which needs to be between 0.8 and 1.5 for an event to pass the following quality cut:

$$0.8 > \frac{Xheight}{CCheight} < 1.5$$
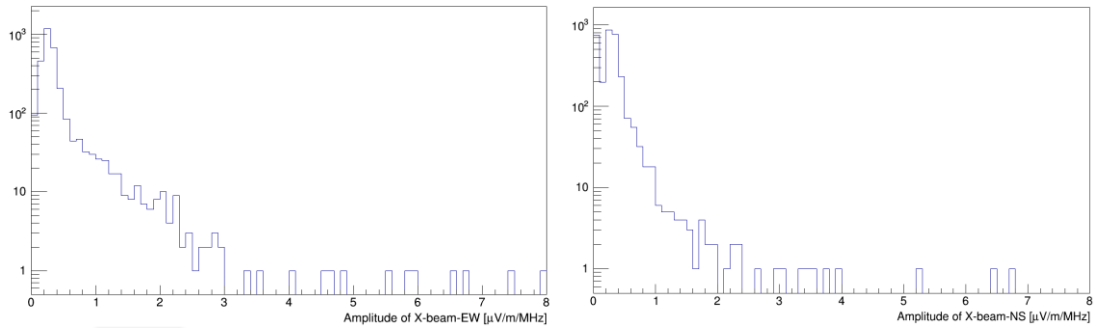
fig. 7.4.1   *Amplitude of X-beam*

left: East-West orientation; right: North-South orientation

7.5   NCCʙᴇᴀᴍAɴᴛᴇɴɴᴀs_EW NCCʙᴇᴀᴍAɴᴛᴇɴɴᴀs_NS

NccbeamAntennas_EW/NS are the numbers of antennas used for the calculation of the CC-beam, so the number of antennas N_{Ant}.
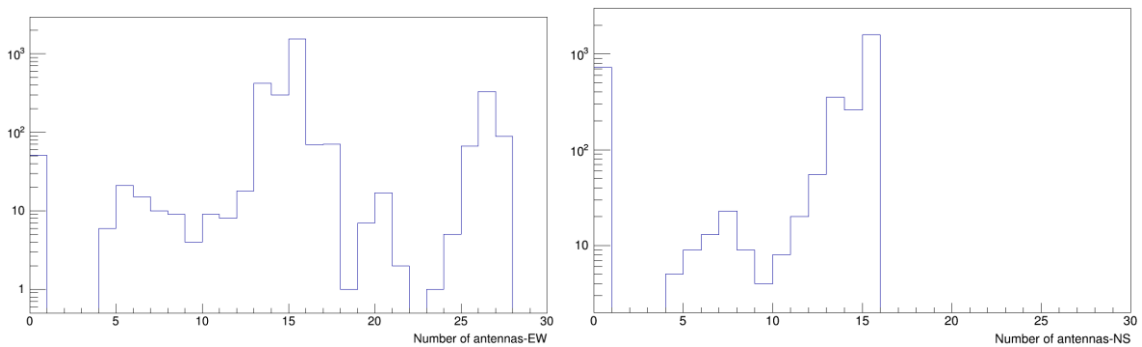
fig. 7.5.1   *number of antennas contributing to CC beam*

left: East-West orientation; right: North-South orientation

This number can vary due to different setups, inactive or malfunctioning antennas.

7.6   CONEANGLE_EW & CONEANGLE_NS

The cone angle is derived during the maximization of the CCbeam, see 7.4. The radio wave front is approximated by a hyperbolic shape, which is parametrized, using the following formula:

$$c\tau(d, z_s) = \sqrt{(dsin\rho)^2 + (cb)^2} + z_s cos\rho + cb$$

With the lateral distance of the antenna to the shower axis d, the distance of the antenna to the shower plane z_s and the two parameters ρ for the opening angle of the asymptotic cone and b describing the time offset between the hyperboloid and the asymptotic cone at the shower axis. The cone angle corresponding to the maximized CCbeam is given here.
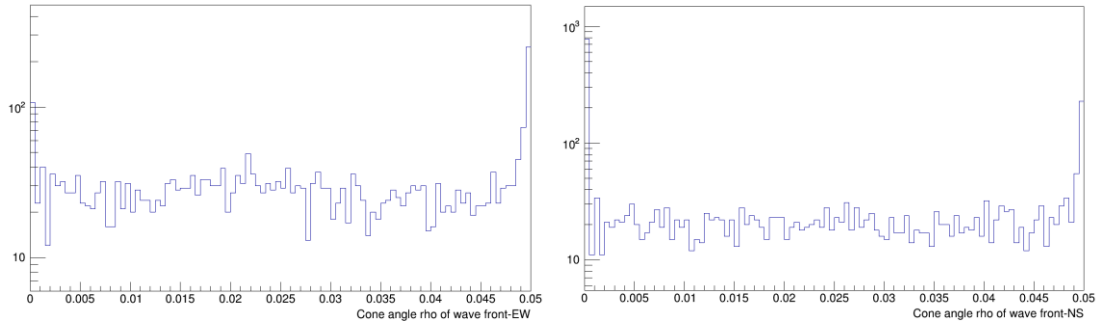
fig. 7.6.1   *cone angle rho of hyperbolic wave front*
                    left: East-West orientation; right: North-South orientation

7.7   ETA_EW & ETA_NS AND EPS_EW & EPS_NS

The lateral distribution, i.e. the amplitude of the radio pulse ε vs the lateral distance to the shower axis d of each antenna, is fitted using an exponential function:

$$\varepsilon(d) = \varepsilon_{100} \cdot exp[-\eta(d - 100m)]$$

with the fit parameters ε_{100} which is the amplitude eps_EW/NS at 100m axis distance, and η which is the lateral slope eta_EW/NS.

This is a simplified assumption assuming a radial symmetry of the radio signal around the shower axis, neglecting the small asymmetry due to the interference of the geomagnetic

and Askaryan effects for the radio emission. The lateral distribution also neglects that for some showers, the radio amplitude first rises until reaching the distance of the Cherenkov cone and decreases only for larger distances. For those events dominated by the rising inner part of the lateral distribution, thus, a negative value of η is expected.
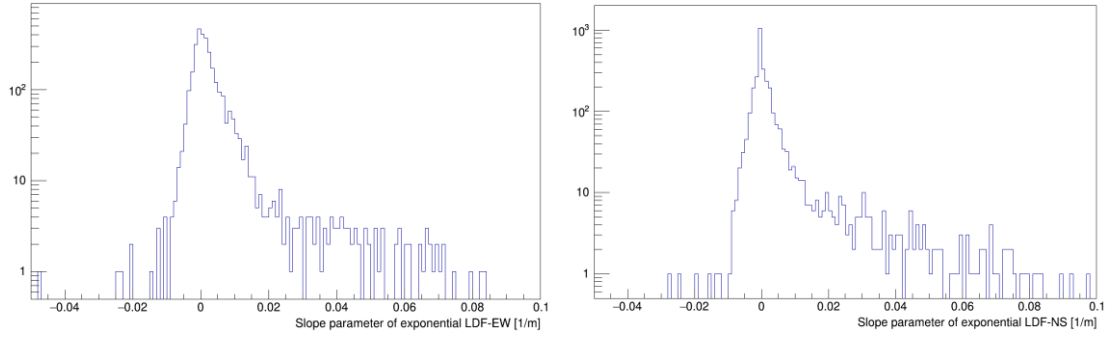
fig. 7.7.1　　*η slope parameter of exponential LDF*

left: East-West orientation; right: North-South orientation
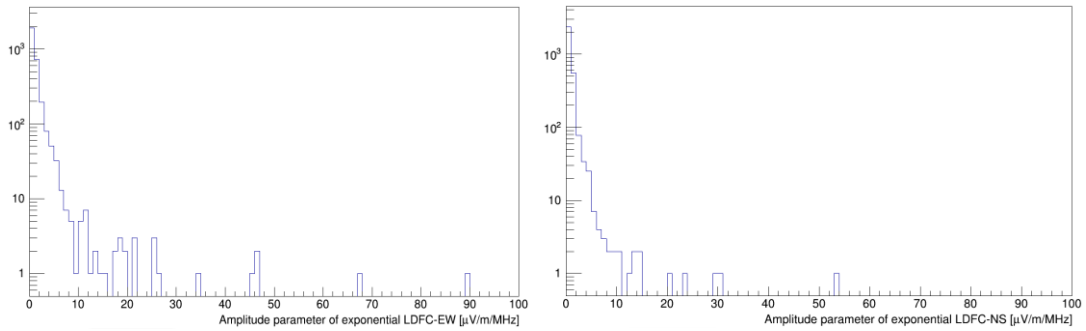
fig. 7.7.2　　*ε amplitude parameter of exponential LDF*

left: East-West orientation; right: North-South orientation

7.8　Geomag_Angle and Geomag_AngleG

The radio signal strongly depends on the angle between the shower axis and the Earth's magnetic field called geomagnetic angle. Therefore, this value is provided here. It is calculated using either the KASCADE or KASCADE-Grande shower coordinates Az/AzG and Ze/ZeG and the direction of the magnetic field in Karlsruhe which is along BAz = 0° and BZe = 64.4°.

113
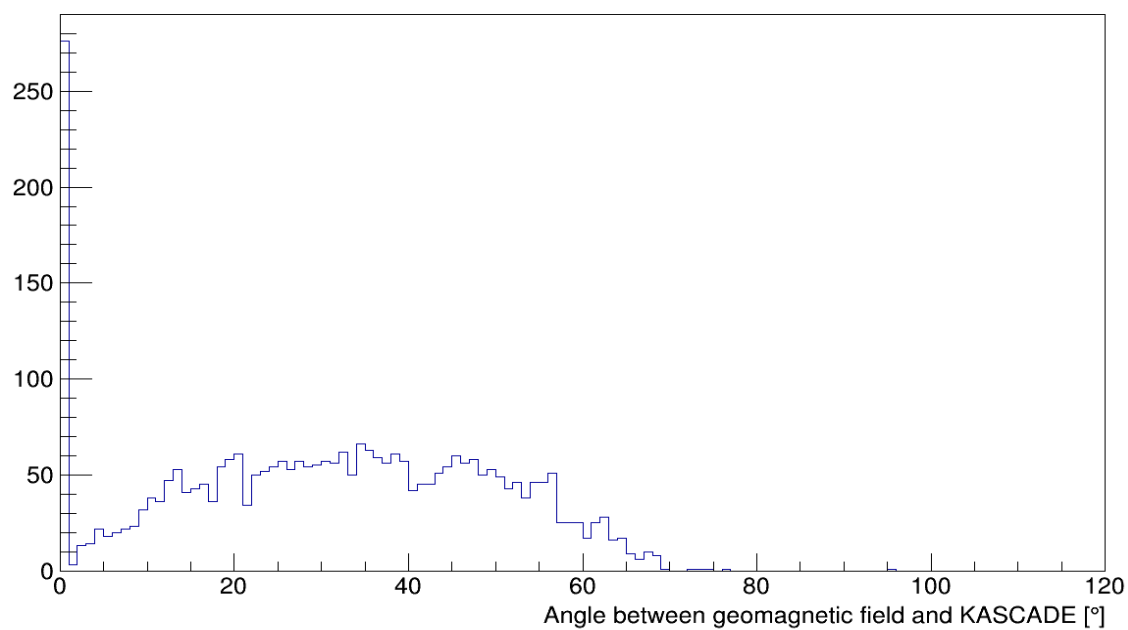
fig. 7.8.1   *angle between geomagnetic field and KASCADE shower axis*
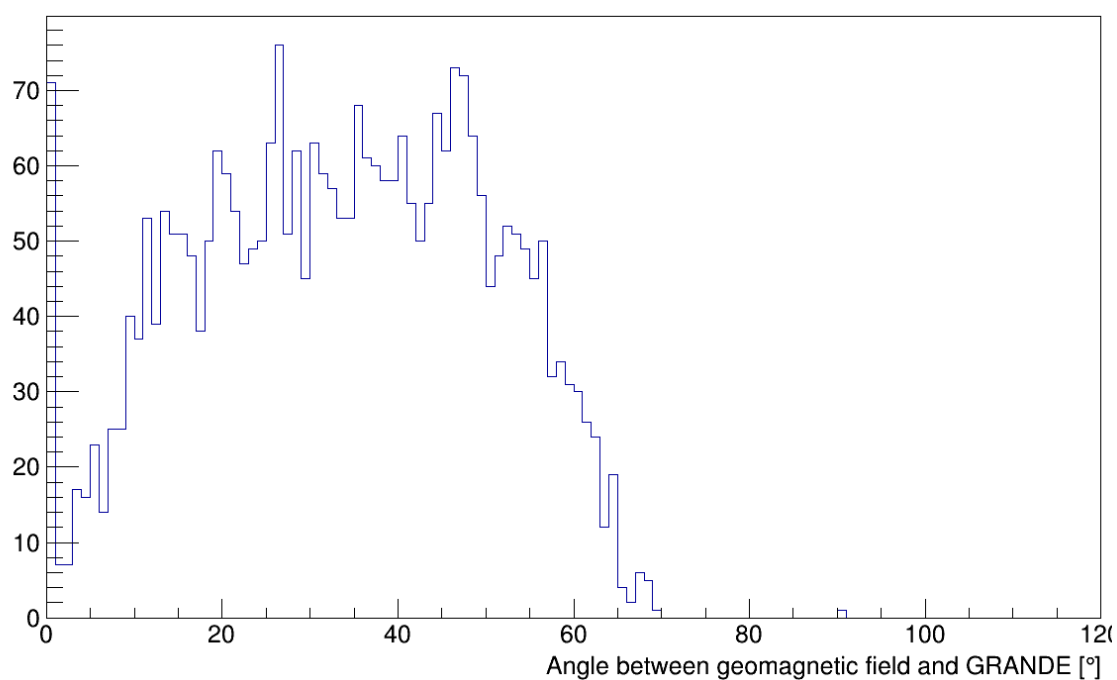
fig. 7.8.2   *angle between geomagnetic field and GRANDE shower axis*

7.9   RECONSTRUCTION

The reconstruction parameter indicates whether KASCADE or KASCADE-Grande input parameters (such as Az, Ze, energy) are used. The decision if the LOPES reconstruction is done using the KASCADE data or the Grande data is taken only from the core position of the reconstructed shower. The reconstruction parameter can either be A=65 for KASCADE("Array") or G=71 for Grande.
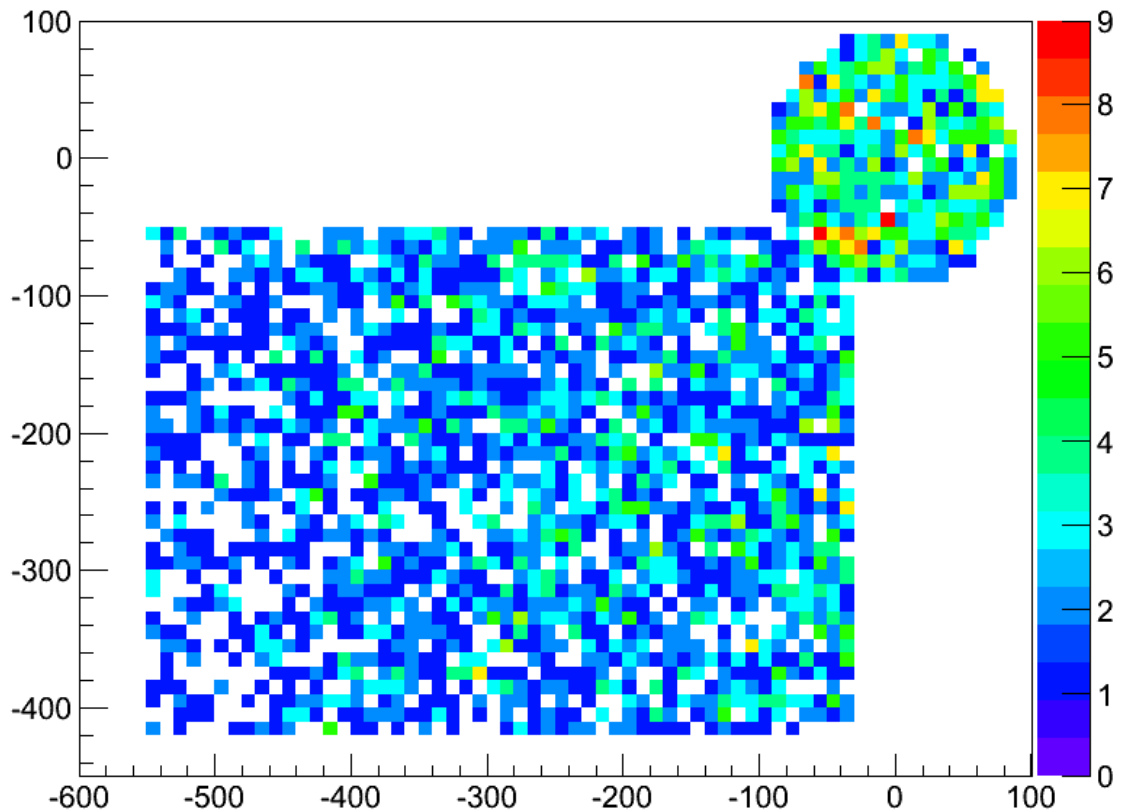
fig. 7.9.1   *core position of the reconstructed showers*

7.10   LOPES COMP ID

The LOPES Component Identifier is a technical parameter to select events with Lopes Radio data directly. The 'LopesCompID' for all Lopes events is set to '1'. If you want to select only data sets with Lopes content you will have to apply a cut in the DataShop from '1' to '1' for the LopesCompID.

7.11 HEIGHT

The height is the amplitude of the radio pulse at each antenna after noise correction and after pulse identification using the time of the CC-beam maximum. The calculation of the CC-beam enables the identification of the pulse induced by the air shower: RFI, e.g., induced by the KASCADE detectors, is usually incoherent while the radio pulse from an air shower is coherent. The CC-beam therefore allows identifying the time of the air-shower signal. This information is used to get the radio pulse amplitude measured by individual antennas. With the timing information from the CC-beam, the maximum pulse amplitude in each antenna is determined by choosing the nearest local maximum of the Hilbert envelope of the trace (i.e., the nearest local maximum of the instantaneous amplitude). For the amplitude at the individual antennas also the influence of noise is considered: Investigations show that noise can increase or decrease the signal depending on the signal-to-noise ratio and a noise correction is applied individually for each antenna correcting for the average effect at the corresponding signal-to-noise ratio.

Note: on the quantity 'LOPES Height' no cuts can be applied

Handling the data array '**Lopes Height'** quantity mostly requires some additional information either on the absolute coordinates of the detector station or on the distance to the reconstructed shower core. Therefore the quantity '**heightS'** is always supplied with the '**height'** values. Furthermore, the number of detector stations with valid '**height'** information ('**heightN'**) is provided as well.

Thus, if the quantity '**Lopes Height'** is selected in the KCDC DataShop you will always be supplied with the following data sets:

heightN	number of active LOPES detector stations for this event [0 … 30]
height	amplitude of the radio pulse [μV/m/MHz]
heightS	detector station ID used for **height** [1…30]

7.11.1 NUMBER OF LOPES DETECTOR STATIONS WITH HEIGHT INFORMATION (HEIGHTN)

The distribution of '**heightN**' is shown in fig. 7.11.1. (left).

Note: This value is always shipped if the 'LOPES Height' Quantity is selected but only in root and hdf5 files not in ASCII.
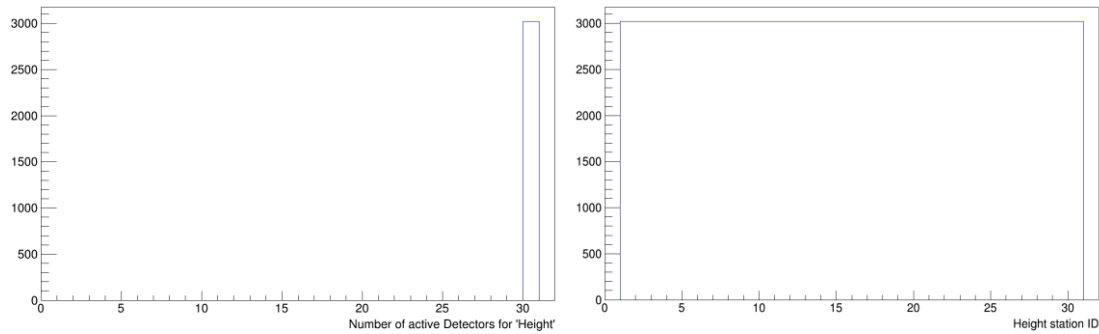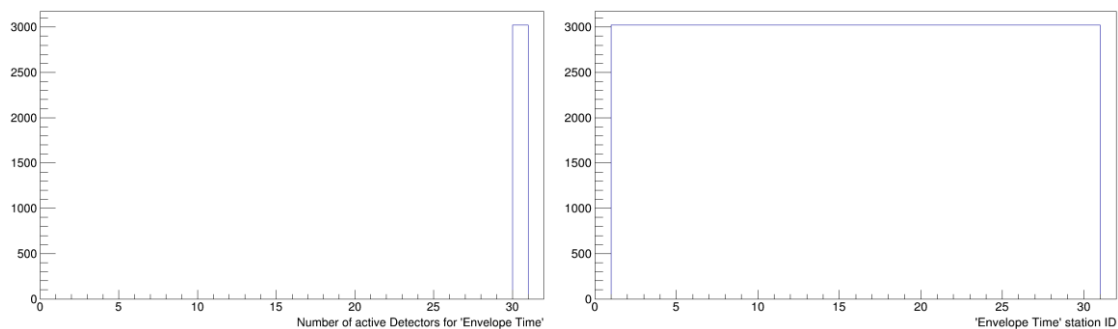

fig. 7.11.1.   *Distribution of the number of active detector stations for 'LOPES Height' (left) and the distribution of station IDs (right)*

7.11.2 STATION ID (HEIGHTS)

The station ID holds the information of the location of the respective detector station. The transformation from the station ID to the LOPES coordinates of the respective LOPES detector station is in detail described in Appendix C. Fig 7.11.1 (right) shows the distribution of station IDs of the active detector stations.

Note: This value is always shipped if the 'LOPES Height' Quantity is selected but only in root and hdf5 files not in ASCII.

7.11.3 HEIGHT PER STATION (HEIGHT)

The '**LOPES Height'** distribution is shown in fig 7.11.2.
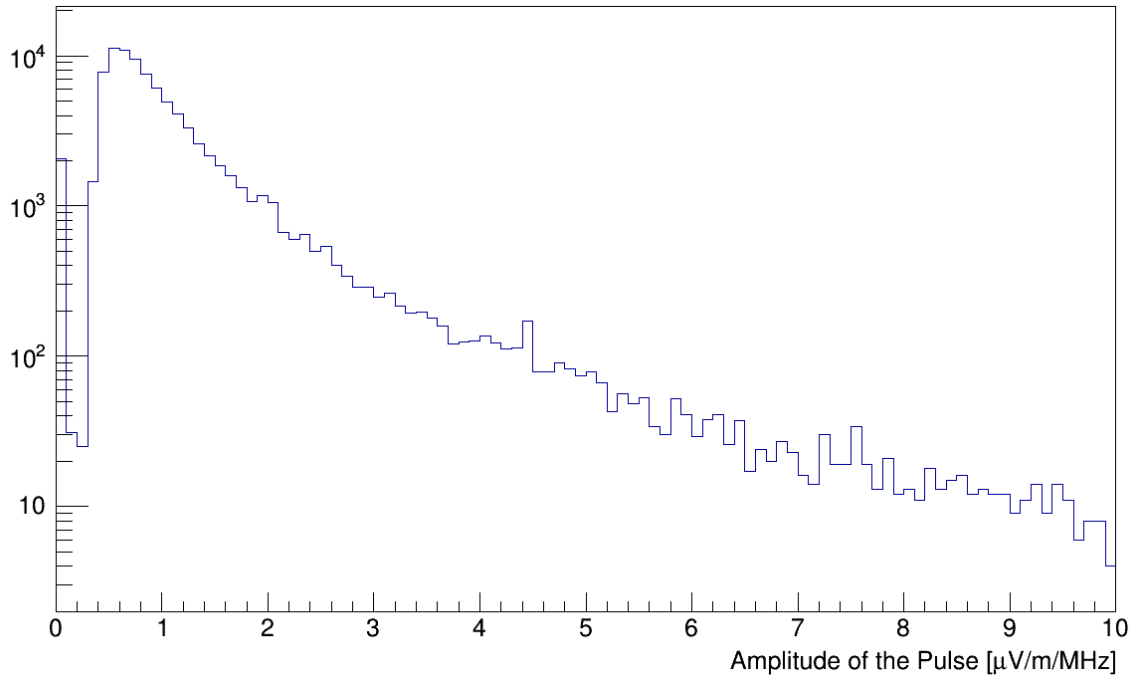
fig. 7.11.2   *amplitude of pulse after noise correction*

7.12   ENVELOPETIME

The envelope time is the time in the trace of each individual antenna at which the pulse amplitude (height) is determined. Consequently, this is the time of the local maximum of the Hilbert envelope closest to the signal arrival time determined by the CC-beam. Typically, it can be up to a few 10 ns earlier or later than this CC-beam time.

Note: on the quantity 'LOPES Envelop Time' no cuts can be applied.

Handling the data arrays '**Lopes Envelope Time**' quantity mostly requires some additional information either on the absolute coordinates of the detector station or on the distance to the reconstructed shower core. Therefore the quantity '**envelopeTimeS**' is always supplied with the '**envelopeTime**' values. Furthermore, the number of detector stations with valid '**envelopeTime**' information ('**envelopeTimeN**') is provided as well.

Thus, if the quantity '**Lopes envelopeTime' is** selected in the KCDC DataShop you will always be supplied with the following data sets:

envelopeTimeN	number of active LOPES detector stations for this event [0 … 30]
envelopeTime	Time of maximum of envelope [ns]
envelopeTime S	detector station ID used for **envelope Time** [1…30]

7.12.1 NUMBER OF LOPES DETECTOR STATIONS WITH ENVELOPETIME INFORMATION (ENVELOPETIMEN)

The distribution of '**envelopeTimeN**' is shown in fig. 7.12.1. (left).

Note: This value is always shipped if the 'LOPES envelopeTime' Quantity is selected but only in root and hdf5 files not in ASCII.
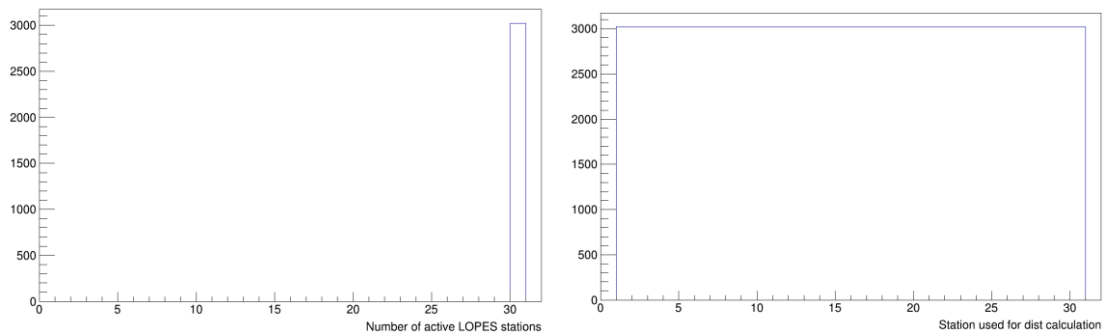

fig. 7.12.1. *Distribution of the number of active detector stations for 'LOPES envelopeTime' (left) and the distribution of station IDs (right)*

7.12.2 STATION ID (ENVELOPETIMES)

The station ID holds the information of the location of the respective detector station. The transformation from the station ID to the LOPES coordinates of the respective LOPES detector station is in detail described in Appendix C. Fig 7.12.1 (right) shows the distribution of station IDs of the active detector stations.

Note: This value is always shipped if the 'LOPES EnvelopeTime' Quantity is selected but only in root and hdf5 files not in ASCII.

7.12.3 ENVELOPE TIME PER STATION (ENVELOPETIME)

The '**LOPES envelopeTime**' distribution is shown in fig 7.12.2.
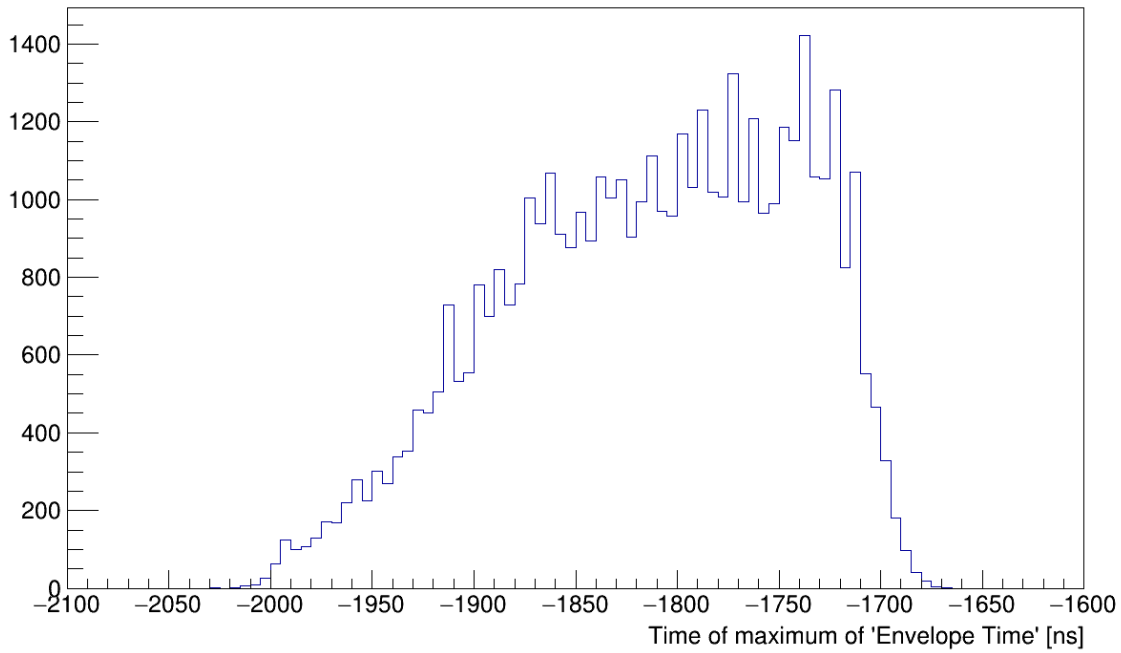
fig. 7.12.2 *time of maximum of envelop*

7.13 DISTANCE TO SHOWER AXIS

The distance **d** is the lateral distance of the antenna position of a single antenna to the shower axis, reconstructed with LOPES, which is used for the reconstruction of the lateral distribution (the standard wave front reconstruction is by the CC-beam, which turned out to be more stable than the reconstruction using the envelopeTime and distance in the individual antennas).

Handling the data array '**Lopes Distance**' quantity mostly requires some additional information either on the absolute coordinates of the detector station or on the distance to the reconstructed shower core. Therefore the quantity '**distanceS**' is always supplied with the '**distance**' values. Furthermore, the number of detector stations with valid **distance** information ('**distanceN**') is provided as well.

Thus, if the quantity '**Lopes Distance**' is selected in the KCDC DataShop you will always be supplied with the following data sets:

distN	number of active LOPES detector stations for this event [0 … 30]
dist	distance to the shower axis [m]
distS	detector station ID used for **dist** [1…30]

7.13.1 NUMBER OF LOPES DETECTOR STATIONS WITH DISTANCE INFORMATION (DISTN)

The distribution of distN is shown in fig. 7.13.1. (left).

Note: This value is always shipped if the 'LOPES Distance' Quantity is selected but only in root and hdf5 files not in ASCII.

fig. 7.13.1.   *Distribution of the number of active detector stations for 'LOPES Distance' (left) and the distribution of station IDs (right)*

7.13.2 STATION ID (DISTS)

The station ID holds the information of the location of the respective detector station. The transformation from the station ID to the LOPES coordinates of the respective LOPES detector station is in detail described in Appendix C. Fig 7.13.1 (right) shows the distribution of station IDs of the active detector stations.

Note: This value is always shipped if the 'LOPES Distance' Quantity is selected but only in root and hdf5 files not in ASCII.

7.13.3 DISTANCES PER STATION (DIST)

The '**LOPES Distance**' distribution is shown in fig 7.13.2.
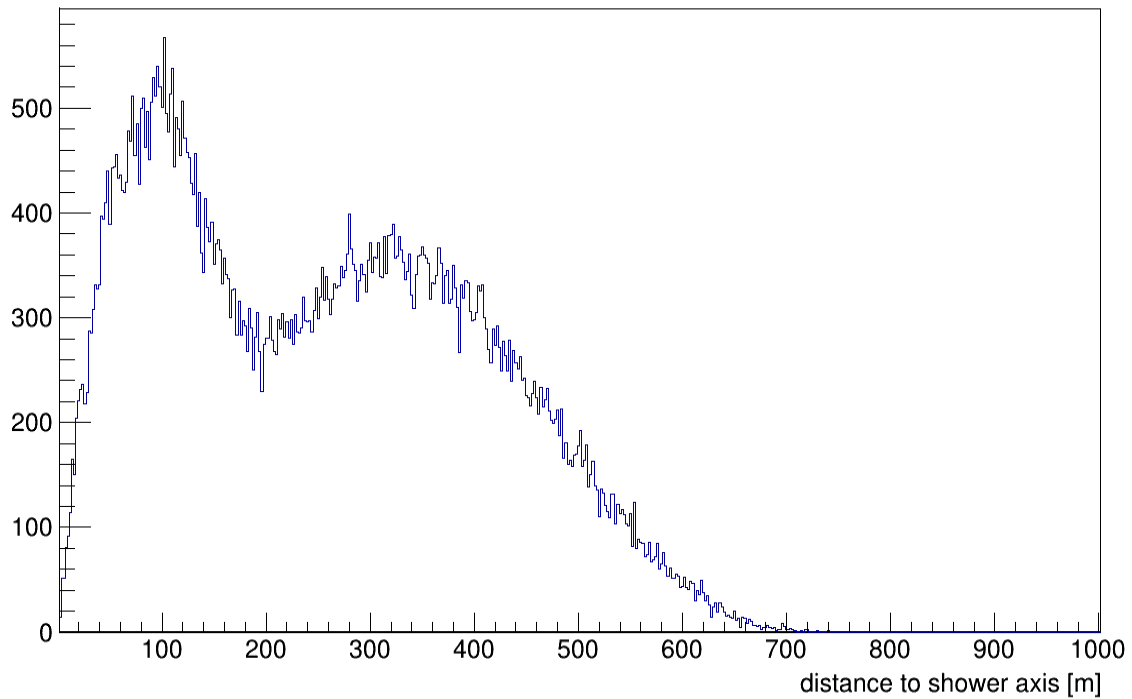
fig. 7.13.2   *distance of antenna position to shower axis*

7.14 POLARIZATION

The polarization is the alignment of the antenna, which is either EW – along the east-west axis or NS – along the north-south axis. This value can change for different setups. For both sets of antennas (EW) and (NS), the reconstruction is run separately and independently from each other.
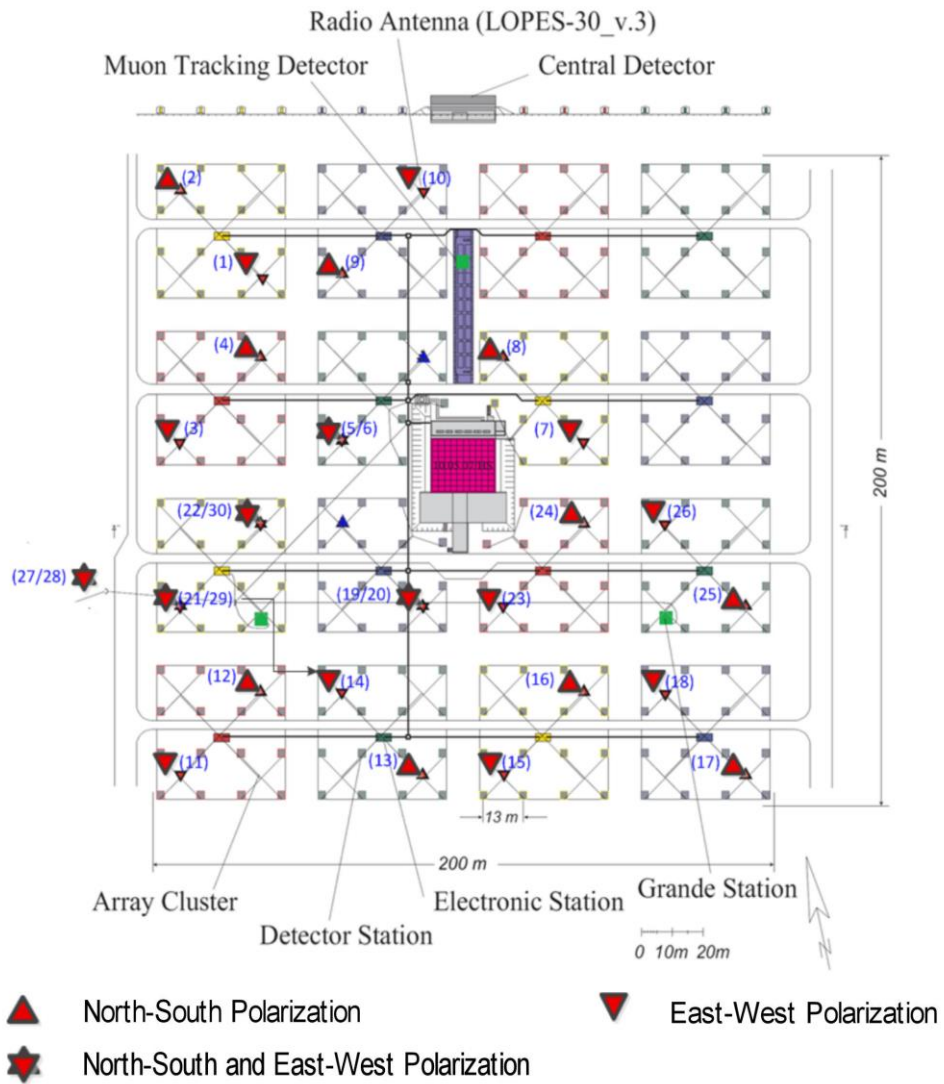
Fig. 7.14.1   *Polarization of the LOPES-30 radio antennas*

In the data sets provided to the users, '0' denotes an antenna polarization in North-South direction, '1' stands for East-West polarization. Five antenna positions are equipped with antennas in both directions (see also app. C).

8 DATA ANALYSIS HELPS

This chapter provides some valuable information on how to deal with the KASCADE and GRANDE data, based on the experience of more than 20 years of data analysis.

8.1 EFFICIENCIES

KASCADE reaches its full detection- and reconstruction efficiency at around $\log(N_e)=5$ which corresponds roughly to a reconstructed energy of about 10^{15} eV. This implies that below this value you will have to deal with efficiency corrections and threshold effects. Some of these effects are described in chapter 4, p.e. the N_μ distribution at low energies in fig. 4.2.2.

The study of the detector efficiency has been done by means Monte Carlo Simulations where the respective efficiency curves for proton- and iron-induced showers have been investigated. The upper picture of fig 8.1.1 shows the pure N_e efficiency curves for trigger efficiency (filled symbols) and in combination with reconstruction efficiency (open symbols). The lower picture indicates that trigger- and reconstruction reaches its full efficiency around 10^{15} eV reconstructed energy. This apparent discrepancy is based on the fact that for reconstruction of the primary energy not only N_e but also the N_μ reconstruction is required. This corresponds to $\log(Ne)>5$ (see chapter 4.2) .

For **GRANDE**, the trigger and reconstruction efficiencies of air showers, after applying all quality and fiducial area cuts as well as the requirement of a successful shower size and muon number reconstruction, are shown in fig 8.1.2 as a function of the simulated total number of charged particles and the primary energy for different primaries. They are computed by means of full simulations of the shower development and detector response. Efficiencies above one are due to cuts on the reconstructed core positions, i.e. events falling outside the selected area can be reconstructed inside. Concerning N_{ch}, primary iron reaches earlier the maximum efficiency, as for lower energy showers the geometrical structure of the Grande array requires already muons for triggering these events.
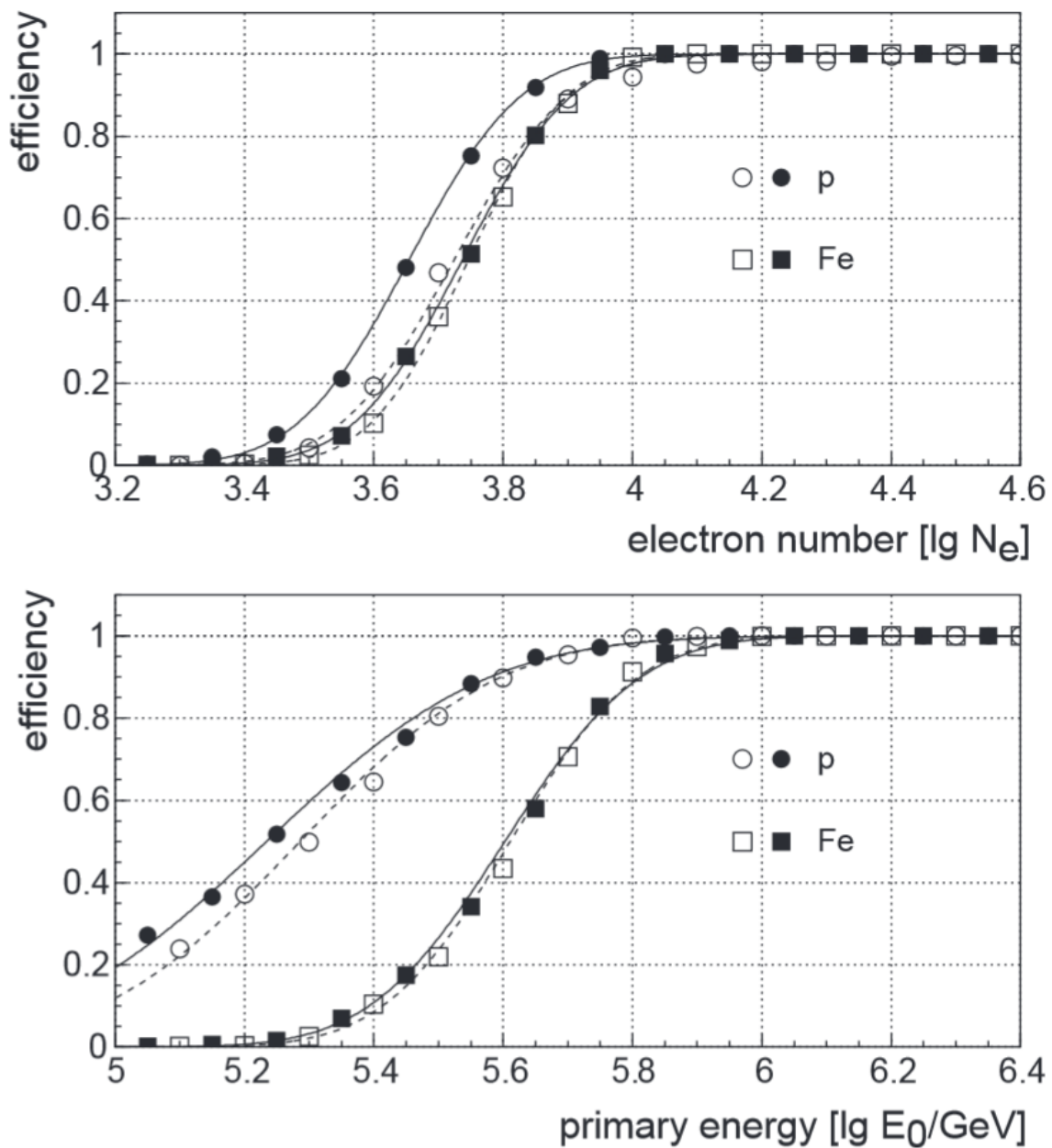
Fig. 8.1.1 *KASCADE detector efficiency for simulated proton- and iron-induced showers (see text); trigger efficiency (filled symbols) combined with reconstruction efficiency (open symbols)*
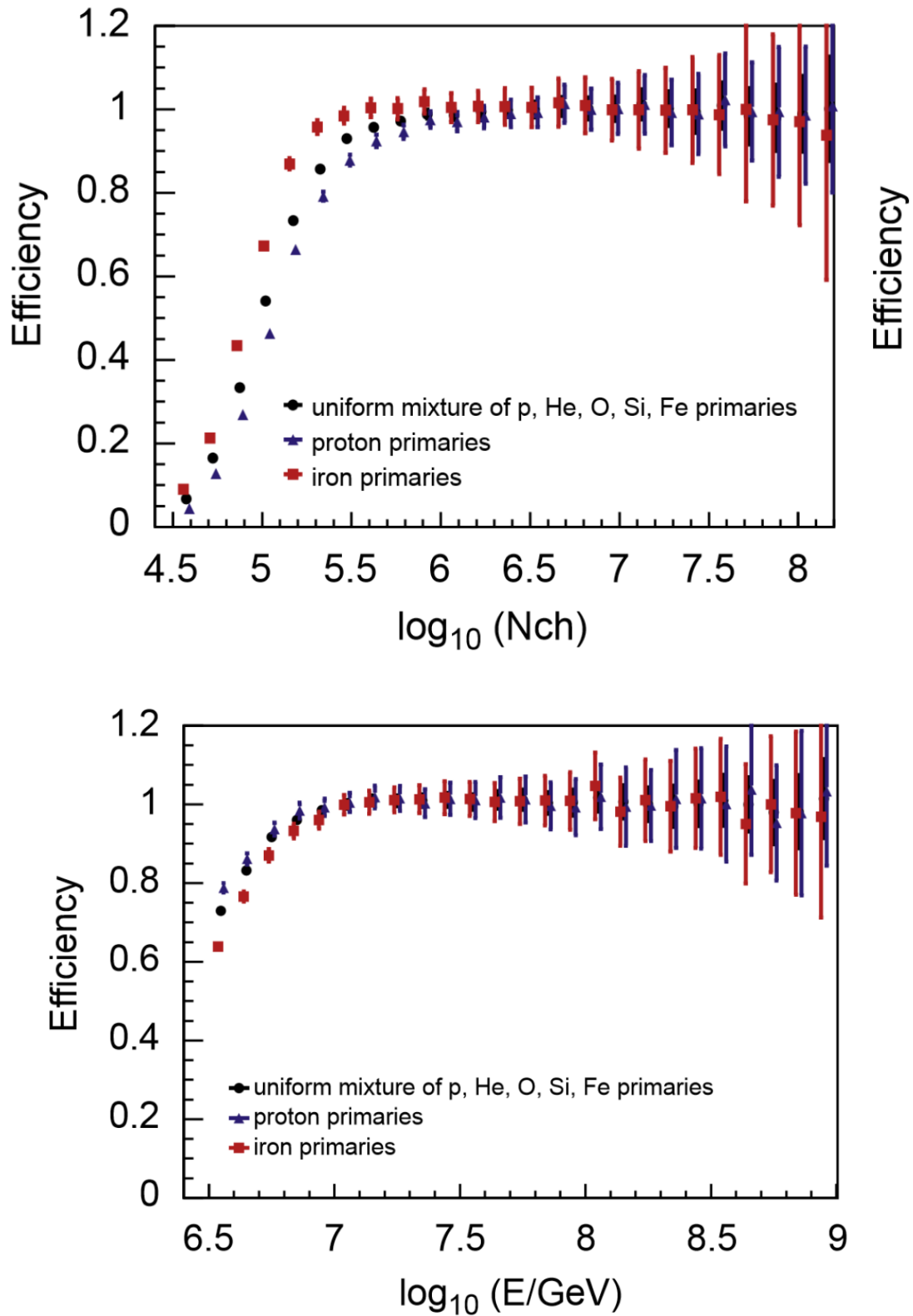
Fig. 8.1.2   *GRANDE Tigger and reconstruction efficiency for different primaries (squares: iron; triangles: protons; circles: uniform mixture of p, He, O, Si, Fe primaries) versus reconstructed shower size (tipper panel) and simulated primary energy (lower panel). For a better visibility, the points for proton and iron assumption are slightly shifted.*

8.2   CUTS

Concerning applied cuts we distinguish between '**Data Selection Cuts'** and '**Advised Cuts'**. The first are already applied on the data published, the latter are highly recommended (see also chapter 8.4.).

8.2.1   DATA SELECTION CUTS KASCADE

The '**Data Selection Cuts KASCADE'** have been applied to the data in a first analysis step using the reconstruction program **KRETA**. These cuts are regarded by the collaboration to be absolutely necessary to guarantee a constant quality of the data sets published.

These Cuts are:

- **the shower reconstruction in the KASCADE Array Processor was successful;**
  all reconstruction steps have been performed without failure.

- **the KASCADE Array has produced a trigger signal**;
  the KASCADE Array was at least one of the trigger sources for the respective event.

- **at most 2 Array clusters may be missing;**
  a whole array cluster can only be missing due to electronic problems. If however more than two clusters out of the 16 are missing at the same time the reconstruction results are not trustworthy anymore.

- **the distance to the shower core is < 91m**;
  the reconstructed shower core is within a 91m radius around the centre of the KASCADE array. This cut is applied to get rid of so called 'border effects' which occur when a shower is reconstructed close to the border and one cannot distinguish if the shower core is inside or outside the array. In this case the lateral density fit function is meaningless.

- **0.1 < AGE < 1.48**;
  KASCADE uses a modified NKG-function to fit the lateral shower shape. Within this function, the age parameter values are limited theoretically to a range from 0.1 to 1.48. Common shower values however range from 0.6 to 1.3.

- **zenith angle ZE < 60°;**
  the KASCADE experiment was designed to record events with a zenith angle well below 60°. Above that value the reconstruction is rather likely to produce nonsense.

- **N_e > 100;**
  this cut is just applied remove the non-physical rubbish (more details see chapter 6.3).

- **N_μ > 100;**
  this cut is just applied remove the nonphysical rubbish (more details see chapter 6.3).

The data published do not contain events which did not survive ALL 'Data Selection Cuts' listed above.

8.2.2   DATA SELECTION CUTS GRANDE

The '**Data Selection Cuts GRANDE**' have mostly been applied while filling the KCDC database.

These Cuts are:

- **7/7 coincidence is present ;**
  all 7 stations from at least on GRANDE hexagon have triggered

- **highest energy deposit is not in a border station**;
  station with max energy deposit is not at the GRANDE array border.

- **the GRANDE array reconstruction was successful;**

- **the shower core is within a well-defined area**;
  the reconstructed shower core has to be within the rectangle -500m - +100m in Y direction and -600m - +100m in X direction with respect to the KASCADE origin. This cut is applied to get rid of so called 'border effects' which occur when a shower is reconstructed close to the border and one cannot distinguish if the shower core is inside or outside the array. In this case the lateral density fit function is meaningless.

- **-0.385 < AGE < 1.485**;
  GRANDE uses a modified NKG-function to fit the lateral shower shape. Within this function, the age parameter values are limited theoretically to a range from -0.385 to +1.485.

- **zenith angle ZE < 40°;**
  the GRANDE experiment was designed to record events with a zenith angle well below 40°. Above that value the reconstruction is rather likely to produce nonsense.

- **N_{ch} > 11111;**
  this cut is applied remove the non-physical rubbish.

- **N_μ > 1500**;
  this cut is applied remove the nonphysical rubbish.

- **no disturbance from synchrotron radiation source ANKA;**
  the synchrotron radiation source ANKA produces disturbances during injection and beam dump which can initiate GRANDE triggers and thus are recorded. Details see chapter 8.6).

8.2.3   DATA SELECTION CUTS CALORIMETER

The '**Data Selection Cuts Calorimeter**' have been applied to the data in a first analysis step using the reconstruction program **KRETA**. For the Hadron Calorimeter data the following cut has been applied:

- **Hadron Calorimeter fully operational**;
  all events where the Central Hadron Calorimeter was not fully operational, for example during construction, are not included in the calorimeter data sets.

- **the hadron reconstruction was successful;**
  at least one hadron in the Calorimeter from the Core Processor or the Single Hadron Processor were reconstructed

8.2.4   DATA SELECTION CUTS LOPES

The '**Quality Cuts LOPES'** have mostly been applied while filling the KCDC database.

- **event is already part of KCDC DataShop**
  only events which were already part of the KCDC DataShop are stored

- **reconstruction parameters from LOPES agree**
  only events where the core position and the incident angle agree with KASCADE-Grande parameters are stored

8.2.5   ADVISED CUTS

The '**Advised Cuts'** are strongly recommended by the KASCADE collaboration. They have been applied in most of our publications.

for KASCADE:

- **zenith angle ZE < 42°;**
  even if the KASCADE experiment recorded events with a zenith angle above 42° we recommend to be careful analysing 'flat showers'. The reconstruction mechanism inside KRETA was fine-tuned to showers between 0° and 42°.

- **0.6 < AGE < 1.3**;
  even though the reconstructed value for the age parameter is between 0.1 and 1.48 a common shower reaches from 0.6 to 1.3.

- **N_e > 100000;**
  this cut is just applied to remove the non-physical rubbish

for GRANDE:

- **fiducial area**
  for our GRANDE data analysis we mostly used the following cuts on the shower core position for the fiducial area (see fig 8.2.1):

X-cut:	-420m < Xc < -50m
Y-cut:	-550m < Yc < -30m
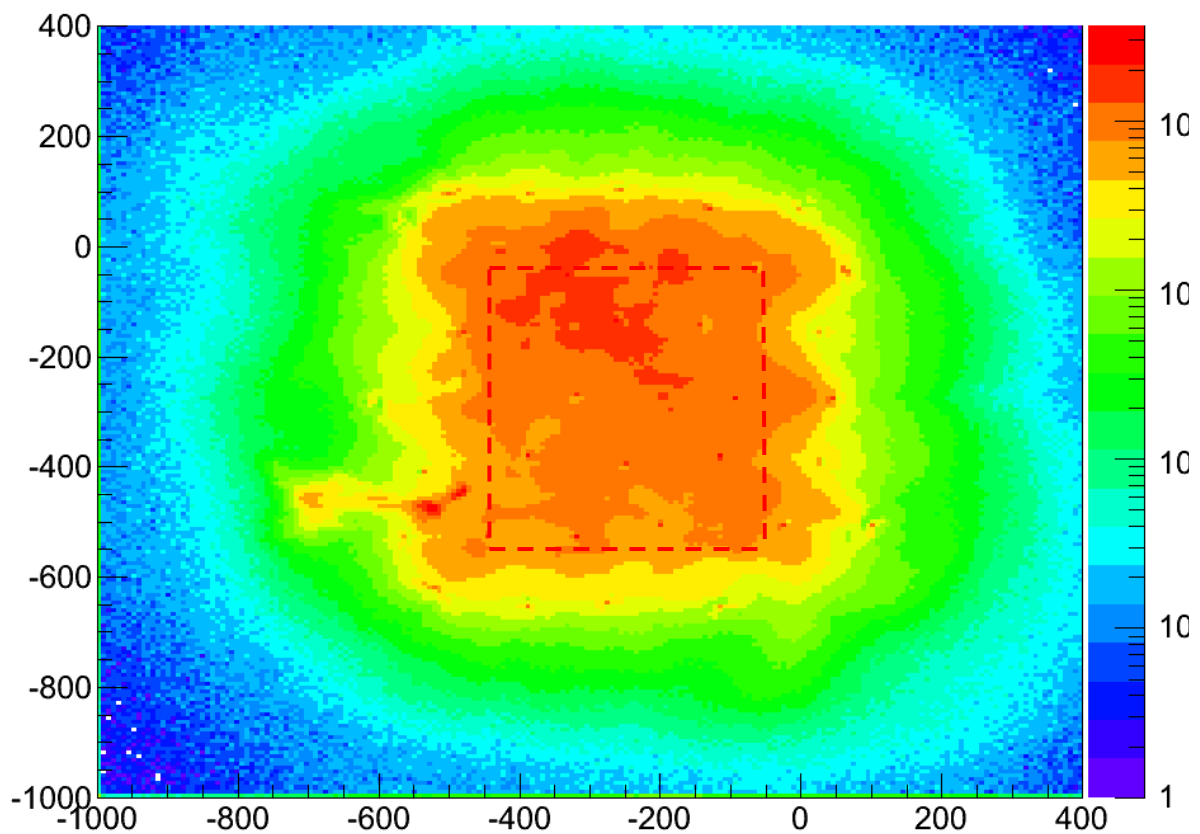
Fig. 8.2.1   *Shower core distribution with GRANDE array detector stations with advised cut*

for LOPES:

- **EfiledMaxAbs < 3000 V/m;**
  the maximum E-field measured by the afield mill has to be <3000 V/m. Above this value the data are likely to be influenced by atmospheric disturbances like thunderstorms.

8.3   EXPERT'S ADVICES

Here are some advices which we think are helpful for people doing analysis with the KCDC data.

- **be careful applying cuts on the quantity 'energy';**
  the quantity energy is a rough estimation based on the measured numbers of electrons (N_e) and the number of muons (N_μ) by means of an "Energy Estimator" who's parameters are deduced with help of a Monte-Carlo Simulation sets optimized for the zenith angle range 0° to 18° (see chapter 4.1.3). It would be advisable to cut on N_e or/and N_μ instead;

- **how to handle the quantities 'Energy Deposit' and 'Arrival Times';**

  as outlined in chapter 4.6, the energy deposit values are only given when the station was working properly. Otherwise, the 'Station ID' (EDepositS) is missing as well as all data for the respective station. The deposit value '0' thus denotes a station which was working but is not a part of the present event. If you are interested in the station co-ordinates please refer to chapter 8.4. and appendix-A. (section 8.5 and appendix-B for GRANDE respectively).

  Basically the same applies for the quantity 'Arrival Times'. But here only stations marked as active e/g-detectors with valid time information are taken into account.

- **the 'row_mapping' file**

  must always be used to match events from different detector components like 'array', 'grande' and 'calorimeter'. When a detector component is missing in the respective event the row_mapping entry is set to '-1';

  C++ code examples how to deal with the row-mapping file can be downloaded.

  For KCDC data:
  https://kcdc.iap.kit.edu/static/txt/KCDC_analyze_example.C.gz ,
  for simulation:
  https://kcdc.iap.kit.edu/static/txt/KCDC_analyze_simulations_example.C.gz .

8.4 CALCULATION OF ARRAY DETECTOR STATION LOCATIONS FROM ID

For the 'Energy Deposits', the 'µ-Energy Deposits' and the 'Arrival Times' in KASCADE, the position of the detector stations is given in so called 'Station IDs' which is a number between 1 and 252 for e/γ-detectors and 192 for µ-detectors. The allocation table and the python-code to calculate the real position of the KASCADE stations in KASCADE coordinates are given in appendix 'A'.

8.5 CALCULATION OF GRANDE DETECTOR STATION LOCATIONS FROM ID

For the 'GRANDE Energy Deposits' and the 'GRANDE Arrival Times' the position of the detectors is given in so called 'Station IDs' which is a number between 1 and 37. The allocation table and to calculate the real position of the respective GRANDE station in KASCADE coordinates are given in appendix 'B'.

8.6 DISTURBANCES FROM ANKA

ANKA is a Synchrotron Radiation Source and a Test Facility and KIT-CN, located in the south-western corner of the GRANDE detector array about 700m away from the centre of the KAS-CADE array. Due to scattered radiation GRANDE measures a disturbance in the measurement during beam injection times and when the beam is dumped in the sense that the GRANDE trigger is activated and events highly inclined coming from south-west are reconstructed. These periods of time as well as times when ANKA was doing 'machine physics' were excluded from the data when filling the mongoDB.

9   KASCADE DATA SHOP

Through the KCDC DataShops we offer the unique possibility to select data sets from a variety of quantities and apply cuts that match your analysis requirements.

We are currently providing two DataShops, the 'KASCADE' DataShop first published in 2013 and continuously extended since then and the newly added DataShop 'COMBINED' (details see separate manual 'KCDC-Combined User Manual').

9.1   KASCADE DATA SHOP OVERVIEW

To have access to the KCDC Data Shops you need to be a registered user as described in chapter 17. You enter the Data Shop via the **'Data Shops'** Menu Item on the KCDC Homepage (https://kcdc.iap.kit.edu/) where you can either submit a new request within **'KASCADE'**, **'Review'** your earlier requests or download predefined data sets called **'Data Preselctions'**.
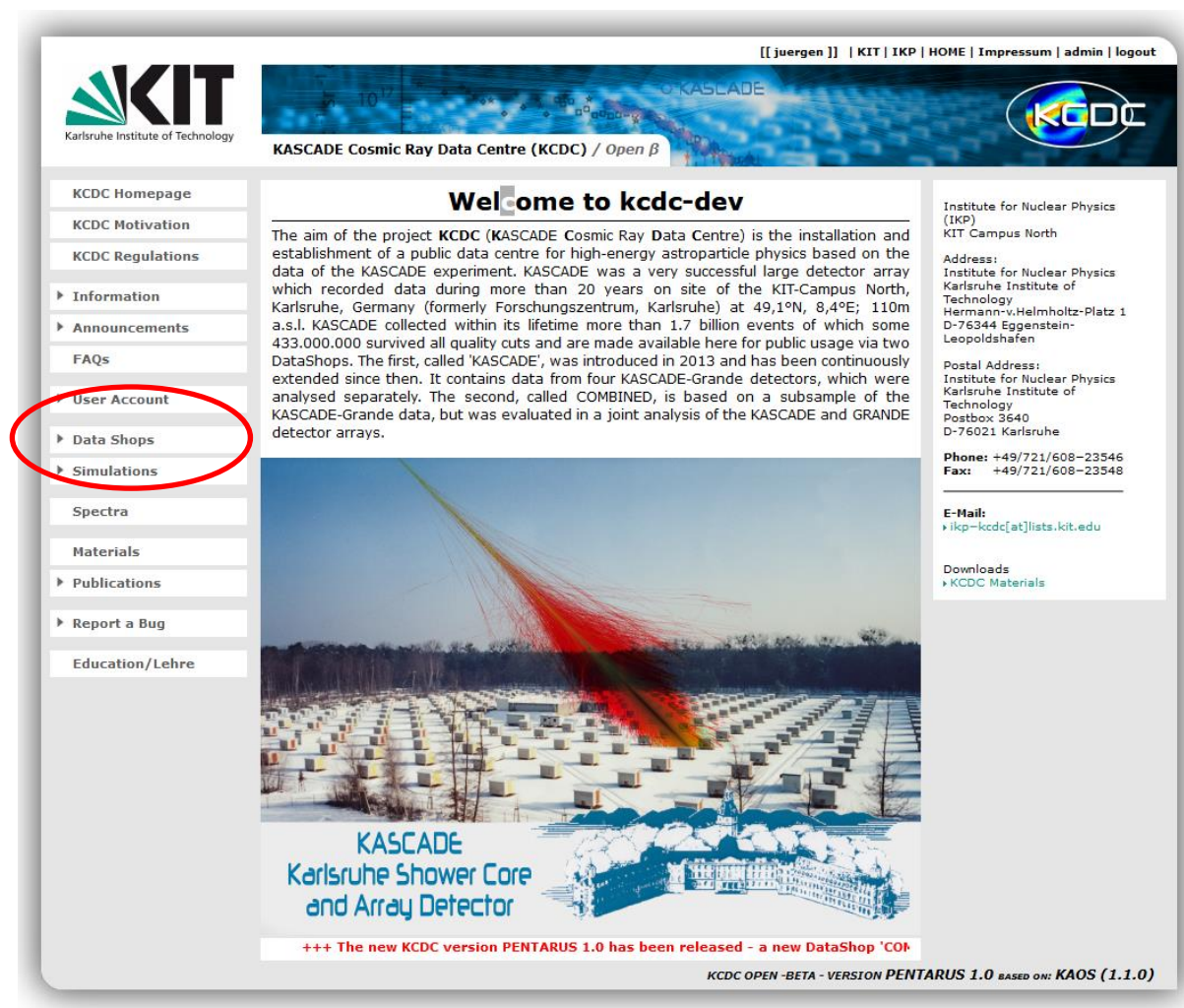
Fig. 9.1.1   *KCDC Homepage*

KASCADE Data Shop

On the right hand side of the shops page invoked by *'KASCADE'* or *'COMBINED'* an information box (orange) is located with some simple helps to find your way through the KCDC Data Shop. This box changes when you *hover* for example over the detector components or later over quantities and cuts.

The link included at the bottom of the 'Welcome to the DataShops' info box will open this manual which holds detailed descriptions on the KASCADE and GRANDE detector components, quantities available and a short way how these quantities are gained from the parameters recorded with the KASCADE experiment.
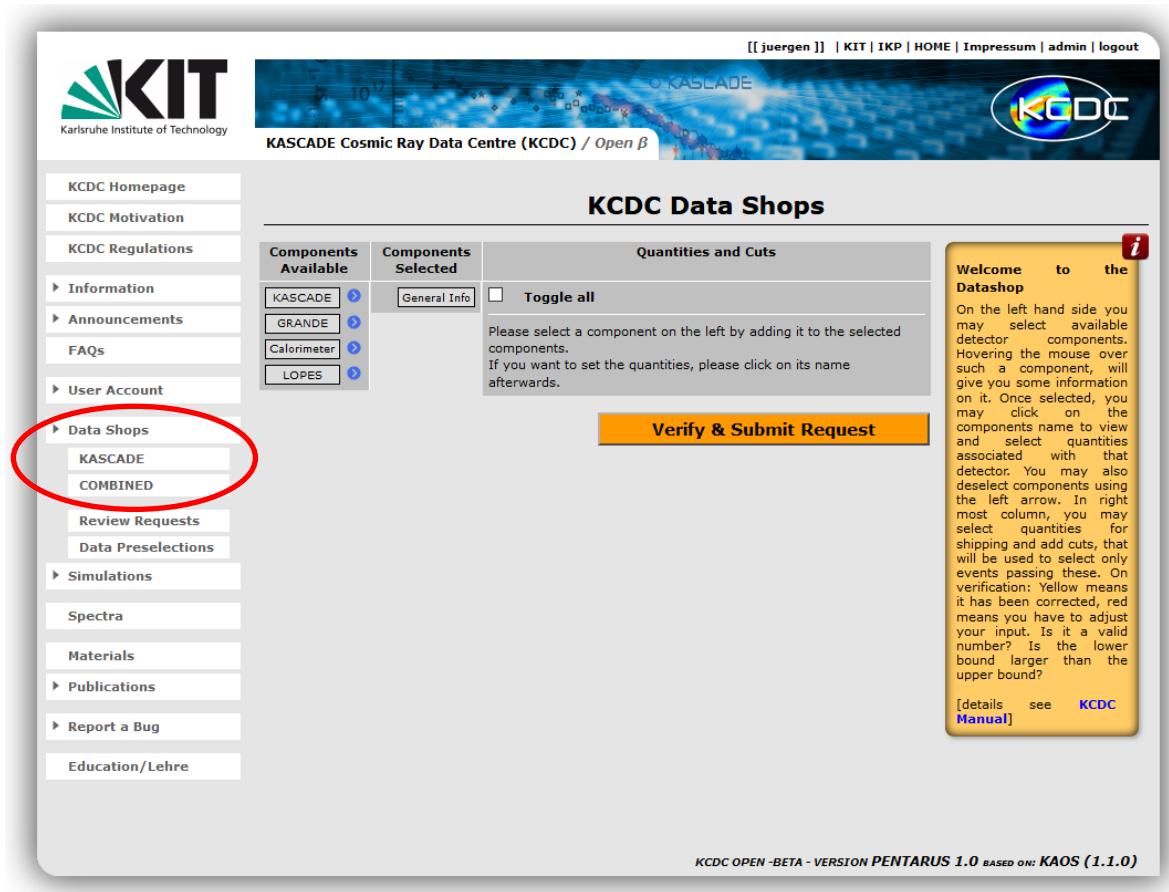
Fig. 9.1.2   *'KASCADE' Data Shop intro page*

Fig. 9.1.3   *Info box with 'hover information' on detector components*

9.2   USER DEFINED SELECTIONS

The column 'Components Available' holds a list of the detector components of the KASCADE-Grande experiment from which quantities are presently available for selection and download. The column '*Components Selected*' holds a list of the detector components selected by the user to select quantities from and to apply cuts to.

To shift a component from '*Components Available'* to *'Components Selected'* and vice versa press the blue arrow of the respective component.

'*General Info'* holds all important event information. As the quantities '*Run Number'* and '*Event Number*' from '*General Info'* cannot be deselected '*General Info'* will always be selected too.

Pressing the *'General Info'* button opens a list of all available quantities with information on their ranges. Here you can select quantities for download and apply cuts by pressing the '*Add Cut'* button for the respective quantity.

Fig. 9.2.1   *Quantities of 'General Info'; 'Run Number' and 'Event Number' are always selected. Please note that 'general' holds all the data arrays like 'E-Deposits' or 'Arrival Times'*

Fig. 9.2.2   *Quantities of 'KASCADE' some are selected by the user*

Fig. 9.2.3   *Quantities of 'Calorimeter' all are selected by the user via 'Toggle all'*

Fig. 9.2.4   *Quantities of 'GRANDE' all are selected by the user via 'Toggle all'*

Fig. 9.2.5   *Quantities of 'LOPES' all are selected by the user via 'Toggle all'*

9.3   USER DEFINED CUTS

To select only a subsample of the KASCADE data available you can apply your own cuts on most of the quantities. No cuts can be applied on quantities where the '*Add Cut*' Button is missing. We do not think that applying cuts makes sense for quantities like '*Micro Time*' or '*Event Number*'. We do as well not offer the cut option for data arrays like '*Energy Deposits*' or '*Arrival Times*' at present.

Fig. 9.3.1   *Applied cuts on 'X Core Position' with some example cuts*

To check and submit your requests press the *'Verify & Submit Request'* –Button.

The summary page gives an overview on your quantities selected for each detector component and on the cuts applied. Additional information on the cuts is provided as well in the last column like:

full range	the full data range for this quantity is selected
user cut	the user has applied cuts which are effective
corrected cut	the user has applied a cut outside the valid range, this cut has been corrected to be within the limits
obsolete now	the user has applied cuts which is beyond the limits, thus the range has been corrected and the selection covers now the full range of data

Fig. 9.3.2   *Check and submit your requests*

9.4   JOB SUBMISSION AND REVIEW

After pressing the '*Submit*' –button you are redirected to your '*Review Requests'* page which holds a complete list of all your requests submitted up to now in all DataShops available. Details see chapter 9.5. '*Job Status Information'.*

9.5   JOB STATUS INFORMATION

The '*Review Requests'* page holds a complete list of all your requests submitted in all DataShops available via the KCDC web portal and enables you to check the present status of your jobs submitted.

Displayed on this page are the date of your request, the data format selected for download and a job status information as described in the table below.

PENDING	job is in the queue to be started
STARTED	job has started
REVOKED	job has been cancelled by the user
SUCCESS	job has been successfully finished data are ready for download
FAILURE	job has failed for some reason
DL EXPIRED	the link to download your data sets is no longer valid
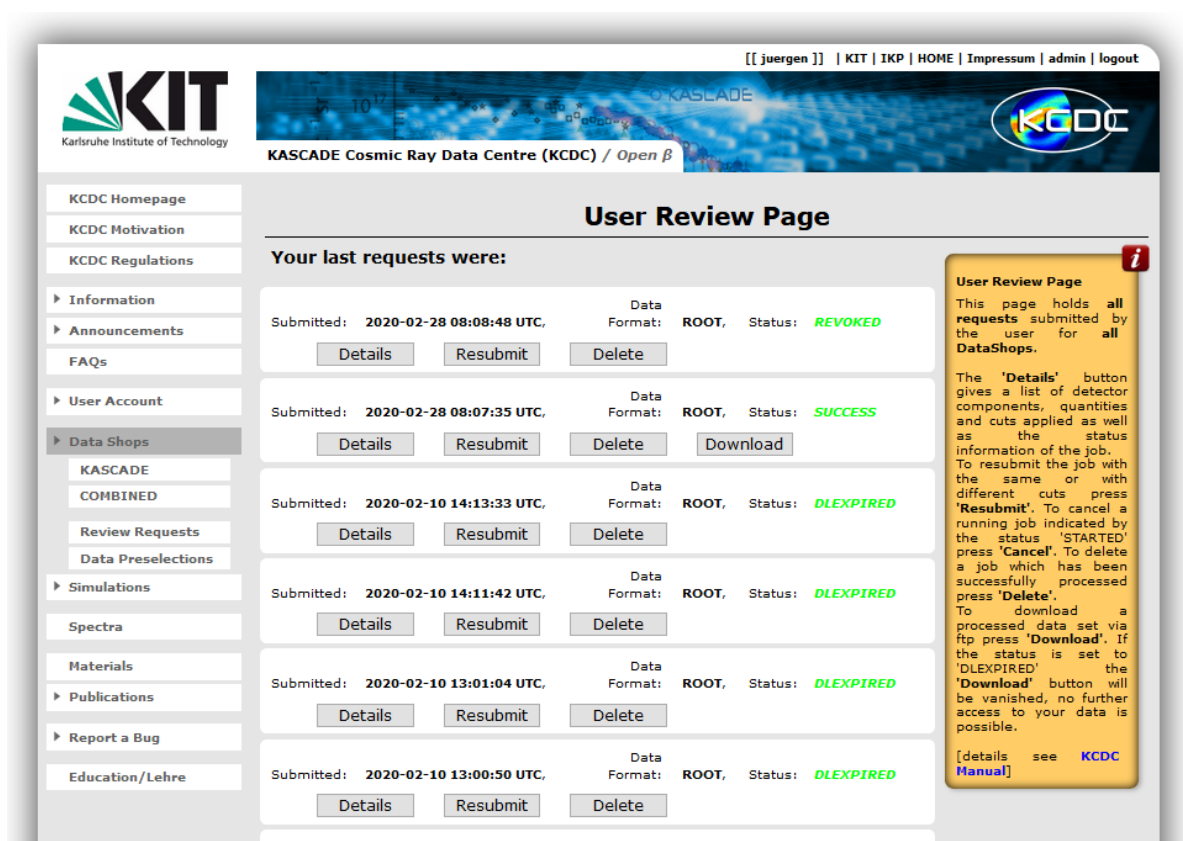
Fig. 9.5.1   *Job 'Review' -page*

On the '*Review*' -page you have several buttons to navigate through your requests. Some of these buttons may change according to the status of the job.

Button	Description	Visibility
Details	shows a list of your request as interpreted by the '*worker*'	switches to 'Hide' when pressed
Resubmit	offers the possibility to resubmit your job and change quantities, selections and cuts	always
Cancel	cancel the job	only while the job is running

		it will change to 'Delete' after the job has finished
Delete	delete the complete request	only when the job is finished
Download	get the link to download your data file	only when successfully finished and the download link has not expired

To get a more detailed list of your requests press the '*Details*' –button

Fig. 9.5.2.   *Details of user selections and cuts*

The information provided here may be different compared to the one displayed on the '*Check & Submit Page'*. This is due do the fact that here only the effective ranges are displayed. Overlapping user defined cuts like in the above example are merged to one effective cut.

9.6   ADVICES TO USE THE DATA SHOP

Using the KCDC Data Shop efficiently requires a little background knowledge how the MongoDB is accessed and how 'Cuts' can speed up your request.

The present MongoDB, which holds the data for the release OCEANUS, has a size of about 2900 GB, which makes it virtually impossible to offer the whole data sample for download. Therefore, restrictions on the user requests and on the file size are vital to guarantee a smooth running. The file size shipped to the user is limited to 50GB to keep the load and the network traffic manageable.

The query to the database uses indices for most of the quantities which can be applied cuts on. We do presently not offer the possibility to cut on the data arrays because it would blow up the query time for the MongoDB enormously.

If you don't exactly know which quantities you need and what cuts to apply, download a small data sample like the one provided for such cases via the 'DataShop' - 'Data Preselections' page. The sample 'KASCADE_SmallDataSample_..._ROOT' (or 'KASCADE_SmallDataSample_..._HDF5' or 'KASCADE_SmallDataSample_..._ASCII') holds about one million events equally distributed over the whole measuring time which corresponds to 0.23% of the whole data sample and should enable you to check the effectiveness of your cuts.

Here are some hints:

- restrict the amount of data in your request by applying as many cuts as possible,
- cutting on energy (dismissing low energetic events) is the most effective cut (see table in chapter 4.1), even though sometimes not advisable (see chapter 8.3)
- the same applies basically for the N_e- and N_μ- quantities,
- download the sample data (~ 1.000.000 events) to check your requirements and make a rough estimation on the number of events (and probably the file size) by applying your cuts before submitting a request,
- cutting on run number or time is sometimes not a good estimator to deduce the number of events for the whole data set because not all components have always been running, and runs have variable lengths,
- contact us in case you need some help iap-kcdc@lists.kit.edu.

9.7 TROUBLESHOOTING

9.7.1 … A GENERAL ERROR INFORMATION OCCURS

Some error information occurring while manoeuvring inside the DataShops is displayed in a red banner on top. Please act according the hints given there.

9.7.2 …THE SUBMITTED REQUEST DOES NOT START?

If you have submitted a request correctly but the status information on the 'Review Page' is not switching from 'pending' to 'started' please try again later. 'Pending' indicates that either there a several requests in the queue waiting to be executed, or that there is problem on the server side of KCDC. Wait for a couple of minutes and if the error persists, resubmit the request using the 'Resubmit' button. If the problem remains please report bugs to the KCDC-Team using the 'Report a Bug' feature.

9.7.3 …THE SUBMITTED REQUEST RETURNS WITH 'FAILURE'

If you have submitted a request and the job status information returns 'FAILURE' please try to resubmit the request using the 'Resubmit' button. If the problem remains please report bugs to the KCDC-Team using the 'Report a Bug' feature.

9.7.4 …DOWNLOADING A PRESELECTION RETURNS WITH ERROR 421

If you have created a new user account and you want to download a preselection from the DataShop's Preselection page, an error might occur indicating your home directory is not available (Error 421). This means that your download directory in the download area has not yet been created. A workaround to this problem is to start a 'New Request'. Once the request is submitted your download directory is available and the preselection ions can be transmitted.

10 DATA RETRIEVAL PROCESS

10.1 GET YOUR DATA

Once a request has been successfully processed the status will change to '*SUCCESS*' and a '*Download*' button will appear.

Fig. 10.1.1   *Request successfully finished → ready for 'Download'*

To start download you have to authenticate in the authentication window popping up. The download link will expire two weeks after your job has been successfully finished. After that, the status will switch to '*DL EXPIRED*' and the '*Download*' button will vanish.

149
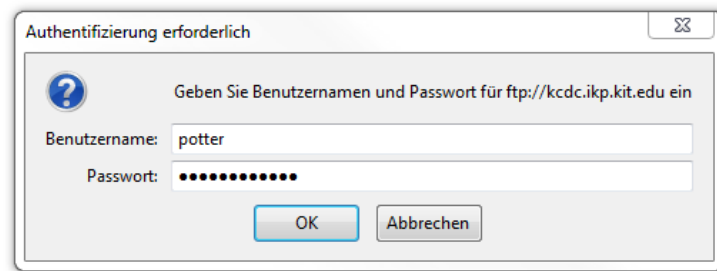
Fig. 10.1.2   *Download authentication window*

11 DATA PRESELECTIONS

If however you are interested in the 'Data Preselections' the DataShop navigation menu offers the option to download data samples directly without selecting quantities and applying cuts. This procedure has the advantage that no time consuming access to the mongoDB is necessary and you will get your data sample immediately. On the other hand, if you know exactly what data you need to perform your analysis it will be most of the time favourable to get your own appropriate data set even if it takes longer.

Preselections of the two detectors published in the KCDC DataShop ('**KASCADE**' and '**COMBINED**') are currently available for download.

The **'SmallDataSample'** data sets hold about 1 million events each, equally distributed over the whole data range meant to be used as a test sample for the user to check their requirements and the cuts to be applied. **'ReducedData'** are data samples not including data arrays like 'Energy Deposits' or 'Arrival Times' per detector station. The column **'size'** should give a rough estimation of the file space required.

The 'Preselections' are invoked via the 'Data Shops' menu item.

11.1 AVAILABLE DATA PRESELECTIONS KASCADE

11.1.1 ASCII DATA PRESELECTIONS KASCADE

ASCII Preselection		
Preselection Set Name	**Description**	**Size**
KASCADE_SmallDataSample_nA_ runs_0877-7417_ASCII	Data sample with every 400th event of the whole data set **1.080.325 events equally distributed;** runs range 877-7417; all detector components except LOPES; all quantities available; no data arrays; no additional cuts applied; Updated with NABOO	93 MB

Data Preselections

ASCII Preselection		
Preselection Set Name	**Description**	**Size**
KASCADE_ReducedData_ runs_0877-4683_ASCII	all KASCADE-Array quantities; run range 877-4683; 143.130.984 KASCADE events; no data arrays; no additional cuts applied; full data sample from the releases VULCAN and MERIDIAN	7.1 GB
KASCADE_ReducedData_ runs_4685-7417_ASCII	all KASCADE quantities; run range 4685-7417; 252.658.250 KASCADE events; no data arrays; no additional cuts applied; Newly added with NABOO	12.9 GB
KASCADE-GRANDE_ReducedData runs_4775-7398_ASCII	all GRANDE quantities; run range 4775-7398; 35.310.393 GRANDE events; no data arrays; no additional cuts applied; Newly added with NABOO	5.0 GB
KASCADE-CALOR_ReducedData_ runs_877-5496_ASCII	all CALORIMETER and KASCADE quantities; run range 877-5496; 100.655.080 CALORIMETER events; no data arrays; no additional cuts applied; Updated with NABOO	9.8 GB
KASCADE_HighEnergyData_ runs_0877-7417_ASCII	Data sample with all events > 15.7 $[\log_{10} eV]$ all quantities; run range 877-7417; 2.537.575 events; no data arrays; Energy cut 15.7 – 19.0$[\log_{10} eV]$ Updated with NABOO	179 MB
KASCADE-LOPES_runs_5534-6821_ASCII	Data sample with LOPES radio events run range 5534-6821; 3058 LOPES events; no data arrays;	541 MB

Data Preselections

ASCII Preselection		
Preselection Set Name	**Description**	**Size**
	no additional cuts applied, Newly added with OCEANUS	

11.1.2 ROOT DATA PRESELECTIONS KASCADE

ROOT Preselection		
Preselection Set Name	**Description**	**Size**
KASCADE_SmallDataSample_nA_ runs_0877-7417_ROOT	Data sample with every 400th event of the whole data set **1.080.325 events equally distributed;** runs range 877-7417; all detector components except LOPES; all quantities available; no data arrays; no cuts applied; Updated with NABOO	93 MB
KASCADE_SmallDataSample_wA_ runs_0877-7417_ROOT	Data sample with every 400th event of the whole data set **1.080.325 events equally distributed;** runs range 877-7417; all detector components; all quantities available; including data arrays; no additional cuts applied; Updated with NABOO	839 MB
KASCADE_ReducedData_ runs_0877-4683_ROOT	all KASCADE-Array quantities; run range 877-4683; 143.130.984 KASCADE events; no data arrays; no additional cuts applied; full data sample from the releases VULCAN and MERIDIAN	6.7 GB
KASCADE_ReducedData_ runs_4685-7417_ROOT	all KASCADE quantities; run range 4685-7417; 252.658.250 KASCADE events; no data arrays;	12.3 GB

Data Preselections

ROOT Preselection		
Preselection Set Name	**Description**	**Size**
	no additional cuts applied; Newly added with NABOO	
KASCADE-GRANDE_ReducedData runs_4775-7398_ROOT	all GRANDE quantities; run range 4775-7398; 35.310.393 GRANDE events; no data arrays; no additional cuts applied; Newly added with NABOO	3.9 GB
KASCADE-CALOR_ReducedData_ runs_877-5496_ROOT	all CALORIMETER and KASCADE quantities; run range 877-5496; 100.655.080 CALORIMETER events; no data arrays; no additional cuts applied; Updated with NABOO	9.9 GB
KASCADE_HighEnergyData_ runs_0877-7417_ROOT	Data sample with all events > 15.7 [$\log_{10}$ eV] all quantities; run range 877-7417; 2.537.575 events; no data arrays; Energy cut 15.7 – 19.0[$\log_{10}$ eV] Updated with NABOO	176 MB
KASCADE-LOPES_runs_5534- 6821_ROOT	Data sample with LOPES radio events run range 5534-6821; 3058 LOPES events; no data arrays; no additional cuts applied, Newly added with OCEANUS	684 MB

11.1.3 HDF5 DATA PRESELECTIONS KASCADE

HDF5 Preselection		
Preselection Set Name	**Description**	**Size**
KASCADE_SmallDataSample_nA_ runs_0877-7417_HDF5	Data sample with every 400th event of the whole data set **1.080.325 events equally distributed;** runs range 877-7417; all detector components; all quantities available; no data arrays; no additional cuts applied; Updated with NABOO	77 MB
KASCADE_SmallDataSample_wA_ runs_0877-7417_HDF5	Data sample with every 400th event of the whole data set **1.080.325 events equally distributed;** runs range 877-7417; all detector components; all quantities available; including data arrays; no additional cuts applied; Updated with NABOO	1400 MB
KASCADE_ReducedData_ runs_0877-4683_HDF5	all KASCADE-Array quantities; run range 877-4683; 143.130.984 KASCADE events; no data arrays; no additional cuts applied; full data sample from the releases VULCAN and MERIDIAN	5.9 GB
KASCADE_ReducedData_ runs_4685-7417_HDF5	all KASCADE quantities; run range 4685-7417; 252.658.250 KASCADE events; no data arrays; no additional cuts applied; Newly added with NABOO	10.8 GB
KASCADE-GRANDE_ReducedData runs_4775-7398_HDF5	all GRANDE quantities; run range 4775-7398; 35.310.393 GRANDE events; no data arrays;	3.2 GB

HDF5 Preselection		
Preselection Set Name	**Description**	**Size**
	no additional cuts applied; Newly added with NABOO	
KASCADE-CALOR_ReducedData_ **runs_877-5496_HDF5**	all CALORIMETER and KASCADE quantities; run range 877-5496; 100.655.080 CALORIMETER events; no data arrays; no additional cuts applied; Updated with NABOO	6.0 GB
KASCADE_HighEnergyData_ **runs_0877-7417_HDF5**	Data sample with all events > 15.7 [$\log_{10}$ eV] all quantities; run range 877-7417; 2.537.575 events; no data arrays; Energy cut 15.7 – 19.0[$\log_{10}$ eV] Updated with NABOO	160 MB
KASCADE-LOPES_runs_5534- **6821_HDF5**	Data sample with LOPES radio events run range 5534-6821; 3058 LOPES events; no data arrays; no additional cuts applied, Newly added with OCEANUS	641 MB

11.2   GET DATA PRESELECTIONS

From the 'Data Shops' – 'Data Preselections' page registered users can download data sets directly (see fig 11.2.1).

Fig. 11.2.1.   *'Data Preselection' for direct download*

12 API (APPLICATION PROGRAMMING INTERFACE)

With release ☰KARA☰AN KCDC provides also an **API** (Application Programming Interface) for data handling. The DataShop API can be used to submit new data requests or to review previous requests within users own application. The main goal is to encourage other astroparticle open data portals not to duplicate data by downloading but to support researchers with a unique interface for data analysis of various experiments.

KCDC is using the quasi-standard of REST (REpresentational State Transfer). REST APIs allows using all functions available on the website to be used through a programmatic interface, for both web and mobile applications. The KCDC API returns data in JavaScript Object Notation (JSON), a format that is commonly used.

The API documentation is available online with Swagger UI:

https://kcdc.iap.kit.edu/datashop/api/docs/index.html

12.1 GET ACCESS

It is necessary to register an account in KCDC. In the API you have to use the encrypted password.

Generate the token in Linux command line (coreutils package):

```
echo -n potter:harry++potter | base64
```

or generate it online https://www.base64encode.org/

12.2 SHELL EXAMPLE

Retrieve the all data with an Energy Range from 17-19eV[log10]. Insert here your username:password in base64 encoding.

API (Application Programming Interface)

```
curl          --insecure          --request          POST          'https://kcdc-
dev.iap.kit.edu/datashop/api/submit' \
--header 'Authorization: Basic cG92dGVyOmhhcnJ5Kytxb3R0ZXI=' \
--header 'Content-Type: application/json' \
--data-raw '
{
    "reconstruction": "",
    "output_format": "ascii",
    "datasets": [
        {
            "name": "array",
            "quantities": [
                {
                    "name": "E",
                    "cuts": [[17, 19]]
                }
            ]
        }
    ]
}'
```

After submit you retrieve immediate the job id

```
{"id":"dbf1e608b6044223afe472125c020d88"}
```

or an error message like

```
{"detail":"Invalid basic header. Credentials not correctly base64 encoded."}
```

Please note that an API started task also show up in the User Job Review Page!

12.3 PYTHON EXAMPLE

```
python3 submit-kcdc.py --user "myusername" --pw "mysecretpassword" --host
"kcdc.iap.kit.edu" --port 443 --https

import argparse
import http.client
import json
import base64
import time
import ssl

def submit_task(conn, auth):
    payload = json.dumps({
        'reconstruction': 'standard',
        'output_format': 'ascii',
        'datasets': [
            {'name': 'array', 'quantities': [{'name': 'E', 'cuts': [[17,
19]]}]}
            ]
    })
    headers = {
        'Authorization': f'Basic {auth}',
        'Content-Type': 'application/json'
```

API (Application Programming Interface)

```python
    }
    conn.request("POST", "/datashop/api/submit", payload, headers)
    data = conn.getresponse().read()
    return json.loads(data.decode("utf-8")).get('id')


def print_status(conn, task_id, auth):
    payload = ''
    headers = {
        'Authorization': f'Basic {auth}'
    }
    conn.request("GET", f'/datashop/api/status/{task_id}', payload, headers)
    res = conn.getresponse()
    data = res.read()
    print(data.decode("utf-8"))


def run_test(conn, auth):
    task_id = submit_task(conn, auth)
    print(f'task has id {task_id}')
    time.sleep(1)
    print_status(conn, task_id, auth)


def get_conn(host: str, port: int, use_https: bool):
    if use_https:
        return  http.client.HTTPSConnection(host,  port,  context=ssl._cre-
ate_unverified_context())
    return http.client.HTTPConnection(host, port)


if __name__ == '__main__':
    parser = argparse.ArgumentParser()
    parser.add_argument('--user', default='test', type=str)
    parser.add_argument('--pw', default='test', type=str)
    parser.add_argument('--host', default='127.0.0.1', type=str)
    parser.add_argument('--port', default=8000, type=int)
    parser.add_argument('--https', action='store_true', dest='https')
    args = parser.parse_args()
    auth  =  base64.b64encode(f'{args.user}:{args.pw}'.encode('utf-8')).de-
code('utf-8')
    #print(auth)
    conn = get_conn(args.host, args.port, args.https)
    run_test(conn, auth)
```

The script returns immediately the status. Because the energy cut is very strict, the job is already in success.

```
task has id 371c406aa277492f8a657d6b4e25bfd3
{"task_id":"371c406aa277492f8a657d6b4e25bfd3","status":"SUCCESS","ex-
pires_at":"2021-02-23T15:46:37.947901Z","submitted_at":"2021-02-
09T15:46:37.947901Z","format":"ascii","down-
load":"https://kcdc.iap.kit.edu/./551/request.zip"}
```

API (Application Programming Interface)

The KCDC Open Data Access via API offers new possibilities of data aggregation for scientists. But is also an important step towards an Astroparticle data lake where decentralized experiment data can be consolidated.

We also would like to encourage the interested public, teacher and training classes to use our data. Continuous use and criticism helps us to further develop and maintain KCDC project.

The '*Shell Script Example'* and the '*Python Example'* mentioned above can be downloaded from the 'Materials' page https://kcdc.iap.kit.edu/materials .

It is planned to give a more detailed description of the API and how to use it in a separate user manual.

13 SPECTRA

The idea behind the Spectra Plugin is to enable the user to download the data sets underlying the Cosmic Ray publications.

13.1 AVAILABLE SPECTRA

At present 102 data sets are available for download from 26 different experiments published between 1984 and 2020 in the energy range 10^{14} to 10^{20} eV. In case of KASCADE and KASCADE-Grande we published as well the data sets from different mass groups like p, he, co, si and fe or heavy and light respectively derived from the unfolding procedure for different high-energy interaction models like QGSJet, EPOS and SIBYLL.

In the following sections, the data sets available are described in more detail. However if you want to get more detailed information you will have to check the original papers and the references therein.

The energy scale of all spectra data is given in [eV] and the flux dJ/dE= E^0*J(E) in [m^{-2} s^{-1} sr^{-1} eV^{-1}]. The errors given are statistical errors only.

Note: if a flux value is given as an upper limit by the experiment, the value is not displayed with the 'Show Data' button. However, it is transferred in the download.

13.1.1 KASCADE

A detailed description of the KASCADE detector is given in chapter 2 of this manual.

"KASCADE"	
Detector	KASCADE
Detector location	49.1°N, 8.4°E ; 110 m asl
Homepage	https://www.iap.kit.edu/kascade
Article Title	The Primary Proton Spectrum of Cosmic Rays Measured with Single Hadrons at Ground Level
Journal	The Astrophysical Journal, 612:914–920
Published	2004
Measuring period	1996-2001

Spectra

DOI	10.1086/422674
ADS	https://ui.adsabs.harvard.edu/abs/2004ApJ...612..914A/
Number of Spectra	1
High Energy Interaction Models used	CORSIKA / QGSJet01
Spectra available	***based on QGSJet01 unfolding*** aSingle Hadron spectrum
Energy Range	$4*10^{12} - 6*10^{15}$ eV

"KASCADE"	
Detector	KASCADE
Detector location	49.1°N, 8.4°E ; 110 m asl
Homepage	https://www.iap.kit.edu/kascade
Article Title	Reconstruction of energy spectra for different mass groups of high-energy cosmic rays
Journal	Thesis Marcel Finger, Karlsruhe 2011
Published	2011
Measuring period	1998/01/01–2010/10/31/
Source	https://web.iap.kit.edu/KASCADE/publication/PhD_Theses/M-Finger-Thesis.pdf
Number of Spectra	24
High Energy Interaction Models used	CORSIKA / QGSJet01 CORSIKA / QGSJet-II-02 CORSIKA / Sibyll 2.1 CORSIKA / EPOS 1.99

Spectra available	***based on QGSJet01 unfolding***
	    all particle spectrum
	    H, He, C, Si, Fe unfolded spectrum
	based on QGSJet-II-02 unfolding
	    all particle spectrum
	    H, He, C, Si, Fe unfolded spectrum
	based on EPOS 1.99 unfolding
	    all particle spectrum
	    H, He, C, Si, Fe unfolded spectrum
	based on SIBYLL 2.1 unfolding
	    all particle spectrum
	    H, He, C, Si, Fe unfolded spectrum

Spectra

Energy Range	$10^{15} - 10^{17}$ eV

"KASCADE"	
Detector	KASCADE
Detector location	49.1°N, 8.4°E ; 110 m asl
Homepage	https://www.iap.kit.edu/kascade
Article Title	KASCADE measurements of energy spectra for elemental groups of cosmic rays: Results and open problems"
Journal	Astroparticle Physics ; 24 ; 2005
Published	2005
Measuring period	1996/10/25-2002/01/15
DOI	10.1016/j.astropartphys.2005.04.001
ADS	"https://ui.adsabs.harvard.edu/abs/2005APh....24....1A/
Number of Spectra	14
High Energy Interaction Models used	CORSIKA / QGSJet01 CORSIKA / Sibyll 2.1
Spectra available	***based on QGSJet01 unfolding*** 　all particle spectrum 　p, he, co, si, fe & heavy unfolded spectrum ***based on SIBYLL 2.1 unfolding*** 　all particle spectrum 　p, he, co, si, fe & heavy unfolded spectrum
Energy Range	$10^{14} - 10^{17}$ eV

13.1.2   KASCADE-Grande

A detailed description of the GRANDE detector is given in chapter 2 of this manual.

"KASCADE-Grande"	
Detector	KASCADE-Grande
Detector location	49.1°N, 8.4°E ; 110 m asl
Homepage	https://www.iap.kit.edu/kascade

Spectra

Article Title	Latest Analysis Results from the KASCADE-Grande Data
Journal	Proceedings, 38th International Cosmic Ray Conference (ICRC 2023) : 26.7.-3.8.2023, Bagoya, Japan
Published	2023
Measuring period	20.12.2003 – 5.11.2012
DOI	10.48550/arXiv.2312.05054
ADS	https://ui.adsabs.harvard.edu/abs/2023arXiv231205054K/
Number of Spectra	9
High Energy Interaction Models used	QGSjet-II-04, EPOS-LHC, SIBYLL 2.3.d
Spectra available	Based on **QGSjet-II-04** unfolding: all particle, light & heavy Based on **EPOS-LHC** unfolding: all particle, light & heavy Based on **SIBYLL 2.3.d** unfolding: all particle, light & heavy
Energy Range	$3*10^{16} – 10^{18}$ eV

"KASCADE-Grande"	
Detector	KASCADE-Grande
Detector location	49.1°N, 8.4°E ; 110 m asl
Homepage	https://www.iap.kit.edu/kascade
Article Title	Measurements of the muon content of EAS in KASCADE-Grande compared with SIBYLL 2.3 predictions
Journal	Proceedings, 35th International Cosmic Ray Conference (ICRC 2017) : 10-20 July, 2017 Bexco, Busan, Korea
Published	2017
Measuring period	
DOI	10.22323/1.301.0316
ADS	https://ui.adsabs.harvard.edu/abs/2017ICRC...35..316A/
Number of Spectra	4

Spectra

High Energy Interaction Models used	CORSIKA / Sibyll 2.3
Spectra available	***based on SIBYLL 2.3 unfolding*** all particle spectrum p, he, co, si, fe unfolded spectra
Energy Range	$3*10^{16} - 10^{18}$ eV

"KASCADE-Grande"	
Detector	KASCADE-Grande
Detector location	49.1°N, 8.4°E ; 110 m asl
Homepage	https://www.iap.kit.edu/kascade
Article Title	KASCADE-Grande energy spectrum of cosmic rays interpreted with post-LHC hadronic interaction models
Journal	Proceedings, 34th International Cosmic Ray Conference (ICRC 2015) : The Hague, The Netherlands, July 30-August 6, 2015
Published	2015
Measuring period	4.9.2003:15:52 - 5.11.2012:11:14
DOI	10.22323/1.236.0359
ADS	https://ui.adsabs.harvard.edu/abs/2015ICRC...34..359B/
Number of Spectra	15
High Energy Interaction Models used	CORSIKA / EPOS LHC CORSIKA / EPOS 1.99 CORSIKA / QGSJet-II-02 CORSIKA / QGSJet-II-04 CORSIKA / Sibyll 2.1
Spectra available	***based on EPOS-LHC unfolding*** all, light, heavy spectra ***based on EPOS 1.99 unfolding*** all, light, heavy spectra ***based on QGSJet-II-02 unfolding*** all, light, heavy spectra ***based on QGSJet-II-04 unfolding*** all, light, heavy spectra ***based on SIBYLL 2.1 unfolding*** all, light, heavy spectra
Energy Range	$10^{16} - 10^{18}$ eV

167

Spectra

“KASCADE-Grande”	
Detector	KASCADE-Grande
Detector location	49.1°N, 8.4°E ; 110 m asl
Homepage	https://www.iap.kit.edu/kascade
Article Title	The KASCADE-Grande energy spectrum of cosmic rays and the role of hadronic interaction models
Journal	Advances in Space Research 53 (2014) 1456–1469
Published	2014
Measuring period	1173 days
DOI	0.1016/j.asr.2013.05.008
ADS	https://ui.adsabs.harvard.edu/abs/2014Ad-SpR..53.1456A/
Number of Spectra	2
High Energy Interaction Models used	CORSIKA / Sibyll 2.1 CORSIKA / EPOS 1.99

Spectra available	**based on SIBYLL 2.1 unfolding**
	  all particle spectrum
	 based on EPOS 1.99 unfolding
	  all particle spectrum

Energy Range	$10^{16} - 2*10^{18}$ eV

“KASCADE-Grande”	
Detector	KASCADE-Grande
Article Title	Ankle-like feature in the energy spectrum of light elements of cosmic rays observed with KASCADE-Grande
Detector location	49.1°N, 8.4°E ; 110 m asl
Homepage	https://www.iap.kit.edu/kascade
Journal	Phsical Review D 87, 081101(R) 2013
Published	2013
Measuring period	
DOI	1550-7998=2013=87(8)=081101(6)
ADS	https://ui.adsabs.harvard.edu/abs/2013PhRvD..87h1101A/

Spectra

Number of Spectra	3
High Energy Interaction Models used	CORSIKA / QGSJet-II-02
Spectra available	**based on QGSJet-II-02 unfolding** all particle spectrum light, heavy spectra
Energy Range	$10^{16} - 3*10^{18}$ eV

"KASCADE-Grande"	
Detector	KASCADE-Grande
Article Title	KASCADE-Grande measurements of energy spectra for elemental groups of cosmic rays
Detector location	49.1°N, 8.4°E ; 110 m asl
Homepage	https://www.iap.kit.edu/kascade
Journal	Astroparticle Physics 47 (2013) 54-66
Published	2013
Measuring period	1318 days
DOI	10.1016/,.astropartphys.2013.06.004
ADS	https://ui.adsabs.har-vard.edu/abs/2013APh....47...54A/
Number of Spectra	6
High Energy Interaction Models used	CORSIKA / QGSJet-II-02
Spectra available	**based on QGSJet-II-02 unfolding** all particle spectrum p, He, C, Si, Fe
Energy Range	$10^{16} - 2*10^{17}$ eV

"KASCADE-Grande"	
Detector	KASCADE-Grande
Detector location	49.1°N, 8.4°E ; 110 m asl
Homepage	https://www.iap.kit.edu/kascade
Article Title	The spectrum of high-energy cosmic rays measured with KASCADE-Grande

Spectra

Journal	Physical Review Letters 107, 171104 (2011)
Published	2012
Measuring period	8.3.2004 – 2.5.2012
ADS	https://ui.adsabs.harvard.edu/abs/2012APh....36..183A/
DOI	10.48550/arXiv.1206.3834
High Energy Interaction Models used	CORSIKA / QGSJet-II-02
Spectra available	*based on QGSJet-II-02 unfolding* all particle spectrum
Energy Range	$10^{16} - 2*10^{18}$ eV

"KASCADE-Grande"	
Detector	KASCADE-Grande
Detector location	49.1°N, 8.4°E ; 110 m asl
Homepage	https://www.iap.kit.edu/kascade
Article Title	Kneelike Structure in the Spectrum of the Heavy Component of Cosmic Rays Observed with KASCADE-Grande
Journal	Physical Review Letters 107, 171104 (2011)
Published	2011
Measuring period	8.3.2004 – 31.12.2010
ADS	https://ui.adsabs.harvard.edu/abs/2011PhRvL.107q1104A/
DOI	10.1103/PhysRevLett.107.171104
High Energy Interaction Models used	CORSIKA / QGSJet-II-03

Spectra available	*based on QGSJet-II-03 unfolding*
	   all particle spectrum
	   light, heavy spectra

Energy Range	$10^{16} - 3*10^{18}$ eV

"KASCADE-Grande"	
Detector	KASCADE-Grande

Spectra

Detector location	49.1°N, 8.4°E ; 110 m asl
Homepage	https://www.iap.kit.edu/kascade
Article Title	Reconstruction of energy spectra for different mass groups of high-energy cosmic rays
Journal	Thesis Marcel Finger, Karlsruhe 2011
Published	2011
Measuring period	8.3.2004 – 31.12.2010
Source	https://web.iap.kit.edu/KASCADE/publication/PhD_Theses/M-Finger-Thesis.pdf
High Energy Interaction Models used	CORSIKA / QGSJet-II-02
Spectra available	**based on QGSJet-II-02 unfolding** all particle spectrum , p, he, co, si, fe spectra
Energy Range	$10^{16} – 10^{18}$ eV

"KASCADE-Grande"	
Detector	KASCADE-Grande
Detector location	49.1°N, 8.4°E ; 110 m asl
Homepage	https://www.iap.kit.edu/kascade
Article Title	Cosmic ray energy spectrum based on shower size measurements of KASCADE-Grande
Journal	Proceedings, 31st International Cosmic Ray Conference (ICRC 2009) : Lodcz, Poland
Published	2009
Measuring period	
ADS	https://ui.adsabs.harvard.edu/abs/2009arXiv0906.4007K/
DOI	10.48550/arXiv.0906.4007
High Energy Interaction Models used	CORSIKA / QGSJet-II-02
Spectra available	**based on QGSJet-II-02 unfolding** allParticle, H, He, C, Si, Fe spectra
Energy Range	$10^{16} – 10^{18}$ eV

The energy in the all-particle spectrum was calibrated assuming all elements (i.e. H, He, C, Si, Fe 20% each). Hence the spectrum is approximately in the range of CNO. For the individual

171

spectra e.g. the Fe spectrum has Fe assuming 100%, therefore it looks larger than the all-particle spectrum.

Later in the PRL paper, the data were selected in *heavy* and *light* and the energy was calibrated separately for them. The sum of the heavy and light spectra is therefore equal to the all-particle spectrum.

13.1.3   AUGER

The **Pierre Auger Observatory**, located in the Argentinian pampa near Malargüe, Mendoza, is the largest cosmic ray Observatory and has been in operation since 2008. With a detection area of 3,000 km^2 it is designed to detect ultra-high-energy cosmic rays with energies beyond 10^{18} eV. The cosmic rays are studied by combining the measurements of a Surface Detector (SD) and a Fluorescence Detector (FD). The SD consists of 1600 Water Cherenkov Detectors (WCDs) on a 1500m triangular grid, covering an area of >3000 km^2, and of additional 61 detectors covering 23.5 km^2 on a 750m grid. The SD is fully efficient at $3*10^{18}$ eV ($3*10^{17}$ eV). The atmosphere above the array is monitored by the 27 telescopes of the FD located in five buildings along the perimeter of the site. 24 telescopes have a field of view of 30°$_x$30° in azimuth and elevation. The FD measurements provide an almost calorimetric estimate of the shower energy but are limited by the atmospheric conditions while the SD measurements are made nearly 100% of the time.

"AUGER"	
Detector	AUGER
Detector location	-35.46271°N -69.58498°E; av. 1400m asl
Homepage	http://auger.org/
Article Title	The energy spectrum of cosmic rays beyond the tumdown around 10^{17} eV as measured with the surface detector of the Pierre Auger Observatory
Journal	Eur. Phys. J. C (2021) 81:966
Published	2021
Measuring period	2014/01/01 - 2018/08/31
DOI	10.1140/epjc/s10052-021-09700-w

Spectra

ADS	https://ui.adsabs.harvard.edu/abs/2021EPJC...81..966A/
High Energy Interaction Models used	
Spectra available	all particle spectrum combined analysis all particle spectrum SD 750
Energy Range	$10^{17} - 1.5*10^{20}$ eV

"AUGER"	
Detector	AUGER
Detector location	-35.46271°N -69.58498°E; av. 1400m asl
Homepage	https://auger.org/
Article Title	Measurement of the energy spectrum of ultra-high energy cosmic rays using the Pierre Auger Observatory
Journal	Proceedings of the 36th International Cosmic Ray Conference (ICRC 2019), Madison, WI, U.S.A.
Published	2019
Measuring period	1/2004 – 12/2017
DOI	10.22323/1.358.0450
ADS	https://ui.adsabs.harvard.edu/abs/2019ICRC...36..450V/
Spectra available	all particle spectrum
Energy Range	$3.5*10^{16} - 1.5*10^{20}$ eV

"AUGER"	
Detector	AUGER
Detector location	-35.46271°N -69.58498°E; av. 1400m asl
Homepage	https://auger.org/
Article Title	The cosmic ray energy spectrum measured using the Pierre Auger Observatory
Journal	Proceedings of the 35th International Cosmic Ray Conference (ICRC 2017), Busan, Korea
Published	2017

Spectra

Measuring period	2004/01 – 2016/12
DOI	10.22323/1.301.0486
ADS	https://ui.adsabs.harvard.edu/abs/2017ICRC...35..486F
High Energy Interaction Models used	CORSIKA / QGSJet-II-04 CORSIKA / Sibyll 2.3 CORSIKA / EPOS-LHC
Spectra available	*based on an* average of QGSJet-II-04, SIBYLL 2.3 and EPOS LHC all particle spectrum
Energy Range	$3.5*10^{17} – 1.5*10^{20}$ eV

"AUGER"	
Detector	AUGER
Detector location	-35.46271°N -69.58498°E; av. 1400m asl
Homepage	https://auger.org/
Article Title	Measurement of the cosmic ray energy spectrum above 10^{18} eV using the Pierre Auger Observatory
Journal	Physics Letters B, Volume 685, Issues 4–5, 8 March 2010, p239-246 and Proceedings of the 31st International Cosmic Ray Conference (ICRC 2009), Lodz, Poland
Published	2009 / 2010
Measuring period	2005/11 – 2008/05
DOI	10.1016/j.physletb.2010.02.013
ADS	https://ui.adsabs.harvard.edu/abs/2010PhLB..685..239A/
High Energy Interaction Models used	CORSIKA / QGSJet-II CORSIKA / Sibyll 2.1
Spectra available	all particle spectrum
Energy Range	$10^{18} – 3*10^{20}$ eV

"AUGER"	
Detector	AUGER
Detector location	-35.46271°N -69.58498°E; av. 1400m asl

Spectra

Homepage	https://auger.org/
Article Title	Observation of the Suppression of the Flux of Cosmic Rays above 4×10^{19}eV
Journal	Phys. Rev. Lett. 101, 061101 (2008)
Published	2008
Measuring period	2004/01/01 – 2007/08/31
DOI	10.1103/PhysRevLett.101.061101
ADS	https://ui.adsabs.har-vard.edu/abs/2008PhRvL.101f1101A/
High Energy Interaction Models used	CORSIKA / QGSJet01
Spectra available	all particle spectrum
Energy Range	$3*10^{18} – 3*10^{20}$ eV

13.1.4 ICE-CUBE

The Ice-Cube Neutrino Observatory is located at the geographic South Pole, with both surface and deeply-buried components. The InIce, component consists of 5160 Digital Optical Modules (DOMs) deployed with 17 m spacing on 86 strings in a 125 m triangular grid formation, at depths from 1450 m to 2450 m below the surface in transparent ice. Each DOM contains a 10 inch Hamamatsu photomultiplier tube and electronics for signal processing and readout.

The surface component, Ice-Top, is an array of pairs of tanks filled with water that has frozen and containing two DOMs each, operating at different PMT gains for increased dynamic range; the pairs of tanks are called stations, and each station is located above a string of the InIce detector. IceTop is operating at a height of 2837 m asl.

"ICE Cube / ICE Top"	
Detector	ICE-Cube / ICE-Top
Detector location	Geographic South Pole, surface at 2837m asl
Homepage	https://www.icecube.wisc.edu/

Spectra

Article Title	Cosmic Ray Spectrum and Composition from PeV to EeV using 3 Years of Data From IceTop and IceCube
Journal	Physical Review D 100, 082002A (2019)
Published	2019
Measuring period	1.6.2010 – 2.5.2013
DOI	10.1103/PhysRevD.100.082002
ADS	https://ui.adsabs.har-vard.edu/abs/2019PhRvD.100h2002A/
High Energy Interaction Models used	CORSIKA / Sibyll 2.1
Spectra available	all particle spectrum, pr, he o, fe
Energy Range	$3.5*10^{15} – 8.0*10^{17}$ eV

13.1.5 ICE TOP

The IceTop air shower array is the surface component of the IceCube Neutrino Observatory at the geographical South Pole. The IceTop array, at an altitude of 2835 m above sea level, consists of 162 tanks filled with clear ice distributed in 81 stations spread over an area of 1 km^2. The analysis was performed using only information from IceTop. The all-particle cosmic ray energy spectrum covers an energy range from $2{,}51*10^{14} – 1.00*10^{16}$ eV. The data published here were taken from June 2010 to May 2011 where the IceTop array consisted of 73 stations.

"ICE-Top"	
Detector	ICE-Top
Detector location	Geographic South Pole, surface at 2835m asl
Homepage	https://www.icecube.wisc.edu/
Article Title	Cosmic ray spectrum from 250 TeV to 10 PeV using Ice-Top
Journal	Physical Review D 102, 122001 (2020)
Published	2020
Measuring period	1/5/2016 – 4/2017
DOI	10.1103/PhysRevD.102.122001

Spectra

ABS	https://ui.adsabs.har-vard.edu/abs/2020PhRvD.102l2001A/
High Energy Interaction Models used	CORSIKA / Sybill 2.1 CORSIKA / QGSJet-II-04
Spectra available	all particle spectra for Sibyll and QGSJet
Energy Range	$2.51 * 10^{14} - 10^{16}$ eV

"ICE-Top"	
Detector	ICE-Top
Detector location	Geographic South Pole, surface at 2835m asl
Homepage	https://www.icecube.wisc.edu/
Article Title	Measurement of the cosmic ray energy spectrum with IceTop-73
Journal	Physical Review D 88, 042004 (2013)
Published	2013
Measuring period	1/6/2010 – 13/5/2011
DOI	10.1103/PhysRevD.88.042004
ABS	https://ui.adsabs.har-vard.edu/abs/2013PhRvD..88d2004A/
High Energy Interaction Models used	CORSIKA / Sibyll 2.1
Spectra available	all particle spectrum
Energy Range	$1.58 * 10^{15} - 1.26 * 10^{18}$ eV

13.1.6 TALE

The Telescope array (TA) experiment is located in the West Desert of Utah, about 150 miles southwest of Salt Lake City, and is the largest cosmic ray detector in the northern hemisphere. In operation since 2008, TA consists of 507 surface detectors, arranged in a square grid of 1.20 km spacing. A total of 38 telescopes are distributed among three fluorescence detector stations at the periphery of the surface detector array. The fluorescence detector telescopes observe the airspace above the surface detector array. As a TA low-energy extension (TALE) ten

new telescopes were added to the 14 of the TA FD and at the site. TALE also incorporates 103 new SD counters arranged in a graded spacing array.

"TALE"	
Detector	TALE
Detector location	39°17'48.8"N 112°54'31.4"W
Homepage	http://www.telescopearray.org/
Article Title	The Cosmic-Ray Energy Spectrum between 2 PeV and 2 EeV Observed with the TALE detector in monocular mode
Journal	The Astrophysical Journal, Volume 865
Published	2018
Measuring period	1.6.2014 – 31.3.2016
DOI	10.3847/1538-4357/aada05
ADS	https://ui.adsabs.harvard.edu/abs/2018ApJ...865...74A/
High Energy Interaction Models used	CORSIKA / CONEX / QGSJet-II-03
Spectra available	monocular spectrum
Energy Range	$2*10^{15} – 2*10^{18}$ eV

13.1.7 AGASA

The large surface array at the Akeno Observatory (35° 47' N, 138° 30' E) to study origin of extremely high-energy cosmic rays is called the Akeno Giant Air Shower Array (AGASA) . AGASA covers an area of about 100 km² and consists of 111 detectors, each 2.2 m² on the ground (surface detectors) and 27 detectors of six different sizes under absorbers (muon detectors). Each surface detector is placed with a nearest-neighbour separation of about 1 km and the detectors are sequentially connected with a pair of optical fibres.

"AGASA"	
Detector	AGASA
Detector location	Akeno, Japan, 35° 47' N, 138° 30' E
Homepage	http://www-akeno.icrr.u-tokyo.ac.jp/AGASA/
Article Title	Energy Determination in the Akeno Giant Air Shower Array Experiment
Journal	Astroparticle Physics Volume 19, Issue 4, July 2003, Pages 447-462
Published	2003
Measuring period	1990/02/17-2002/07/31
DOI	10.1016/S0927-6505(02)00243-8
ADS	https://ui.adsabs.harvard.edu/abs/2003APh....19..447T/
High Energy Interaction Models used	AIRES / QGSJET, SIBYLL CORSIKA / QGSJET, SIBYLL COSMOS / QCDJET
Spectra available	all particle spectrum
Energy Range	$3.5*10^{18} - 3*10^{20}$ eV

13.1.8   AKENO

The AKENO air shower array consists of two parts, a 20 km^2 array and a packed region in one corner of the array with the size of about 1km^2. The 1km^2 array consists of 156 scintillation detectors, each of area 1 m^2 which are distributed over an area of about 1 km^2 with a detector spacing of 120 m, and 30 m in three regions each of area (90x90) m^2, where clusters of detectors are in operation to observe the showers whose total number of particles is below $10^{6.5}$. The 20 km^2 array consists of 19 detectors, each of area 2.25 m^2, and four detectors, each of area 1.0 m^2, which are arranged with an inter-detector spacing of about 1 km.

"AKENO"	
Detector	AKENO
Detector location	Akeno, Japan, 35° 47' N, 138° 30' E
Homepage	http://www-akeno.icrr.u-tokyo.ac.jp/AGASA/
Article Title	Energy spectrum of primary cosmic rays between $10^{14,5}$ and 10^{18} eV

Spectra

Journal	J. Phys. G Nucl. Phys. 10 (1984) 1295-1310
Published	1984
Measuring period	1/1979-3/1983
DOI	10.1088/0305-4616/10/9/016
ADS	https://ui.adsabs.har-vard.edu/abs/1984JPhG...10.1295N/
High Energy Interaction Models used	
Spectra available	all particle spectrum
Energy Range	$4*10^{14} – 5*10^{18}$ eV

"AKENO"	
Detector	AKENO
Article Title	Energy spectrum of primary cosmic rays between $10^{14,5}$ and 10^{18} eV
	Energy spectrum of primary cosmic rays above 1017.0 eV determined from extensive air shower experiments at Akeno
Journal	Astrophysical Journal 424(1994) 491-502
Published	1992
DOI	0305-4616/84/091295+16$02.25
	0954-3899/92/020423+20$04.50
Spectra available	all particle spectrum
Energy Range	$4*10^{14} – 5*10^{18}$ eV
Data Taking	1981 – 3/1990 (from the 1 km^2 array only)

13.1.9   Fly's Eye

The Fly's Eye I is an atmospheric fluorescence detector located at the Dugway Proving Grounds in Utah consists of 67 spherical mirrors, 1.5 diameter each. The mirrors are arranged to view the whole sky. In 1986 a second detector (Fly's Eye II) 3.4 km away came into full operation. It consists of 36 mirrors with the same design, viewing only half of the night sky in the direction of Fly's Eye I.

Spectra

Data from the monocular mode between 1983 and 1992 are shown as well as stereo data recorded between 1986 and 1992.

The '**Oh-My-God particle'** was an UHECR particle detected on 15 October 1991 by the Fly's Eye camera. Its energy was estimated as $(3.2\pm0.9)\times10^{20}$ eV. Assuming it was a proton, for which mc^2 is 938 MeV, this means it was traveling at 0.999 999 999 999 999 999 999 9951 times the speed of light with a Lorentz facotor of $3.2*10^{11}$. At this speed, if a photon were traveling alongside the particle, it would take over 215,000 years for the photon to gain a 1 cm lead.

"Fly's Eye"	
Detector	Fly's Eye monocular
Detector location	Dugway, Utah, USA; 40°N, 113°W
Homepage	http://www.telescopearray.org/index.php/history/the-fly-s-eye-1981-1993
Article Title	The cosmic-ray energy spectrum observed by the Fly's Eye
Journal	Astrophysical Journal 424(1994) 491-502
Measuring period	1983/02 - 1992/07
DOI	10.1086/173906
ADS	https://ui.adsabs.harvard.edu/abs/1994ApJ...424..491B/
Published	1994
Spectra available	*Fly's Eye I* (monocular mode) all particle spectrum
Energy Range	$10^{17} – 3*10^{20}$ eV

"Fly's Eye"	
Detector	Fly's Eye stereo
Detector location	Dugway, Utah, USA; 40°N, 113°W
Homepage	http://www.telescopearray.org/index.php/history/the-fly-s-eye-1981-1993
Article Title	The cosmic-ray energy spectrum observed by the Fly's Eye
Journal	Astrophysical Journal 424(1994) 491-502

Spectra

Measuring period	1986/11 - 1992/07
DOI	10.1086/173906
ADS	https://ui.adsabs.harvard.edu/abs/1994ApJ...424..491B/
Published	1994
Spectra available	*Fly's Eye I* (stereo mode) all particle spectrum
Energy Range	$2*10^{17} - 4*10^{19}$ eV

13.1.10 HiRes I & II

The experiment consists of two detector stations (HiRes-I and HiRes-II) located in Utah, 12.6 km apart. Each station is assembled from telescope modules (22 at HiRes-I and 42 at HiRes-II) pointing at different parts of the sky, covering nearly 360° in azimuth, and 3°–17° (HiRes-I) and 3°–31° (Hires-II) in elevation. Each telescope module collects and focuses UV light from air showers using a spherical mirror of 3.7 m² effective area. A cluster of 256 photomultiplier tubes is placed at the focal plane of each mirror and serves as the camera for each telescope. The field of view of each PMT subtends a 1° diameter cone on the sky.

"HiRes I & II"	
Detector	HiRes I
Detector location	Dugway, Utah, USA; 40°N, 113°W
Homepage	
Article Title	First Observation of the Greisen-Zatsepin-Kuzmin Suppression
Journal	Physical Review Letters 100, 101101 (2008)
Published	2008
Measuring period	06/1997 - 06/2006
DOI	10.1103/PhysRevLett.100.101101
ADS	https://ui.adsabs.harvard.edu/abs/2008PhRvL.100j1101A/
High Energy Interaction Models used	CORSIKA / SIBYLL & QGSJET
Spectra available	all particle spectrum
Energy Range	$3*10^{18} - 2*10^{20}$ eV

13.1.11 JACEE

The Japanese-American Cooperative Emulsion Experiment (JACEE) was studying the interactions and energy spectra of cosmic ray nuclei at energies above 1 TeV/nucleon. The experiments were performed on a series of twelve balloon flights, including several long duration Australia to South America and Antarctic circumpolar flights. The spectra of proton and helium were recorded. The spectra provided are given in [GeV/Nucleon].

"JACEE"	
Detector	JACEE
Detector location	Balloon, southern hemisphere
Homepage	https://www.mpi-hd.mpg.de/hfm/HEGRA/HEGRA.html
Article Title	Cosmic-Ray Proton and Helium Spectra: Results from the JACEE Experiment
Journal	Astrophysical Journal , 502 (1998) 278-283
Published	1998
Measuring period	5/1979 – 12/1995 (flights 1-12)
DOI	10.1086/305882
ADS	https://ui.adsabs.harvard.edu/abs/1998ApJ...502..278A/
Spectra available	proton & helium spectrum
Energy Range	$10^{12} - 10^{15}$ eV

"JACEE"	
Detector	JACEE
Detector location	Balloon, southern hemisphere
Homepage	https://www.mpi-hd.mpg.de/hfm/HEGRA/HEGRA.html
Article Title	Elemental Abundance of High Energy Cosmic Rays
Journal	Nuclear Physics B (Proc. Suppl.) 60B (1998) 83-92
Published	1998
Measuring period	5/1979 – 12/1995 (flights 1-12)
DOI	10.1016/S0920-5632(97)00503-3

Spectra

ADS	https://ui.adsabs.har-vard.edu/abs/1998NuPhS..60...83T/
Spectra available	All Particle, CNO group, Ne-S group, Fe
Energy Range	$10^{10} - 10^{15}$ eV

13.1.12 CASA-Mᵢₐ

The Chicago Air Shower Array (CASA) was a ultra high high-energy astrophysics experiment operating in the 1990s. The full CASA detector, consisting of 1089 detectors began operating in 1992 in conjunction with a second instrument, the Michigan Muon Array (MIA), under the name **CASA-MIA**. MIA was made of 1024 underground muon detectors. MIA was located at the Dugway Proving Grounds southwest of Salt Lake City, Utah.

The CASA stations are spaced 15 m apart on a square grid. The MIA scintillation counters are arranged in 16 patches, each of which contains 64 individual counters buried 3 meters underground.

CASA-MIA worked in conjunction with several other experiments at the same site: the Broad Laterial Non-imaging Cherenkov Array (**BLANCA**), the Dual Imaging Cherenkov Experiment (**DICE**) and the **Fly's Eye HiRes** prototype experiment.

"CASA-Mia"	
Detector	CASA-Mia
Detector location	40° 12' 0" N, 112° 48' 0" W at 1450 m asl
Homepage	https://en.wikipedia.org/wiki/Chicago_Air_Shower_Array
Article Title	The cosmic ray energy spectrum between 10^{14} and 10^{16} eV
Journal	Astroparticle Physics 10 (1999),4, p 291-302
Published	1999
Measuring period	1/1992 – 06/1999
DOI	10.1016/S0927-6505(98)00070-X

Spectra

ADS	https://ui.adsabs.harvard.edu/abs/1999APh....10..291G/
High Energy Interaction Models used	MOCCA
Spectra available	all particle spectrum
Energy Range	$10^{14} - 10^{16}$ eV

13.1.13 CASA-Blanca

The CASA-Blanca detector was located at the Dugway Proving Grounds southwest of Salt Lake City, Utah. During BLANCA runs, CASA consisted of 957 scintillation counters covering an area of 0.2 km², detecting the charged particles in air showers. BLANCA consisted of 144 angle-integrating detectors which recorded the lateral distribution of air shower Cherenkov light working in conjunction with **CASA-Mia.**

"CASA-BLANCA"	
Detector	CASA-BLANCA
Detector location	40° 12' 0" N, 112° 48' 0" W at 1450 m asl
Homepage	https://en.wikipedia.org/wiki/Chicago_Air_Shower_Array
Article Title	A Measurement of the Cosmic Ray Spectrum and Composition at the Knee
Journal	Astroparticle Physics 15 (2001),4, p 49-64
Published	2001
Measuring period	1/1997 – 05/1998
DOI	10.1016/S0927-6505(00)00139-0
ADS	https://ui.adsabs.harvard.edu/abs/2001APh....15...49F/
High Energy Interaction Models used	CORSIKA / QGSJet
Spectra available	all particle spectrum
Energy Range	$2*10^{14} - 6.5*10^{16}$ eV

13.1.14 EAS-Top

The EAS-TOP array is located at Campo Imperatore, Italy, 2005 m a.s.l. (above the underground Gran Sasso laboratories), at 820 g cm^{-2} atmospheric depth. Its electromagnetic detector is made of 35 scintillator modules, 10 m^2 each, split into 16 individual scintillators. The modules are separated by 20 m in the central region and 80 m at the edges of the array.

"EAS-Top"	
Detector	EAS-Top
Detector location	42°26'N; 13°33'E
Homepage	https://gallery.lngs.infn.it/en/gallery/past-experiment/eastop/
Article Title	The EAS size spectrum and the cosmic ray energy spectrum in the region 10^{15}-10^{16} eV
Journal	Astroparticle Physics 10(1999) l-9
Published	1999
Measuring period	1.1.1992 – 31.12.1999
DOI	10.1016/S0927-6505(98)00035-8
ADS	https://ui.adsabs.harvard.edu/abs/1999APh....10....1E/
High Energy Interaction Models used	CORSIKA / QGSjet, Sibyll
Spectra available	all particle spectrum
Energy Range	10^{15} – $2*10^{16}$ eV

13.1.15 DICE

The two DICE Cherenkov telescopes are located at the CASA/MIA site in Dugway, Utah. They each consist of a 2 m diameter spherical mirror with a focal plane detector of 256 close packed hexagonal photomultipliers. The telescopes are on fixed mounts separated by 100 m.

"DICE"	
Detector	DICE
Detector location	40°12N, 112°48'W
Homepage	
Article Title	Elemental composition of cosmic rays near the knee by multiparameter measurements of air showers
Journal	Astroparticle Physics 13 (2000) 137–130
Published	2000
Measuring period	1994/07 – 1996/03
DOI	10.1016/S0927-6505(99)00117-6
ADS	https://ui.adsabs.harvard.edu/abs/2000APh....13..137S/
High Energy Interaction Models used	CORSIKA / VENUS
Spectra available	all particle spectrum
Energy Range	$4*10^{14} – 3*10^{17}$ eV

13.1.16 HEGRA

The High Energy Gamma Ray Astronomy (HEGRA) experiment was located on nearly on top of the Roque de los Muchachos, La Palma island, Spain at a height of 2200 m a.s.l. (790 g/cm^2). It consisted of several detector types for observing secondary particles or light from particle cascades in the atmosphere (Extensive Air Showers, EAS). The EAS detected by HEGRA are produced by cosmic ray particles in the energy range 10^{12} to 10^{16} eV. With its various types of detectors, HEGRA was taking data between 1987 and 2002. Another detector type for the Cherenkov light was AIROBICC (AIrshower Observation by Angle Integrating Cherenkov Counters) with one large photomultiplier looking at the sky above it. 49 of these detectors were spread in a 7-by-7 grid to observe the amplitude and the time of arrival of the front of Cherenkov light. Another 48 were added later on.

In the present analysis, only data of the scintillator array and part of the AIROBICC array were used.

Spectra

"HEGRA"	
Detector	HEGRA
Detector location	28°45.7'N; 17°53,5'W at 2200 m asl
Homepage	https://www.mpi-hd.mpg.de/hfm/HEGRA/HEGRA.html
Article Title	Energy spectrum and chemical composition of cosmic rays between 0.3 and 10 PeV determined from the Cherenkov-light and charged-particle distributions in air showers
Journal	Astron. Astrophys. 359, 682–694 (2000)
Published	2000
Measuring period	1987 - 1998
DOI	10.48550/arXiv.astro-ph/9908202
ADS	https://ui.adsabs.harvard.edu/abs/2000A%2526A…359..682H
High Energy Interaction Models used	CORSIKA / QGSJet
Spectra available	all particle spectrum $(E(Ns)_p$
Energy Range	$3*10^{14} - 10^{16}$ eV

13.1.17 RUNJOB

RUNJOB was a Japanese and Russian balloon flight experiment which launched balloons in 1995 and 1996 from Kamchatka peninsula. The payload consisted of emulsion chambers with a total exposure of 231 m² h covering an energy range of 10-500 TeV for protons.

"RUNJOB"	
Detector	RUNJOB
Detector location	Balloon flight
Homepage	
Article Title	Cosmic-ray spectra and composition in the energy range 10-1000 TeV per particle obtained by the RUNJOB experiment
Journal	The Astrophysical Journal, 628:L41–L44
Published	2005

Spectra

Measuring period	1995 -1997 + 1999
DOI	10.1086/432715
ADS	https://ui.adsabs.harvard.edu/abs/2005ApJ...628L..41D/
Spectra available	allParticle, H, He, C-N-O, Ne-Mg-Si, Fe
Energy Range	$7*10^{11} – 2*10^{15}$ eV

"RUNJOB"	
Detector	RUNJOB
Detector location	Balloon flight
Homepage	
Article Title	Composition and energy spectra of cosmic-ray primaries in the energy range 10^{13} - 10^{15} eV/particle observed by Japanese-Russian joint balloon experiment
Journal	Astroparticle Physics 16 (2001) 13-46
Published	2001
Measuring period	1995 -1996
DOI	10.1016/S0927-6505(00)00163-8
ADS	https://ui.adsabs.harvard.edu/abs/2001APh....16...13A/
Spectra available	allParticle, H, He, C-N-O, Ne-Mg-Si, Fe
Energy Range	$10^{13} – 5*10^{14}$ eV

13.1.18 HAVERAH PARK

At Haverah Park close to Leeds, UK, a 12 km^2 air shower array of water-Cherenkov detectors, was operational from 1967–1987 to measure cosmic rays in the energy range 10^{17}–10^{20} eV. Air showers recorded by the Haverah Park array during the years 1974–1987 have been re-analysed and published. The spectrum published is generated under the assumption of a bi-modal composition of 34% proton and 66% iron.

"Haverah Park" 2003	
Detector	Haverah Park
Detector location	Near Leeds, UK, 53°58'N, 1°38'W, 220m asl

Spectra

Homepage	http://www.ast.leeds.ac.uk/haverah/havpark.shtml
Article Title	The energy spectrum of cosmic rays in the range $3*10^{17}$–$4*10^{18}$ eV as measured with the Haverah Park array
Journal	Astroparticle Physics 19 (2003) 47–60
Published	2003
Measuring period	1974 – 1987
DOI	10.1016/S0927-6505(02)00188-3
ADS	https://ui.adsabs.harvard.edu/abs/2003APh....19...47A/
High Energy Interaction Models used	CORSIKA / QGSJet98
Spectra available	proton spectrum
Energy Range	$3*10^{17}$ – $4*10^{18}$ eV

"Haverah Park" 1985	
Detector	Haverah Park
Detector location	Near Leeds, UK, 53°58'N, 1°38'W, 220m asl
Homepage	http://www.ast.leeds.ac.uk/haverah/havpark.shtml
Article Title	The cosmic ray spectrum above 10(19) EV at Volcano Ranch and Haverah Park
Journal	Conference Contributions 19th ICRC 1985, San Diego USA
Published	1985
Measuring period	
DOI	
ADS	https://articles.adsabs.har-vard.edu//full/1985ICRC....9..475L
High Energy Interaction Models used	
Spectra available	proton spectrum
Energy Range	$2*10^{17}$ – $2*10^{20}$ eV

"Haverah Park" 1979	
Detector	Haverah Park
Detector location	Near Leeds, UK, 53°58'N, 1°38'W, 220m asl
Homepage	http://www.ast.leeds.ac.uk/haverah/havpark.shtml
Article Title	The energy Spectrum ans Arrival Difection Distribution of Cosmic Rays with Energies above 10^{19} Electronvolts
Journal	The Astrophysical Journal, 236:L71-L75, 1980
Published	1979
Measuring period	
DOI	10.1086/183201
ADS	https://ui.adsabs.harvard.edu/abs/1980ApJ...236L..71C/
High Energy Interaction Models used	
Spectra available	proton spectrum
Energy Range	$2*10^{17} - 2*10^{20}$ eV

13.1.19 TUNKA -25 & -133

The TUNKA-13 array comprises 13 phototubes with 37cm photocathode diameter, set up in a square of 240m side length. The distance between the stations was 85 m.

The Tunka-25 array incorporated 25 optical stations distributed over 340×340m^2 area. The distance between individual optical stations was 85 m. The array had 0.5° angular resolution and 1-PeV energy threshold and operated between 2000 and 2006.

The Tunka-133 array consists of 175 wide-angle optical detectors placed to cover an area of 3 km^2 . The detectors are grouped into 25 clusters, each with 7 detectors (six hexagonally-arranged detectors and one in the centre). The distance between the detectors in the cluster is 85 m. Nineteen clusters were installed in a circle of 500m radius with 6 clusters placed at a distance 700-1000m from the array centre.

Spectra

"TUNKA"	
Detector	TUNKA-13
Detector location	51°48'35" N, 103°4'2" O, 675m a.s.l.
Homepage	http://dbserv.sinp.msu.ru/tunka/
Article Title	The first results of TUNKA-13 EAS Cherenkov light experiment
Journal	ICRC 1997
Published	1997
Measuring period	120 hours of moonless nights
DOI	10.1142/3653
ADS	https://ui.adsabs.harvard.edu/abs/1997ICRC....4..129G/
Spectra available	all particle spectrum
Energy Range	$2*10^{14} - 8*10^{16}$ eV

"TUNKA"	
Detector	TUNKA-25
Detector location	51°48'35" N, 103°4'2" O, 675m a.s.l.
Homepage	http://dbserv.sinp.msu.ru/tunka/
Article Title	Measurement of Cosmic Ray Primary Energy with the Atmospheric Cherenkov Light Technique in Extensive Air Showers
Journal	Nucl.Phys.B Proc.Suppl 165 (2007) 74-80
Published	2007
Measuring period	1999 – 2000 (140 hours of moonless nights)
DOI	10.1016/j.nuclphysbps.2006.11.012
ADS	https://ui.adsabs.harvard.edu/abs/2007NuPhS.165...74K
High Energy Interaction Models used	CORSIKA / SIBYLL & QGSJet
Spectra available	all particle spectrum
Energy Range	$8*10^{14} - 2*10^{17}$ eV

Spectra

"TUNKA"	
Detector	TUNKA-133
Detector location	51°48'35" N, 103°4'2" O, 675m a.s.l.
Homepage	http://dbserv.sinp.msu.ru/tunka/
Article Title	Results from Tunka-133 (5 years observation) and from the Tunka-HiSCORE prototype
Journal	EPJ Web of Conferences 121 , 03004 (2016)
Published	2016
Measuring period	2009 - 2014
DOI	10.1051/epjconf/201612103004
ADS	https://ui.adsabs.har-vard.edu/abs/2016EPJWC.12103004P/
High Energy Interaction Models used	CORSIKA / QGSJet-II-04
Spectra available	all particle spectrum
Energy Range	$7*10^{15} - 2*10^{18}$ eV

"TUNKA"	
Detector	TUNKA-133 (2020)
Detector location	51°48'35" N, 103°4'2" O, 675m a.s.l.
Homepage	http://dbserv.sinp.msu.ru/tunka/
Article Title	New Results from Tunka-133
Journal	Astropart.Physics 117 (2020)102406
Published	2020
Measuring period	2009 - 2019
DOI	10.1016/j.astropartphys/2019.102406
ADS	https://ui.adsabs.har-vard.edu/abs/2020APh...11702406B
High Energy Interaction Models used	CORSIKA / QGSJet-II-04
Spectra available	all particle spectrum
Energy Range	$7*10^{15} - 2.5*10^{18}$ eV
Data taking	2009 – 2019

13.1.20 TUNKA -REX

The Tunka Radio Extension (Tunka-Rex) is a digital antenna array located in the Tunka Valley in Siberia, which measures the radio emission of cosmic-ray air-showers with energies of $10^{16.5}$ - $10^{18.5}$ eV in the frequency band of 30-80 MHz. The array is externally triggered by the Tunka-133 air-Cherenkov timing array (during nights) and by the Tunka-Grande array of particle detectors (remaining time). Starting with 18 antenna stations in 2012, Tunka-Rex reached 57 antenna stations in 2016 in a 1 km² dense core extended with 6 satellite detectors reaching the total area of 3 km³. Starting from 2019 the most of the antenna stations are decommissioned leaving 16 antenna stations in the field for the education and diagnostic purposes.

"TUNKA-Rex"	
Detector	TUNKA-Rex
Detector location	51°48'35" N, 103°4'2" O, 675m a.s.l.
Homepage	http://dbserv.sinp.msu.ru/tunka/
Article Title	Seven years of Tunka-Rex operation
Journal	ICRC 2019
Published	2019
Measuring period	2012– 2018
DOI	10.22323/1.358.0319
ADS	https://ui.adsabs.harvard.edu/abs/2019ICRC...36..319K/
High Energy Interaction Models used	CORSIKA / QGSJet-II-04
Spectra available	all particle spectrum
Energy Range	$2*10^{17} – 1*10^{18}$ eV

13.1.21 TAIGA-HISCORE

The TAIGA-HiSCORE ("High Sensitivity Cosmic Rays and gamma Explorer") is an array of wide-angle integrating air Cherenkov stations to detect the Cherenkov radiation from EASs. TAIGA-HiSCORE is a part of TAIGA ("Tunka Advanced Instrument for cosmic ray physics and Gamma

Astronomy") and is a complex, hybrid detector system for ground-based gamma-ray astronomy from a few TeV to several PeV, and for cosmic ray studies from 100 TeV to several 100's of PeV. TAIGA is situated in the TUNKA-Valley and includes TAIGA-HiSCORE –, and Tunka-133 – an integrating air Cherenkov array.

"TAIGA-HiScore 2022"	
Detector	TAIGA-HiScore
Detector location	51°48'35" N, 103°4'2" O
Homepage	https://taiga-experiment.info/
Article Title	Cosmic-Ray Research at the TAIGA Astrophysical Facility: Results and Plans
Journal	Journal of Experimental and Theoretical Physics, Volume 134, Issue 4, p.469-478
Published	2022
Measuring Period	327 h
DOI	10.1134/S1063776122040136
ADS	https://ui.adsabs.harvard.edu/abs/2022JETP..134..469A/
High Energy Interaction Models used	QGSjet-II-04
Spectra available	all particle spectrum
Energy Range	$10^{14} - 10^{16}$ eV

13.1.22 TIBET-II

The Tibet-II air-shower array was carried out at Yangbajing (4,300 m a.s.l., 606 g/cm2) in Tibet, China to obtain the energy spectra of primary protons and heliums. From three year operation, these energy spectra are deduced between 1015 and 1016 eV. The Tibet hybrid experiment, consisting of emulsion chambers, burst detectors and the Tibet-II air-shower array, composed of 221 scintillation counters each placed on a 15 m square grid with an enclosed area of 36,900 m2 was operated at Yangbajing in Tibet during the period from November 1996 through August 1999 and a total live time of 699.2 days.

"TIBET-II"	
Detector	TIBET-III
Detector location	90.53° E, 30.11° N; 4300m asl, Yangbejing, China
Homepage	https://www.icrr.u-tokyo.ac.jp/em/index.html
Article Title	Are protons still dominant at the knee of the cosmic-ray energy spectrum?
Journal	Physics Letters B, Volume 632, Issue 1, p. 58-64
Published	2005
Measuring Period	11/1996 – 8/1999
DOI	10.1016/j.physletb.2005.10.048
ADS	https://ui.adsabs.harvard.edu/abs/2006PhLB..632...58T/
High Energy Interaction Models used	CORSIKA / SIBYLL 2.1 & QGSJet01
Spectra available	particle spectra H & He proton dominated (QGSjet + PD) particle spectra H & He proton dominated (SIBYLL + PD) particle spectra H & He heavy dominated (QGSjet + HD) particle spectra H & He heavy dominated (SIBYLL + HD)
Energy Range	$4*10^{14} – 2*10^{16}$ eV

13.1.23 TIBET-III

The Tibet air-shower experiment has been operated at Yangbajing (E 90° 31', N 30°06'; 4300 m a.s.l.) in Tibet, China. The Tibet-I surface array was constructed in 1990 using 65 plastic scintillation detectors placed on a lattice with 15 m spacing. This array was gradually expanded to the Tibet-II (1994) and Tibet-III (1999) arrays. Finally it consists of 761 fast timing counters with 28 density counters surrounding them. In the inner 36,900 m^2, fast timing counters are deployed at 7.5m lattice intervals.

"TIBET-III"	
Detector	TIBET-III
Detector location	90.53° E, 30.11° N; 4300m asl
Homepage	https://www.icrr.u-tokyo.ac.jp/em/index.html

Spectra

Article Title	The All-Particle Spectrum of Primary Cosmic Rays in the Wide Energy Range from 10^{14} to 10^{17} eV Observed with the Tibet-III Air-Shower Array
Journal	Astrophysical Journal 687(2008)1165-1179
Published	2008
Measuring Period	11/2000 – 10/2004
DOI	10.1086/529514
ADS	https://ui.adsabs.har-vard.edu/abs/2008ApJ...678.1165A/
High Energy Interaction Models used	CORSIKA / SIBYLL 2.1 & QGSJet01
Spectra available	particle spectrum proton dominated (QGSjet + PD) particle spectrum heavy dominated (QGSjet + HD) particle spectrum heavy dominated (Sibyll + HD)
Energy Range	10^{14} – $2*10^{17}$ eV

13.1.24 YAKUTSK

The Yakutsk array is located at Oktyomtsy near Yakutsk, Russia (61.7°N 129.4°E), 100m a.s.l. (1020 g cm^{-2}). It consists of 58 ground-based and six underground scintillation detector stations for measuring charged particles (electrons and muons) and 48 detectors for observing the atmospheric Cherenkov light. During the more than 30 years of its lifetime, the Yakutsk array has been re-configured several times; the total area covered by the detectors was maximal in about 1990 (S_{eff} ~17 km^2). In the central part of the array, there is a denser domain with 100–250m detector spacing. During the whole observation period, approximately 10^6 showers of primary energy above 10^{15} eV were detected; the three highest energy events selected with the axes within the array area and zenith angle $\Theta<60°$ have an energy E > 10^{20} eV. The twosub-array C1 and C2 have been put together into one spectrum.

"YAKUTSK"	
Detector	Yakutsk
Homepage	

Spectra

Article Title	Measuring extensive air showers with Cherenkov light detectors of the Yakutsk array: the energy spectrum of cosmic rays
Journal	New Journal of Physics, Volume 11, Issue 6, id. 065008 (2009)
Published	2009
Measuring period	
DOI	10.1088/1367-2630/11/6/065008
ADS	https://ui.adsabs.harvard.edu/abs/2009NJPh...11f5008I/
High Energy Interaction Models used	CORSIKA / QGSJet01
Spectra available	all particle spectrum
Energy Range	$10^{15} - 10^{20}$ eV

"YAKUTSK"	
Detector	Yakutsk
Homepage	
Article Title	Particle and Atmospheric Cherenkov Light Denisty Spaectra of large EAS at fixed Core Distances
Journal	Proc. 16th ICRC (Kyoto), 1979, 8, 168
Published	1979
Measuring period	
DOI	10.1086/183201
ADS	https://ui.adsabs.harvard.edu/abs/1980ApJ...236L..71C/
High Energy Interaction Models used	
Spectra available	all particle spectrum
Energy Range	$3*10^{17} - 10^{20}$ eV

13.1.25 GAMMA

The GAMMA installation is a ground-based array of 33 surface detection stations and 150 underground muon detectors, located at the south side of Mount Aragats in Armenia. The elevation of the GAMMA facility is 3200 m above sea level. The surface stations of the EAS array contain plastic scintillation detectors with dimensions of 1×1×0.05 m^3. 150 underground muon detectors are compactly arranged in the underground hall under 2.3 kg cm^2 of concrete and rock.

"GAMMA"	
Detector	GAMMA 2008
Detector location	Mt. Aragats, Armenia, 40°25'N; 44°15'E at 3200m asl
Homepage	
Article Title	All-particle primary energy spectrum in the 3-200 PeV energy range
Journal	J. Phys. G: Nucl. Part. Phys. 35(2008) 115201
Published	2008
Measuring period	2004 - 2006
DOI	10.1088/0954-3899/35/11/115201
ADS	https://ui.adsabs.harvard.edu/abs/2008JPhG...35k5201G/
High Energy Interaction Models used	CORSIKA / SIBYLL
Spectra available	all particle spectrum
Energy Range	$3*10^{15} - 2*10^{17}$ eV

"GAMMA"	
Detector	GAMMA 2014
Detector location	Mt. Aragats, Armenia, 40°25'N; 44°15'E at 3200m asl
Homepage	
Article Title	Sharp knee phenomenon of primary cosmic ray energy spectrum
Journal	Physical Review D. 89 (2014) 123003
Published	2014

Spectra

Measuring period	2003 - 2007
DOI	10.1103/PhysRevD.89.123003
ADS	https://ui.adsabs.har-vard.edu/abs/2014PhRvD..89l3003T/
High Energy Interaction Models used	CORSIKA / SIBYLL
Spectra available	all particle spectrum, H, He, O-group, Fe-group
Energy Range	$10^{15} - 3*10^{17}$ eV

13.1.26 MAKET-ANI

The MAKET-ANI surface array includes 92 particle density detectors consisting of 5 cm thick plastic scintillators. Sixty eight detectors have 1 m² area, the remaining 24 are 0.09 m². The central part of the detector consists of 73 scintillators and is arranged in a rectangle of 85*65 m² . Fifteen and four 1 m³ scintillators of the same type are placed at two remote locations at a distance of 95 m and 65 m from the center of the array. In order to estimate the zenith and azimuth angles, the 19 detectors out of 92 are equipped with timing readouts to measure the timing of the appearance of the EAS front.

"Maket-ANI"	
Detector	Maket-ANI
Detector location	40°25'N; 44°15'E at 3200m asl
Article Title	Study of extensive air showers and primary energy spec-tra by MAKET-ANI detector on mountain Aragats
Homepage	http://crd.yerphi.am
Journal	Astroparticle Physics, 28 (2007) 58-71
Published	2007
Measuring period	1007 - 2004
DOI	10.1016/j.astropartphys.2007.04.005
ADS	https://ui.adsabs.harvard.edu/abs/2007APh....28...58C/
High Energy Interaction Models used	CORSIKA / QGSJet01, NKG Mode

Spectra

Spectra available	all particle spectrum, light(p, he) and heavy (c, si, fe) component spectra
Energy Range	$5*10^{14} - 9*10^{16}$ eV

13.1.27 MSU-EAS

The MSU EAS array had the area of 0.5 km^2 and contained 77 charged particle density detectors (consisted of the Geiger-Mueller counters) for determination of the EAS size Ne employing the empirical lateral distribution function and 30 scintillator detectors which measured particle arrival times necessary for determi-nation of the EAS arrival direction. In addition to the surface detectors which recorded mostly electron-photon component of an EAS, the array included also four underground muon detectors, also consisted of Geiger-Mueller counters, located at the depth of 40 meters of water equivalent. These detectors recorded muons with energies above 10 GeV. A muon detector with the area of 36.4 m^2 was located at the center of the array while other three stations had the area of 18.2 m^2 and were located at the distances between 150 m and 300 m from the center. The scintillator detectors were located at the same points as the Geiger-Mueller counters. The position of the shower core was determined with the precision of $\sim$10 m. The precision of determination of the arrival direction was $\sim$3°. The number of particles in the shower was determined with the accuracy $\sim$(15−20)%.

"MSU-EAS"	
Detector	MSU-EAS
Detector location	
Article Title	Energy spectrum of cosmic rays at energies $5*10^{15}$-$5*10^{17}$ eV"
Homepage	
Journal	ICRC-1991
Published	1991
Measuring period	
DOI	1991ICRC....2...85F
ADS	https://ui.adsabs.harvard.edu/abs/1991ICRC....2...85F/
High Energy Interaction Models used	AIRES / QGSJET-01

Spectra available	all particle spectrum
Energy Range	$5 \times 10^{15} - 5 \times 10^{17}$ eV

13.1.28 MT. NORIKURA

The arrangement of the Air Shower Experiment at Mt.Norikura (Honshu, Japan) consists in 192 scintillation detectors, distributed rather evenly over the area of 160m x 220m^2 at an atmospheric depth of 735g/cm^2. About 80 of them are arranged with 5m separation making double the density at the central part. With this packed and sparse configuration, the size of EAS between 5×10^4 to 10^8 was measured. The total running time is 1.9×10^7 sec corresponds to ~220 days of data taking. The total number of EAS used for analysis is 1.7×10^6.

"Mt. Norikura"	
Detector	Mt. Norikura
Detector location	36.11°N, 137.55°E, 2770m asl
Homepage	https://www.icrr.u-tokyo.ac.jp/en/facility/4222/
Article Title	Energy spectrum and chemical composition of primary cosmic rays above 100TeV derived from the size spectrum at Mt.Norikura
Journal	ICRC-1997
Published	1997
Measuring period	
DOI	10.1103/PhysRevD.96.122001
ADS	https://ui.adsabs.harvard.edu/abs/1997ICRC....4..117I/
High Energy Interaction Models used	semi Monte Carlo simulation code GENAS
Spectra available	all particle spectrum
Energy Range	$5 \times 10^{14} - 10^{17}$ eV

13.1.29 HAWC

The HAWC Observatory (High Altitude Water Cherenkov Experiment) is an air shower array located at 4100 m a.s.l. on the slopes of Vulcan Sierra Negra in the state of Puebla., Mexico. HAWC is designed to detect air showers produced by primary gamma rays in the 500 GeV to

100 TeV energy range, but its altitude and physical dimensions permit measurements of primary hadronic cosmic rays up to multi-PeV energies.

The detector comprises a 22,000 m² array of 294 close-packed Water Cherenkov Detectors, each consisting of a 4 .5 m tall and 7.3 m diameter cylindrical steel tank filled with 188,000 liters of purified water. Four PMTs attached on the floor and facing upwards, observe the Cherenkov light produced when secondary particles (primarily electrons, positrons and gamma rays) from air showers enter the tank.

"HAWC 2021"	
Detector	HAWC
Detector location	19°0'N; 97°18.42'W at 4100 m asl
Homepage	https://www.hawc-observatory.org
Article Title	The all-particle cosmic ray energy spectrum measured with HAWC
Journal	ICRC 2021, Berlin Germany
Published	2021
Measuring period	2018/01 - 2019/12
DOI	10.22323/1.395.0330
ABS	https://ui.adsabs.harvard.edu/abs/2022icrc.confE.330M/
High Energy Interaction Models used	QGSJet-II-04
Spectra available	all particle spectrum
Energy Range	$10^{13} - 10^{15}$ eV

The total running time is 234 days from 8 June 2016 to 17 February 2017. The total up-time efficiency was ~92% and the mean trigger rate was ~25 kHz.

The data set consists of 8.42 x 10^9 events with a mean energy of ~3 TeV.

"HAWC-2017"	
Detector	HAWC

Detector location	19°0'N; 97°18.42'W at 4100 m asl
Homepage	https://www.hawc-observatory.org
Article Title	All-particle cosmic ray energy spectrum measured by the HAWC experiment from 10 to 500 TeV
Journal	Physical Review D; Phys. Rev. D 96, 122001 (2017)
Published	2017
Measuring period	2016/06/08 - 2017/02/17
DOI	10.1103/PhysRevD.96.122001
ADS	https://ui.adsabs.harvard.edu/abs/2022icrc.confE.330M/
High Energy Interaction Models used	QGSJet-II-03
Spectra available	all particle spectrum
Energy Range	$10^{13} - 5*10^{14}$ eV

The observation period used was taken from January, 2018 to December, 2019, with a total duration of 703 days. After the event selection, the experimental data set has a total of 1.5x1010 showers.

13.1.30 NUCLEON

The NUCLEON satellite experiment is designed to directly investigate above the atmosphere the energy spectra of cosmic-ray nuclei and the chemical composition (Z=1-30) in the energy range of 2-500 TeV (below the "knee"). The primary energy is reconstructed by registration of spatial density of the secondary particles. The particles are generated by the first hadronic inelastic interaction in a carbon target. Then additional particles are produced in a thin tungsten converter, by electromagnetic and hadronic interactions.

NUCLEON it is placed on board the RESURS-P 2 satellite. The spacecraft s orbit is a Sun-synchronous one, with an inclination of 97.276 and a middle altitude of 475 km. The satellite was launched on 26 December, 2014.

"NUCLEON"	
Detector	NUCLEON
Detector location	Satellite
Homepage	
Article Title	Energy spectra of abundant cosmic-ray nuclei in the NU-CLEON experiment
Journal	Advances Space Research, 64 (12), 2019
Published	2019
Measuring period	2015/07 – 2017/06
DOI	10.1016/j.asr.2019.10.004
ADS	https://ui.adsabs.harvard.edu/abs/2019Ad-SpR..64.2546G/
High Energy Interaction Models used	QGSJet
Spectra available	all particle spectrum, H, He, C, Ne, O, Mg, Si, Fe
Energy Range	$8.0*10^{12} – 1.0*10^{15}$ eV

13.1.31 VOLCANO RANCH

The **Volcano Ranch experiment** was an array of particle detectors in Volcano Ranch, New Mexico, used to measure ultra-high-energy cosmic rays. The array was built by John Linsley and Livio Scarsi in 1959. On February 22, 1962, Linsley observed an air shower at Volcano Ranch created by a primary particle with an energy greater than 10^{20} eV, the highest energy cosmic ray particle ever detected at the time. Linsley continued to operate Volcano Ranch until 1978.

"Volcano Ranch"	
Detector	Volcano Ranch
Detector location	35 ° 9'N 106 ° 47'W
Homepage	
Article Title	The cosmic ray spectrum above 10(19) Ev at Volcano Ranch and Haverah Park
Journal	Conference Contributions 19th ICRC 1985, San Diego USA

Spectra

Published	1985
Measuring period	1963/01-1975/12
DOI	
ADS	https://articles.adsabs.harvard.edu//full/1985ICRC....9..475L
High Energy Interaction Models used	
Spectra available	all particle spectrum
Energy Range	$7.0*10^{17} - 2.0*10^{20}$ eV

"Volcano Ranch"	
Detector	Volcano Ranch
Detector location	35 ° 9'N 106 ° 47'W
Homepage	
Article Title	The Energy Spectrum and Arrival Direction Distribution of Cosmic Rays with Energies above 10^{19} Electronvolts
Journal	The Astrophysical Journal 236:L71- L75, 1980
Published	1975
Measuring period	1963/01- 1975/01
DOI	10.1086/183201
ADS	https://ui.adsabs.harvard.edu/abs/1980ApJ...236L..71C
High Energy Interaction Models used	
Spectra available	all particle spectrum
Energy Range	$7.0*10^{17} - 3.0*10^{19}$ eV

13.1.32 ATIC-2

The balloon-born experiment **ATIC-2 (Advanced Thin Ionization Calorimeter)** is designated for measuringt he composition and energy spectra of primary cosmic rays in the energy range from approximately 5O GeV to 100-200 TeV per particle with the element-to-element charge resolution from protons to iron, and the electron spectrum of primary cosmic rays.

Spectra

The ATIC instrument performed a stratospheric flight about the South Pole from December 29th 2002 to January 18th 2003.

"ATIC-2"	
Detector	ATIC
Detector location	Flight near geographic South Pole
Homepage	https://cosmicray.umd.edu/atic-home
Article Title	Energy Spectra of Abundant Nuclei of Primary Cosmic Rays from the Data of ATIC-2 Experiment: Final Results
Journal	Bulletin of tho Russian Academy of Science: Physics, 2009. Vol 73, No.5, pp. 564-567
Published	2009
Measuring period	29.12.2002 – 18.1.2003
DOI	10.3103/S1062873809050098
ADS	https://ui.adsabs.har-vard.edu/abs/2009BRASP..73..564P/
Spectra available	all particle spectrum, H, He, C, O, Ne, Mg, Si, Fe
Energy Range	$5.0*10^{10} – 2.0*10^{14}$ eV

13.1.33 TIC

Thin Ioinization Calorimeter(TIC) was flown for 76 hours onbord a balloon in northern Canada in August 1994 in order to measure cosmic rays all-particle spectrum in the energy range from 100 GeV to 10 TeV. The altitue of the flight varied from 4 to 8 g/cm². Nearly 2.000.000 events were recorded.

"TIC"	
Detector	TIC
Detector location	Flight over Canada
Homepage	

Article Title	Data sets from: "Energy Spectra of Abundant Nuclei of Primary Cosmic Rays from the Data of ATIC-2 Experiment: Final Results"
Journal (org)	Izv.Ross. Akad. Nauk, Ser. Fiz. 61, 1181 (1997).
Published	1997
Measuring period	August 1994
DOI	
ADS	
Spectra available	all particle spectrum
Energy Range	$2.0*10^{11} - 1.0*10^{14}$ eV

13.1.34 GRAPES-3

The **GRAPES-3** observatory located in Ooty, India at an altitude of 2200m meter is designed to study the origin, acceleration and propagation of cosmic rays through measurement of extensive air showers, induced by primary cosmic rays or gamma rays entering the Earth's atmosphere in Tev to PeV energies. GRAPES-3 is designed with a high-density array of 400 plastic scintillator detectors (SDs) with an interdetector separation of 8 m which is spread over an area of 25 000 m^2.

"GRAPES-3"	
Detector	GRAPES-3
Detector location	Ooty, India, 11°23.428876' , 76°39.84444", 2200 m asl
Homepage	https://www.tifr.res.in/grapes3/
Article Title	Evidence of a Hardening in the Cosmic Ray Proton Spectrum at around 166 TeV Observed by the GRAPES-3 Experiment
Journal	Physical Review Letters, Volume 132, Issue 5, 2019
Published	2019
Measuring period	1.1.2014 – 26.10.2015
DOI	10.1103/PhysRevLett.132.051002

Spectra

ADS	https://ui.adsabs.har-vard.edu/abs/2024PhRvL.132e1002V/
Spectra available	proton spectrum
Energy Range	$5.0*10^{13} - 2.0*10^{15}$ eV

13.1.35 ARGO

The **ARGO–YBJ** experiment is a full-coverage air shower detector located at the Yangbajing Cosmic Ray Observatory (Tibet, China, 4300 m asl). The high altitude, combined with the full-coverage technique, allows the detection of extensive air showers in a wide energy range and offer the possibility of measuring the cosmic ray proton plus helium spectrum down to the TeV region, where direct balloon/space-borne measurements are available. The ARGO–YBJ experiment is made of a single layer of resistive plate chambers surrounded by a partially instrumented guard ring designed to improve the event reconstruction. The detector is made of 1836 RPCs, arranged in 153 clusters each made of 12 chambers.

"ARGO"	
Detector	ARGO
Detector location	90°26'E and 30°13'N. Tibet, CN, 4300m asl
Homepage	https://argo.na.infn.it/
Article Title	Cosmic ray proton plus helium energy spectrum measured by the ARGO-YBJ experiment in the energy range 3–300 TeV
Journal	Physical Review D 91, 112017
Published	2015
Measuring period	11/2007 – 2/2013
DOI	10.1103/PhysRevD.91.112017
ADS	https://ui.adsabs.har-vard.edu/abs/2015PhRvD..91k2017B/
Spectra available	H+He spectrum
Energy Range	$4.0*10^{12} - 2.5*10^{14}$ eV

13.1.36 ARGO+LHAASO

The data were collected simultaneously by ARGO-YBJ and a single wide field of view Cherenkov telescope located at the Yangbajing Cosmic Ray Observatory. The Cherenkov telescope is located 79 m away the center of the ARGO-YBJ central carpet in the southeast direction. The telescope (named WFCT-02) has been operated starting from 2008. Another similar instrument (named WFCT-01) is 99 m off the center of the ARGO-YBJ carpet in the northwest direction. Both WFCT-01 and WFCT-02 are the prototypes of the future telescopes of the LHAASO experiment.

"ARGO+LHAASO"	
Detectors	ARGO and LHAASO (prototype)
Detector location	90°26'E and 30°13'N. Tibet, CN, 4300m asl
Homepage	https://argo.na.infn.it/
Article Title	Knee of the cosmic hydrogen and helium spectrum below 1 PeV measured by ARGO-YBJ and a Cherenkov telescope of LHAASO
Journal	Physical Review D 92, 082005
Published	2015
Measuring period	12/2010 – 2/2012
DOI	10.1103/PhysRevD.92.092005
ADS	https://ui.adsabs.harvard.edu/abs/2015PhRvD..92i2005B/
Spectra available	H+He spectrum
Energy Range	$1.5*10^{14} – 2.5*10^{15}$ eV

13.1.37 CREAM

The balloon-borne CREAM experiment has measured elemental spectra of cosmic rays from protons to iron nuclei since 2004. It has flown six times, circumnavigating the Antarctic continent with ∼161 days of accumulated exposure.

The **CREAM-I** comprised of a suite of particle detectors to determine the charge and energy of the very high energy particles. The detector configuration included a timing charge detector (TCD), a transition radiation detector (TRD) with a Cerenkov detector (CD), a silicon charge detector (SCD), hodoscopes (HDS), and a tungsten/scintillating fibre calorimeter. The first

Spectra

Long Duration Balloon (LDB) flight of the CREAM-I payload was launched from McMurdo Station, Antarctica on2004 December 16. It subsequently circumnavigated the South Pole three times for a record-breaking duration of 42 days. The flight was terminated on 2005 January 27. The instrument float altitude remained between 37 and 40 km through most of the flight.

"CREAM-I"	
Detectors	CREAM-I (balloon experiment)
Homepage	https://cosmicray.umd.edu/cream/
Article Title	Cosmic Ray proton and helium spectra from the first CREAM flight
Journal	The Astrophysical Journal, 728:122 (8pp)
Published	2011
Measuring period	12/2010 – 2/2012
DOI	110.1088/0004-637X/728/2/122
ADS	https://ui.adsabs.harvard.edu/abs/2015PhRvD..92i2005B/
Spectra available	H, He spectrum
Energy Range	$8*10^{11} – 2*10^{14}$ eV

The instrument for **CREAM-II** included a redundant system for particle identification, consisting of a timing-charge detector (TCD), a Cherenkov detector (CD), a pixelated silicon charge detector (SCD), and a sampling imaging calorimeter (CAL) designed to provide a measurement of the energy of CR nuclei in the multi-TeV region. The CREAM-II instrument was launched from McMurdo station in Antarctica on 2005 December 16th. The balloon circled the South Pole twice at a float altitude between 35 and 40 km. The flight was terminated on 2006 January 13th, 28 days after the launch.

"CREAM-II"	
Detectors	CREAM-II (balloon experiment)
Homepage	https://cosmicray.umd.edu/cream/
Article Title	Cosmic Ray proton and helium spectra from the first CREAM flight
Journal	The Astrophysical Journal, 707:593
Published	2009
Measuring period	12/2005 – 1/2006

DOI	10.1088/0004-637X/707/1/593
ADS	https://ui.adsabs.harvard.edu/abs/2009ApJ...707..593A/
Spectra available	C, O, Ne, Mg, Si, Fe-spectra
Energy Range	$2.5*10^{10} - 7.5*10^{12}$ eV

The **CREAM-III** payload had a successful 29-day flight around the Antarctic continent. It was launched on a long duration balloon from Williams Field near McMurdo station, Antarctica on 2007 December 19th, and it landed on 2008 January 17th. The float altitude during the flight was between 37 and 40 km. The CREAM-III instrument included a tungsten/scintillating fiber calorimeter, a dual-layer silicon charge detector (SCD), a Cherenkov camera (CherCam), a Cherenkov detector (CD), and a timing charge detector (TCD).

"CREAM-III"	
Detectors	CREAM-III (balloon experiment)
Homepage	https://cosmicray.umd.edu/cream/
Article Title	Cosmic Ray proton and helium spectra from the first CREAM flight
Journal	The Astrophysical Journal, 839:5
Published	2017
Measuring period	12/2007 – 1/2008
DOI	10.3847/1538-4357/aa68e4
ADS	https://ui.adsabs.harvard.edu/abs/2017ApJ...839....5Y/
Spectra available	H, He-spectra
Energy Range	$3*10^{11} - 2*10^{14}$ eV

13.1.38 H.E.S.S.

H.E.S.S. is a system of Imaging Atmospheric Cherenkov Telescopes to investigates cosmic gamma rays in the GeV to TeV energy range. The name H.E.S.S. stands for **H**igh **E**nergy **S**tereoscopic **S**ystem. H.E.S.S. is located in Namibia, near the Gamsberg mountain at 1830m asl. The detection of high energy gamma rays with the H.E.S.S. telescopes is based on the imaging air Cherenkov technique. The H.E.S.S. instrument used for this measurement consists of four CTs each equipped with a 960 pixel camera.

Spectra

"H.E.S.S."	
Detectors	H.E.S.S.
Homepage	https://www.mpi-hd.mpg.de/hfm/HESS/
Article Title	First ground-based measurement of atmospheric Cherenkov light from cosmic rays
Journal	Phys Rev D
Published	2007
Measuring period	2004 - 2006
DOI	10.1103/PhysRevD.75.042004
ADS	https://ui.adsabs.harvard.edu/abs/2007PhRvD..75d2004A/
Spectra available	Fe spectrum (with SIBYLL and QGSjet)
Energy Range	$1.5*10^{13} - 1.4*10^{14}$ eV

13.1.39 VERITAS

VERITAS (Very Energetic Radiation Imaging Telescope Array System) is a ground-based gamma-ray instrument operating at the Fred Lawrence Whipple Observatory (FLWO) in southern Arizona, USA. It is an array of four 12m optical reflectors for gamma-ray astronomy in the GeV - TeV energy range. These imaging Cherenkov telescopes are deployed such that they have the highest sensitivity in the VHE energy band (50 GeV - 50 TeV), with maximum sensitivity from 100 GeV to 10 TeV. Each telescope has a mirror area of about $100m^2$, consisting of 350 hexagonal with a focal length of 12m.

"VERITAS"	
Detector	VERITAS
Detector location	Fred Lawrence Whipple Observatory (FLWO) in southern Arizona, USA, 31°40.51N; 110°57.124W
Homepage	https://veritas.sao.arizona.edu/
Article Title	Measurement of the Iron Spectrum in Cosmic Rays by VERITAS
Journal	Phys Rev D
Published	2018, 98
Measuring period	9/009 – 5/2012
DOI	10.1103/PhysRevD.98.022009

Spectra

ADS	https://ui.adsabs.har-vard.edu/abs/2018PhRvD..98b2009A/
High Energy Interaction Models used	CORSIKA / QGSJet-II-03
Spectra available	Fe spectrum
Energy Range	$2*10^{13} - 3.5*10^{14}$ eV

13.1.40 SOKOL

The SOKOL satellite experiment was performed in 1985–1986. The ionization calorimeter was mounted on the Kosmos-1713 satellite. The device consisted of two Cherenkov charge detectors and 10 iron absorber layers separated by scintillator detectors. Light signals from these detectors were registered using photomultiplier tubes.

The SOKOL experiment was performed to investigate cosmic rays at the energy range 10^{12}–10^{14} eV. The energy spectra of various groups of nuclei were reconstructed.

"SOKOL"	
Detector	SOKOL
Detector location	Satellite edxperiment
Homepage	
Article Title	Energy spectra of cosmic rays above 2 TeV as measured by the "SOKOL" apparatus
Journal	ICRC 1993
Published	1993
Measuring period	1985<y - 1986
DOI	
ADS	https://ui.adsabs.harvard.edu/abs/1993ICRC....2...17I/
Spectra available	All particle, H, He, CNO, NeMgSi, Fe spectra
Energy Range	$2*10^{10} - 3*10^{14}$ eV

"SOKOL-2"	
Detector	SOKOL
Detector location	Satellite edxperiment
Homepage	
Article Title	The mass composition of cosmic rays according to data obtained in the SOKOL-2 satellite experiment
Journal	Advances in Space Research 60 (2017) 1578–1582
Published	2017
Measuring period	1985 -1986
DOI	10.1016/j.asr.2017.07.008
ADS	https://ui.adsabs.harvard.edu/abs/2017Ad-SpR..60.1578T/
Spectra available	All particle, H, He, CNO, NeMgSi, Fe spectra
Energy Range	$2*10^{10} – 3*10^{14}$ eV

13.1.41 TELESCOPE ARRAY (TA)

TA is a hybrid detector that uses air fluorescence detectors (FD) combined with a ground array covering an energy range from 4 PeV to over 100 EeV.

The Telescope Array(TA) experiment, located in Millard County, Utah, USA, is measuring the ultra high energy cosmic rays since 2008 and it is the largest cosmic ray detector in the northern hemisphere. The TA has three fluorescence detector (FD) stations overlooking a surface detector array of 507 counters, each consisting of 2 layers of $3m^2 \times 1.2cm$ scintillators. The counters are positioned on a 1200m grid and span a $680m^2$ area on the ground in total. The three TA FD stations are Black Rock Mesa (BR), Long Ridge (LR), and Middle Drum (MD). Both BR and LR have 10 telescopes each, with 256 pixels per telescope that use 10 MHz FADC readout system, and each station covers 108° in azimuth and 3° to 33° degrees in elevation. TA MD has 14 telescopes, with 256 pixels per telescope that use sample and hold electronics, and the station covers 112° in azimuth and 3° to 31° degrees in elevation. The main TA detectors have been in operation since March 2008.

"Telescope Array"	
Detector	Telescope Array
Detector location	Millard County, Utah, USA,
Homepage	
Article Title	Highlights from the Telescope Array Experiment
Journal	Proceedings of the 21st ISVHECRI 2022.
Published	2023
Measuring period	
DOI	10.48550/arXiv.2209.03591
ADS	https://ui.adsabs.har-vard.edu/abs/2022arXiv220903591S/
Spectra available	All particle
Energy Range	$10^{18} - 3*10^{20}$ eV

13.2   GET SPECTRA

To get spectra published with the respective detector component choose either the DOI (Digital Object Identifier) or the Detector itself and load the data sets.

With the format settings, you can select directly the scaling and the spectral index of the request, which will be invoked by pressing the 'Load' button again.

A click inside the box where the papers are displayed will allow you to select the plots and download the data sets.

Note for MAC/Safari users: The drop-down menus in the 'Select-Option' Boxes do not work properly with some Safari Browsers. Please give the 'Detector' or the 'DOI' directly as listed or use other browsers.

Spectra

Fig. 13.2.1.   *"Spectra' selection page*

14 DATA FORMATS

14.1 ASCII

ASCII is a plain text data format. The KCDC data sets released with WOLF-359 and VULCAN have only been transferred in ASCII data format. Due to a rapidly increasing number of parameters and meta information we changed to *HDF5* and *root* file format respectively for coming releases. However, ASCII will be provided too but only for non-array quantities. If an array quantity like '*Muon Energy Deposit'* or '*Arrival Time'* is selected the ASCII format button will no longer be available.

For **ASCII** format up to six files are transmitted, depending on the detector components selected.

infos.txt	holds information on your requests, like the quantities selected and the cuts applied
array.txt	data sets of the KASCADE array quantities
grande.txt	data sets of the GRANDE array quantities
calorimeter.txt	data sets of the CALORIMETER quantities
lopes.txt	data sets of the LOPES quantities
general.txt	general event information
row_mapping.txt	event table, 'active/inactive' information on detector components
EULA.pdf	End User Licence Agreement

As it is possible that one or more detector components are missing in the respective event (due to for example repairs etc.), the file **'row_mapping.txt'** is provided the user. It contains a row number for each component and is set to '-1' if the component was missing.

14.2 ROOT

ROOT is an object-oriented framework developed by CERN aimed at solving the data analysis challenges of high-energy physics.

Data Formats

For **ROOT** format only three files are transmitted

infos.txt   holds information on your requests, like the quantities selected
and the cuts applied

events.root   root data sets for all selected quantities including 'row_map'

EULA.pdf   End User Licence Agreement

The root file contains one tree for each detector component and a tree to map the entries for

the selected detector components for each event (see fig. 14.2.1.).
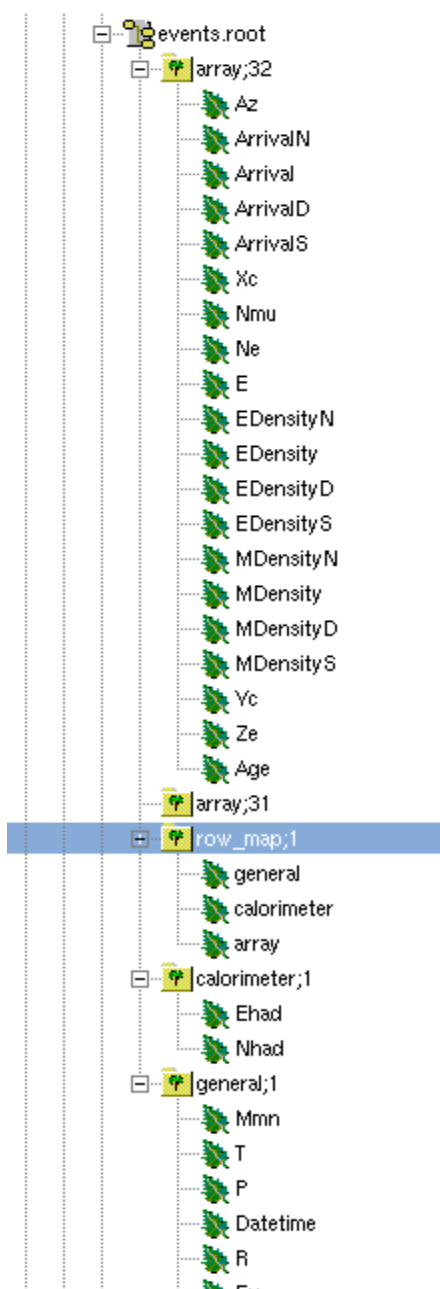
Fig. 14.2.1.   *ROOT –trees example*
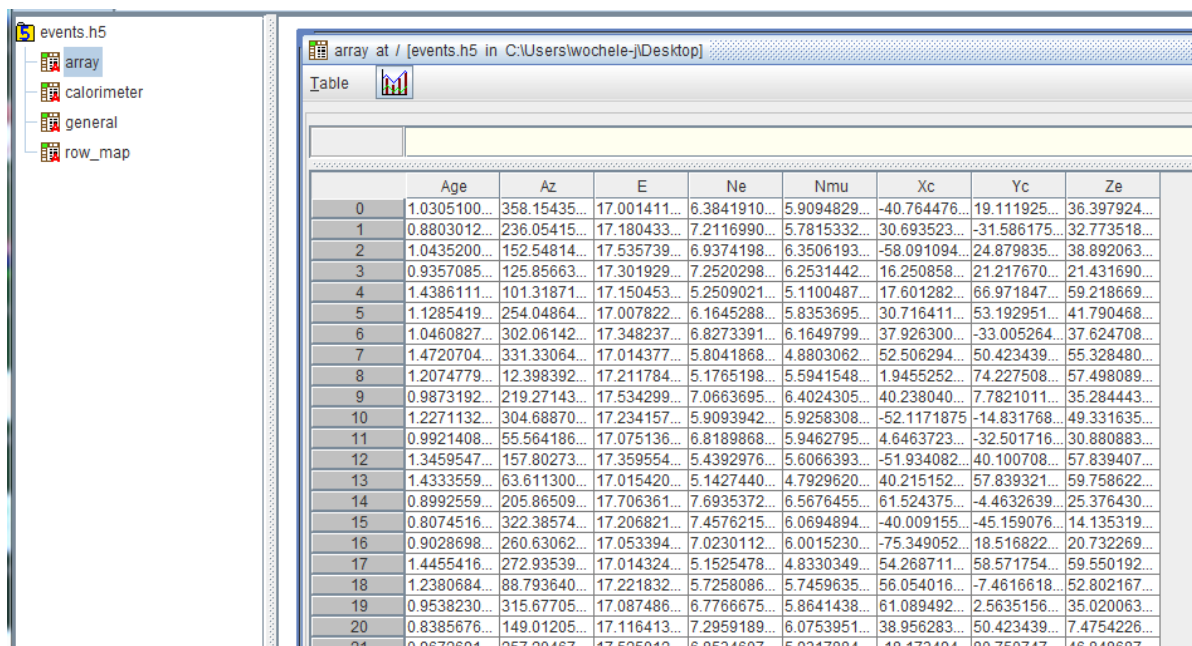
14.3   HDF5

Hierarchical Data Format (HDF) is a file format designed to store and organize large amounts of numerical data objects and a wide variety of metadata. HDF is a unique technology suite that makes possible the management of extremely large and complex data collections with no limit on the number or size of data objects. HDF is freely available distribution supported by many commercial and non-commercial software platforms, including Java, C, C++, Fortran 90 and Python. HDF provides a rich set of integrated performance features that allow for access time and storage space optimizations.

For **HDF5** format only three files are transmitted

infos.txt	holds information on your requests, like the quantities selected and the cuts applied
events.h5	hdf5 data sets for all selected quantities including 'row_map'
EULA.pdf	End User Licence Agreement

The h5 file will contain one table for each detector component and a table to map the entries for the selected detector components for each event (see fig. 14.3.1.).

Fig. 14.3.1.   *HDF5 –tree & data tables example*

KCDC provides the **HDF5** data format from the release ᴍᴇʀɪᴅɪᴀɴ.

14.4   GENERAL DATA HANDLING

The **row_mapping** information always provided with the data sets can be used to deselect time periods where a detector component was missing. In the present status this applies to the Hadron '*Calorimeter*' and to '*GRANDE*'. A deselected detector component is set to '-1' in the row_mapping file as shown in the example of fig 14.4.1 where the calorimeter was not active for some time. The event counter for this component was not increased.

calorimeter	general	array
0	0	0
1	1	1
2	2	2
:		
9687	9687	9687
9688	9688	9688
9689	9689	9689
9690	9690	9690
-1	9691	9691
-1	9692	9692
-1	9693	9693
-1	9694	9694
:		
-1	10044	10044
-1	10045	10045
-1	10046	10046
-1	10047	10047
9691	10048	10048
9692	10049	10049
9693	10050	10050
.		

Fig. 14.4.1.   *Example of 'row_mapping.txt'*

If the order of events is important for the analysis (for example if you want to estimate the effective running time of the experiment by plotting the time difference between two subsequent events) you have to sort the data of the ASCII data file. As the run number [R] and the event number within one run [Ev] are both in increasing orders in time, a combination of those two quantities, which are for various reasons always shipped with the data, gives a correct sequence of the data sets. If the Global Time [GT] is selected it can be used in the same way to sort the data sample. But have in mind that at a data rate of ~4Hz Gt must not be unique.

14.5   PROBLEMS WHILE HANDLING THE DATA FILES

14.5.1 WARNING WHEN OPENING ROOT FILES

The root files are created using the 'ROOT 6' version. If you open the *events.root* file with a different version you might get some warnings as outlined below which can be ignored.

```
root [1] Warning in <TStreamerInfo::BuildCheck>:
  The StreamerInfo of class TTree read from file events.root
  has the same version (=19) as the active class but a different checksum.
  You should update the version to ClassDef(TTree,20).
  Do not try to write objects with the current class definition,
  the files will not be readable.
```

> Warning in <TStreamerInfo::CompareContent>: The following data member of
> the on-file layout version 19 of class 'TTree' differs from
> the in-memory layout version 19:
>   double fWeight; //
> :
> :

14.5.2 32-bit LINUX Systems

As the files transmitted can be rather large, we strongly recommend using a 64-bit system. There is p.e. a 2GB file-size limit in LINUX. This limit is deeply embedded in the versions of Linux for 32-bit CPUs so there is no workaround for this situation.

15   DATA SET HISTORY

This chapter holds information on the data sets (Quantities) published in the various KCDC releases and how these quantities were derived from the data measured by KASCADE.

15.1   DATA SETS FOR WOLF359

The data sets for the KCDC release WOLF359 (released on 4.11.2013) were recorded between 25.10.1996 and 20.12.2003 with the KASCADE Array detector and processed with the KASCADE reconstruction program KRETA, Version V1.18/05 (Library compiled 20140804). The event selection is based on the requirements listed below, invoked by cuts adapted during data pre-processing using KRETA version V1.15/00.

Requirements	
the shower reconstruction in the KASCADE Array Processor did not fail	**and**
there was an Array trigger	**and**
the distance of the core to Array centre < 91 m (radial cut)	**and**
0.0 < AGE < 1.5	**and**
zenith angle ZE < 60°	**and**
missing clusters < 3	**and**
NE > 100	**and**
NMU > 100	

From all events recorded during this period of time 158,718,853 events survived all quality cuts applied and were stored in the KCDC *MySql* database. This data sample was called *FullData* and represents the basis on which all user cuts were applied then.

The complete ranges of the Quantities published in WOILF359 are described in the table below.

Data Set History

	Quantity	Full Range
Energy	E	1.0e14 to 1.0e18 (log10) eV
Core Position X	XC	-91.0 m to + 91.0 m
Core Position Y	YC	-91.0 m to + 91.0 m
Zenith Angle	ZE	0.0° to 60.0°
Azimuth Angle	AZ	0.0° to 360.0°
Number of Electrons	SIZE	1.0e1 to 1.0e8 (log10)
Number of Muons	NMU	1.0e1 to 5.0e6 (log10)
Date	YMD	19961025 to 20031219
Hour	HMS	0.0 to 235959.0
Global Time	GT	846,252,788 to 1,071,878,399
Micro Time	MMN	0.0 to 999,999,999.0
Run Number	IRUN	282 to 4683
Event Number	IEVE	1.0 to 4,100,000.0
Air Temperature	T200	-20.0° to +50°
Air Pressure	P200	980.0 to 1030.0 hPa

Moreover some Preselections had been published which we thought might be of special interest for some applications.

Selection Name	Cut(s) applied	Nr of Events
Full Data	no Cuts	158,718,853
High Energy	5.0e15 < E < 1.0e18	1,156,873
Vertical Showers	0.0 < ZE < 5.0 °	5,999,889

The data are available only in ASCII data format no matter whether ‚Full Data' or ‚Selections' are requested.

15.2   DATA SETS FOR VULCAN

The data sets for the KCDC release ᐯᑌᒪᑕᗩᑎ (released on 12.11.2014) were recorded between 25.10.1996 and 20.12.2003 with the KASCADE Array detector and the central Hadron Calorimeter. The events were processed with the KASCADE reconstruction program KRETA, Version V1.18/05 (Library compiled 20140804). The event selection is based on the requirements listed below, invoked by cuts adapted during data pre-processing using the same KRETA version.

Requirements	
the shower reconstruction in the KASCADE Array Processor did not fail	**and**
there was an Array trigger	**and**
the distance of the core to Array centre < 91 m (radial cut)	**and**
0.0 < AGE < 1.5	**and**
zenith angle ZE < 60°	**and**
missing clusters < 3	**and**
NE > 100	**and**
NMU > 100	

Originally, 657,987,334 events were recorded during this period of time. After all these quality cuts applied 159,612,095 events survived and were stored in the KCDC *MongoDB*. This data sample was called *FullData* and represents the basis on which all user cuts were applied.

From all quantities measured and reconstructed in KASCADE by KRETA 16 parameters were made available for public usage in the first place. The Quantity *'AGE'* was newly added.

On 12.12.2014 KCDC release ᐯᑌᒪᑕᗩᑎ.ᎧᎩ has been published with two additional quantities, the '*Number of Hadrons*' and the '*Energy of Hadrons*'.

In this version some Quantities names have been changed. Furthermore, the former Quantity '*SIZE*' which represented in ᗯᎧᒪᖴᒞᎩᎩ the number of charged particles has been transferred to '*Ne*', the real number of electrons. This change is the reason for the differences in

some spectra compared to WOLF-359 and for the different number of events in the preselections published.

The complete ranges of the Quantities published in VULCAN and VULCAN.OI is described in the table below.

	Quantity	Full Range
Energy	E	1.0e14 to 1.0e18 (log10) eV
Core Position X	XC	-91.0 m to +91.0 m
Core Position Y	YC	-91.0 m to +91.0 m
Zenith Angle	ZE	0.0° to 60.0°
Azimuth Angle	AZ	0.0° to 360.0°
Number of Electrons	Ne	1.0e1 to 1.0e8 (log10)
Number of Muons	Nmu	1.0e1 to 5.0e6 (log10)
AGE	AGE	0.1 to 1.48
Date	YMD	19961025 to 20031219
Hour	HMS	0.0 to 235959.0
Global Time	GT	846,252,788 to 1,071,878,399
Micro Time	MT	0.0 to 999,999,999.0
Run Number	R	282 to 4683
Event Number	EV	1.0 to 4,100,000.0
Air Temperature	T	-20.0° to +50°
Air Pressure	P	980.0 to 1030.0 hPa
Hadron Energy	Ehad	-1, 0; 0.0 to 1.0e16 (log10) eV
Hadron Number	Nhad	-1.0, 0.0 to 511.0

Moreover some Preselections had been published which we thought might be of special interest for some applications.

Selection Name	Cut(s) applied	Nr of Events
Full Data	no Cuts	159,612,095
High Energy	5.0e15 < E < 1.0e18	865,597
Vertical Showers	0.0 < ZE < 5.0 °	6,033,402
Hadrons	0.0 < Ehad < 1.0e16 0.0 < Nhad < 511.0 0.0° < ZE < 30.0° 0.19 < YC < 10.19 m -5.0 < XC < +5.0 m	119,090

We restricted ourselves on scalar quantities for the VULCAN release. Publishing data arrays requires a redesign of the data shop, which will be done in the release MERIDIAN.

The data are available only in ASCII data format no matter whether ‚Full Data' or ‚Selections' are requested.

15.3   DATA SETS FOR MERIDIAN

The data sets for the KCDC release MERIDIAN   (released on 12/2015) were recorded between 8.5.1998 and 20.12.2003 with the KASCADE Array detector and the central Hadron Calorimeter. The events were processed with the KASCADE reconstruction program KRETA, Version V1.19/08 (Library compiled 20150109). The event selection is based on the requirements listed below, invoked by cuts adapted during data pre-processing using KRETA version V1.18/05. Going to a newer version of our reconstruction program was necessary because the version used for earlier releases could not handle field arrays as required here.

Requirements	
the shower reconstruction in the KASCADE Array Processor did not fail	**and**
there was an Array trigger	**and**
the distance of the shower core to Array centre < 91 m (radial cut)	**and**
0.1 < AGE < 1.48	**and**
zenith angle ZE < 60°	**and**
missing clusters < 3	**and**
NE > 100	**and**
NMU > 100	

Originally 582,754,488 events were recorded during this period of time. After all these quality cuts applied 147,739,495 events survived and were stored in the KCDC *MongoDB*. This data sample was called *FullData* and represents the basis on which all user cuts were applied.

From all quantities measured and reconstructed in KASCADE by KRETA 20 parameters were made available for public usage in MERIDIAN. The Quantities *'Electron Density'* , 'Muon *Density*' and '*Arrival Times'* were newly added.

The complete ranges of the Quantities published in MERIDIAN are described in the table below.

	Quantity	Full Range
Energy	E	13.0 to 18.0 (log10) eV
Core Position X	Xc	-91.0 m to + 91.0 m
Core Position Y	Yc	-91.0 m to + 91.0 m
Zenith Angle	Ze	0.0° to 60.0°
Azimuth Angle	Az	0.0° to 360.0°
Number of Electrons	Ne	2.0 to 8.7 (log10)

Number of Muons	Nmu	2.0 to 7.7 (log10)
AGE	AGE	0.1 to 1.48
Date & Time	Datetime	19,980,508 to 20,031,220
Global Time	Gt	894,645,350 to 1,071,891,549 s
Micro Time	Mt	0.0 to 999,999,999.0
Run Number	R	877 to 4683
Event Number	Ev	1.0 to 4,100,000.0
Air Temperature	T	-20.0° to +50.0 °C
Air Pressure	P	960.0 to 1040.0 hPa
Hadron Energy	Ehad	0; 10.0 to 16.0 (log10) eV
Hadron Number	Nhad	0.0 to 511.0
Electron Density	EDensity	0.0 to 2000.0 part/m²
Muon Density	MDensity	0.0 to 100.0 part/m²
Arrival Times	Arrival	-1000.0 to 2000.0 ns
Additional Quantities provided with 'Electron Densities'		
Distance to Shower Core	EDensityD	0.0 to 200.0 m
Number of active stations	EDensityN	0.0 to 252.0
Station ID	EDensityS	1 to 252
Additional Quantities provided with 'Muon Densities'		
Distance to Shower Core	MDensityD	0.0 to 200.0 m
Number of active stations	MDensityN	0.0 to 192.0
Station coordinate	MDensityS	1 to 252 m
Additional Quantities provided with 'Arrival Times'		

Distance to Shower Core	ArrivalD	0.0 to 200.0 m
Number of active stations	ArrivalN	0.0 to 252.0
Station coordinate	ArrivalS	1 to 252

Important note:

We offer in MERIDIAN about 11% less data than in the former releases WOLF 359 and VULCAN. This reflects the fact that all KASCADE publications are based on data sets with the same trigger conditions. Earlier runs (between 282 and 876) were recorded with a higher trigger threshold resulting in a frequency of about 2Hz. From 8.5.1998 (run 877) we lowered the threshold to roughly double the data rate. All subsequent runs up to the last KAS-CADE run 7417 are recorded under the same trigger conditions. In order to ensure as far as possible a constant data quality for the whole data sample, we decided to reduce the data set offered.

15.4   DATA SETS FOR NABOO

The data sets for the KCDC release NABOO 1.0 (released on 1/2017) were recorded between 8.5.1998 and 15.1.2013, thus covering the whole measuring period of KASCADE and KASCADE-Grande. The data were recorded with the KASCADE Array detectors, the Grande Array detectors and the Central Hadron Calorimeter. The events were processed with the KASCADE reconstruction program KRETA, Version V1.19/09 (Library compiled 20160216). The event selection is based on the requirements listed below, invoked by cuts adapted during data pre-processing using KRETA version V1.18/05. Going to a newer analysis version of our reconstruction program was necessary because the version used for earlier KCDC releases could not handle field arrays as required here.

Two different data selections were merged:

   - the KASCADE Array data selection partly used for the previous publications

    - the GRANDE Array data selection used for the data sets recorded with the Grande detectors.

In the table below the number of events published for the three detector components is listed

Detector	Nr of Events
KASCADE	395,789,234
GRANDE	35,310,393
CALORIMETER	100,655,080

15.4.1 KASCADE Array Data Sets

Requirements for ARRAY data sets	
the shower reconstruction in the KASCADE Array Processor did not fail	**and**
there was an Array trigger	**and**
the distance of the shower core to Array centre < 91 m (radial cut)	**and**
0.1 < AGE < 1.48	**and**
zenith angle Ze < 60°	**and**
missing clusters < 3	**and**
Ne > 100	**and**
Nmu > 100	

Originally 1.7 billion events were recorded during this period of time. After all these quality cuts applied 433,209,340 events survived and were stored in the KCDC **MongoDB**. This data sample was called **FullData** and represents the basis on which all user cuts were applied.

From all quantities measured and reconstructed in KASCADE by KRETA 20 parameters were made available for public usage. In MERIDIAN the Quantities *'Electron Density'* , 'Muon

Density' and '*Arrival Times*' were newly added. In NABOO the Quantities '*Electron Density*' and '*Muon Density*' were replaced by '*Electron Energy Deposit*' and '*Muon Energy Deposit*'. The reason is outlined in detail chapter 4.6.

The complete ranges of the Quantities published in NABOO are described in the table.

	Quantity	Full Range
Energy	E	13.0 to 18.0 (log10) eV
Core Position X	Xc	-91.0 m to + 91.0 m
Core Position Y	Yc	-91.0 m to + 91.0 m
Zenith Angle	Ze	0.0° to 60.0°
Azimuth Angle	Az	0.0° to 360.0°
Number of Electrons	Ne	2.0 to 8.7 (log10)
Number of Muons	Nmu	2.0 to 7.7 (log10)
AGE	AGE	0.1 to 1.48
Date & Time	Datetime	19980508 to 20130115
Global Time	Gt	894,645,350 to 1,358,242,843 s
Micro Time	Mt	0.0 to 999,999,999.0
Run Number	R	877 to 7417
Event Number	Ev	1 to 4,100,000
Air Temperature	T	-20.0° to +50.0 °C
Air Pressure	P	960.0 to 1040.0 hPa
Hadron Energy	Ehad	0; 10.0 to 16.0 (log10) eV
Hadron Number	Nhad	0.0 to 511.0
Electron Energy Deposit	EDeposit	0.0 to 30,000.0 MeV
Muon Energy Deposit	MDeposit	0.0 to 1000.0 MeV

Arrival Times	Arrival	-1550.0 to 2550.0 ns
Additional Quantities provided with 'Electron Energy Deposits		
Number of active stations	EDepositN	0.0 to 252.0
Station ID	EDepositS	1 to 252
Additional Quantities provided with 'Muon Energy Deposits'		
Number of active stations	MDepositN	0.0 to 192.0
Station coordinate	MDepositS	1 to 252 m
Additional Quantities provided with 'Arrival Times'		
Distance to Shower Core	ArrivalD	0.0 to 200.0 m
Number of active stations	ArrivalN	0.0 to 252.0
Station coordinate	ArrivalS	1 to 252

15.4.2 GRANDE ARRAY DATA SETS

Requirements for GRANDE data sets	
all 7 stations from at least on GRANDE hexagon have triggered (7/7 coincidence, see chapter 3.1)	**and**
station with max energy deposit is not at the GRANDE array border	**and**
the reconstruction was successful	**and**
at least 12 GRANDE stations available for time fit	**and**
-0.385 < Age < 1.485	**and**
zenith angle Ze < 40°	**and**
Nch > 11111	**and**
Nmu > 1500	**and**
no disturbance from synchrotron radiation source ANKA	

Originally 88,459,522 events were recorded from 20.12.2003 and 5.11.2012. After all these quality cuts applied 35,310,393 events survived and were stored in the KCDC *MongoDB*. This data sample was called *GrandeFullData* and represents the basis on which all user cuts for the GRANDE data sets are applied.

From all quantities measured and reconstructed in KASCADE-Grande by KRETA nine parameters were made available for public usage in NABOO. The Quantities *'Grande Energy Deposit'* , and 'Grande *Arrival Times'* are data arrays. A detailed description is given in chapter 6.

The complete ranges of the GRANDE Quantities published in NABOO are described in the table below.

	Quantity	Full Range
Grande Core Position X	Xc	-500.0 m to + 100.0 m
Grande Core Position Y	Yc	-600.0 m to + 100.0 m
Grande Zenith Angle	Ze	0.0° to 40.0°
Grande Azimuth Angle	Az	0.0° to 360.0°
Grande Number of charged particles	Nch	11111. to 9.0 (log10)
Grande Number of Muons	Nmu	1500. to 8.0 (log10)
Grande AGE	Age	-0.385 to 1.485
Grande Energy Deposit	GDeposit	0.0 to 100,000.0 MeV
Grande Arrival Times	GArrival	1000.0 to 10,000.0 ns
Additional Quantities provided with 'Grande Energy Deposits'		
Number of active Grande stations	GDepositN	0.0 to 37.0
Grande Station ID	GDepositS	1 to 37
Additional Quantities provided with 'Grande Arrival Times'		

Number of active Grande stations	GArrivalN	0.0 to 37.0
Grande Station coordinate	GArrivalS	1 to 37

15.5   Data Sets for OCEANUS

The data sets for the KASCADE, GRANDE and the CALORIMETER published with KCDC release OCEANUS (released on 11/2019) were recorded between 8.5.1998 and 15.1.2013, thus covering the whole measuring period of KASCADE and KASCADE-Grande (details see chapter 14.4). The data were recorded with the KASCADE Array detectors, the Grande Array detectors and the Central Hadron Calorimeter. The events were processed with the KASCADE reconstruction program KRETA, Version V1.19/09 (Library compiled 20160216). The event selection is based on the requirements listed below, invoked by cuts adapted during data pre-processing using KRETA version V1.18/05. Going to a newer analysis version of our reconstruction program was necessary because the version used for earlier KCDC releases could not handle field arrays as required here.

In addition data recorded with the LOPES radio detection devices have been added as a new detector component 'LOPES'. As the radio data were not part of the KASCADE data stream, the events have been merged offline by means of the transmitted time stamps. LOPES data were recorded in the time range 25.7.2005 (Run 5534) to 26.10.2009 (Run 6821). From this period 3058 events survived all quality cuts and have been added to the KCDC DataShop.

Concerning KASCADE and GRANDE two different data selections were merged:

    - the KASCADE Array data selection partly used for the previous publications

    - the GRANDE Array data selection used for the data sets recorded with the Grande detectors.

For LOPES a separate data collection was used, merged offline with the KASCADE and GRANDE data.

In the table below the number of events published for the 4 detector components is listed

Data Set History

Detector	Nr of Events
KASCADE	395,789,234
GRANDE	35,310,393
CALORIMETER	100,655,080
LOPES	3,058

15.5.1 LOPES Radio Antenna Data Sets

Requirements for LOPES data sets	
the radio data have been analysed and reconstructed using the KASCADE or GRANDE reconstructed parameters	**and**
the parameters reconstructed by LOPES (like core position and angles) agree with either KASCADE or GRANDE reconstructed parameters	**and**
the events reconstructed are already published in KCDC	

From all quantities measured and reconstructed in LOPES with a stand-alone program outside of KRETA, 22 parameters were made available for public usage in OCEANUS. The Quantities *'Height'* , *'Envelop Time'*, *'Distance'* and *'Polarization'* are data arrays. A detailed description is given in chapter 7.

The complete ranges of the GRANDE Quantities published in OCEANUS are described in the table below.

	Quantity	Full Range
E-Field Max	E-FieldMax	0 -50,000 V/m
Azimuth East-West	Azimuth EW	0 – 360°
Azimuth North-South	Azimuth NS	0 – 360°
Elevation East-West	Elevation EW	40 – 90°
Elevation North-South	Elevation NS	40 – 90°
CC Height East-West	CC Height EW	0 - 20 µV/m/MHz

Data Set History

CC Height North-South	CC Height NS	0 - 20 µV/m/MHz
X Height East-West	X Height EW	0 - 20 µV/m/MHz
X Height North-South	X Height NS	0 - 20 µV/m/MHz
Cone Angle East-West	ConeAngle EW	$0 - 0.1$ rad
Cone Angle North-South	ConeAngle NS	$0 - 0.1$ rad
NCC Beam Antenna East-West	NCCbeamAnt EW	0 - 30
NCC Beam Antenna North-South	NCCbeamAnt NS	0 - 30
Eta East-West	Eta EW	$-0.04 - 0.1$ 1/m
Eta North-South	Eta NS	$-0.04 - 0.1$ 1/m
Eps East-West	Eps EW	0 - 100 µV/m/MHz
Eps North-South	Eps NS	0 - 100 µV/m/MHz
Geomagnetic Angle	Geomag_Angle	$0 - 120°$
Geomagnetic Angle Grande	Geomag_AngleG	$0 - 120°$
Reconstruction Index	Reconstruction	65 or 71 [A or G]
Envelope Time	LOPES envelope Time	$-2500 - -1600$ ns
Height	LOPES-Height	$0 - 60$ µV/m/MHz
Distance	LOPES-Distance	$0 - 800$ m
Polarization	LOPES-Polar	NS or EW or both
LopesCompID	Identifier	0 or 1

The parameter **LopesCompID** was introduced as an identifier for data sets, which contain LOPES events.

239

15.6 DATA SETS FOR PENTARUS

With the release PENTARUS 1.0 we introduced for the first time a second DataShop, called '**COMBINED'**. It offers data from the joint analysis of the 'KASCADE' and 'GRANDE' detector arrays of the KASCADE-Grande experiment.

A detailed explanation of the properties and contents of this new DataShop can be found in a separate manual, the '**KCDC-Combined User Manual**', which can be called up via the 'Materials' main menu item.

The data previously published in KCDC are still available via the DataShop **'KASCADE'.** Some inconsistencies in the data content of the KASCADE mongoDB have been cleared.

15.7 DATA SETS FOR SKARAGAN

With the release SKARAGAN 1.0 we introduced for the first time a DataShop not directly connected to KASCADE-Grande, the 'Makte-Ani' DataShop. Published are data sets from the Makewt-Ani detector system, placed on Mt. Aragats (Aragats Cosmic Ray Observatory, Armenia), 3200m above the sea level at 40°25'N, 44°15'E operating at an atmospheric depth of ~700g/cm^2 running between 1997 and 2007.

A short explanation of the properties and contents of this new DataShop can be found in a separate manual, the '**Maket-Ani User Manual**', which can be viewed via the 'Materials' main menu item.

16 PUBLICATIONS

In the 'Publications' menu item two types of publications are listed: KCDC publications KCDC based publications.

16.1 KCDC PUBLICATIONS

Publications describing the web portal of the KASCADE Cosmic Ray Data Centre, the data sets offered for download and the procedures how to handle the data as well as some basic information on the KASCADE detector components. These publications are released by the KCDC-Team.

16.2 KCDC BASED PUBLICATIONS

Papers and conference contributions using KCDC data sets downloaded from the web portal.

17 MATERIALS

The menu item 'Materials' contains a collection of information of interest for the KCDC user. The main components are the various manuals for the different DataShops published via the KCDC web portal. Furthermore, software helps and interesting information about the use of the KCDC data are provided.

17.1 KCDC MANUALS

A manual is provided for each DataShop published via the KCDC web portal. It contains information about the respective experiment, data acquisition and data analysis and, as far as possible, detailed descriptions of the published parameters. This information is intended to contribute to the broadest possible understanding of the data provided in order to enable efficient data analysis by the KCDC user.

Furthermore, manuals for the associated simulations are provided (if available) separately, which hold information about how these simulations were created and how they can be used.

Detector	Manual	Remark
KASCADE-Grande	KCDC User Manual	general KCDC user manual with measured data from the KASCADE, GRANDE, Central CALORIMETER and the LOPES detectors and all relevant information concerning the KCDC web portal
KASCADE-Grande	KCDC Simulations User Manual	simulations correlated with the KASCADE-Grande measurement data
COMBINED	KCDC-Combined User Manual	user manual for the combined data analysis
COMBINED	KCDC-Combined Simulations Manual	simulations correlated with the COMBINED data analysis
Maket-Ani	Maket-Ani User Manual	user manual for the Maket-Ani data analysis

17.2   KCDC Software Helps

'Software Helps' contains program fragments as a little help for the users. Currently included are C-programs, which describe the merging of the different data trees using 'row_mapping' and a Python fragment to calculate the X- and Y-positions of the KASCADE-Arrays detector stations necessary to analyse the energy deposits of muons and electron/gammas.

18 USER ACCOUNT

All changes and manipulations of your user account including creating, closing and monitoring can be invoked via the 'User Account' menu item (see fig.18.1.)

Fig. 18.1.   *Access to your user account*

18.1 CREATE ACCOUNT

To create a new account press the respective button of the menu item and provide all necessary information. Mandatory information is listed in the yellow information box on the right hand side. You have to accept the 'End User License Agreement' (EULA) and the 'Privacy Policy'. Press 'Register' to submit your request.

You will get an email with a link to confirm your request similar to:

User Account

> *Hello user `potter`.*
> *Please use the following link to activate your account!*
> *kcdc.iap.kit.edu/account/create/confirm/NA/46z-b8aca5ecdc0aa2e949ff/ (Click)*
> *Your KCDC Team*

If you encounter that the link (click) is not clickable please put the confirmation link directly to your browser's URL. In case of success you will be redirected to the *'User Profile'* page.

Fig. 18.1.1.   *KCDC user registration page*

18.2   LOGIN / LOGOUT

The *'Login'* / *'Logout'* button is a toggle button. You can either use the button of the navigation menu or the one in the metanavigation menu (header) to login or logout. Since version QUALO released on May 2nd 2022 there are three ways you login to KCDC (fig. 18.2.1.).:

User Account

- if you are a registered user you can login with your username and password. Otherwise, you are asked to register. After login in the user profile page will be displayed holding all the information of your account;

- if you are a member the 'Institute for Astroparticle Physics' (IAP) at KIT you can login with your KIT account on a local Keycloak server;

- if you are registered in Helmholtz, you can login via the Helmholtz AAI directly. If you login via Helmholtz AAI your email address and your credentials will not be transferred to KCDC. Thus, if you want to receive a mail when your job has finished you have to add both in the 'User Profile' menu item in your 'User Account' (see chapter 18.3.).

The latter two procedures are still in an experimental stage.

Fig. 18.2.1   *KCDC user login page*

18.3   USER PROFILE

Here you can change your profile settings like name and email address by editing the field list and pressing the 'Apply Changes' button.

Fig. 18.3.1   *KCDC user profile page*

18.4   CHANGE & RESET PASSWORD

To change the password give old and new password (twice). A valid password requires at least 6 characters.

If however you have forgotten your password use the 'Reset Password' button to order a new password. You just have to supply your username press the 'order reset-key' and a new pass-word will be sent to the address corresponding to this username. Confirming this links redi-rects you to a kcdc page where you can change the password.

User Account

Fig. 18.4.1   *KCDC change password page*
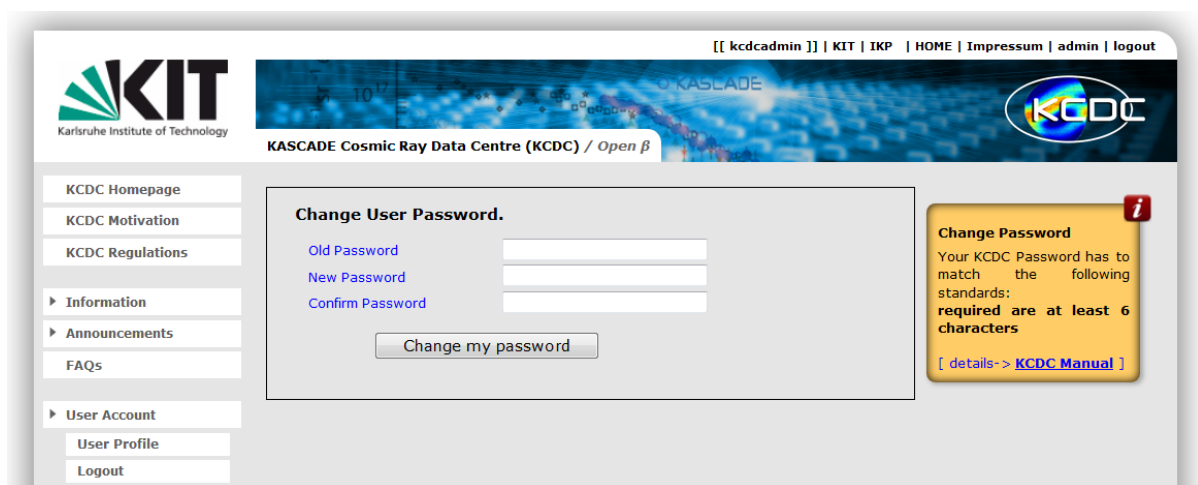
18.5   CLOSE ACCOUNT

Use the '*Close Account'* button to delete your account for good. You just have to provide your password and press the 'Close Account' button.

Note: Closing your account is a non-reversible action so please be careful!

If you want to continue using KCDC data you will have to re-register a new account.
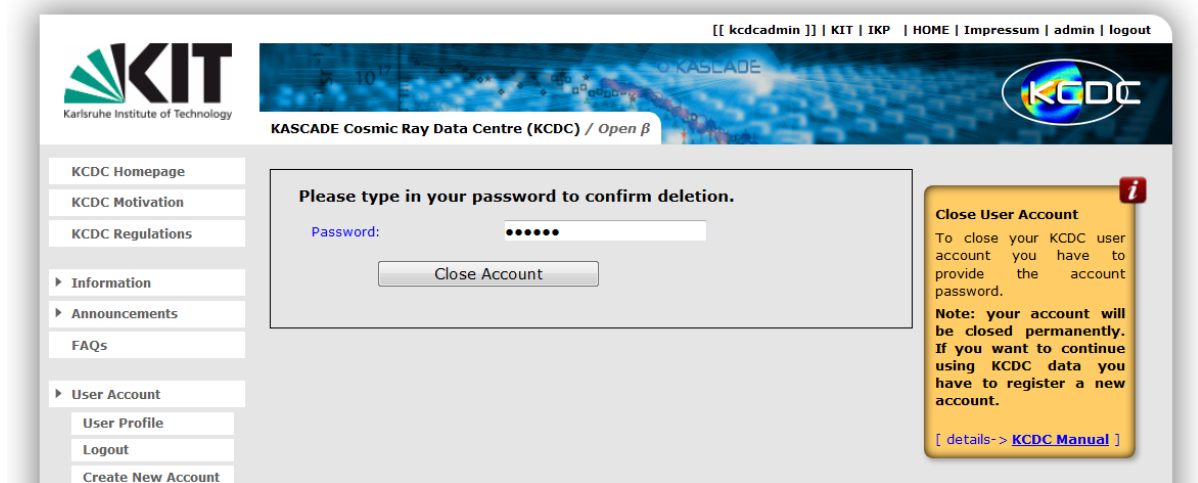

Fig.18.5.1   *Close your KCDC account*

18.6   PRIVACY

This site uses a local piwik analytics server to track usage of the website. The data are only used for site improvement and to report usage statistics for the public authorities. We declare that by no means user specific data will be passed to third party.

18.6.1   WHEN DO WE COLLECT PRIVACY DATA AND HOW DO WE USE THEM?

When you view the KCDC website the webserver stores the used IP, date and what pages are accessed in his log files for 14 days. This helps us to identify service problems or intrusion.

We track page views and downloads with *MAMOTO* (former piwik) analytics to learn about the customer needs. Further we have to report usage statistics anonymized to the public financiers. If you set "do-not-track" in your browser we respect that.

Cookies are used to store the session ID of the browser, a *Cross Site Request Forgery* protection cookie and the analytics cookies used by *MAMOTO*.

When you register as a KCDC user your data will be transferred encrypted to our web service and stored in a local database. This information is used to provide you a personal file share and inform you via email about the status of the job processing.

18.6.2   WHEN DO WE DELETE THE DATA?

When you close your account all your account data are deleted.

You may deactivate or restrict the transmission of cookies by changing the settings of your web browser. Cookies that are already stored may be deleted at any time.

18.6.3   HOW DO WE SECURE YOUR PRIVACY DATA?

Only KCDC administrators have access to the user database and KCDC server. The data will reside also on a system backup with limited administrator access.

We use encrypted connections and limit access to the database to the minimum. We will never share or publish privacy data.

Analytics statistics are stored anonymized.

18.6.4 YOUR OPTIONS AND RIGHTS

If you do not want to register to use KCDC you can always mail us to find an alternative access to the data. You can at any time ask us to delete your data.

19   CONTACT US

To get in touch with us you can either send us an email or use the ‚Bug Report' feature.

19.1   BUG REPORT

To report a bug use the 'Send a Bug Report' button. There you add some information on the troubling url and give a detailed description of the problem. As many problems are connected to incompatibilities of web browsers, please provide us the name and version of the browser which raised the problem. If you want to send us screen shot please use the mailing option iap-kcdc@lists.kit.edu. Pressing the submit button will send the report.

The KCDC team will be automatically informed and will respond as soon as possible.

Fig. 19.1.1   *'Send a Bug Report' main page*

Contact us

The response dialog can be viewed via the 'List reported Bugs' page by pressing 'view reply'. There you can send another message as long as the status information 'already resolved' is set to 'no' (see fig 19.1.2). Furthermore, you will get an email telling you that you received an answer from the KCDC-team. If we think that the problem is resolved the status will be set to 'yes' and the reply box will disappear.

In case of a report of common interest we will publish the answer on our FAQs page.
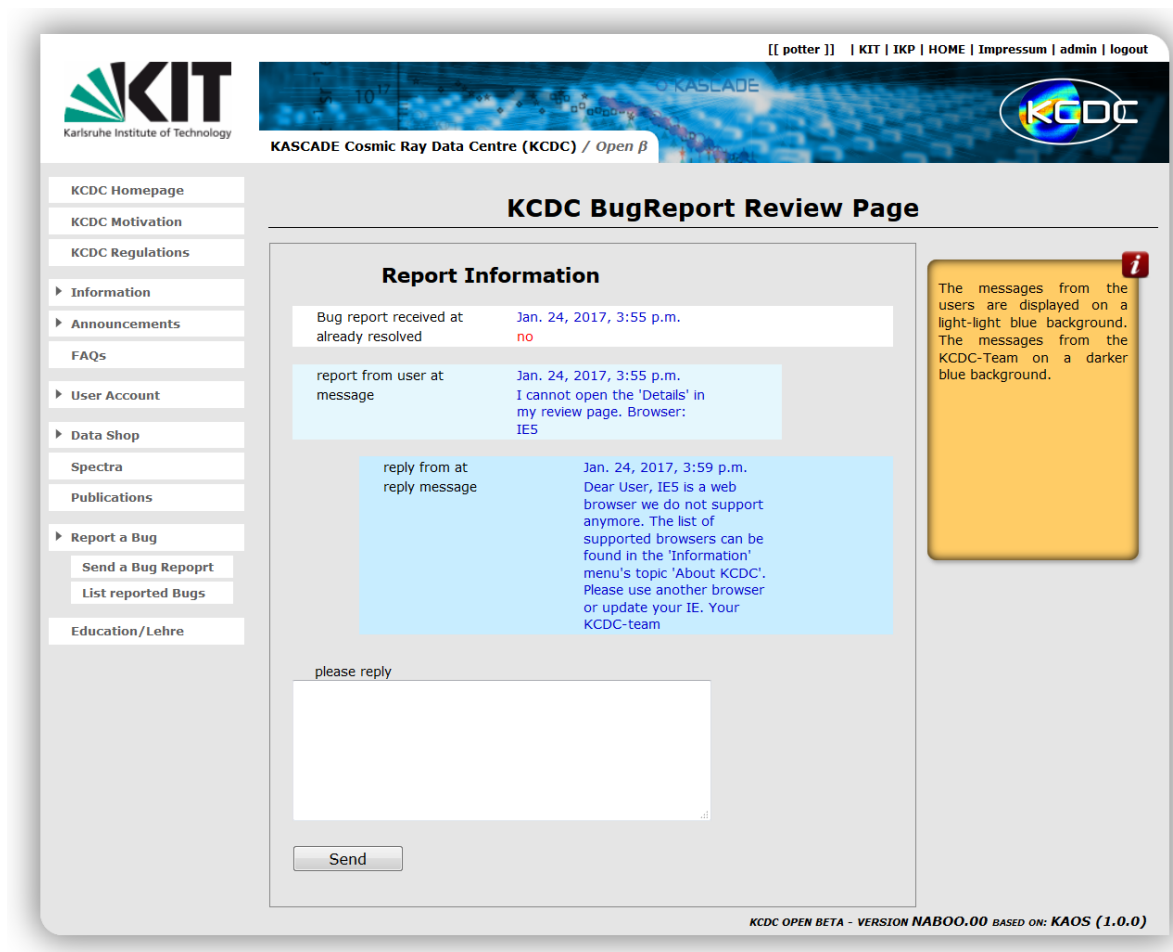
Fig. 19.1.2   *"List reported Bugs' page*

19.2   MAIL

If you have special questions which are not related to a bug do not hesitate to send us an email at ' iap-kcdc@lists.kit.edu '.

Contact us

As we are permanently trying to improve our software we are thankful for any feedback we

get from your side.

The *'Education/Lehre'* page holds a compilation of interesting lessons within the vast field of cosmic radiation to illustrate the processes within and outside of our atmosphere by means of the data sets of the KASCADE experiment.

Fig. 20.1.   *Education page in KCDC*

The colours of the frames indicate the rating of the exercise:

red	'heavy stuff' with special knowledge
yellow	'medium heavy' with little basic knowledge
green	'rather easy' without basic knowledge
blue	'finger exercise'

The link at the bottom of each exercise opens a pdf-file with descriptions of the exercise, comments on where to get more information, hints how to solve the problem and where to get the data. A complete solution with a discussion of the results is a well provided in the pdf-file which can be downloaded and printed.

This collection will be extended in cooperation with interested teachers and pupils to increase the understanding of the cosmic radiation.

These exercises are presently available in German and in English. Pressing the respective flag in the top right corner switches the language.

21   RELEASE PHILOSOPHY AND OUTLOOK

Always remember that this whole thing was started by a mouse.

Walt Disney (1901-1966).

21.1   KCDC RELEASE PHILOSOPHY

In KCDC we distinguish between:

- **Major Release**, where we change the release name, is introduced when either the published data sets have been changed/extended or if a significant change has occurred in the software;

- **Minor Release**, where we change only the Version number, usually means the functional expansion of the KCDC web portal like publishing data or information for the user which are not implemented in the data shop itself for example offering the simulations via download pages;

- **Patches / Updates,** where we change only the sub-version number, usually is a bug fix or the introduction of new tutorials.

OCEANUS 1.0

Subversion name: **Patch / Update**
Version name: **Minor Release**
Release name: **Major Release**

21.2   MANUAL IN PROGRESS

This is not a finished work. We are going to improve the descriptions in this manual and add more information to help users with different physics knowledge to work with the KASCADE data. The KCDC-Team is quite aware of the fact that not all details concerning data acquisition and data analyses can be described in this manual. Furthermore, the plots shown in chapters 4 to 7 are only examples, mostly based on a subsample of the data sets published. So applying user cuts either in the KCDC Data Shop or in your own analysis can change these spectra drastically.

If you encounter any problem or you have any question please do not hesitate to ask.

21.3 NEXT MILESTONES

Check on https://kcdc.iap.kit.edu/announcements/developerNews the next milestones for KCDC web application and release of new observables in KCDC data shop.

21.4 ACKNOWLEDGEMENT

We want to thank Prof. Dr. Blümer to pick up the responsibility of OPEN ACCESS in this project, to encourage and support the team in setting up this web application.

Special thanks to Dr H.-J. Mayer who supported us whith his expertise on the data analysis program KRETA with fruitful discussions and detailed answers even though he is no longer working for KASCADE-Grande.

We are grateful to Dr Frank Schröder and Dr Katrin Link for their untiring help in integrating the LOPES data into KCDC and in creating the LOPES documentation.

22 REFERENCE LIST

22.1 KCDC

The KASCADE Cosmic-ray Data Centre KCDC: Releases and Future Perspectives

4th International Workshop on Data Life Cycle in Physics (DLC 2020), Online,

08.06.2020 – 10.06.2020

Data Structure Adaption from Large-Scale Experiment for Public Re-Use

3rd International Workshop on Data Life Cycle in Physics (DLC 2019), Irkutsk, Russia,

02.04.2019 – 07.04.2019

The KASCADE Cosmic-ray Data Centre KCDC: Granting Open Access to Astroparticle Physics Research Data

The European Physical Journal C (2018) →publication to be cited

A new release of the KASCADE Cosmic Ray Data Centre (KCDC)

35th International Cosmic Ray Conference (ICRC)

Bexco, Busan, Korea; 12. - 20.7.2017

The KASCADE Cosmic-ray Data Centre (KCDC)

34th International Cosmic Ray Conference (ICRC)

The Hague, Netherlands; 30.7. - 6.8.2015

The KASCADE Cosmic-ray Data Centre (KCDC)

24th European Cosmic Ray Symposium (ECRS)

Kiel, Germany; 1. - 5.9.2014

The KASCADE Cosmic ray Data Centre - providing open access to astroparticle physics research data

Helmholtz Open Access Webinars on Research Data Webinar

15; 8. - 12.11.2013

KCDC - publishing research data from the KASCADE experiment

Helmholtz Open Access Workshop

DESY, Hamburg; 11.6.2013

22.2   KASCADE

The Cosmic-Ray Experiment – KASCADE

Nuclear Instruments and Methods; A513 (2003) p490-510

A Warm-liquid Calorimeter for Cosmic-ray Hadrons

Nuclear Instruments and Methods; A427 (1999) 528-542

22.3   KASCADE-Gʀᴀɴᴅᴇ

The KASCADE-Grande experiment

Nuclear Instruments and Methods; A620 (2009) p202-216

22.4   LOPES

The LOPES radio antennas

Nucl.Instr. and Meth.A604 (2009) 1-8

Nucl.Instr. and Meth.A969 (2012) 100-109

22.5   Mᴀᴋᴇᴛ-Aɴɪ

The ANI experiment: on the investigation of interactions from hadrons and nuclei in the energy range 103-105 TeV

Nuclear Instruments and Methods in Physics Research A323 (1992) 104 - l07

Status Report on "MAKET-ANI" Experiment

International Cosmic Ray Conference, Vol. 1, held August 28-September 8, 1995 in Rome, Italy.

Extension of the GAMMA muon underground detectors for studies of the longitudinal air shower development

FZK Report 6215 p90-97

EAS size spectrum for 1 · 105 < Ne < 5 · 107 measured by the MAKET installation

FZK Report 6215 p51-54

Investigation of the integral EAS size spectra in the knee region

FZK Report 6215 p55-60

The EAS Size Spectrum measured at ANI Cosmic Ray Observatory in the region of Knee

26th International Cosmic Ray Conference 1999

Status of the Experiment ANI. The first stage-Installation "GAMMA"

Proceedings of ICRC 1999

The Dependence of the Age Parameter from EAS Size and Zenith Angle of Incidence

arXiv:astro-ph/0002077v1 3 Feb 2000

Determination of the EAS Attenuation Length from Data of the ANI Experiment

Astro-ph/0002076v1 3 Feb 2000

Determination of angular accuracy of the MAKET ANI surface array

Proceedings of ICRC 2001: 818

Investigation of extensive air shower development using large slant depth of atmosphere

Proceedings of ICRC 2001; 2001ICRC....1.165S

Determination of primary energy spectra from MAKET ANI data

Proceedings of ICRC 2001: 93

Concept and layout of the EAS delayed particles arrival time distribution measurements at Aragats cosmic ray observatory

Proceedings of ICRC 2001: 818

The cosmic ray energy spectrum around the knee measured with the GAMMA array at Mt. Aragats

J. Phys. G: Nucl. Part. Phys.28(2002) 2317–2328

Light and Heavy Cosmic-Ray Mass Group Energy Spectra as Measured by the MAKET-ANI Detector

The Astrophysical Journal, 603:L29–L32, 2004 March 1

The Size Spectra of Extensive Air Showers in the "Knee" region Measured by MAKET-ANI Detector

29th International Cosmic Ray Conference Pune (2005) 6, 93-96

Study of extensive air showers and primary energy spectra by MAKET-ANI detector on mountain Aragats

Astroparticle Physics 28 (2007) 58–71

Cosmic Ray research in Armenia

Advances in Space Research 44 (2009) 1183–1193

Particle bursts from thunderclouds: Natural particle accelerators above our heads

Physical Review D83,062001 (2011)

lOth anniversary of the MAKET -ANI results on the energy spectra at "knee" energies

A. Chilingarian

EAS data classification into light and heavy mass groups by MAKET installation

http://crd.yerphi.am/ANI_Collaboration_Scientific_Papers_Reports

22.6 WEB –LINKS

For nore information on KASCDE/KASCADE see:

https://web.iap.kit.edu/KASCADE/

For nore information on KCDC see:

https://kcdc.iap.kit.edu/

For more infpormation on Maket-Ani see:

http://crd.yerphi.am

Berlin declaration:

https://openaccess.mpg.de/Berlin-Declaration

23 GLOSSARY

CC-Beam
The CC-Beam (cross-correlation beam) is the result of the interferometry combination of radio antennas. This is done by calculating the cross-correlation of all antenna pairs. So each signal of one antenna is multiplied by the signals of all other antennas. These values are then averaged. The square root is thus the value of the CC beam, keeping the sign as the sign of the CC beam. This indicates whether the original signals were coherent or not. The CC beam of a coherent signal is always positive, while incoherent noise gives a value close to zero, as contributions of different signs are averaged out. An anti-phase signal in the antenna pairs provides a negative value for the CC beam.

COMBINED
We use the name **COMBINED** as a synonym for combined data analysis of the KASCADE and the GRANDE detector systems of the KASCADE-Grande experiment. The combined analysis merges the advantages of the formerly separated KASCADE and GRANDE analyses and leads to a consistent spectrum in the energy range 10^{15} to 10^{18} eV. The aim of the combined analysis was to utilize this improved reconstruction to get one single, consistent energy spectrum.

CORSIKA
CORSIKA (**CO**smic **R**ay **SI**mulations for **KA**scade) is a program package for detailed simulation of extensive air showers initiated by high-energy cosmic ray particles. Protons, light nuclei up to iron, photons, and many other particles may be treated as primaries.

The particles are tracked through the atmosphere until they undergo reactions with the air nuclei or - in the case of instable secondaries – decay.

CRES
CRES (**C**osmic **R**ay **E**vent **S**imulation) is code package for the simulation of the signals / energy deposits in all detector components of KASCADE/KASCADE-Grande as response to an extensive air shower as simulated with **CORSIKA**.

KAOS

KAOS is the acronym for **K**arlsruhe **A**stroparticlephysics **O**pen data **S**oftware. It has been written in the context of the KASCADE Cosmic Ray Data Centre ([KCDC](#)), a web portal designed for the publication of scientific data recorded with the [KASCADE experiment](#). **KAOS** is implemented using a plugin-based design with a focus on easy extensibility and modifiability in order to work also outside the context of KCDC.

KRETA

KRETA (**K**ascade **R**econstruction of **Ext**ensive **A**ir showers) is the main data analysis engine of the KASCADE/KASCADE-Grande Experiment. KRETA is written in Fortran77 and makes extensive use of the CERN library and its various software packages.

MIP

Minimum ionizing particles (MIPS) are charged particles, which embody the minimum ionizing losses in substances. This situation occurs when the kinetic energy of particles is at least twice larger than their rest mass. For example, electrons (or protons) can be considered as minimum ionizing particles when their kinetic energy is greater than 1 MeV (or GeV 2). Since the ionization losses of these particles are only weakly dependent on their momentum, it is generally accepted that minimum ionizing particles produce an even distribution of free charge carriers along their paths. Muons for example suffer an energy loss of roughly 1.5 MeV/cm when passing through a plastic scintillator.

P-Beam

The P-beam (power beam) is calculated as the root of the average power of all antennas, which is always positive. However, it cannot be determined whether a signal is coherent or not.

Quantity

The KASCADE variables published in the KCDC web portal are called quantities

SDC

Shower **D**isc **C**oordinates. The sketch below illustrates how the radii R1 and R2 are calculated in SDC.
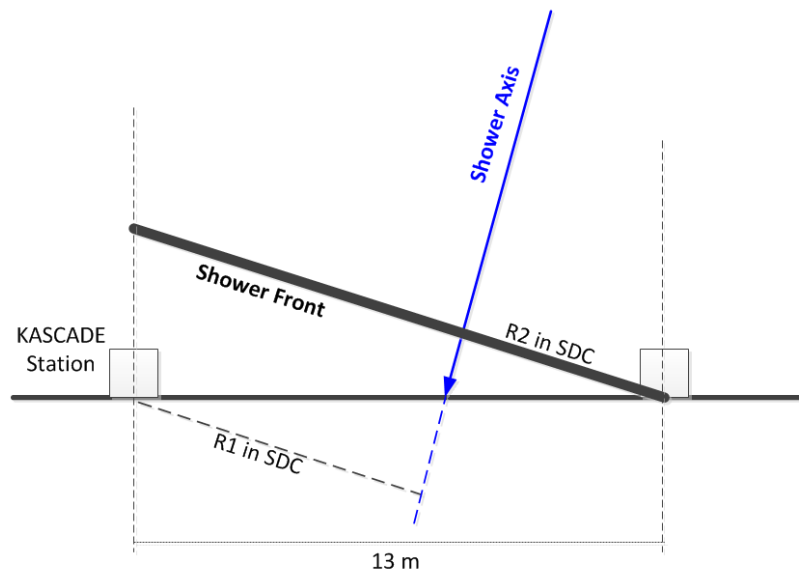
ZEBRA   **ZEBRA** is a memory management system and part of the CERN library. ZEBRA allows a dynamic creation of data structures at execution time as well as the manipulation of those structures.

24 APPENDIX

24.1 APPENDIX A

Correlation between station ID as given in the data arrays and the x- and y-positions in KAS-CADE coordinates. The positions are given in [m]. The column 'Detect' shows the detectors installed (number of e/γ and μ detectors). The red numbers indicate that the station is dislocated from the regular grid. Four stations in the centre of the KASCADE array are missing, their positions are blocked by the central calorimeter. The scheme of the nomenclature is illustrated in fig. A.1.

St-ID	X- Y-Position [m]	Detect	St-ID	X- Y-Position [m]	Detect	St-ID	X- Y-Position [m]	Detect
1	-97.5 / -97.5	2 e/γ & 4μ	85	-19.5 / -45.5	4 e/γ	169	6.5 / 32.5	4 e/γ
2	-84.5 / -97.5	2 e/γ & 4μ	86	-6.5 / -45.5	4 e/γ	170	19.5 / 32.5	4 e/γ
3	-84.5 / -84.5	2 e/γ & 4μ	87	-6.5 / -32.5	4 e/γ	171	19.5 / 45.5	4 e/γ
4	-97.5 / -84.5	2 e/γ & 4μ	88	-19.5 / -32.5	4 e/γ	172	6.5 / 45.5	4 e/γ
5	-71.5 / -97.5	2 e/γ & 4μ	89	-19.5 / -19.5	4 e/γ	173	58.5 / 6.5	2 e/γ & 4μ
6	-58.5 / -97.5	2 e/γ & 4μ	90	-6.3 / -18.5	4 e/γ	174	71.5 / 6.5	2 e/γ & 4μ
7	-58.5 / -84.5	2 e/γ & 4μ	91	-19.5 / -6.5	4 e/γ	175	71.5 / 19.5	2 e/γ & 4μ
8	-71.5 / -84.5	2 e/γ & 4μ	92	-45.5 / -19.5	4 e/γ	176	58.5 / 19.5	2 e/γ & 4μ
9	-71.5 / -71.5	2 e/γ & 4μ	93	-32.5 / -19.5	4 e/γ	177	84.5 / 6.5	2 e/γ & 4μ
10	-58.5 / -71.5	2 e/γ & 4μ	94	-32.5 / -6.5	4 e/γ	178	97.5 / 6.5	2 e/γ & 4μ
11	-58.5 / -58.5	2 e/γ & 4μ	95	-45.5 / -6.5	4 e/γ	179	97.5 / 19.5	2 e/γ & 4μ
12	-71.5 / -58.5	2 e/γ & 4μ	96	6.5 / -45.5	4 e/γ	180	84.5 / 19.5	2 e/γ & 4μ
13	-97.5 / -71.5	2 e/γ & 4μ	97	19.5 / -45.5	4 e/γ	181	84.5 / 32.5	2 e/γ & 4μ
14	-84.5 / -71.5	2 e/γ & 4μ	98	19.5 / -32.5	4 e/γ	182	97.5 / 32.5	2 e/γ & 4μ
15	-84.5 / -58.5	2 e/γ & 4μ	99	6.5 / -32.5	4 e/γ	183	97.5 / 45.5	2 e/γ & 4μ
16	-97.5 / -58.5	2 e/γ & 4μ	100	32.5 / -45.5	4 e/γ	184	84.5 / 45.5	2 e/γ & 4μ
17	-45.5 / -97.5	2 e/γ & 4μ	101	45.5 / -45.5	4 e/γ	185	58.5 / 32.5	2 e/γ & 4μ
18	-32.5 / -97.5	2 e/γ & 4μ	102	45.5 / -32.5	4 e/γ	186	71.5 / 32.5	2 e/γ & 4μ
19	-32.5 / -84.5	2 e/γ & 4μ	103	32.5 / -32.5	4 e/γ	187	71.5 / 45.5	2 e/γ & 4μ
20	-45.5 / -84.5	2 e/γ & 4μ	104	32.5 / -19.5	4 e/γ	188	58.5 / 45.5	2 e/γ & 4μ
21	-19.5 / -97.5	2 e/γ & 4μ	105	45.5 / -19.5	4 e/γ	189	-97.5 / 58.5	2 e/γ & 4μ
22	-6.5 / -97.5	2 e/γ & 4μ	106	45.5 / -6.5	4 e/γ	190	-84.5 / 58.5	2 e/γ & 4μ
23	-6.5 / -84.5	2 e/γ & 4μ	107	32.5 / -6.5	4 e/γ	191	-84.5 / 71.5	2 e/γ & 4μ
24	-19.5 / -84.5	2 e/γ & 4μ	108	7.5 / -19.5	4 e/γ	192	-97.5 / 71.5	2 e/γ & 4μ
25	-19.5 / -71.5	2 e/γ & 4μ	109	19.5 / -19.5	4 e/γ	193	-71.5 / 58.5	2 e/γ & 4μ
26	-6.5 / -71.5	2 e/γ & 4μ	110	19.5 / -6.5	4 e/γ	194	-58.5 / 58.5	2 e/γ & 4μ

St-ID	X- Y-Position [m]	Detect	St-ID	X- Y-Position [m]	Detect	St-ID	X- Y-Position [m]	Detect
27	-6.5 / -58.5	2 e/γ & 4μ	111	58.5 / -45.5	2 e/γ & 4μ	195	-58.5 / 71.5	2 e/γ & 4μ
28	-19.5 / -58.5	2 e/γ & 4μ	112	71.5 / -45.5	2 e/γ & 4μ	196	-71.5 / 71.5	2 e/γ & 4μ
29	-45.5 / -71.5	2 e/γ & 4μ	113	71.5 / -32.5	2 e/γ & 4μ	197	-71.5 / 84.5	2 e/γ & 4μ
30	-32.5 / -71.5	2 e/γ & 4μ	114	58.5 / -32.5	2 e/γ & 4μ	198	-58.5 / 84.5	2 e/γ & 4μ
31	-32.5 / -58.5	2 e/γ & 4μ	115	84.5 / -45.5	2 e/γ & 4μ	199	-58.5 / 97.5	2 e/γ & 4μ
32	-45.5 / -58.5	2 e/γ & 4μ	116	97.5 / -45.5	2 e/γ & 4μ	200	-71.5 / 97.5	2 e/γ & 4μ
33	6.5 / -97.5	2 e/γ & 4μ	117	97.5 / -32.5	2 e/γ & 4μ	201	-97.5 / 84.5	2 e/γ & 4μ
34	19.5 / -97.5	2 e/γ & 4μ	118	84.5 / -32.5	2 e/γ & 4μ	202	-84.5 / 84.5	2 e/γ & 4μ
35	19.5 / -84.5	2 e/γ & 4μ	119	84.5 / -19.5	2 e/γ & 4μ	203	-84.5 /97.5	2 e/γ & 4μ
36	6.5 / -84.5	2 e/γ & 4μ	120	97.5 / -19.5	2 e/γ & 4μ	204	-97.5 /97.5	2 e/γ & 4μ
37	32.5 / -97.5	2 e/γ & 4μ	121	97.5 / -6.5	2 e/γ & 4μ	205	-45.5 / 58.5	2 e/γ & 4μ
38	45.5 / -97.5	2 e/γ & 4μ	122	84.5 / -6.5	2 e/γ & 4μ	206	-32.5 / 58.5	2 e/γ & 4μ
39	45.5 / -84.5	2 e/γ & 4μ	123	58.5 / -19.5	2 e/γ & 4μ	207	-32.5 / 71.5	2 e/γ & 4μ
40	32.5 / -84.5	2 e/γ & 4μ	124	71.5 / -19.5	2 e/γ & 4μ	208	-45.5 / 71.5	2 e/γ & 4μ
41	32.5 / -71.5	2 e/γ & 4μ	125	71.5 / -6.5	2 e/γ & 4μ	209	-19.5 / 58.5	2 e/γ & 4μ
42	45.5 / -71.5	2 e/γ & 4μ	126	58.5 / -6.5	2 e/γ & 4μ	210	-6.5 / 58.5	2 e/γ & 4μ
43	45.5 / -58.5	2 e/γ & 4μ	127	-97.5 / 6.5	2 e/γ & 4μ	211	-6.5 / 71.5	2 e/γ & 4μ
44	32.5 / -58.5	2 e/γ & 4μ	128	-84.5 / 6.5	2 e/γ & 4μ	212	-19.5 / 71.5	2 e/γ & 4μ
45	6.5 / -71.5	2 e/γ & 4μ	129	-84.5 / 19.5	2 e/γ & 4μ	213	-19.5 / 84.5	2 e/γ & 4μ
46	19.5 / -71.5	2 e/γ & 4μ	130	-97.5 / 19.5	2 e/γ & 4μ	214	-6.5 / 84.5	2 e/γ & 4μ
47	19.5 / -58.5	2 e/γ & 4μ	131	-71.5 / 6.5	2 e/γ & 4μ	215	-6.5 / 97.5	2 e/γ & 4μ
48	6.5 / -58.5	2 e/γ & 4μ	132	-58.5 / 6.5	2 e/γ & 4μ	216	-19.5 / 97.5	2 e/γ & 4μ
49	58.5 / -97.5	2 e/γ & 4μ	133	-58.5 / 19.5	2 e/γ & 4μ	217	-45.5 / 84.5	2 e/γ & 4μ
50	71.5 / -97.5	2 e/γ & 4μ	134	-71.5 / 19.5	2 e/γ & 4μ	218	-32.5 / 84.5	2 e/γ & 4μ
51	71.5 / -84.5	2 e/γ & 4μ	135	-71.5 / 32.5	2 e/γ & 4μ	219	-32.5 / 97.5	2 e/γ & 4μ
52	58.5 / -84.5	2 e/γ & 4μ	136	-58.5 / 32.5	2 e/γ & 4μ	220	-45.5 / 97.5	2 e/γ & 4μ
53	84.5 / -97.5	2 e/γ & 4μ	137	-58.5 / 45.5	2 e/γ & 4μ	221	6.5 / 58.5	2 e/γ & 4μ
54	97.5 / -97.5	2 e/γ & 4μ	138	-71.5 / 45.5	2 e/γ & 4μ	222	19.5 / 58.5	2 e/γ & 4μ
55	97.5 / -84.5	2 e/γ & 4μ	139	-97.5 / 32.5	2 e/γ & 4μ	223	19.5 / 71.5	2 e/γ & 4μ
56	84.5 / -84.5	2 e/γ & 4μ	140	-84.5 / 32.5	2 e/γ & 4μ	224	6.5 / 71.5	2 e/γ & 4μ
57	84.5 / -71.5	2 e/γ & 4μ	141	-84.5 / 45.5	2 e/γ & 4μ	225	32.5 / 58.5	2 e/γ & 4μ
58	97.5 / -71.5	2 e/γ & 4μ	142	-97.5 / 45.5	2 e/γ & 4μ	226	45.5 / 58.5	2 e/γ & 4μ
59	97.5 / -58.5	2 e/γ & 4μ	143	-45.5 / 6.5	4 e/γ	227	45.5 / 71.5	2 e/γ & 4μ
60	84.5 / -58.5	2 e/γ & 4μ	144	-32.5 / 6.5	4 e/γ	228	32.5 / 71.5	2 e/γ & 4μ
61	58.5 / -71.5	2 e/γ & 4μ	145	-32.5 / 19.5	4 e/γ	229	32.5 / 84.5	2 e/γ & 4μ
62	71.5 / -71.5	2 e/γ & 4μ	146	-45.5 / 19.5	4 e/γ	230	45.5 / 84.5	2 e/γ & 4μ
63	71.5 / -58.5	2 e/γ & 4μ	147	-19.5 / 6.5	4 e/γ	231	45.5 / 97.5	2 e/γ & 4μ
64	58.5 / -58.5	2 e/γ & 4μ	148	-6.3 / 24.5	4 e/γ	232	32.5 / 97.5	2 e/γ & 4μ
65	-97.5 / -45.5	2 e/γ & 4μ	149	-19.5 / 19.5	4 e/γ	233	6.5 / 84.5	2 e/γ & 4μ

St-ID	X- Y-Position [m]	Detect	St-ID	X- Y-Position [m]	Detect	St-ID	X- Y-Position [m]	Detect
66	-84.5 / -45.5	2 e/γ & 4μ	150	-19.5 / 32.5	4 e/γ	234	19.5 / 84.5	2 e/γ & 4μ
67	-84.5 / -32.5	2 e/γ & 4μ	151	-6.5 / 32.5	4 e/γ	235	19.5 / 97.5	2 e/γ & 4μ
68	-97.5 / -32.5	2 e/v & 4μ	152	-6.5 / 45.5	4 e/γ	236	6.5 / 97.5	2 e/γ & 4μ
69	-71.5 / -45.5	2 e/γ & 4μ	153	-19.5 / 45.5	4 e/γ	237	58.5 / 58.5	2 e/γ & 4μ
70	-58.5 / -45.5	2 e/v & 4μ	154	-45.5 / 32.5	4 e/γ	238	71.5 / 58.5	2 e/γ & 4μ
71	-58.5 / -32.5	2 e/γ & 4μ	155	-32.5 / 32.5	4 e/γ	239	71.5 / 71.5	2 e/γ & 4μ
72	-71.5 / -32.5	2 e/γ & 4μ	156	-32.5 / 45.5	4 e/γ	240	58.5 / 71.5	2 e/γ & 4μ
73	-71.5 / -19.5	2 e/γ & 4μ	157	-45.5 / 45.5	4 e/γ	241	84.5 / 58.5	2 e/γ & 4μ
74	-58.5 / -19.5	2 e/γ & 4μ	158	19.5 / 6.5	4 e/γ	242	97.5 / 58.5	2 e/γ & 4μ
75	-58.5 / -6.5	2 e/γ & 4μ	159	19.5 / 19.5	4 e/γ	243	97.5 / 71.5	2 e/γ & 4μ
76	-71.5 / -6.5	2 e/γ & 4μ	160	10.2 / 24.1	4 e/γ	244	84.5 / 71.5	2 e/γ & 4μ
77	-97.5 / -19.5	2 e/v & 4μ	161	32.5 / 6.5	4 e/γ	245	84.5 / 84.5	2 e/γ & 4μ
78	-84.5 / -19.5	2 e/γ & 4μ	162	45.5 / 6.5	4 e/γ	246	97.5 / 84.5	2 e/γ & 4μ
79	-84.5 / -6.5	2 e/γ & 4μ	163	45.5 / 19.5	4 e/γ	247	97.5 / 97.5	2 e/γ & 4μ
80	-97.5 / -6.5	2 e/γ & 4μ	164	32.5 / 19.5	4 e/γ	248	84.5 / 97.5	2 e/γ & 4μ
81	-45.5 / -45.5	4 e/γ	165	32.5 / 32.5	4 e/γ	249	58.5 / 84.5	2 e/γ & 4μ
82	-32.5 / -45.5	4 e/γ	166	45.5 / 32.5	4 e/γ	250	71.5 / 84.5	2 e/γ & 4μ
83	-32.5 / -32.5	4 e/γ	167	45.5 / 45.5	4 e/γ	251	71.5 /97.5	2 e/γ & 4μ
84	-45.5 / -32.5	4 e/γ	168	32.5 / 45.5	4 e/γ	252	58.5 /97.5	2 e/γ & 4μ

Fig. A.1   *The scheme of the counting of the array station IDs (1 ... 252)*

Appendix

python-code fragment to calculate x- and y-positions of the KASCADE-Arrays detector stations from the station IDs.

```python
def get_station_locs():
    dstcl = 5200.                              // width of array cluster
    dstqa = 2600.                              // width of one sub-cluster
    dstas = 1300.                              // distance between stations
    sddy = [-1., -1., 1., 1.]                  // count matrix X
    sddx = [-1., 1., 1., -1.]                  // count matrix Y
    iasn = 0
    real_iasn = 0
    stations = {}

    for icl in range(1, 17):
        ycl = (float(floor((icl-1)/4))-1.5)*dstcl
        xcl = (float(fmod(icl-1, 4))-1.5)*dstcl

        for j in range(0,4):
            yqa = ycl + 0.5 * dstqa*sddy[j]
            xqa = xcl + 0.5 * dstqa*sddx[j]
            for k in range(0,4):
                yas = yqa + 0.5 * dstas*sddy[k]
                xas = xqa + 0.5 * dstas*sddx[k]
                iasn += 1

                if yas < -dstas or yas > dstas or xas < -dstas or xas > dstas:
                    real_iasn += 1
                    iccdd = icl * 100 + fmod(iasn-1, 16) + 1

    #   stations dislocated from the regular grid
                    if iccdd == 610:                   # ID 90
                        xas += 23.0
                        yas += 100.
                    elif iccdd == 713:                 # ID 108
                        xas += 100.
                    elif iccdd == 1007:                # ID 148
                        xas += 20.
                        yas += 495.9
                    elif iccdd == 1104:                # ID 160
                        xas += 366.5
                        yas += 461.0

                    stations[str(real_iasn)] = [xas/100., yas/100.]
    return stations
```

24.2 APPENDIX B

Correlation between the GRANDE station ID as given in the Grande data arrays and the x- and y-positions in KASCADE coordinates. The positions are given in [m] in reference to the KAS-CADE array centre. The red numbers indicate that the station has been moved during the lifetime of Grande.

Date of validity for the positions given in the table below is 20.12.2003 – 5.11.2012

St-ID	X- Y- Z-Position [m]	St-ID	X- Y- Z-Position [m]	St-ID	X- Y- Z-Position [m]
1	-0.14 / 65.33 / 2.47	14	-260.09 / -136.2 / 1.52	27	-533.7 / -409.1 / 0.87
2	-131.3 / 70.87 / 2.05	15	-377.5 / -145.0 / 1.67	28	101.2 / -507.6 / 1.74
3	-257.0 / 101.7 / 1.96	16	-481.5 / -155.5 / 1.83	29	-24.72 / -507.6 / 1.90
4	-384,8 / 96.12 / 0.84	17	44.09 / -276.6 / 1.65	30	-196.5 / -504.1 / 1.81
5	-499.6 / 95.51 / 1.81	18	-95.83 / -276.0 / 1.29	31	-317.9 / -529.2 / 1.84
6	64.48 / -42.03 / 1.15	19	-195.4 / -272.6 / 1.63	32	-443.3 / -525.9 / 1.95
7	-64.99 / -41.42 / 1.11	20	-319.8 / -267.6 / 1.92	33	-566.5 / -526.4 / 0.63
8	-211.2 / -40.54 / 1.47	21	-481.5 / -234.9 / 1.59	34	-111.9 / -654.9 / 1.90
9	-329.0 / -49.29 / 1.86	22	-608.3 / -281.8 / 0.94	35	-275.0 / -645.4 / 1.71
10	-426.1 / -7.66 / 1.46	23	24.79 / -391.3 / 1.32	36	-389.1 / -653.3 / 1.71
11	-569.8 / 46.42 / 1.90	24	-112.9 / -383.6 / 1.66	37	-517.9 / -620.8 / 1.96
12	24.21 / -156.6 / 1.31	25	-249.8 / -392.0 / 1.48		
13	-140.1 / -143.8 / 1.53	26	-386.5 / -382.1 / 1.84		

24.2.1 MODIFICATIONS OF THE GRANDE STATION POSITIONS

Stations 8 and 30 had to be moved from their original locations by several meters. Their positions and the matching *dates of validity* are outlined in the table below.

St-ID	X- Y- Z-Position [m]	valid from	valid until
8	-211.2 / -40.54 / 1.47	20.12.2003 00:00	23.09.2005 12:00
8	-224.4 / -33.68 / 2.03	23.09.2005 12:00	5.11.2012 23:59
30	-196.5 / -504.1 / 1.81	20.12.2003 00:00	11.05.2011 00:00
30	-193.9 / -525.0 / 1.81	11.05.2011 00:00	5.11.2012 23:59

24.3   APPENDIX C

Correlation between the LOPES antenna ID as used in LOPES and the x- and y-positions in LOPES- (C.1) and KASCADE-coordinates (C.2).

24.3.1   C.1 - LOPES COORDINATES

Ant-ID	X-Position [m]	Y-Position [m]	Z-Position [m]	Polarization
1	79.73	-45.60	1.12	NS
2	111.59	-63.98	1.05	EW
3	36.31	-84.52	1.19	NS
4	54.80	-52.61	1.13	EW
5	22.72	-34.17	1.07	EW
6	22.72	-34,17	1.07	NS
7	2.18	41.15	1.21	NS
8	34.48	22.88	1.16	EW
9	72.72	-20.68	1.06	EW
10	91.02	11.28	0.96	NS
11	-64.10	-111.95	1.27	NS
12	-45.77	-79.76	1.30	EW
13	-84.46	-36.48	1.35	EW
14	-52.31	-54.49	1.25	NS
15	-91.37	-11.36	1.38	NS
16	-72.91	20.41	1.47	EW
17	-111.81	63.48	1.53	EW
18	-79.92	45.56	1.53	NS
19	-34.37	-22.83	1.28	EW
20	-34.37	-22.83	1.28	NS
21	-13.70	-97.84	1.53	EW
22	4.51	-65.93	1.50	EW
23	-41.18	2.16	1.32	NS
24	-22.79	33.43	1.21	EW
25	-61.46	77.65	1.43	EW
26	-29.63	59.18	1.28	NS
27	-7.55	-127.63	1.39	NS
28	-7.55	-127.63	1.39	EW
29	-13.70	-97.84	1.53	NS
30	4.51	-65.93	1.50	NS

Appendix

In LOPES coordinates the positions of the antennas are given in [m] with reference to the KASCADE array centre. But unlike the KASCADE coordinate system, the X-axis points north, the Y-axis points east and the system rotates anti-clockwise. The red numbers indicate that the antenna has been moved during the lifetime of LOPES as outlined in the table below.

24.3.2 C.2 - KASCADE Coordinates

Ant-ID	X-Position [m]	Y-Position [m]	Z-Position [m]	Polarization
1	-62.60	56.24	1.12	NS
2	-91.08	90.83	1.05	EW
3	-91.09	12.80	1.19	NS
4	-65.17	39.04	1.13	EW
5	-38.94	12.93	1.07	EW
6	-38.94	12.93	1.07	EW
7	39.12	12.93	1.21	NS
8	13.00	39.28	1.16	EW
9	-39.08	64.72	1.06	EW
10	-13.06	90.78	0.96	NS
11	-91.15	-91.29	1.27	NS
12	-64.91	-65.13	1.30	EW
13	-12.98	-91.08	1.35	EW
14	-38.81	-64.80	1.25	NS
15	13.07	-91.14	1.38	NS
16	38.86	-64.97	1.47	EW
17	90.65	-91.17	1.53	EW
18	64.98	-65.12	1.53	NS
19	-12.98	-39.16	1.28	EW
20	-12.98	-39.16	1.28	EW
21	-90.80	-38.95	1.53	EW
22	-64.79	-12.99	1.50	EW
23	12.91	-39.16	1.32	NS
24	38.25	-13.19	1.21	EW
25	91.08	-38.87	1.43	EW
26	64.89	-13.02	1.28	NS
27	-121.14	-40.85	1.39	NS
28	-121.14	-40.85	1.39	NS
29	-90.80	-38.95	1.53	EW
30	-64.79	-12.99	1.50	EW

Appendix

In KASCADE coordinates the positions of the antennas are as well given in [m] with reference to the KASCADE array centre, but in this coordinate system, the X-axis points east, the Y-axis points north and the system rotates clockwise. The red numbers indicate that the antenna has been moved during the lifetime of LOPES as outlined in the table below.

24.3.3 C.3 - Modifications of the LOPES antenna positions

In the beginning of the measurements called 'LOPES-30' (see fig. C.3.1) all antennas were aligned in East-Western direction. These alignments have been changed for several antennas but their positions remained unchanged.

| Ant-ID	action	valid from	valid until
27	alignment moved to NS	10.8.2006 12:00	end of measurement
29	alignment moved to NS	10.8.2006 12:00	end of measurement
30	alignment moved to NS	10.8.2006 12:00	end of measurement
3	alignment moved to NS	8.12.2006 10:44	end of measurement
6	alignment moved to NS	8.12.2006 10:44	end of measurement
7	alignment moved to NS	8.12.2006 10:44	end of measurement
10	alignment moved to NS	8.12.2006 10:44	end of measurement
11	alignment moved to NS	8.12.2006 10:44	end of measurement
14	alignment moved to NS	8.12.2006 10:44	end of measurement
15	alignment moved to NS	8.12.2006 10:44	end of measurement
18	alignment moved to NS	8.12.2006 10:44	end of measurement
20	alignment moved to NS	8.12.2006 10:44	end of measurement
23	alignment moved to NS	8.12.2006 10:44	end of measurement
26	alignment moved to NS	8.12.2006 10:44	end of measurement
27	alignment moved to NS	8.12.2006 10:44	end of measurement
29	alignment moved to NS	8.12.2006 10:44	end of measurement
30	alignment moved to NS	8.12.2006 10:44	end of measurement
1	alignment moved to NS	24.1.2007 13:15	end of measurement
19	interchanged with ant-20	17.1.2008 11:40	end of measurement
20	interchanged with ant-19	17.1.2008 11:40	end of measurement
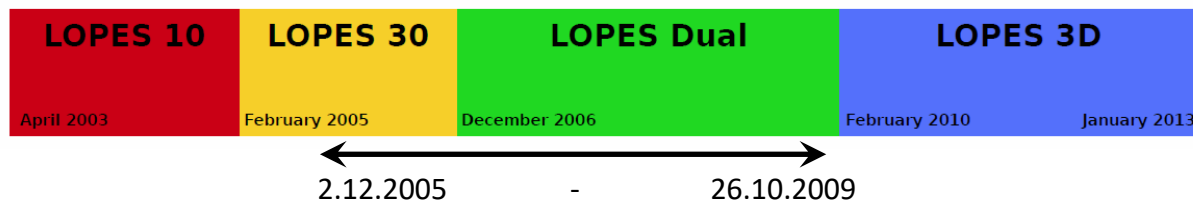
Fig.C.3.1 *Overview of the different LOPES setups and the time range where data are available in KCDC*

Before December 2005 no proper amplitude calibration is available and after October 2009 the reconfiguration to the Tripole setup started and due to the different antenna type no combined analysis was done.